NORTHWESTERN UNIVERSITY

Activity- and drug-induced plasticity of synaptic and intrinsic properties in pyramidal neurons of the rat hippocampus

A DISSERTATION

SUBMITTED TO THE GRADUATE SCHOOL
IN PARTIAL FULFILLMENT OF THE REQUIREMENTS

for the degree

DOCTOR OF PHILOSOPHY

Field of NEUROSCIENCE

By

Shannon Jessie Moore

Evanston, Illinois
December 2008

Abstract

Activity- and drug-induced plasticity of synaptic and intrinsic properties in pyramidal neurons of the rat hippocampus

Shannon Jessie Moore

The vertebrate brain, which is made up of a vast array of individual neurons, is responsible for controlling numerous functions and behaviors, including distinguishing between visual cues, learning to navigate in a new environment, or making complex decisions. These neurons form specific networks that receive, process, and integrate chemical and electrical signals. Generally, a chemical signal, called a neurotransmitter, activates specific receptors on the dendrites of a neuron. These receptors, either directly or indirectly, cause a change in the transmembrane voltage of the neuron, due to an exchange of charged ions (primarily sodium, potassium, or calcium; Na^+, K^+, and Ca^{2+}, respectively) through particular ion channels. The resulting electrical signal propagates from the dendrites towards the soma, where, if a critical threshold is reached, an action potential is triggered. The action potential travels along the axon, where it can cause release of neurotransmitter, beginning the process in another neuron. Changes, caused by specific patterns of activity or chemical modulation, in any of the receptors or channels that detect or transmit these signals can have important implications for information processing in the network.

My work explores plasticity of synaptic and intrinsic properties in the hippocampus, a region that has been strongly linked to spatial and declarative memory. Chapter 1 provides a brief introduction to hippocampal function, anatomy, and plasticity. Chapter 2 explores plasticity exhibited at synapses formed at different locations on the dendritic tree in CA1 neurons, demonstrating that inputs, even from the same presynaptic region, may be independently regulated. Chapter 3 begins with examining locomotor sensitization induced by withdrawal from repeated exposure to amphetamine. I then move on to investigate withdrawal-induced alterations in intrinsic excitability in the subiculum, providing a link between neuronal and behavioral changes that may underlie the transition from drug use to drug abuse. Chapter 4 investigates how patterned activity in the subiculum leads to robust and distinct changes in intrinsic burst firing, which may be important for propagating processed hippocampal information to various downstream cortical and subcortical targets. Chapter 5 reports the results of several additional experiments that further elucidate cellular processes involved in the induction and expression of burst plasticity, in addition to presenting possible models for the mechanisms by which an enhancement or suppression of burst firing may be achieved. Chapter 6 presents a summary of the experimental data with attention given to incorporating these results into the larger body of scientific work. Taken together, the data presented here add to our understanding of the mechanisms by which experience may alter neuronal processing in the hippocampus, and may lead to novel targets for the treatment of disorders affecting memory systems, including drug addiction and Alzheimer's disease.

Acknowledgements

I have many people to thank for both their scientific and personal support over the years as I have worked on and completed my graduate studies. Dr. Donald Cooper provided an introduction into the mechanics of patch-clamp electrophysiology. My committee members, Drs. Gianmaria Maccaferri and Catherine Woolley have provided invaluable advice and encouragement as I have navigated the stages of my scientific career. Gianmaria, thanks for all your support over the years. Catherine, I always knew I could pester you with questions or ideas, and that you would take the time to listen, discuss, and help me grow. More informally, but no less importantly, Dr. Indira Raman has always had an open door and I've appreciated her input on a number of topics. Finally, I must thank my advisor Dr. Nelson Spruston, without whose insight, advice, and direction none of this would have been possible. Nelson, I have learned much from you about the tangible and non-tangibles of being a great thinker, scientist, and advisor.

On a day-to-day basis, members of the Spruston, Raman, and Woolley labs have always been happy to talk about projects and results - or to just grab a cup of coffee and chat about the weather. In particular, Dr. Catherine Kaczorowski has not only been my scientific inspiration, but has also shaped the person I am today. Austin Graves has been a great source of support, laughter, friendship and has helped tremendously during the writing of this tome. Finally, to my parents, who have been cheering me on from the very beginning - thanks for all that you have done for me. And now, as the Walrus said, the time has come to talk of many things… Thanks for listening.

TABLE OF CONTENTS

Figure List

Table List

List of Abbreviations

***Note: Abbreviations for pharmacological agents used in experiments are not included here, but can be found in the List of Pharmacological Agents below.**

2-AG: 2-arachidonylglycerol (retrograde signal, acting at CB1 receptors)

AC: adenylyl cyclase (enzyme that serves as a primary effector in an intracellular signaling pathway)

ACh: acetylcholine (neurotransmitter)

ACSF: artificial cerebrospinal fluid (perfusion solution)

AD: Alzheimer's disease (disproportionately affects the elderly, behavioral characterized by increasingly severe memory deficits)

ADP: afterdepolarization (voltage depolarization following an action potential)

AHP: afterhyperpolarization (voltage hyperpolarization following an action potential)

AMPAR: α-amino-3-hydroxy-5-methyl-4-isoxazolepropionic acid receptor (ionotropic glutamate receptor, excitatory)

AMPH: amphetamine (psychostimulant)

bAP: backpropagating action potential (somatically generated action potential that actively propagates into the apical, radial oblique, and basal dendritic branches)

BS: burst spiking neuron (in the subiculum, a neuron that fires bursts rather than single action potentials at threshold)

Ca^{2+}: calcium

CA: cornu ammonis (used to denote different hippocampal subfields)

CaMKII: calcium calmodulin-dependent kinase II (kinase, activated by the Ca^{2+} binding protein calmodulin, which phosphorylates myriad proteins)

cAMP: cyclic adenosine monophosphate (diffusible second messenger that activates the downstream protein kinase PKA)

CB1: type I cannabinoid receptor

DA: dopamine (neurotransmitter)

DAG: diacylglycerol (membrane-bound second messenger that activates the downstream protein kinase PKC)

DG: dentate gyrus (subfield of the hippocampus)

DIC: differential interference contrast (microscopy visualization technique)

EC: entorhinal cortex (region comprising the primary cortical input to the hippocampus)

EPSC: excitatory postsynaptic current

EPSP: excitatory postsynaptic potential

ERK: extracellular signal-regulated kinase (kinase that phosphorylates myriad proteins)

E-S: EPSP-to-spike (probability that an EPSP will elicit an action potential)

EW: early withdrawal (2 days since repeated AMPH treatment)

fEPSP: field EPSP (excitatory response recorded extracellularly from a population of neurons)

G protein: guanine nucleotide-binding protein (membrane protein that, upon ligand binding, exchanges guanosine diphosphate for guanosine triphosphate, releasing the α subunit, which results in activation of a primary effector to initiate a second messenger signaling cascade)

$GABA_A$, $GABA_B$ receptor: γ-aminobutyric acid receptor, subtype A and B (ionotropic and metabotropic receptors, respectively, for GABA, inhibitory)

GCL: granule cell layer (layer of principal cells in the DG)

iGluR: ionotropic glutamate receptor (consisting of AMPAR and NMDAR, excitatory)

IP_3: inositol-1,4,5-triphosphate (diffusible second messenger that binds to receptors on the endoplasmic reticulum, resulting in Ca^{2+} release from intracellular stores)

ISI: inter-spike interval (time between action potentials)

K^+: potassium

LW: late withdrawal (14 days since repeated amphetamine)

LTD: long-term depression (long-lasting decrease in synaptic efficacy)

LTP: long-term potentiation (long-lasting increase in synaptic efficacy)

mAChR: muscarinic acetylcholine receptor (metabotropic receptor for ACh)

mGluR: metabotropic glutamate receptor (subtypes are denoted by a number; for example, mGluR1 is metabotropic glutamate receptor, subtype 1)

MF: mossy fiber (axons from granule cells that synapse on CA3 pyramidal dendrites)

Mg^{2+}: magnesium

ML: molecular layer (dendritic region of the DG)

Na^+: sodium

NAc: nucleus accumbens (region in the brain reward circuit)

NMDAR: N-methyl-D-aspartate receptor (ionotropic glutamate receptor, excitatory)

Ni^{2+}: nickel

PARA: parasubiculum (region immediately adjacent to the EC)

PIP_2: phosphotidylinositol 4,5-biphosphate (membrane phospholipid that can produce two second messengers, DAG and IP_3, in a reaction catalyzed by PLC)

PFC: prefrontal cortex (region involved in decision making and executive control; part of the brain reward circuit)

PKA: protein kinase A (kinase that phosphorylates myriad proteins)

PKC: protein kinase C (kinase that phosphorylates myriad proteins)

PLC: phospholipase C (enzyme that catalyzes the breakdown of PIP_2 into two second messengers, DAG and IP_3)

PRE: presubiculum (region immediately adjacent to the subiculum)

PP: perforant path (axons from layers II/III of the EC that synapse at distal locations on pyramidal neurons in the subiculum and in SLM in CA1)

RS: regular spiking neuron (in the subiculum, a neuron that fires single action potentials rather than bursts at threshold)

SAL: saline

SC: Schaffer collaterals (axons from CA3 that synapse in SR and SO of CA1)

sEPSC: simulated excitatory postsynaptic current (somatic current injection designed to mimic an EPSC)

sEPSP: simulated excitatory postsynaptic potential (response to a sEPSC)

SL: stratum lucidum (in CA3 only, dendritic layer between SP and SR; contains apical dendrites)

SLM: stratum lacunosum-moleculare (dendritic layer furthest [most superficial] from SP in the CA subfields; contains apical dendrites and dendritic tuft)

SO: stratum oriens (dendritic layer deep to SP in the CA subfields; contains basal dendrites)

SP: stratum pyramidale (layer of principal cells in the CA subfields)

SR: stratum radiatum (dendritic layer between SP and SLM in the CA subfields; contains apical dendrites and radial oblique branches)

STDP: spike timing-dependent plasticity (protocol used to induce plasticity, the direction of which depends on the relative timing between presynaptic input and postsynaptic output)

SUB: subiculum (subfield of the hippocampus)

TBS: theta-burst stimulation (protocol, based on activity recorded during spatial exploration *in vivo*, used induce plasticity; consists of 5 synaptic stimuli at 100 Hz, repeated at 5 Hz)

TLE: temporal lobe epilepsy (a disease characterized by seizures)

TRP: transient receptor potential receptors (family of non-selective cation channels)

VTA: ventral tegmental area (region of the brain reward circuit)

vSUB: ventral subiculum (region of the subiculum particularly involved in the brain reward circuit)

List of Pharmacological Agents

***Note: All drugs are bath-applied in *in vitro* hippocampal slice experiments, unless otherwise stated.**

AM251: 600 nM; CB1 receptor antagonist

Amphetamine (AMPH): 2.5 mg/kg for *in vivo* injections; 25 - 50 μM for acute application in hippocampal slice experiments

Atropine: 1-10 μM; general mAChR antagonist

1,2-bis(o-aminophenoxy)ethane-N,N,N',N'-tetraacetic acid (BAPTA): 10 mM; fast Ca^{2+} chelator (included in internal recording solution)

CGP52432: 3 μM; $GABA_BR$ antagonist

CGP55845: 1 μM; $GABA_BR$ antagonist

6-cyano-7-nitroquinoxaline-2,3-dione (CNQX): 20 μM; competitive AMPAR antagonist

D-amino-5-phosphonopentanoate (D-AP5): 50 μM; non-competitive NMDAR antagonist

Kynuernic acid: 2.5 mM; competitive antagonist for AMPAR and NMDAR

LY367385: 25 μM; specific group I, subtype 1 mGluR antagonist

MK-801: 20 μM; competitive NMDAR blocker

2-methyl-6-(phenylethynyl)-pyridine (MPEP): 10 μM; specific group I, subtype 5 mGluR antagonist

SR95531: 2-4 μM; $GABA_AR$ antagonist

Telenzipine: 50 nM; specific mAChR M_1 subtype antagonist

Thapsigargin: 2 μM; Ca^{2+}-ATPase inhibitor (included in internal recording solution)

Tetrodotoxin (TTX): 50 nM-500 nM; a voltage-gated Na^+ channel antagonist

U-73122: 25 μM; PLC inhibitor

Chapter 1:

Introduction

Function of the hippocampus

In vertebrates, the cerebral cortex is responsible for higher-level cognitive processing and is primarily responsible for complex brain functions such as decision making, awareness, and memory. The hippocampus, which is the phylogenetically oldest region of the cerebral cortex, was named in the mid-1500s by Italian anatomist Giulio Cesare Aranzi because, when dissected out from the medial temporal lobe of human brain, it bore a striking resemblance to a seahorse ("hippocampus" is the Greek word for "seahorse"; see Figure 1.1).

Over the past centuries, many functions for the hippocampus have been proposed, including a role in olfaction, emotion, and attention (Andersen et al., 2007). Currently, the most widely accepted view of hippocampal function is that it plays prominent role in spatial learning and declarative memory formation. Although not the first suggestion of a role for temporal lobe structures in learning and memory, pioneering work by William Scoville and Brenda Milner was instrumental in firmly establishing and supporting this idea.

In the 1950s, Scoville, a neurosurgeon, performed 30 operations in which bilateral medial-temporal lobe resections were made to varying extents in an effort to reduce or eliminate psychotic symptoms, particularly in schizophrenic patients. In general, these surgeries had the advantages of sparing patients' pre-operative personalities (unlike

frontal lobotomies) and lacking the development of post-operative seizures (unlike partial lobotomies of other regions). Therefore, when a young and otherwise normal patient, now known as H.M., was referred to Scoville because of severe and intractable epilepsy, Scoville decided to try this surgical procedure to reduce epileptic seizures in what was a "frankly experimental" approach. In the radical operation, nearly all of the tissue from H.M.'s medial temporal lobes was bilaterally removed. Although the surgery appeared to be successful in relieving epileptic symptoms, it created a new and severe problem. H.M. now exhibited profound memory deficits for events that had taken place after and just prior to the operation. This observation prompted Scoville and Milner to further examine the other patients who had received temporal lobe resections. In all cases in which the hippocampus was bilaterally affected, at least some memory impairment was noted. Furthermore, the extent of damage to the hippocampus was positively correlated with the extent of the observed memory deficit (Scoville and Milner, 1957). These interesting and unexpected findings became the impetus for extensive research focused on the hippocampus as a primary center for learning and memory in vertebrates.

The hippocampus and disease

The hippocampus has been implicated in a number of diseases that profoundly affect human society, including Alzheimer's disease (AD), epilepsy, and drug addiction. Cell death, disrupted neurotransmission, and non-specific or inappropriate alterations in intrinsic properties of hippocampal neurons may play a prominent role in the pathophysiology of these, and potentially other, disorders.

Epilepsy affects up to 1% of the total human population (Sander and Shorvon, 1996), and temporal lobe epilepsy (TLE) accounts for 60% of all partial epilepsies (those that begin in one specific region of the brain). Data from human patients combined with animal models (particularly in the rat) have demonstrated three main types of changes in the hippocampus that contribute to the development of TLE. These factors are: structural changes, including cell loss and subregion atrophy (Mutel et al., 2000); changes in chemical neurotransmission, such as increased excitatory drive (Blumcke et al., 2000; Wu and Leung, 2003) and loss of inhibitory tone (Denslow et al., 2001; Martin and Sloviter, 2001); and enhancement of neuronal excitability, mediated via decreased action potential threshold (Bernard and Wheal, 1996), downregulation of dendritic A-type K^+ channels (Bernard et al., 2004), and increased burst firing (Troyer et al., 1992; Jensen and Yaari, 1997; Su et al., 2002). Hyperexcitability, manifest as spontaneous or evoked seizure-like events, has been demonstrated in hippocampal subfields concomitantly (Surmeier and Foehring, 2004), as well as specifically in the dentate gyrus (DG) (Muller and Misgeld, 1991; Scharfman, 1994), CA3 (Ishihara et al., 1993; Queiroz and Mello, 2007), and CA1 (Alger and Nicoll, 1980; Beau and Alger, 1998). Interestingly, recent work has suggested that the subiculum is responsible for gating the spread of discharges to extrahippocampal regions (Benini and Avoli, 2005), and therefore may be critical component controlling the propagation or termination of epileptic seizures (Stafstrom, 2005).

AD, which disproportionately affects the elderly (Hebert et al., 2003), is the most common cause of dementia worldwide. One of the most prominent behavioral

phenotypes of AD, is loss of declarative memory, which intensifies with disease progression (Walker et al., 2007). Decreased hippocampal volume is strongly associated with AD, and can distinguish the disease from normal aging with a high degree of specificity (Jack et al., 1997). In an animal model of AD (and in normal aging studies [Power et al., 2002]), the excitability of CA1 neurons, controlled by the amplitude of the afterhyperpolarization (AHP), is a critical determinant of the ability to learn (Disterhoft et al., 2004). Furthermore, pharmacological interventions that reduced the amplitude of the AHP rescued hippocampus-dependent learning in normally aged mice, as well as in a genetic model of AD (Ohno et al., 2006). Together, these results suggest that restoring or enhancing neuronal excitability in the hippocampus may represent a therapeutic target for the treatment of AD in humans.

Drug addiction is perhaps one of the most economically draining disorders affecting society, with nearly $200 billion lost in direct and indirect costs due to decreased productivity, crime, and treatment in the United States alone (Office of National Drug Control Policy, 2004). Almost 60% of Americans will use an illicit drug at least once in their lifetimes, yet only a fraction of those will become drug abusers. The transition from casual to compulsive drug use involves a “hijacking” of neural circuitry normally involved in pleasure, motivation, and learning (Robinson and Berridge, 2003). This brain reward circuit, which includes the hippocampus, nucleus accumbens (NAc), ventral tegmental area (VTA), and prefrontal cortex (PFC; Figure 1.2), is potently activated by drugs of abuse, even moreso than by “natural” stimuli such as food (Kalivas and Volkow, 2005). For example, amphetamine produces a supraphysiological increase

in dopamine (DA) by reversing the DA transporter (DAT) and prolongs dopaminergic neurotransmission by blocking reuptake (Heikkila et al., 1975a; Heikkila et al., 1975b). Psychostimulants, such as amphetamine, are characterized by their ability to enhance locomotor behaviors, such as exploration, rearing, and grooming (Fray et al., 1980; Gold et al., 1988). Amphetamine-induced locomotion is greatly attenuated by specific lesions of the ventral hippocampus (Burns et al., 1993), although locomotor sensitization, which occurs with repeated psychostimulant exposure, is not affected (Wolf et al., 1995; Browman et al., 1996). Conversely, stimulation of the ventral subiculum increases extracellular DA levels in NAc, and results in DA D1 receptor-dependent hyperlocomotion (Taepavarapruk et al., 2000). Hippocampal projections have been shown to gate cortical input to NAc by driving the transition from a quiescent ("down") state to an active ("up") state (O'Donnell and Grace, 1995), which may contribute to activation of goal-directed behaviors, such as drug-seeking. Perhaps most intriguing is the demonstration that stimulation of glutamatergic hippocampal efferents induces a reinstatement of drug-seeking behavior after previous extinction, which may provide a model for relapse in human patients (Vorel et al., 2001).

Hippocampal anatomy

Nearly all of the terminology used in describing the hippocampus comes from the work of two pioneering neuroanatomists, Santiago Ramón y Cajal, and his student, Rafael Lorente de Nó (Ramón j Cajal, 1893; Lorente de Nó, 1933, 1934). In spite, or perhaps because, of this historical terminology, there is a lack of consensus in the primary

literature as to which regions comprise the hippocampus. For the purposes of this thesis, I will use the term "hippocampus" to include the dentate gyrus (DG), the cornu ammonis (CA) subfields (CA1-CA4 [Lorente de Nó, 1934]; CA4 is usually referred to as the hilus, and is generally included as part of the DG [Amaral, 1978]), and the subiculum (Figure 1.3). The hippocampal subfields are three-layered cortices composed of a single cellular layer containing principal excitatory neurons and two to three dendritic layers which are highly, though not exclusively, laminar. In DG, the principle neurons, elliptically-shaped granule cells, are located in a U- or V-shaped granule cell layer (GCL) with unipolar cone-shaped dendritic arbors extending superficially (towards the hippocampal fissure or the ventricular surface) into the molecular layer (ML). The CA subfields are distinguished by principle cells with triangularly-shaped soma, which are therefore called pyramidal cells. These reside in a relatively thin and densely packed layer called stratum pyramidale (SP). All pyramidal cells have dendrites extending both below (deep to) and above (superficial to) SP. Basal dendrites (so called because they originate from the base of the triangularly-shaped soma) extend below SP into the dendritic layer called stratum oriens (SO). Apical dendrites (originating from the apex of the triangular soma) extend into the increasingly superficial (and distal from the soma) dendritic layers of stratum lucidum (SL; only present in CA3), stratum radiatum (SR), and stratum lacunosum-moleculare (SLM), respectively. The subiculum also contains pyramidal cells, which are indistinguishable morphologically from those in CA1. However, subicular pyramidal cells do not form the tightly packed cellular layer seen in the CA subfields; rather, they become progressively more dispersed along the superficial-

deep axis as distance from CA1 increases (closer to presubiculum). Furthermore, the relatively distinct dendritic layers observed in CA1 disappear and are replaced by the molecular layer of the subiculum, which can be divided into a deep portion (roughly continuous with SR) and a superficial portion (roughly continuous with SLM). As in other hippocampal subfields, basal dendrites are deeper, relative to the soma, and apical dendrites extend superficially.

It should also be noted that each of these regions may contain one or more different types of interneurons which are usually classified on the basis of their axonal arborization and their unique staining patterns for one or more molecular markers (such as parvalbumin, cholecystokinin, or somatostatin). These interneurons generally form inhibitory synaptic connections with principle neurons in each region, and are important in shaping the integration properties of the local circuits in the hippocampus. Because of the diversity and complexity of hippocampal interneurons (for review, see Maccaferri and Lacaille, 2003) , and because it is difficult to stimulate both excitatory and inhibitory afferents in a physiological manner in an *in vitro* slice preparation, I have focused on the effects of excitatory neurotransmission in my thesis.

Intrinsic and extrinsic connectivity of the hippocampus

Unlike many other brain regions, there are very few reciprocal connections between hippocampal subfields (Ramón j Cajal, 1893), resulting in a largely unidirectional flow of information (see Figure 1.4). A logical place to begin a discussion of synaptic connections is in the entorhinal cortex (EC), which provides the major

cortical input pathway to the hippocampus. The perforant path (PP; so called because it perforates, or transects, the subiculum [Ramón j Cajal, 1893]) is largely composed of axons from superficial EC (although a minor component comes from deep layers [Steward and Scoville, 1976]); axons arising mainly in layer II cross the hippocampal fissure and target granule cells dendrites in the molecular layer (ML) and CA3 pyramidal neurons in stratum lacunosum moleculare (SLM), while layer III axons run along the dorsal edge of the hippocampal fissure and contact CA1 dendrites (see below). In DG, the organization of this projection is such that axons originating in lateral EC form synapses in the outermost third of the ML, while axons from medial EC synapse in the middle third (Steward, 1976; Witter and Amaral, 1991). No EC contacts are made in the innermost third of the molecular layer (Amaral and Lavenex, 2007). Similarly, in CA3, projections from lateral EC terminate in the most superficial regions of SLM, while projections from medial EC terminate in deeper areas of SLM. No synaptic contacts are formed between EC axons and CA3 neurons in stratum radiatum (SR) or stratum lucidum (SL) (Witter, 1993).

Granule cell axons, which are called mossy fibers (MFs) due to the presence of relatively large presynaptic boutons (Amaral and Dent, 1981), project almost exclusively to the CA3 subfield. In proximal CA3 (close to DG), MFs form synapses in stratum oriens (SO) on basal dendrites, and in the narrow SL region on apical dendrites (Blackstad et al., 1970). Moving more distally in CA3 (towards CA2), the synapses become increasingly confined to SL. The MF projection ends precisely at the border of CA3 and CA2, and, in fact, the lack of DG input is one of the defining features of CA2

(Amaral and Lavenex, 2007). SR, the layer superficial to SL in CA3, contains the majority of the apical dendritic arbor, and is where the numerous recurrent projections from other CA3 pyramidal cells form synaptic contacts. SLM, superficial to SR, receives synaptic connections from layer II EC, but proximally located CA3 neurons (close to DG) do not have dendritic arbors that extend into SLM (Amaral and Lavenex, 2007). Therefore, EC input to CA3 neurons becomes increasingly more prominent moving from proximal to distal CA3 (approaching CA2).

In between CA3 and CA1 is a narrow band of pyramidal cells that Lorente de Nó recognized as a separate subregion, which he called CA2 (Lorente de Nó, 1934). Like CA1 neurons, these cells do not receive input from DG, but like CA3 neurons, they form extensive recurrent collaterals within CA2. Although not as well studied as other hippocampal subfields, anatomical and histochemical evidence suggests that these neurons do indeed form a distinct region (Amaral and Lavenex, 2007).

CA3 axons, called Schaffer collaterals (SC) after Károly Schaffer who first described them (Amaral and Lavenex, 2007), provide the major input to CA1, making synaptic connections on both basal dendrites in SO and apical dendrites in SR (Ishizuka, 2001). Proximal CA3 (closest to DG) preferentially innervates distal CA1 (by the CA1/subiculum border), while distal CA3 (near CA2) projects more heavily to proximal CA1 (near CA2) (Ishizuka, 2001). Unlike CA3 pyramidal cells, CA1 neurons have very few, if any, recurrent connections. An additional feature of CA1 is that the most superficial portions of the apical dendrites (those closest to the hippocampal fissure, which are in SLM) receive synaptic input from a distinct set of afferent fibers originating

in layer III of EC (these are fibers in the PP that do not cross the hippocampal fissure) (Ramón j Cajal, 1893). The organization of the EC projections to CA1 is topographical (rather than laminar, as in DG): axons from lateral EC target distal CA1 (close to the CA1/subiculum border), while axons from medial EC target proximal CA1 (close to the CA1/CA2 border) (Amaral and Lavenex, 2007).

Moving from CA1 into the subiculum, the pyramidal cell layer widens and laminar dendritic layers of CA1 (SR and SLM) end, to be replaced by the molecular layer (O'Mara et al., 2001). Dendrites in the deep region of the molecular layer, which is continuous with SR, receive dense innervation from CA1 axons (Amaral et al., 1991). Dendrites in the more superficial region, which is roughly continuous with SLM, receive synaptic contacts from PP axons arising in layer III EC (O'Mara et al., 2001). Both CA1 and EC projections to the subiculum are topographically organized (Witter and Groenewegen, 1990). Proximal CA1 (at the CA1/CA2 border) projects to distal subiculum (near the subiculum/presubiculum border) while distal CA1 projects to proximal subiculum (both at the CA1/subiculum border) (Tamamaki et al., 1987). Meanwhile, lateral EC projects to proximal subiculum, while medial EC projects to distal subiculum (Figure 1.4) (Witter and Amaral, 1991). Additionally, subicular neurons exhibit a higher degree of recurrent collateral connections than do CA1 neurons.

Subicular efferents, in turn, form the major output pathway of the hippocampus (Swanson and Cowan, 1977), projecting to a variety of cortical and subcortical targets. These include prominent connections with layer V of EC (which also receives a minor projection directly from CA1) , the amygdaloid complex (Kemppainen et al., 2002), the

septal nucleus and adjacent NAc (Witter et al., 1990; Ishizuka, 2001) , and the prefrontal cortex (Jay and Witter, 1991; Verwer et al., 1997). Therefore, the impact of processed hippocampal information is controlled by synaptic and intrinsic properties of subicular neurons, which are well-placed to influence a diverse array of functions and behaviors.

Electrophysiological characteristics of CA1 and the subiculum

Studies comparing CA1 and subicular pyramidal neurons have revealed very few differences in electrical properties between the two populations (Staff et al., 2000). Whole-cell current-clamp recordings demonstrated that both have resting membrane potentials between -60 and -70 mV and action potential thresholds at ~ -45 mV. CA1 neurons exhibited an after-hyperpolarization (AHP) following a single action potential; instead, subicular neurons had an after-depolarization (ADP). However, there is one key difference: a majority of subicular pyramidal neurons fire action potentials in high frequency clusters ("bursts") while CA1 pyramidal neurons generally display tonic firing of single action potentials (Figure 1.5) (Staff et al., 2000).

In vitro recordings from subicular pyramidal neurons have revealed two broad classifications: burst-firing and regular-firing neurons (Taube, 1993). There are no significant differences in morphological characteristics such as dendritic structure or passive membrane properties between these two populations (Staff et al., 2000), although burst-firing cells tend to be found deeper in the subiculum, while regular-firing cells tend to be more superficially located (Greene and Totterdell, 1997). There is also some

evidence that burst-firing and regular-firing cells differ with respect to local connections, as well as their extrinsic targets. Deep cells, which are mostly burst-firing, have axons that run along the basal-apical dendritic axis, and remain relatively close to the dendritic arbor of their cell of origin, forming a crude column. Conversely, more superficially located cells, which tend to be regular-firing, have axons that spread out orthogonally to the dendritic axis and extend over a larger area of the region (Harris et al., 2001). Furthermore, when activated antidromically, burst-firing cells were recruited only when presubiculum was stimulated, and never when entorhinal cortex (EC) was stimulated; regular-firing cells showed the opposite organization and were only recruited with EC stimulation (Stewart, 1997).

However, active electrophysiological characteristics, such as voltage-gated conductances, do vary between burst-firing and regular-firing neurons. For example, burst-firing neurons exhibit a pronounced voltage "sag" in response to a hyperpolarizing current injection, which is a measure of hyperpolarization-activated current (I_h) (Stewart and Wong, 1993). Interestingly, somatic voltage-clamp recordings showed that burst-firing neurons had larger amplitude Ca^{2+} tail currents compared to regular-firing neurons. Furthermore, strong burst-firing neurons (those that, in whole-cell recordings where a sustained depolarizing current was applied, continued to fire bursts throughout the duration of the injection) had the largest Ca^{2+} tail currents; CA1 pyramidal neurons, on the other hand, had the smallest (Jung et al., 2001). Local application of specific Ca^{2+} channel antagonists to the dendrites was ineffective at preventing burst firing, but high concentrations of Ni^{2+} puffed on the soma blocked burst firing (Jung et al., 2001).

Therefore, burst firing in the subiculum appears to be due to activation of voltage-gated Ca^{2+} channels by depolarization from a Na^{+}-dependent action potential. The resulting Ca^{2+} tail current produces an ADP that, if sufficiently large, can reach threshold to trigger another Na^{+}-dependent action potential. Other depolarizing, non-inactivating currents, particularly persistent Na^{+} current, have been suggested to underlie burst firing in subicular pyramidal neurons (Golomb et al., 2006). In fact, any conductance that provides additional depolarization after a Na^{+}-dependent action potential can increase the probability of reaching threshold for subsequent action potentials, but the intrinsic mechanism for generating burst firing appears to be dependent on the Ca^{2+} tail current (Jung et al., 2001).

Action potential bursts likely have special consequences for neuronal circuits (Lisman, 1997). Bursts are "information rich" in that they are sufficient to relay information about a stimulus (Livingstone et al., 1996). In fact, in some cases, such as defining tuning curves in auditory cortex (Cattaneo et al., 1981a, 1981b) and spatial maps of hippocampal place cells (Otto et al., 1991), considering bursts alone provides more refined representations than when single action potentials are included. Furthermore, bursts can induce changes in synaptic strength through the induction of long-term potentiation (LTP) or long-term depression (LTD). In CA1, when one burst (4 pulses at 100 Hz) was delivered at the peak of a carbachol-induced theta oscillation, LTP was observed; conversely, when the burst was delivered at the trough, previously potentiated synapses were depressed (Huerta and Lisman, 1995). Even without cholinergic modulation, one burst (5 pulses at 100 Hz) is sufficient to induce LTP in the Schaffer

collateral pathway in CA1 (Remy and Spruston, 2007). Burst firing is likely so efficacious because bursts represent a robust signal that is reliably propagated; regardless of the initial probability of release at a synapse, a burst containing just two action potentials increases release probability to over 95% (Stevens and Wang, 1995). Because of their strong effect on downstream targets, bursts can drive transitions between bistable membrane voltage states (for example, the up- and down-states in NAc), thereby gating other excitatory input (O'Donnell and Grace, 1995). Furthermore, the strong influence of burst firing may be used as a signal for important or novel events (Cooper, 2002), and confer salient information about the environment (such as a cue associated with a food or drug reward) (Martin and Ono, 2000).

Metabotropic receptor signaling

In addition to ionotropic receptors, which are directly gated ion channels, another class of receptors, metabotropic receptors, influence ligand- or voltage-gated ion channels indirectly. This class of receptors includes metabotropic glutamate receptors (mGluRs), muscarinic acetylcholine receptors (mAChRs), and γ-aminobutyric acid $(GABA)_B$ receptors, among others, which are part of the guanine nucleotide-binding protein (G protein) subfamily of metabotropic receptors. In general, activation of these receptors releases a subunit of the G protein, which activates an effector (typically an enzyme) that can produce a diffusible (or membrane-bound) second messenger (Figure 1.6). This second messenger may act directly on ion channels, but more often, initiates a biochemical cascade that results in protein kinase activation and/or Ca^{2+} release from

intracellular stores, which both affect the biochemical state of the neuron. The second messenger produced, and thus the downstream targets engaged, depends on the type of G protein coupled to the activated receptor. There are generally multiple subtypes of each metabotropic receptor, coupled to different G proteins, so one neurotransmitter may recruit varied intracellular signaling pathways, depending on the unique expression pattern of receptor subtypes. mGluRs are ubiquitously expressed in the hippocampus (Shigemoto et al., 1997) and participate in the regulation of many cellular processes, so I will focus on their activation and transduction mechanisms as an example of the functional consequences of metabotropic receptor signaling.

Eight mGluR subtypes have been identified, which can be divided into three groups, based on their sequence homology. Group I contains subtypes 1 and 5, group II contains subtypes 2 and 3, and group III contains 4, 6, 7, and 8 (Conn and Pin, 1997). Furthermore, these different groups have distinct transduction mechanisms. Activation of group I mGluRs releases the α subunit of the G protein G_q, which stimulates phospholipase C (PLC) (Sugiyama et al., 1987). PLC catalyzes a reaction in which the breakdown of phosphotidylinositol 4,5-biphosphate (PIP_2), a membrane phospholipid, produces diacylglycerol (DAG), which remains membrane-bound and leads to the activation of protein kinase C (PKC), and inositol-1,4,5-triphosphate (IP_3), which can freely diffuse through the cytosol and activate IP_3 receptors on intracellular Ca^{2+} stores, leading to Ca^{2+} release (Masu et al., 1991; Abe et al., 1992). On the other hand, activation of either group II (Tanabe et al., 1992; Tanabe et al., 1993) or group III (Okamoto et al., 1994) mGluRs releases the α subunit of the G protein $G_{i/o}$, which inhibits the activity of

adenylyl cyclase (AC). AC stimulates production of cyclic adenosine monophosphate (cAMP), which binds to the regulatory subunit of protein kinase A (PKA), freeing the catalytic subunit to phosphorylate downstream target proteins. However, because $G_{i/o}$ inhibits AC production, stimulation of group II or group III mGluRs reduce the activity of PKA in the cell, and thus would lead to a decrease in the phosphorylation state of downstream proteins.

Numerous studies have examined the electrophysiological roles of mGluR activation, and not surprisingly, have found a variety of effects (for review, see Anwyl, 1999). These include inhibition and potentiation of voltage-gated ionic conductances, modulation of excitatory transmitter release, and induction and modulation of synaptic plasticity. For example, in several brain regions, including neocortex (Sayer et al., 1992; Swartz, 1993; Choi and Lovinger, 1996), hippocampus (Swartz and Bean, 1992; Sahara and Westbrook, 1993; Swartz et al., 1993), and cerebellum (Chavis et al., 1994; Chavis et al., 1995), agonists of group I, II, or III mGluRs have been shown to inhibit L- and N-type Ca^{2+} channels. As would be predicted for a G protein-mediated effect, the inhibition of L-type channels appears to depend on a diffusible second messenger (Sayer et al., 1992; Chavis et al., 1995). Interestingly, however, inhibition of N-type channels was prevented by techniques that block membrane-delimited signaling, but not intracellular signaling, which implies that the G protein (or a subunit) may interact directly with N-type channels to inhibit the conductance (Swartz and Bean, 1992). On the other hand, mGluR agonists have also been reported to potentiate both L- and N- type currents in

ganglion and cerebellar cultures (Rothe et al., 1994; Chavis et al., 1995; Chavis et al., 1996), demonstrating that the complexity of the effects mediated by mGluR activation.

The evidence supporting a role for mGluR in modulation of excitatory neurotransmitter release first came from the observation that a glutamate analog, AP4, depressed transmission at perforant path (PP) synapses in dentate gyrus (DG) (Dong et al., 2005). After the elucidation of mGluR, the reversible suppression of excitatory neurotransmission in CA1 in rat hippocampal slices was demonstrated using a non-specific agonist (Baskys and Malenka, 1991a, 1991b; Desai et al., 1999). Since then myriad pharmacological studies using selective agonists have demonstrated presynaptic effects for mGluRs, particularly group II and group III, and occasionally group I (for review, see Anwyl, 1999).

Most recently, mGluRs have been shown to mediate long-lasting changes in synaptic strength. Activation by a non-specific agonist induced long-term potentiation (LTP) in CA1 (Bortolotto et al., 1994; Bortolotto and Collingridge, 1995; Manahan-Vaughan and Reymann, 1997), DG (O'Connor et al., 2005), and cerebellum (Rossi et al., 1996). Further, tetanically induced LTP was occluded by prior induction of mGluR-mediated LTP, suggesting a common molecular mechanism of maintenance and/or expression (Bortolotto and Collingridge, 1993). Interestingly, mGluR activation can also contribute to synaptic plasticity by priming synapses for future plasticity (so-called metaplasticity), without inducing changes in synaptic strength immediately. When CA1 neurons had previously been exposed to a group I mGluR agonist, subsequent LTP, induced by tetanic stimulation, displayed a greater magnitude increase than when the

mGluR agonist was not applied (Cohen and Abraham, 1996). Additionally, this protocol caused an enhancement of intrinsic neuronal excitability, evidenced by increased excitatory postsynaptic potential-to-spike (E-S) coupling, which may have facilitated LTP induction (Cohen et al., 2002).

A final level of complexity in metabotropic receptor signaling involves synergistic actions between multiple G protein-coupled receptors. One source of synergy comes from direct interactions between metabotropic receptors, such as in the formation of heteromers (Enz, 2007). In Purkinje neurons, $GABA_B$ receptors formed complexes with mGluR1 and potentiated responses of the mGluRs to glutamate through an interaction with extracellular Ca^{2+} (Tabata et al., 2004). Interestingly, this effect persisted in the presence of pertussis toxin, a G protein inhibitor, demonstrating that the $GABA_B$-mediated sensitization of mGluR1 was not mediated through canonical $G_{i/o}$ signaling (Tabata et al., 2004). Heteromeric interactions between metabotropic receptors can also synergistically potentiate intracellular signaling. Complexes formed of mGluR1 and adenosine A_1 receptors in a transfected cell line (similar to the heteromers observed in primary cortical cultures) significantly potentiated receptor-evoked Ca^{2+} signaling (Ciruela et al., 2001). In another study, coactivation of mGluR5 and adenosine A_2 receptors in neostriatal slices exponentially increased phosphorylation of a downstream signaling molecule (DARPP-32). The results of pharmacological manipulations suggested that mGluR potentiated adenosine A_2 receptor-mediated production of cAMP (Nishi et al., 2003). A functional role for metabotropic synergism in mediating behavior has been demonstrated as well. Infusion of a specific group II mGluR into the nucleus

accumbens (NAc) had no effect on locomotor activity alone, but potentiated locomotor responses in the presence of dopamine (DA) D1 receptor agonists (David and Abraini, 2001).

Taken together, the data support many roles for metabotropic receptor signaling, from canonical recruitment of specific intracellular signaling cascades to a contribution to metaplasticity. Further, the effects of metabotropic receptor activation may be mediated by G protein-dependent or -independent interactions. These receptors are likely targets for modulation, and may contribute to the induction or expression of neuronal and behavioral output.

Synaptic plasticity in the hippocampus

Pyramidal neurons in the hippocampus have been estimated to receive up to 30,000 excitatory inputs (usually from glutamatergic presynaptic boutons onto dendritic protuberances called spines). The idea that memories are stored by specific changes in connections between neurons was perhaps first proposed in the mid-1800s by Alexander Bain who stated “for every act of memory … there is specific grouping or co-ordination … by virtue of specific growths in the cell-junctions” (Bain, 1855). Nearly one hundred years later, Donald Hebb put forth a detailed theoretical hypothesis of how these changes might occur in a network (Hebb, 1949). He suggested that when one cell “repeatedly or persistently” contributes to causing a second cell to fire, a structural or chemical (metabolic) change takes place, in one or both cells, such that the impact of the first cell on the second is increased.

However, it was not until 1973 that experimental evidence emerged to support this idea. Tim Bliss and Terje Lømo, while recording in the dentate gyrus (DG) of anesthetized rabbits, observed that brief (3-15 seconds) high frequency stimulation of perforant path (PP) inputs resulted in potentiated field excitatory postsynaptic potentials (fEPSPs; recorded extracellularly, representing the response of a population of cells). This enhancement could be observed for hours after the brief tetanic stimulation, and so was called long-term potentiation (LTP) (Bliss and Lømo, 1973). Since this groundbreaking discovery, LTP has generated considerable interest as a possible cellular mechanism underlying learning and memory. LTP has several characteristics that make it an attractive model. For example, induction of LTP is *selective* in that only inputs which were specifically stimulated display increased efficacy (Andersen et al., 1977; Lynch et al., 1977), *cooperative* in that enough inputs must be synchronously active to reach a threshold level of depolarization (McNaughton et al., 1978; Levy and Steward, 1979), and *associative* in that strong depolarization at one group of synapses can lead to strengthening of a less strongly activated group of synapses, which wouldn't have been potentiated if activated alone (McNaughton et al., 1978; Levy and Steward, 1979). These features are also characteristic of many declarative memories: memories are formed for specific facts or events (selectivity); multiple characteristics of an object or event can combine to reach threshold for memory (cooperativity); and important or significant characteristics or events can cause other, less noteworthy facts to be remembered in concert (associativity). Furthermore, LTP has been demonstrated in a number of regions shown to be critically involved in the acquisition, storage, and/or retrieval of memories,

including the hippocampus (Jarrard, 1993; Shen et al., 1994), prefrontal cortex (Laroche et al., 1990), and cerebellum (Crepel and Jaillard, 1991).

The locus of both the induction and expression of LTP have been the subjects of vigorous debate. Arguably, the most extensive work on the mechanisms underlying LTP has been carried out in the hippocampus, where two distinct forms have been demonstrated: N-methyl-D-aspartate (NMDAR)-dependent LTP at Schaffer collateral (SC) synapses in CA1 and NMDAR-independent LTP at mossy fiber (MF) synapses in CA3. Detailed experiments in these two regions have provided a wealth of information about the presynaptic and postsynaptic mechanisms of synaptic plasticity.

At SC synapses in CA1, it is almost universally agreed that the locus of induction is postsynaptic. Several lines of evidence support this conclusion. The induction of LTP at these synapses requires postsynaptic depolarization (Kelso et al., 1986; Gustafsson et al., 1987), activation of NMDARs (Collingridge et al., 1983), and a rise in intracellular Ca^{2+} (Lynch et al., 1983). The requirement for depolarization is likely due to the voltage-dependent Mg^{2+} block of NMDARs (Mayer et al., 1984; Nowak et al., 1984). NMDARs are permeable to Ca^{2+} (MacDermott et al., 1986), so their activation causes a significant, but transient, increase in Ca^{2+} concentration in the postsynaptic spine. This brief Ca^{2+} signal is then thought to initiate second messenger cascades, likely involving myriad protein kinases (such as calcium calmodulin-dependent kinase II (CaMKII); for review, see Lisman et al., 2002), which ultimately engage the cellular mechanisms underlying LTP induction.

For years, the locus of LTP expression at SC synapses in CA1 has been much more controversial. Some studies reported that, while LTP induction could be blocked by postsynaptic manipulations, LTP expression was unaffected, suggesting a presynaptic mechanism (Malinow et al., 1989). A hypothesis put forth to explain these results was that LTP is mediated by a persistent increase in the probability of release of neurotransmitter from the presynaptic terminal. One line of evidence which supported this idea was the observation that, after LTP induction, the coefficient of variation (CV; the standard deviation divided by the mean) of the amplitudes of excitatory postsynaptic currents (EPSCs) was decreased (Bekkers and Stevens, 1990; Malinow and Tsien, 1990). The CV is inversely related to quantal content (the average number of activated synapses that release neurotransmitter) because as more synapses release neurotransmitter in response to stimulation, the standard deviation of the EPSC amplitudes (and thus the CV) decreases. Another result that further supported this conclusion was that, after LTP induction, the number of failures (synaptic stimulation that resulted in no [measurable] synaptic response) decreased (Kullmann and Nicoll, 1992). Failure of a postsynaptic response after stimulation was assumed to be a result of a lack of neurotransmitter release; therefore, if the probability of release increased, the number of failures would be expected to decrease. Finally, it was reported that these changes occurred with no increase in the amplitude of the unitary synaptic response, seeming to rule out a contribution from a postsynaptic increase in α-amino-3-hydroxy-5-methyl-4-isoxazolepropionic acid receptor (AMPAR) function (Stevens and Wang, 1994).

On the other hand, increased AMPAR function or number would increase the amplitude of evoked excitatory postsynaptic potentials (EPSPs), which is a hallmark of LTP. For example, phosphorylation of AMPARs, which can occur at multiple sites, increases the open probability (Banke et al., 2000) as well as the conductance through the channel (Derkach et al., 1999), and changes in phosphorylation of AMPARs have been observed after the induction of LTP (Lee et al., 1983). Additionally, the demonstration that NMDAR activation or postsynaptic depolarization, which have both been shown to be required for the induction of LTP, resulted in insertion of the AMPAR subunit GluR1 into dendritic membranes supported a potential postsynaptic mechanism for LTP expression (Lu et al., 2001; Pickard et al., 2001).

These two seemingly contradictory sets of results were in large part resolved by elegant experiments that demonstrated the existence of synapses containing only NMDARs (and no AMPARs), which were thus are functionally silent (not able to contribute to the synaptic response near resting membrane potentials because of the voltage-dependent Mg^{2+} block of the NMDAR) (Isaac et al., 1995). Furthermore, these "silent synapses" were converted to functional synapses (containing AMPARs and therefore able to respond to synaptic activation at hyperpolarized potentials) by an LTP-inducing protocol (Liao et al., 1995). Studies of neurotransmission at single synapses (which can be recruited by minimal stimulation) demonstrated no changes in probability of neurotransmitter release, but, when release did occur, the resulting EPSC amplitudes were larger, on average, than before LTP induction (Isaac et al., 1996). In this light, initial experiments demonstrating decreased variance of the amplitudes of the synaptic

responses and decreased number of failures were reinterpreted as reflecting insertion of AMPAR into synapses which previously contained only NMDAR (Malenka and Nicoll, 1997, 1999). Thus, after insertion, these "converted" synapses respond to glutamate release, where they did not previously, increasing the variance in the response, and decreasing the number of observed failures. The ability of AMPARs to be recruited to synapses previously containing only NMDAR has been demonstrated in hippocampal cell cultures (Liao et al., 1995). Taken together, these results provide strong support for a postsynaptic mechanism for expression of NMDAR-dependent LTP at SC synapses in CA1.

Conversely, at MF synapses in CA3, the locus of LTP (MF-LTP) induction has garnered the most debate and remains controversial. Support for a presynaptic mechanism of induction comes largely from experiments that demonstrate postsynaptic manipulations have no effect on MF-LTP induction, while manipulations affecting presynaptic terminals abolish the induction. For example, unlike LTP in CA1, induction of MF-LTP has been shown not to require NMDAR activation, postsynaptic depolarization, or a rise in postsynaptic Ca^{2+} (Zalutsky and Nicoll, 1990; Mellor and Nicoll, 2001) and, further, persisted in antagonists of excitatory postsynaptic receptors (Castillo et al., 1994). However, removing extracellular Ca^{2+} prevented the induction of MF-LTP, suggesting that Ca^{2+} entry into the presynaptic terminal was a critical component of LTP induction (Castillo et al., 1994).

On the other hand, a number of studies have implicated a critical postsynaptic contribution to the induction of MF-LTP by demonstrating that postsynaptic

manipulations, particularly chelating Ca^{2+} or preventing depolarization (Williams and Johnston, 1989; Jaffe and Johnston, 1990), reduced or prevented the induction of MF-LTP. Furthermore, MF-LTP could be induced, even in the presence of ionotropic glutamate receptor antagonists, via mGluR-mediated release of Ca^{2+} from intracellular stores (Yeckel et al., 1999).

Some resolution to these conflicting results has come from a study that showed short trains of high-frequency stimulation resulted in Hebbian plasticity, which could be blocked by a number of postsynaptic manipulations, while long trains of high-frequency stimulation led to non-Hebbian plasticity that was unaffected by postsynaptic manipulations (Urban and Barrionuevo, 1996). Therefore, it may be that the specific protocol used to induce MF-LTP recruit different induction mechanisms. A more intriguing possibility has been suggested by the finding that MF-LTP was markedly reduced in the presence of postsynaptic inhibitors of EphB receptor tyrosine kinases or the extracellular application of soluble B-ephrins (which are endogenous ligands for EphB receptors) (Contractor et al., 2002). These results support a model in which MF-LTP induction depends on a rise in postsynaptic Ca^{2+} to stimulate EphB receptor activation, which would promote retrograde signaling through interaction with presynaptic ephrins. In this case, the results which have been interpreted as a presynaptic locus for MF-LTP induction may reflect a disruption of either ephrin-EphB receptor interaction or downstream ephrin signaling.

In either case, a wealth of evidence supports the idea that the locus of MF-LTP expression is presynaptic. For example, paired-pulse facilitation, an indirect but common

measure of the probability of release, is decreased after LTP, which indicates a higher probability of release in response to the first stimulus (Zalutsky and Nicoll, 1990). Optical quantal analysis performed by confocal microscopy has demonstrated both an increase in the number of active release sites as well as an increase in probability of release at release sites that were already active (Reid et al., 2004). A more precise method to assess the involvement of a presynaptic mechanism in MF-LTP has demonstrated that in mice lacking Rab3A (which is a small GTP-binding protein thought to be critically involved in mediating neurotransmitter release at MF synapses) MF-LTP is absent, suggesting that presynaptic signaling leads to a long-lasting alteration in the neurotransmitter release machinery at MF-CA3 synapses (Castillo et al., 1997).

Intrinsic plasticity in the hippocampus

In a physiological setting, action potential firing depends both on synaptic input received as well as the unique identity and distribution of ion channels throughout the neuron. As discussed in the previous section, an abundance of research has focused on plasticity of synaptic properties as a cellular correlate of learning and memory. Much less work, however, has focused on activity-dependent changes in the intrinsic properties of neurons, which may represent a significant means by which neurons may alter their integration, processing, and output in response to internal or external stimuli (Figure 1.7).

Bliss and Lømo's (1973) initial report of long-term potentiation (LTP) also noted an increase in the amplitude of the population spike, which reflects synchronous action

potential firing of many neurons. A larger amplitude population spike is indicative of a greater number cells generating an action potential, suggesting that there was an increased probability of firing for any given granule cell. An increase in firing probability would be expected based solely on the potentiation of the field excitatory postsynaptic potentials (fEPSPs; recorded extracellularly, representing the response from a population of neurons); however, even if the stimulus intensity was decreased to evoke fEPSPs of the same amplitude as before plasticity was induced, the population spike was larger than that observed during baseline [called EPSP-to-spike (E-S) potentiation] (Bliss and Lømo, 1973). This demonstrated that another long-lasting process, in addition to potentiation of excitatory synapses, was induced by tetanic stimulation in the dentate gyrus (DG).

One explanation for these findings is that tetanic stimulation induced plasticity at inhibitory synapses in addition to LTP at excitatory connections. In this case, the increase in firing probability would result from an altered balance between excitatory and inhibitory drive, perhaps via a decrease in feed-forward inhibition. However, another possibility is that voltage-gated (intrinsic) conductances were also modified in an activity-dependent manner, and that these changes served to increase the overall neuronal excitability of granule cells. A number of studies have attempted to resolve this question by examining E-S potentiation in the presence of γ-aminobutyric acid (GABA)ergic receptor antagonists. If E-S potentiation persists, it can not be (solely) due to a decrease in inhibitory drive, and must involve changes in intrinsic conductances. On the other hand, preventing E-S potentiation by blocking GABAergic receptors supports the idea that decreased inhibitory drive underlies the increased probability of action potential

firing. Thus far, the results have been conflicting. A number of groups have reported that E-S potentiation is blocked by GABAergic antagonists (Gustafsson et al., 1987; Chevaleyre and Castillo, 2003; Cooper et al., 2003), but others have found that E-S potentiation persisted in the presence of GABAergic antagonists (Chavez-Noriega et al., 1990; Jester et al., 1995; Liao et al., 1995; Campanac and Debanne, 2008). It seems, therefore, that at least a component of E-S potentiation, in some conditions, may reflect changes in the intrinsic, voltage-gated conductances of neurons.

A stronger link between alterations in neuronal firing properties and intrinsic conductances was demonstrated in cell culture. Lobster stomatogastric ganglion neurons exhibit burst firing *in vivo* when receiving synaptic input. Conversely, when maintained in culture for 2 days, ganglion neurons responded to depolarizing current injections with regular (tonic) firing (similar to the firing profile exhibited when pharmacologically isolated in the ganglion). However, long-term isolation (3 days or longer in culture) resulted in a re-emergence of burst firing (Turrigiano et al., 1994), which was paralleled by alterations in voltage-gated conductances, including an up-regulation of Na^+ and Ca^{2+} currents, and a down-regulation of a (likely A-type) K^+ current (Turrigiano et al., 1995). Together, these results suggest that a chronic absence of normal excitatory input induces plasticity of intrinsic conductances, which promote the ability to generate burst firing endogenously, so that stable activity patterns are maintained.

More rapid induction of intrinsic plasticity has been demonstrated in acute cerebellar slices (Aizenman and Linden, 2000). In deep cerebellar nuclei neurons, tetanic synaptic stimulation or direct depolarization via somatic current injection resulted in a

gradual, but persistent increase in the number of action potentials elicited by a depolarizing current injection. Because only somatic current injection was used to elicit action potential firing, this increase can not be due to changes in synaptic drive, and therefore must be mediated by alterations in voltage-gated channels throughout the neuron. The induction of this plasticity required Ca^{2+} entry, either via NMDAR activation (synaptic tetanus), or through voltage-gated Ca^{2+} channels (somatic depolarization), and, in most neurons, was correlated with a reduction in action potential threshold. These results demonstrate that plasticity of intrinsic conductances can be rapidly induced by physiological activity patterns, resulting in a global increase in the neuronal response to depolarizing input.

Several studies have demonstrated that changes in synaptic and intrinsic properties can be induced concurrently. In cerebellar granule cells in acute slices, pairing membrane depolarization with high frequency stimulation of mossy fibers resulted in LTP of excitatory postsynaptic currents (EPSCs) (D'Angelo et al., 1999) and an increase in neuronal excitability, reflected by an increase in input resistance and a decrease in action potential threshold (Armano et al., 2000). Induction of both synaptic and intrinsic plasticity required postsynaptic depolarization and N-methyl-D-aspartate receptor (NMDAR) activation, suggesting that they may be mediated by the same molecular mechanisms. In hippocampal slices, LTP induction in CA1 pyramidal neurons via a theta-burst protocol also resulted in an increase in dendritic excitability, evidenced by an increase in the amplitude of backpropagating action potentials (bAPs) and a corresponding increase in the associated Ca^{2+} signal (Frick et al., 2004). LTP and

increased dendritic excitability were both blocked by NMDAR antagonists; however, cell-attached patch-clamp recordings from dendrites showed that plasticity induction was accompanied by a reduction in A-type K^+ channel function (evidenced by a hyperpolarizing shift in the steady-state inactivation curve), which would enhance backpropagation, but is unlikely to mediate the expression of LTP. Taken together, these results suggest that synaptic activation may be required for the induction of changes in intrinsic properties, but that distinct mechanisms may underlie the expression of synaptic and intrinsic plasticity.

To investigate whether changes in intrinsic excitability, like changes in synaptic strength, can be bidirectionally regulated, a spike-timing dependent (STDP) protocol was used to induce plasticity in CA1 neurons from hippocampal slices (Campanac and Debanne, 2008). As predicted from previous work (Bi and Poo, 1998), a pre-before-post pairing resulted in LTP of EPSPs, and, conversely, a post-before-pre pairing resulted in long-term depression (LTD). Interestingly, induction of LTP was accompanied by E-S potentiation (in the presence of $GABA_A$ antagonists), while induction of LTD was accompanied by E-S depression (Campanac and Debanne, 2008). As in previous studies, both synaptic and intrinsic plasticity induction (potentiation and depression) required the activation of NMDARs, suggesting that these two forms of plasticity may represent a redundant mechanism for information storage.

Thus far, the experiments regarding intrinsic plasticity have demonstrated a global increase in neuronal excitability (for example, by decreasing action potential threshold, or increasing action potential backpropagation along the apical dendrite), which would be

predicted to boost excitatory inputs arriving at any location on the dendritic tree. Campanac and Debanne also addressed the specificity of intrinsic plasticity by recording from two independent pathways, only one of which was stimulated with the STDP protocol. Both synaptic and intrinsic plasticity (LTP and E-S potentiation or LTD and E-S depression) were only induced in the pathway that was stimulated, while no changes in EPSP amplitude or E-S coupling were observed in the unstimulated pathway (Campanac and Debanne, 2008). This result demonstrates that, like synaptic plasticity, intrinsic plasticity can be input specific, which preserves a large capacity for information storage.

A recent study has demonstrated that specific changes in dendritic excitability can be restricted to individual dendritic compartments (Losonczy et al., 2008). Two-photon uncaging of glutamate onto basal or radial oblique branches of CA1 pyramidal neurons initiated a dendritic spike that propagated to the soma. Somatic recording detected the resulting non-linear voltage deflection, which was composed of a fast Na^+-channel-dependent and a slow NMDAR-dependent component, and fluorescence imaging detected the strength of the associated Ca^{2+} signal. In some braches, strong dendritic spike propagation was observed, corresponding to a relatively large amplitude somatic voltage deflection and a Ca^{2+} signal that did not attenuate over moderately long distances (~60 μm). However, in the majority of branches, uncaging resulted in weak dendritic spike propagation, producing only a small amplitude somatic voltage deflection and a Ca^{2+} signal that attenuated dramatically within a short distance (<40 μm) from the site of stimulation. Interestingly, when a theta-patterned induction stimulus was delivered to a weak branch (which consisted of pairing uncaging of glutamate to elicit dendritic spikes

and somatic current injection to generate bAPs), the strength of the branch was persistently enhanced. Evoking dendritic spikes alone (by uncaging glutamate) did not result in branch strength potentiation, but this plasticity could be induced by uncaging in the presence of carbachol, a cholinergic agonist. In both cases, branch strength potentiation was specific to the stimulated branch, and did not affect other, unstimulated branches. Taken together, these results suggest that the contribution of individual dendritic branches in neuronal integration can be specifically regulated in an activity- and state-dependent manner.

The potential importance of intrinsic plasticity as a mechanism mediating learning and memory has been demonstrated *in vivo* by training on a hippocampus-dependent task. In a trace eye-blink conditioning paradigm, a tone signifies that an air puff will be delivered to the eye, after some delay (the trace period). Rabbits learn to blink in order to avoid the air puff, which is mildly aversive. Recordings in CA1 pyramidal neurons from naïve rabbits that had not been exposed to the task, rabbits that were able to learn the task (learners), and rabbits that were unable to learn the task (non-learners) demonstrated that, 24 hours after training, learners had a significantly reduced afterhyperpolarization (AHP) compared to non-learners and naïve rabbits (Moyer et al., 1996). However, 7 days after training, the AHP in learners had returned to an amplitude comparable to that observed in non-learners and naïve rabbits, although behavioral performance remained stable (Moyer et al., 1996). Therefore, this transient reduction in the AHP, which is likely mediated by alterations in Ca^{2+}-dependent K^{+} conductances (Disterhoft et al., 1993; Moyer et al., 1996), appears to be permissive for learning the task, but is not required for expression of

the learned behavior. Intriguingly, cholinergic modulation reduces the AHP and enhances learning in aged animals, which usually have larger AHPs and can not learn the task (Disterhoft et al., 1999; Disterhoft and Matthew Oh, 2003). This suggests that an interplay may exist between glutamatergic neurotransmission and behavioral states which upregulate cholinergic tone, providing a generalized mechanism for the induction of plasticity of intrinsic excitability, which may be required for some forms of learning and memory.

Plasticity and drugs of abuse

One of the most prevalent diseases involving neuroadaptations in the brain is drug addiction. The reinforcing effects of nearly all habit-forming drugs appear to be mediated by disruption of signaling within the mesolimbic dopaminergic system and related structures, which together comprise the brain reward circuit (Wise, 1998). The major regions of the reward circuit are the ventral tegmental area (VTA), nucleus accumbens (NAc), prefrontal cortex (PFC), amygdala, and subiculum (Figure 1.2) (Kalivas and Volkow, 2005). The VTA contains dopaminergic neurons, which are activated in response to salient environmental cues (such as presentation of a drug). The NAc contains γ-aminobutyric acid (GABA)ergic (inhibitory) medium spiny neurons that target the ventral pallidum, which leads to motor output via the basal ganglia, and therefore provide an interface between the limbic system and the motor pathway. The PFC is usually designated as the region responsible for decision making and formulating goal-directed behaviors, which are critical to drug-seeking. The amygdala provides an emotional context in which behaviors take place, while the subiculum, via input from

CA1 and the entorhinal cortex (EC), is likely involved in supplying a spatial framework and encoding factual information about motivationally salient events.

Psychomotor stimulants (or psychostimulants), such as cocaine and amphetamine, powerfully activate the mesolimbic system by inhibiting and/or reversing dopaminergic transporters, thereby preventing reuptake and causing further (non-stimulus dependent) release of dopamine (DA) (Heikkila et al., 1975a; Heikkila et al., 1975b). As a result, these drugs have been used extensively in animal models of addiction to characterize behavioral and cellular neuroadaptations that may underlie the transition from drug use to drug abuse.

Behavioral changes induced by repeated experience with psychostimulants can be divided into two major classes: increased drug seeking (incentive sensitization) and enhanced locomotor responses to acute drug presentation (psychomotor sensitization), either over time or compared to drug-naïve animals (Robinson and Berridge, 2003). Incentive is generally quantified by measuring the amount work an animal will do to obtain a drug reward. For example, following a period of *ad libitum* access to cocaine, rats will robustly press a lever in an attempt to obtain the drug (Di Ciano and Everitt, 2002), even in spite of aversive stimuli (Vanderschuren and Everitt, 2004).

Acute exposure to amphetamine in drug-naïve animals significantly increases locomotion, exploration, and, at higher doses, results in stereotyped behaviors such as rearing and grooming (Fray et al., 1980). In animals that have been previously exposed to amphetamine, acute exposure boosts the expression of these behaviors even further (Segal and Mandell, 1974; Segal et al., 1980). Psychomotor sensitization is often used as

an indicator of addiction because it is relatively easy to measure, and depends, at least in part, on brain regions that comprise the reward circuit, particularly NAc (Paulson and Robinson, 1991; Wyvell and Berridge, 2000).

These observed behavioral adaptations are likely mediated by changes in neuronal properties of cells in the reward circuit. Recent work has focused on identifying and characterizing neuroadaptations that occur in response to repeated exposure to psychostimulants. Most of the alterations that have been identified are transient, and thus can not underlie the maintenance or expression of behavioral sensitization (Dong et al., 2005), which can persist for years in rodents (Paulson et al., 1991), and possibly a lifetime in humans. However, these short-term neuroadaptations may be permissive for or required to induce other changes that are responsible for the manifestation of addiction-related behaviors.

Because a disruption in dopaminergic signaling appears to be an integral component in mediating addiction, most studies have examined drug-induced alterations in VTA. Transient neuroadaptations in this region generally result in enhanced basal activity levels and increased dopaminergic neurotransmission. Specifically, these alterations include decreased sensitivity of DA autoreceptors on presynaptic butons (Ackerman and White, 1990; Dong et al., 2005), enhanced sensitivity of α-amino-3-hydroxy-5-methyl-4-isoxazolepropionic acid (AMPA) receptors (Zhang et al., 1997) and increased expression of both AMPA and N-methyl-D-aspartate (NMDA) receptor subunits on dopaminergic neurons (Fitzgerald et al., 1996), and increased Ca^{2+} signaling in dopaminergic axon terminals (Pierce and Kalivas, 1997).

In contrast, in NAc neurons, repeated exposure to psychostimulants results in a persistent enhancement of inhibitory responses mediated by DA D1 receptors (Henry et al., 1989; Higashi et al., 1989), which is temporally paralleled by the expression of behavioral sensitization to cocaine (Henry and White, 1995). In addition to alterations due to repeated exposure to psychostimulants, withdrawal also induces changes in NAc neurons. *In vitro* recordings have demonstrated a reduction in whole-cell Na^+ and Ca^{2+} currents after 3 days of abstinence from repeated amphetamine, which is mediated by enhanced D1-dependent cyclic adenosine monophosphate (cAMP) and protein kinase A (PKA) signaling (Zhang et al., 1998; Zhang et al., 2002). This decreased response to excitatory inputs, particularly from cortical regions (Thomas et al., 2001), may contribute to flattened affect and decreased motivation exhibited during short-term withdrawal from psychostimulants.

Although relatively understudied compared to VTA and NAc, repeated psychostimulant experience has also been demonstrated to modulate activity in other regions of the brain reward circuit. For example, recurring cocaine treatment results in an increased capacity of future exposure to elevate extracellular glutamate in VTA and NAc, which may contribute to sensitization of locomotor behaviors (Pierce et al., 1996; Reid and Berger, 1996). Withdrawal from repeated amphetamine treatment transiently decreases neuronal excitability in the ventral subiculum (Cooper et al., 2003), which gates PFC input to NAc neurons (O'Donnell and Grace, 1995), thereby further reducing NAc responses to excitatory drive. The current challenge is to link these neuroadaptations

to the emergence and maintenance of addiction-related behaviors, in the hope of identifying targets to prevent or ameliorate the impact of drugs of abuse.

Work presented

In this section, I will briefly describe the projects that comprise my thesis work. I will also outline my contributions to each project.

Chapter 2: Distance- and location-dependent plasticity at Schaffer collateral synapses on CA1 pyramidal neurons. The idea for this project was motivated from work by Dr. Jason Hardie. In this project, I investigated whether there were differences in the magnitude of synaptic plasticity at Schaffer collateral synapses at different locations on CA1 pyramidal neurons. I performed all electrophysiological recordings and data analysis reported in this chapter.

Chapter 3: Psychostimulant-induced plasticity of intrinsic neuronal excitability in subicular pyramidal neurons. This study was performed in collaboration with Dr. Donald Cooper and Dr. Nathan Staff. We aimed to characterize neuronal excitability of subicular pyramidal neurons from amphetamine-treated rats. Further, we assayed locomotor sensitization in time-matched populations to compare the time course of electrophysiological and behavioral changes observed. For this project, I performed all the electrophysiological recordings and analysis to examine the effects of acute amphetamine application neuronal excitability (Figure 3.7). Further, I contributed to the

electrophysiological recordings which demonstrated that the amplification of subthreshold properties was Na^+-channel dependent, and that the effect of amphetamine was occluded in the presence of TTX (Figures 3.3 and 3.4). I was involved in treating rats with amphetamine, and contributed to the collection and analysis of behavioral data. Finally, I was responsible for performing three-dimensional reconstructions of regular firing and burst firing neurons (Figure 3.1). A version of this study was published in the Journal of Neuroscience (Cooper et al., 2003).

Chapter 4: Bidirectional plasticity of intrinsic burst firing in subicular pyramidal neurons. The initial idea of investigating changes in burst firing in an *in vitro* hippocampal slice was conceived by Dr. Donald Cooper. In this project, I focused on inducing and characterizing changes in neuronal burst firing, which is mediated by intrinsic conductances. The receptors and intracellular signaling pathways required for the induction of these changes were elucidated. I conducted all recordings and data analysis. A manuscript regarding this project has been submitted to Neuron and is under review.

Chapter 5: Possible mechanisms of induction and expression of burst plasticity in subicular pyramidal neurons. This chapter presents additional unpublished data from experiments designed to explore the induction and expression mechanisms of burst plasticity. Furthermore, possible models regarding the mechanisms of induction and expression are presented. I performed all electrophysiological recordings and data analysis reported in this chapter.

Figures

Figure 1.1 Comparison of the hippocampus and seahorse.

On the left, the hippocampus, dissected from a human brain. On the right, a seahorse, for which the structure is named. Reprinted from Andersen et al., 2007.

Figure 1.1

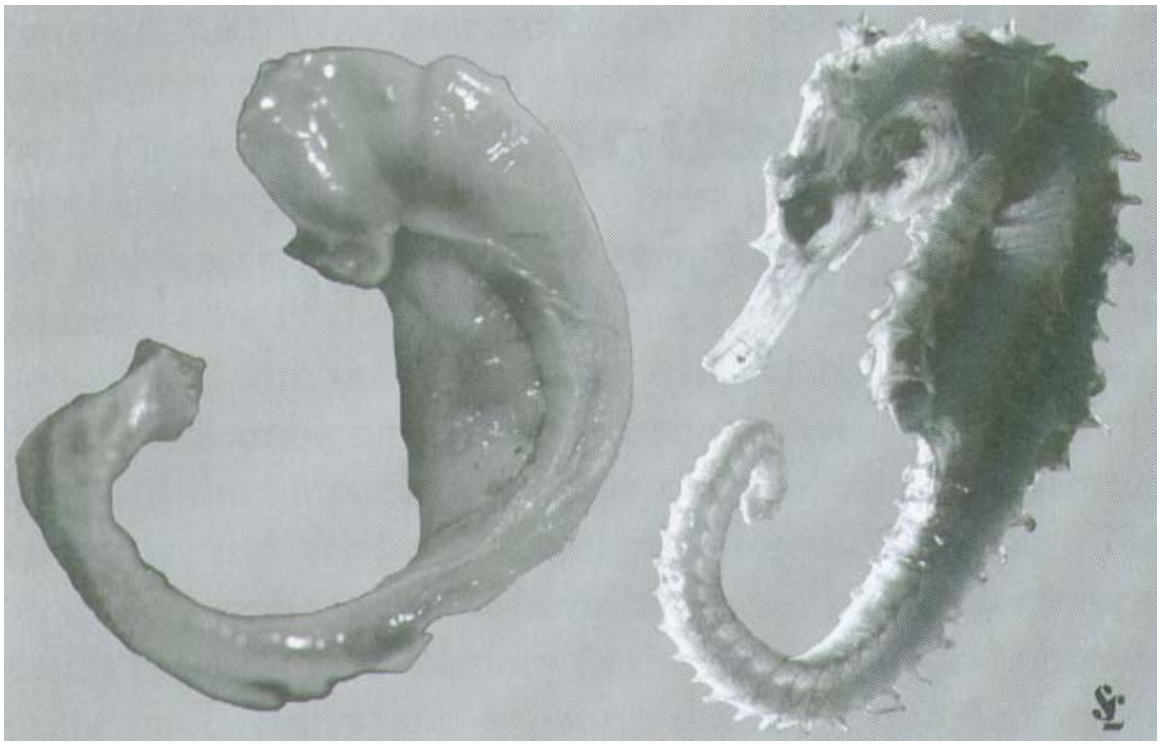

Figure 1.2 Schematic of reward circuitry.

Major regions comprising the reward circuit in the brain. Colored arrows denote the identity of the neurotransmitter used by projections from each region: red - glutamate, blue - GABA and/or neuropeptides, yellow - GABA, green - dopamine. Note that there are reciprocal connections between each of the glutamatergic regions, which are not denoted for clarity. Adapted from Kalivas and Volkow, 2005.

Figure 1.2

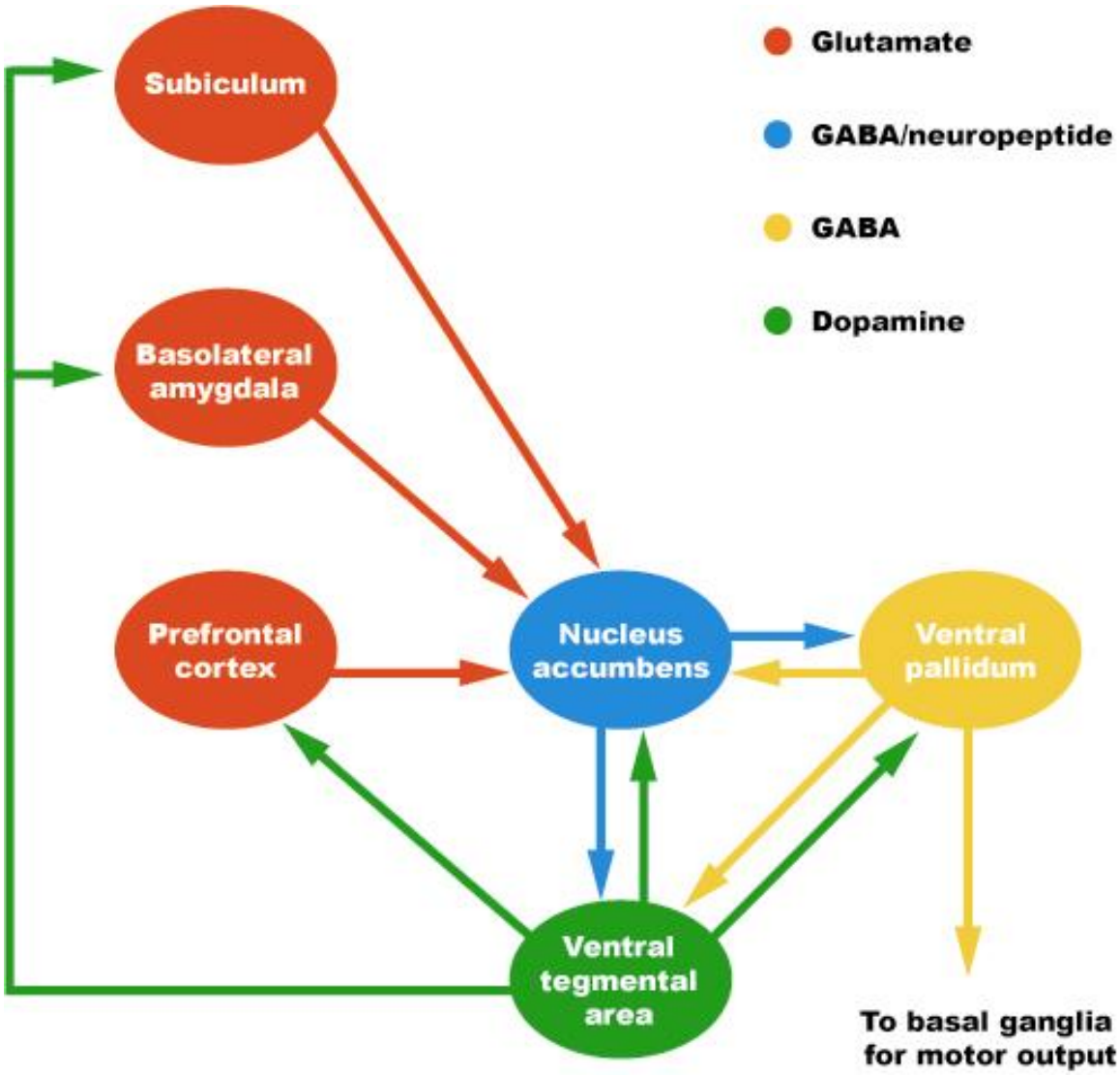
Glutamate
GABA/neuropeptide
GABA
Dopamine
Subiculum
Basolateral amygdala
Prefrontal cortex
Nucleus accumbens
Ventral pallidum
Ventral tegmental area
To basal ganglia for motor output

Figure 1.3 Anatomy of the hippocampus.

The hippocampus as depicted by two early 20th century neuroanatomists. **Left,** Drawing by Santiago Ramón y Cajal. Note that arrows show Ramón y Cajal's hypotheses about the direction of information flow into and through the hippocampus, which proved to be largely correct. **Right,** Drawing by Rafael Lorenete de Nó, detailing the anatomy and delineation between hippocampal subfields (Lorente de Nó, 1934). Reprinted from Andersen et al., 2007.

Figure 1.3

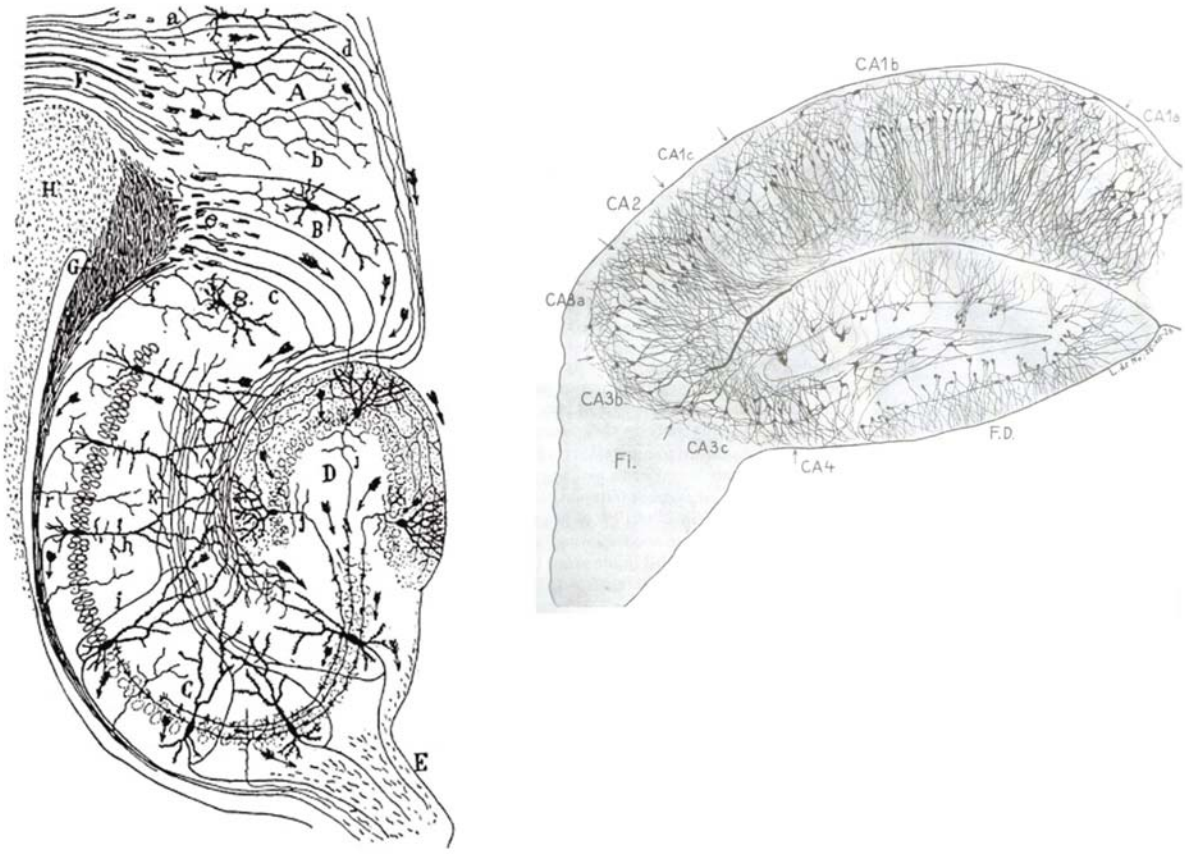

Figure 1.4 Connectivity of the hippocampus.

Left, Schematic of the hippocampal subfields, with major synaptic pathways shown. **Right,** Summary of the topographical organization of intrinsic and extrinsic connections within the hippocampus. Abbreviations are as follows: entorhinal cortex (EC), parasubiculum (Para), presubiculum (Pre), subiculum (Sub), lateral entorhinal area (LEA), and medial entorhinal area (MEA). Proximal (Prox) and distal (Dist) regions are indicated for each subfield. Reprinted from Andersen et al., 2007.

Figure 1.4

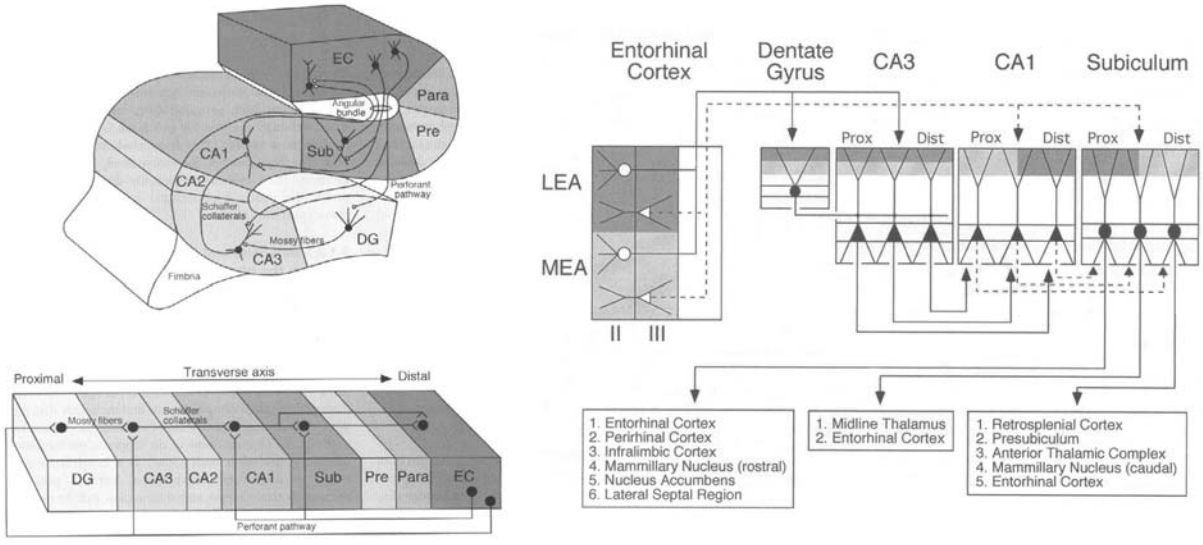
EC
Para
Pre
Sub
CA1
CA2
CA3
DG
Angular bundle
Perforant pathway
Schaffer collaterals
Mossy fibers
Fimbria
Proximal
Transverse axis
Distal
DG
CA3
CA2
CA1
Sub
Pre
Para
EC
Perforant pathway
Entorhinal Cortex
Dentate Gyrus
CA3
CA1
Subiculum
LEA
MEA
II
III
Prox
Dist
1. Entorhinal Cortex
2. Perirhinal Cortex
3. Infralimbic Cortex
4. Mammillary Nucleus (rostral)
5. Nucleus Accumbens
6. Lateral Septal Region
1. Midline Thalamus
2. Entorhinal Cortex
1. Retrosplenial Cortex
2. Presubiculum
3. Anterior Thalamic Complex
4. Mammillary Nucleus (caudal)
5. Entorhinal Cortex

Figure 1.5 Firing patterns of CA1 and subicular pyramidal neurons.

Examples of action potential firing in CA1 and subicular (SUB) pyramidal cells. Note that there are two distinct classes of firing patterns in the subiculum, regular firing and burst firing. Burst firing neurons can be further divided into weak (one burst before a transition to regular firing) and strong (multiple bursts before a transition to regular firing) categories. Scale bars apply to all traces and insets respectively. Insets show a magnified view of the first action potential or burst. Adapted from Staff et al., 2000.

Figure 1.5

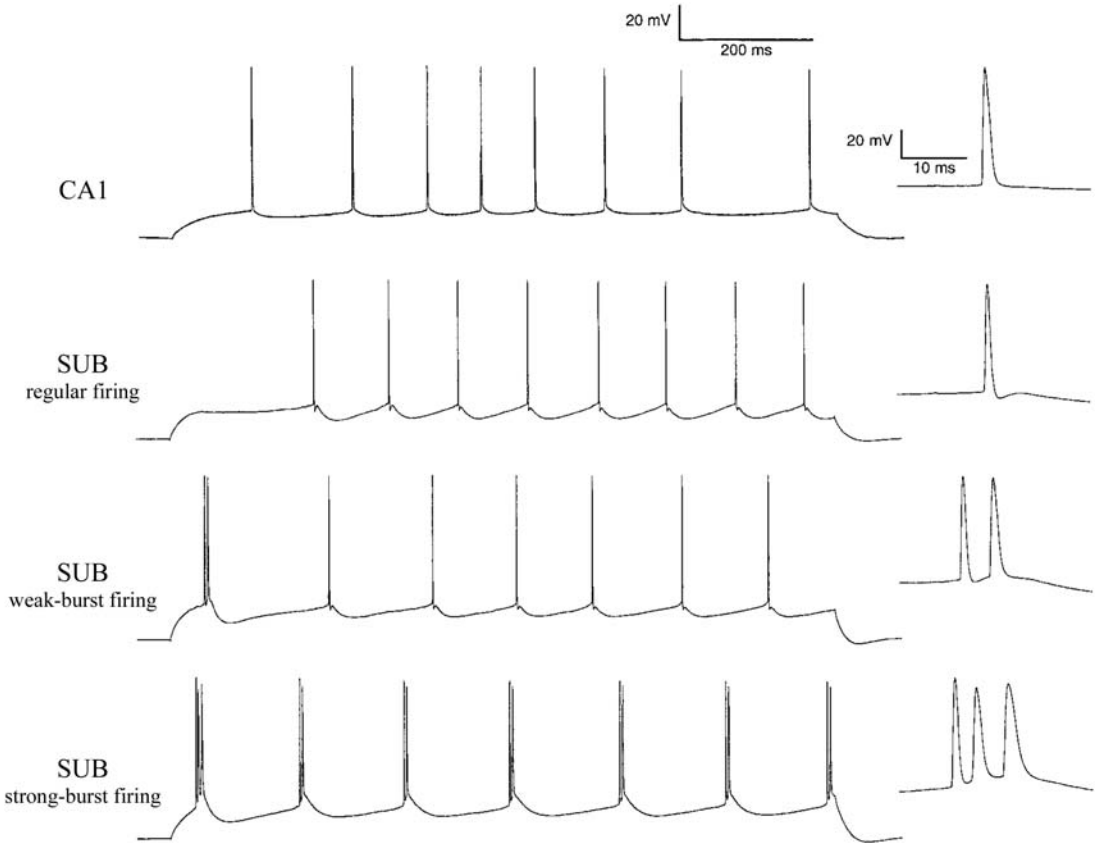
20 mV
200 ms
20 mV
10 ms
CA1
SUB
regular firing
SUB
weak-burst firing
SUB
strong-burst firing

Figure 1.6 Schematic of G-protein coupled receptor signal transduction pathways.

Left, Schematic showing the generalized structure of G-protein coupled receptor signaling. **Right,** Specific G-protein signaling pathway, coupled to metabotropic glutamate receptor subtypes 1 and 5 (mGluR1 and mGluR5). Reprinted from Kandel et al., 2000.

Figure 1.6

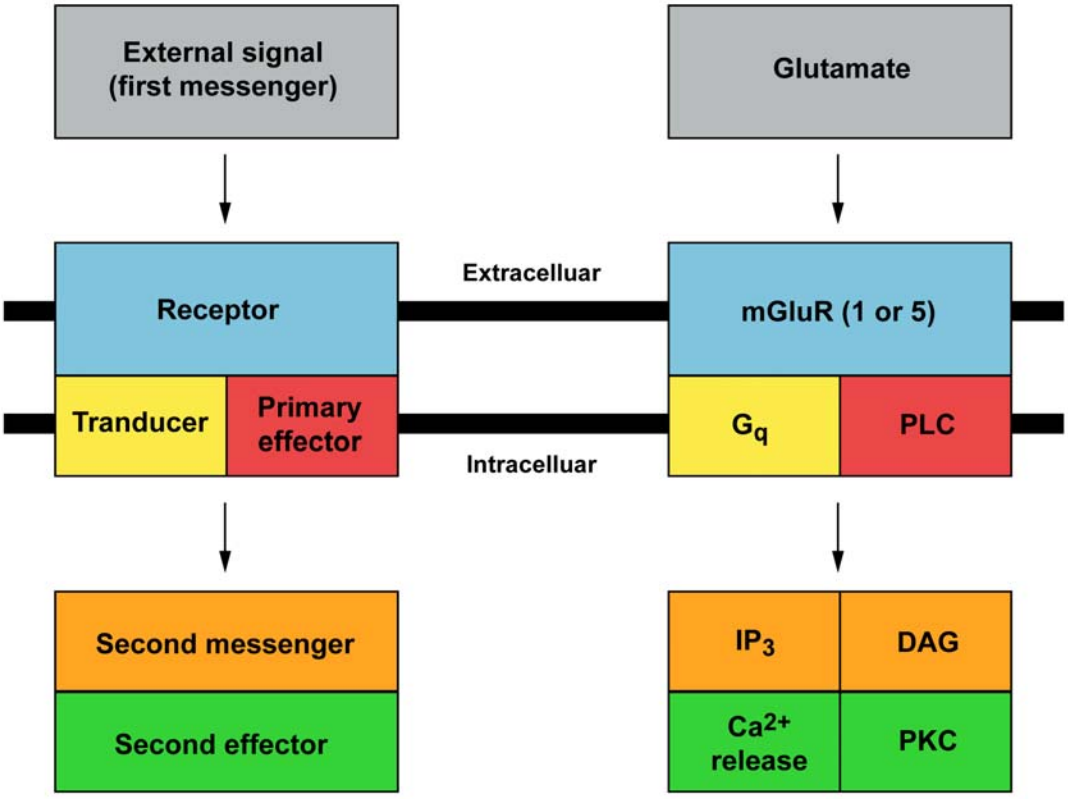
External signal
(first messenger)
Glutamate
Receptor
Extracelluar
mGluR (1 or 5)
Tranducer
Primary
effector
Intracelluar
G_q
PLC
Second messenger
Second effector
IP_3
DAG
Ca^{2+}
release
PKC

Figure 1.7 Diagram of activated and affected regions in models of synaptic and intrinsic plasticity.

Synaptic plasticity causes changes only at the synapses (or at synapses very close to those) activated during induction. Conversely, intrinsic plasticity causes changes in the excitability of a region (for example, the apical dendrite) of or an entire neuron globally.

Figure 1.7

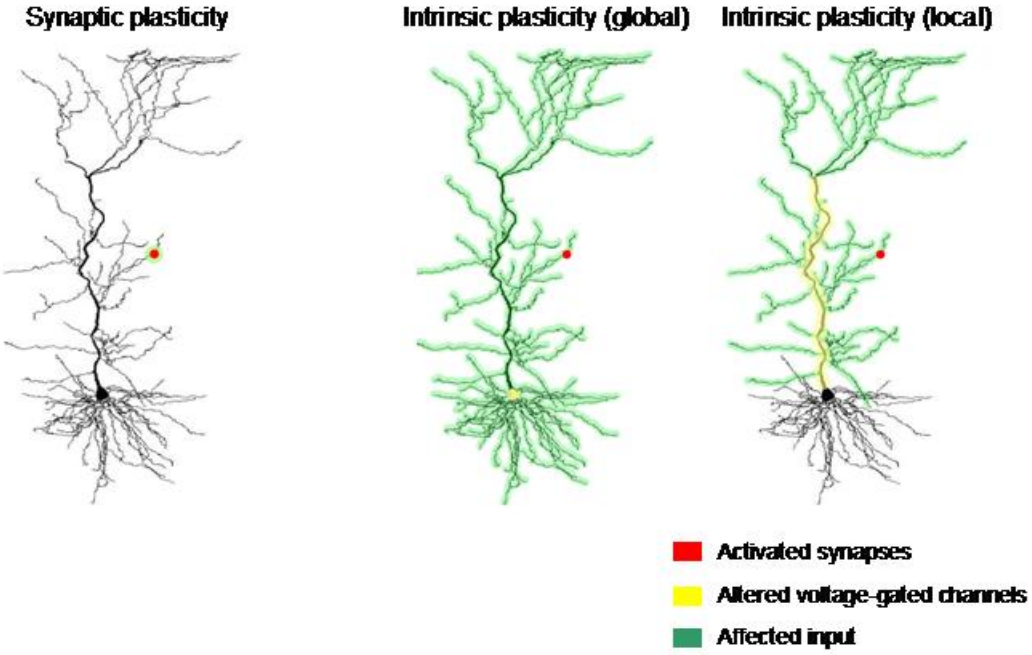
Synaptic plasticity
Intrinsic plasticity (global)
Intrinsic plasticity (local)
Activated synapses
Altered voltage-gated channels
Affected input

Chapter 2:

Distance- and location-dependent plasticity at Schaffer collateral synapses on CA1 pyramidal neurons

Abstract

Synaptic plasticity, often expressed as changes in the strength of connections between neurons, is widely regarded as the leading candidate for a cellular mechanism underlying learning and memory. Since the initial description of long-term potentiation (LTP), a variety of protocols have been shown to induce changes in synaptic strength, and these vary with respect to the frequency, number, and strength of stimulation. However, the question of whether plasticity is differentially induced at synapses formed on different locations of a neuron has remained largely unexplored. To this end, we used whole-cell current-clamp recordings to examine the synaptic plasticity observed at Schaffer collateral (SC) fibers impinging on different regions of the CA1 dendritic arbor. We found that synaptic plasticity was differentially induced, depending on the location of the synapses formed. SC synapses in distal stratum radiatum (SR) exhibited LTP that was blocked by antagonists of N-methyl-D-aspartate receptors (NMDARs) while SC synapses in proximal SR and stratum oriens (SO) exhibited long-term depression (LTD). Interestingly, LTD in proximal SR was dependent on activation of type 1 cannabinoid (CB1) receptors, and further, could be converted to LTP by antagonists of group I metabotropic glutamate receptors (mGluRs). However, SC synapses in stratum oriens

(SO) exhibited LTD that was not affected by mGluR antagonism. Taken together, these results demonstrate that synapses formed by fibers originating in the same region support distinct forms of synaptic plasticity, which depend on activation of unique receptor types in specific dendritic regions.

Introduction

In the late 1800s, neuroanatomist Ramón y Cajal was one of the first to suggest that changes in connections between neurons may provide the foundation for learning and memory (Andersen et al., 2007). Donald Hebb provided a theoretical framework for this idea when he proposed that when one cell "repeatedly or persistently" contributes to evoking action potentials in a second cell, the strength of the connection between the two will be increased (Hebb, 1949). Experimental evidence to support these assertions came when Bliss and Lømo, working in the anesthetized rabbit, found that repeatedly stimulating axons in the perforant path (PP; efferents from entorhinal cortex [EC]) increased the size of the response elicited in field potential recordings in the dentate gyrus (DG), which they called LTP (Bliss and Lømo, 1973). Subsequently, LTP (and its correlate, LTD) has received considerable attention as a potential molecular mechanism underlying learning and memory.

A variety of protocols, which differ with respect to the number and frequency of stimulations, have been shown to induce LTP. For example, LTP can be induced by a short period of tetanic (high-frequency) stimulation (such as 100 Hz for 1 s) or by longer periods of lower intensity stimulation (such as theta-burst stimulation (TBS), which usually consists of 5 synaptic stimuli at 100 Hz, repeated once every 200 ms for 3-5 s). Both the strength of the presynaptic input and the timing relative to postsynaptic output (action potential firing) have also been shown to impact the magnitude and direction of synaptic plasticity (Sjostrom et al., 2001). In layer 5 visual cortical neurons, pairing weak input with postsynaptic output 10 ms later, repeated at 10-50 Hz, induced LTP, while no

change was observed when this pairing was repeated at 0.1 Hz. However, if the strength of the presynaptic input was increased, LTP induction at 0.1 Hz could be rescued. On the other hand, when the relative timing was varied so that output preceded input by 10 ms, LTD was induced at frequencies up to 20 Hz (Sjostrom et al., 2001).

In addition to these synaptic strength- and pattern-dependent differences, the induction of synaptic plasticity may also depend on differences in synapse-specific properties, such as location or sensitivity to neuromodulation. For example, in CA1, back-propagating action potentials (bAPs) can induce LTP in SR but not SLM (Magee and Johnston, 1997), possibly because bAPs fail to invade distal dendritic regions (Callaway and Ross, 1995; Golding et al., 2001). Instead, synapses in SLM appear to require strong stimulation, leading to the cooperative activation of dendritic spikes, which can induce LTP (Golding et al., 2002). Synapses in SR and SLM are also differentially sensitive to neuromodulation. Carbachol, a cholinergic agonist, produces strong suppression of evoked excitatory postsynaptic potentials (EPSPs) at synapses in SR, but much weaker suppression of EPSPs at synapses in SLM (Hasselmo and Schnell, 1994).

To explore differences in the induction of synaptic plasticity at synapses from the same input pathway at different dendritic locations, we performed whole-cell current-clamp recordings from CA1 pyramidal neurons while recruiting SC inputs at distinct dendritic locations. We placed an extracellular stimulating electrode in either distal SR, proximal SR, or SO to activate SC fibers from CA3. Our results demonstrate that synapses formed at different locations on CA1 pyramidal neurons exhibit different levels of synaptic plasticity, and that the induction of this plasticity depends on specific

activation of receptors in different dendritic compartments. This may represent a universal mechanism by which input from distinct regions or networks influences synaptic changes in neurons, leading to formation of specific memories.

Methods

Animals – Male Wistar rats, aged 25-45 days, were used for all experiments. Animals were colony housed on a 12-hour light/dark cycle with free access to food and water. All animal procedures were approved by the Northwestern University Animal Care and Use Committee.

Solutions – Artificial cerebrospinal fluid (ACSF) consisted of (in mM): 125 NaCl, 2.5 KCl, 25 $NaHCO_3$, 1.25 NaH_2PO_4, 1 $MgCl_2$, 2 $CaCl_2$, and 25 dextrose (all from Fisher Scientific, Pittsburgh, PA). The pH of the ACSF was 7.2-7.4 and the osmolarity was 305-320 mOsm. ACSF was always oxygenated by constant bubbling with a gas mixture of 95% O_2/5% CO_2. Internal recording solution consisted of (in mM): 115 K-gluconate, 20 KCl, 10 sodium phosphocreatine (Na_2-Pcr), 10 HEPES, 2 MgATP, and 0.3 NaGTP with 0.10% biocytin for subsequent determination of morphology (all from Sigma-Aldrich, St. Louis, MO, except KCl and HEPES, which were from Fisher Scientific). 1 M KOH was used to pH the internal solution to 7.3-7.4. The osmolarity was 272-295 mOsm.

ACSF used to perfuse slices in the recording chamber always included 2 μM SR95531, a γ-aminobutyric acid $(GABA)_A$ antagonist (Sigma-Aldrich), and 3 μM CGP52432, a $GABA_B$ antagonist (Tocris-Cookson, Bristol, UK) (control conditions).

Where noted, one of the following antagonists or combinations of antagonists (all from Sigma-Aldrich unless otherwise indicated) was also included in the perfusion ACSF and present for the entire duration of recording: the NMDAR antagonists D-2-amino-5-phosphonopentanoate (D-AP5, 50 μM) and MK-801 (20 μM); the group I metabotropic glutamate (mGluR) receptor subtype 1 and subtype 5 antagonists LY367385 (25 μM) and 2-methyl-6-(phenylethynyl)-pyridine (MPEP, 10 μM), respectively (both Tocris-Cookson); or the CB1 receptor antagonist AM251 (600 nM, Tocris-Cookson).

Slice preparation and experimental setup – Rats were anesthetized with halothane, then decapitated. Following decapitation, the brain was rapidly removed and placed in ice-cold ACSF. A blocking cut was made to each hemisphere at 60^{o} to the horizontal plane before mounting with ventral side up. Transverse hippocampal slices, 300 μm thick, were made with a Vibratome 3000 (Ted Pella, Inc., Redding, CA), transferred to a storage chamber, and incubated at 32-35 ^{o}C for 20-30 min. Afterwards, the chamber was maintained at room temperature.

Prior to electrophysiological recordings, slices were transferred to a submerged chamber and maintained at 32-35 ^{o}C by constant perfusion of warmed ACSF, at a rate of approximately 1 mL/s. A Zeiss Axioskop (Oberkochen, Germany) equipped with differential interference contrast (DIC) optics was used in conjunction with a Hamamatsu camera system to visually identify CA1 pyramidal cells. Recording pipettes were fabricated (Flaming/Brown Micropipette Puller, Sutter Instruments, Novato, CA) from thick-walled borosilicate capillary glass (Garner Glass Company, ID = 1.2 ± 0.05 mm,

OD = 2.0 ± 0.05 mm) and filled with the K-gluconate-based internal solution to obtain a 3-5 MΩ open-tip resistance in the bath. Using a motorized micromanipulator (Sutter Instruments), the recording pipette was positioned on a pyramidal cell and negative pressure was applied by mouth suction to form a GΩ seal. Brief pulses of negative pressure were then used to break through the membrane in the patch pipette and achieve whole-cell configuration.

To evoke synaptic responses, an extracellular stimulating pipette, fabricated from borosilicate theta glass (Sutter Instruments) was filled with ACSF and placed (by using a separate motorized micromanipulator, Sutter Instruments) 50-150 μm away from the site of the whole-cell recording in distal SR (near the border of SR and SLM), proximal SR (near the border of SR and stratum pyramidale [SP]), or SO. On the apical dendritic side, the border between SR and SLM was distinguished by the prominent appearance of vertically-oriented dendrites in SR and horizontally-oriented axons in SLM (see Figure 2.1).

Electrophysiological recordings – Whole-cell current-clamp recordings of CA1 pyramidal neurons in rat hippocampal slices were made through patch pipettes containing a silver chloride-coated electrode connected to an amplifier (Dagan BVC-700, Minneapolis, MN). Only cells that had a resting potential between -56 and -70 mV at break-in were used.

A subthreshold synaptic response, evoked by stimulation of one pathway (either PP or SC), was monitored once every 20 seconds. The synaptic stimulus (0.2 ms square

current pulse through the extracellular bipolar electrode; Axon stimulus isolator) was set to elicit excitatory postsynaptic potentials (EPSPs) of 2-5 mV. A 10-minute period (baseline) during which no run-up or run-down of the EPSP amplitude was observed was recorded before the plasticity induction stimulus was given.

To induce synaptic plasticity, 40 pulses at 5 Hz were delivered via the extracellular stimulating electrode (a total of 8 s of stimulation). The strength of the stimulus was increased 2-to-3-fold over that used during the monitoring phase so that action potentials were evoked. At least one action potential was evoked from each pulse, and, in some cases where facilitation occurred, up to 3 action potentials were evoked per pulse.

All neurons were held at membrane potentials between -63 mV and -67 mV for the duration of the recordings. Cells that required more than 250 pA of current to maintain these potentials were excluded from the dataset. Bridge balance and capacitance compensation were monitored and adjusted throughout the duration of each experiment; recordings in which the series resistance exceeded 45 MΩ were excluded from the data set. Cells were generally recorded from for a total of 50-70 minutes.

Data acquisition and statistical analysis – Voltage responses were filtered at 5 kHz, digitized at 50 kHz, and stored via an ITC-16 analog-to-digital converter (Instrutech, Port Washington, NY) on a Dell Dimension PC. All acquisition and analysis procedures were custom programmed in IGOR Pro (Wavemetrics, Lake Oswego, OR). Statistical analyses of group data were performed using one- or two-factor repeated measures ANOVA with

Prism software (GraphPad Software, Inc., San Diego, CA). When a significant main effect was detected with ANOVA tests, Bonferroni's post-hoc correction was applied to determine significance between pairwise comparisons. Unless stated otherwise, average values (either in representative or group data) are the mean of all values collected in 10-minute bins. Error bars are standard deviation (within one cell) or standard error of the mean (group data).

Results

The direction of synaptic plasticity evoked in CA1 is distance-dependent

Whole-cell current clamp recordings of CA1 pyramidal neurons were used to measure EPSPs during low-frequency (0.05 Hz) stimulation of afferent fibers. Only one set of synapses was used in each experiment, recruited separately based on the position of the extracellular stimulating electrode. After recording EPSPs for a 10-minute baseline period, the plasticity-induction stimulus was given, consisting of 40 synaptic pulses at 5 Hz, at a strength sufficient to elicit action potential firing (induction). At SC synapses in distal SR, induction resulted in LTP, as evidenced by a long-lasting increase in the amplitude of the synaptic response (Figure 2.2A). However, at SC synapses in proximal SR and SO, induction resulted in LTD, as evidenced by a long-lasting decrease in the amplitude of the synaptic response (Figure 2.2B,C). These results demonstrate that synapses formed at different distances from the soma exhibit differential induction of synaptic plasticity.

LTP, but not LTD, requires NMDAR activation

The role of the NMDAR in the induction of synaptic plasticity has been well-established (Bliss and Collingridge, 1993). Therefore, we tested whether NMDAR activation was required for the induction of synaptic plasticity at SC synapses by performing experiments in the presence of NMDAR antagonists (50 μM D-AP5, a competitive antagonist, and 20 μM MK-801, a non-competitive antagonist). NMDAR blockade prevented the induction of LTP at SC synapses in distal SR, but did not affect LTD induction at SC synapses in proximal SR (Figure 2.3). This suggests that while a NMDAR-mediated increase in Ca^{2+} may be required for LTP induction, other mechanisms control the induction of LTD.

Blockade of group I mGluR activation converts LTD into LTP

More recently, studies have focused on the roles of mGluR activation in synaptic plasticity. For instance, in CA1, group I mGluRs have been found to be involved in both LTP and LTD induction (Anwyl, 1999). We investigated whether mGluR activation was involved in induction of the synaptic plasticity we observed at SC synapses in CA1 by performing experiments in the presence of antagonists of both subtypes which comprise group I mGluRs (25 μM LY367385 to block subtype 1 [mGluR1], and 10 μM MPEP to block subtype 5 [mGluR5]). Antagonism of group I mGluRs did not affect the plasticity induced at either SC synapses in distal SR or at SC synapses in SO, where LTP and LTD, respectively, were still observed (Figure 2.4A,C). However, at SC synapses in proximal SR, group I mGluR antagonists blocked the induction of LTD. Furthermore, when LTD

was prevented, the induction stimulus resulted in LTP instead (Figure 2.4B). This suggests that group I mGluR activation can differentially influence the induction of synaptic plasticity, depending on where the input impinges upon the dendritic tree, and may therefore act as a molecular switch between LTD and LTP.

LTD induction requires CB1 receptor activation

Endocannabinoids, produced in postsynaptic neurons, form a class of retrograde signaling molecules that can induce short- and long-term synaptic plasticity by modulating neurotransmitter release from presynaptic neurons (Akers et al., 1986). We tested whether endocannabinoid signaling was involved in the induction of synaptic plasticity by performing experiments in the presence of an antagonist for the CB1 receptor (600 nM AM251). The CB1 receptor antagonist blocked LTD induction at SC synapses in proximal SR, but did not prevent LTP induction at SC synapses in distal SR (Figure 2.5). This suggests that LTD may be induced by a long-lasting reduction in glutamate release at SC synapses.

Discussion

We have shown that synapses formed by the same presynaptic fibers but targeting distinct regions of a dendritic tree exhibit differential induction of synaptic plasticity, and that this plasticity is mediated by activation of specific receptors. SC synapses in distal SR exhibit NMDAR-dependent LTP that is insensitive to group I mGluR or CB1 receptor

blockade. Conversely, SC synapses in proximal SR, exhibit CB1 receptor-dependent LTD that is insensitive to NMDAR blockade, but can be converted to LTP in the absence of group I mGluR-mediated signaling. SC synapses in SO also exhibit LTD, but, unlike SC synapses in proximal SR, this is unaffected by blockade of group I mGluRs.

Characteristics that may confer synapse-specific plasticity in CA1 pyramidal neurons

There are several possibilities that may explain the differential effects on synaptic plasticity observed in our experiments. One potential difference is a distance-dependent disparity in the amount of dendritic depolarization evoked by synaptic stimulation. Although there were no differences in the average EPSP amplitude recorded during baseline (SLM = 4.2 ± 0.5 mV; SR = 4.8 ± 0.4 mV; SO = 3.9 ± 0.5 mV; $p = 0.42$, one-factor ANOVA) or the number of somatically generated action potentials during induction (SLM = 73 ± 12; SR = 68 ± 9; SO = 69 ± 15; $p = 0.95$, one-factor ANOVA), a great degree of attenuation, which can be up to 100-fold in computer simulations of CA1 neurons (Golding et al., 2005), occurs as electrical events propagate from distal synapses towards the soma. This powerful attenuation may obscure an accurate reflection of the magnitude of depolarization that occurs at distal synapses, and thus may mask dendritic large local voltage deflections (Magee and Cook, 2000), or possibly dendritic spikes, which may be more efficacious at inducing LTP (Golding et al., 2002).

A second possibility is that location-dependent synaptic plasticity may be conferred by differential subcellular localization of receptors. Our experiments provide some evidence in support of this idea, because group I mGluR antagonists affected the

induction of synaptic plasticity only at proximal SR synapses, while having no effect on plasticity induced at distal SR or SO synapses. Few studies have been aimed at quantitatively determining the distribution of mGluR subtypes in CA1, but the results of one immunohistological experiment suggest that differences in the distribution of group I mGluRs do exist (Shigemoto et al., 1997). Staining for mGluR5 is very intense in SR and SO, but weaker in SLM. Staining for mGluR1 is generally much weaker throughout CA1, although there may be some expression in SR. Thus, the pattern of activation of specific group I mGluR receptor subtypes in different dendritic regions may contribute to differential induction of synaptic plasticity. However, it is likely that other factors, such as the availability of components of intracellular signaling cascades or activation of additional types of receptors (such as the CB1 receptor), are also important because even in regions that appear to have similar group I mGluR expression patterns, differential results were observed after induction (i.e. LTP in distal SR but LTD in proximal SR).

A third alternative is that the sets of fibers targeting different regions of CA1 may arise in different populations of CA3 neurons (or, for example, from different locations along the septal-temporal axis [Amaral and Lavenex, 2007]), and that these have unique presynaptic properties that result in differential induction of synaptic plasticity. Canonically, CB1 receptors are expressed on interneuron terminals and their activation by a retrograde signal inhibits GABAergic neurotransmission (Akers et al., 1986). This pathway can not explain our results, as both $GABA_A$ and $GABA_B$ receptors were blocked throughout the course of our experiments. However, in several brain regions, including the hippocampus, activation of CB1 receptors has been shown to directly inhibit

glutamate release from excitatory presynaptic terminals (Chevaleyre et al., 2006; Németh et al., 2008). Therefore, a possibility that may explain our results is that CB1 receptors are present at terminals of SC fibers targeting CA1 dendrites in proximal SR, but not distal SR. Interestingly, one effect of group I mGluR activation is the production of 2-arachidonoylglycerol (2-AG), via catalysis of diacylglycerol (DAG), which is an endogenous agonist of CB1 receptors (Chevaleyre and Castillo, 2003; Edwards et al., 2006). mGluR-mediated production of a retrograde messenger that acts at CB1 receptors may underlie the mGluR and CB1 receptor-dependent LTD observed at proximal SR synapses.

Taken together, these results suggest that LTP in CA1 pyramidal cells depends on NMDAR activation, possibly to increase depolarization or to trigger dendritic spikes. LTP induction may be overridden by an LTD-inducing process that depends on group I mGluR activation in CA1 neurons. This may be due to a requirement for production of a retrograde signal, such as 2-AG, which acts on CB1 receptors on presynaptic excitatory terminals to reduce glutamate release. In this model, group I mGluRs, CB1 receptors, or both would be restricted to SC synapses in proximal SR (and possibly SO), producing the location-dependent synaptic plasticity we observed.

Location-dependent synaptic plasticity may affect neuronal integration

Neurons in many regions receive convergent input from several distinct neuronal populations, each carrying specialized information. These diverse inputs may be segregated, targeting one area of a dendritic tree, or may be dispersed over the entire

neuronal compartment. Several mechanisms have been proposed by which synapses at different locations may enhance their relative contribution to overall neuronal excitability. For example, increasing the size and/or strength of synapses remote from the soma ("synaptic scaling") may be a way to overcome the powerful attenuation that would otherwise render those synapses ineffective in contributing to action potential generation (Andrasfalvy and Magee, 2001; Nicholson et al., 2006). Another possibility is that certain inputs are more efficacious during particular behavioral states in the presence of specific neuromodulators. For example, cholinergic modulation during awake, alert states may increase the relative contribution of PP synapses because they are less inhibited by muscarinic receptor activation than their SR counterparts (Hasselmo and Schnell, 1994). Likewise, the relative contributions of synapses impinging on the dendritic tree at different locations may be regulated by the level of presynaptic activity. Our experiments suggest that during periods of low activity, when it is likely that less glutamate can diffuse beyond the synaptic cleft to activate mGluR located extrasynaptically. LTP is more easily induced by coincident presynaptic input and postsynaptic output mediated by synapses in proximal SR compared to periods of high activity, when mGluR activation results in LTD induction at these synapses. In this case, the influence of synaptic activation in distal SR would be greatest during periods of relatively high activity, when other inputs are comparatively suppressed.

Our results provide an additional mechanism by which separate inputs may differentially affect neuronal output. We show that synaptic activity may be more effective at inducing distinct forms of synaptic plasticity (LTP or LTD) at specific inputs.

Furthermore, this effect depends on the particular combination of presynaptic and postsynaptic receptors expressed at the synapse. This may represent a universal mechanism by which the relative importance of information from a particular set of inputs is enhanced relative to other inputs targeting the same neuron.

Figures

Figure 2.1 A representative stained CA1 pyramidal neuron in a hippocampal slice.

On the left is an image showing the soma and dendritic arborization of a CA1 pyramidal cell, stained with biocytin. On the right is the same image, with relevant borders depicted. The thin black line denotes the hippocampal fissure, separating CA1 from dentate gyrus (DG). The dashed lines indicate dendritic layers in CA1: stratum lacunosum moleculare (SLM), containing the most distal parts of the apical dendrite where perforant path (PP) synapses are formed; stratum radiatum (SR), containing more proximal regions of the apical dendrite, where Schaffer collateral (SC) synapses are formed; and stratum oriens (SO), containing basal dendrites, also targeted by SC fibers. Stratum pyramidale (SP) forms a tightly packed layer containing CA1 pyramidal cell bodies. The thick black line denotes the border between SO and the alveus, which contains CA1 axon fibers. Note the axon from the stained cell entering the alveus (arrow). Also visible is the border between CA1 and the subiculum (SUB), where pyramidal cell bodies begin to spread out to form a more disperse cellular layer.

Figure 2.1

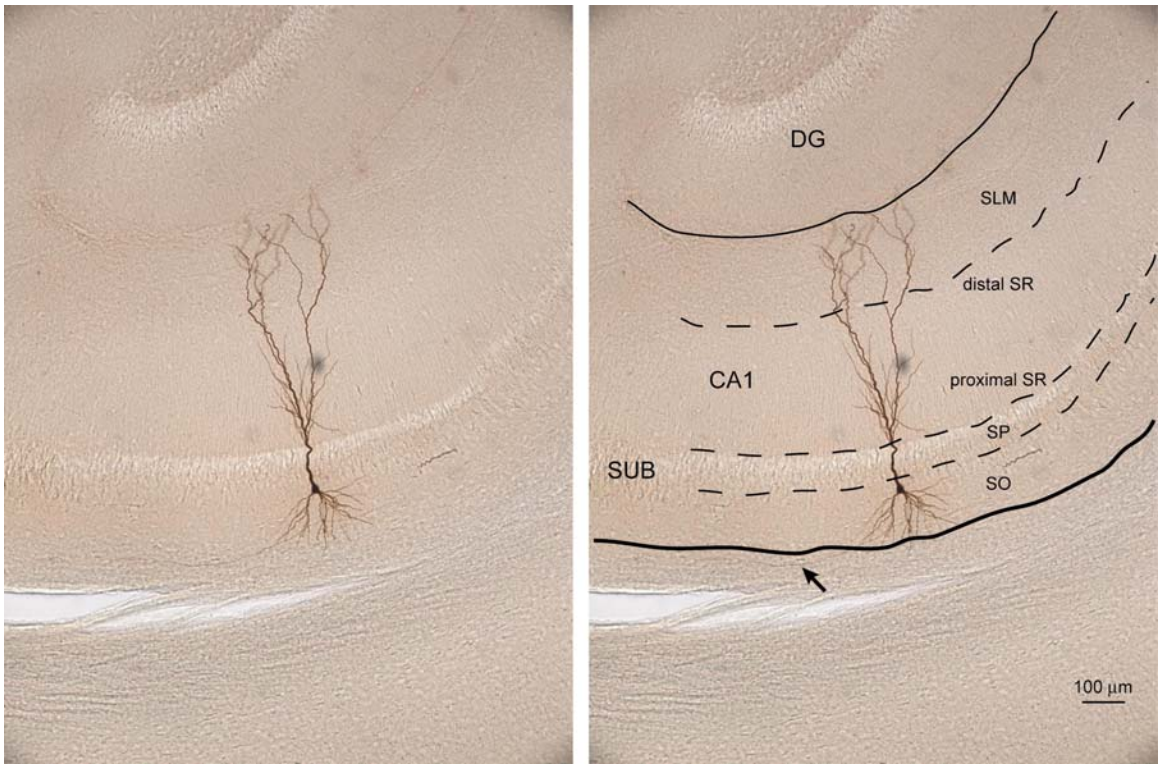

Figure 2.2 Induction results in distance-dependent synaptic plasticity in CA1 pyramidal neurons.

For all panels, graphs on the left show data collected from a representative cell for each configuration, and graphs on the right show the average data for the group. Small open circles (black) are the raw data, while large open circles (red) show the average amplitude (± standard deviation) in 10-minute bins. Filled circles (red) show the average (± s.e.m.) for all cells recorded in the given configuration. Arrows indicate the time at which the plasticity-induction stimulus was given (t = 0 min). Dashed lines represent the amplitude during the baseline period. Significance levels, calculated by a repeated measures ANOVA with Bonferroni post-hoc comparisons, are * = $p < 0.05$, ** = $p < 0.01$, *** = $p < 0.001$. Insets show representative excitatory postsynaptic potentials (EPSPs), recorded before (black) and after (red) induction. The scale bars in A. apply to all insets.
A. Stimulation of Schaffer collateral (SC) synapses in distal stratum radiatum (SR) resulted in long-term potentiation (LTP), evidenced by a long-lasting increase in EPSP amplitude ($n = 6$; $p < 0.0001$, repeated measures ANOVA). **B.** Stimulation of SC synapses in proximal SR resulted in long-term depression (LTD), evidenced by a long-lasting decrease in EPSP amplitude ($n = 8$; $p < 0.01$, repeated measures ANOVA). **C.** Simulation of SC synapses in stratum oriens (SO) resulted in LTD, evidenced by a long-lasting decrease in EPSP amplitude ($n = 6$; $p < 0.0001$, repeated measures ANOVA).

Figure 2.2

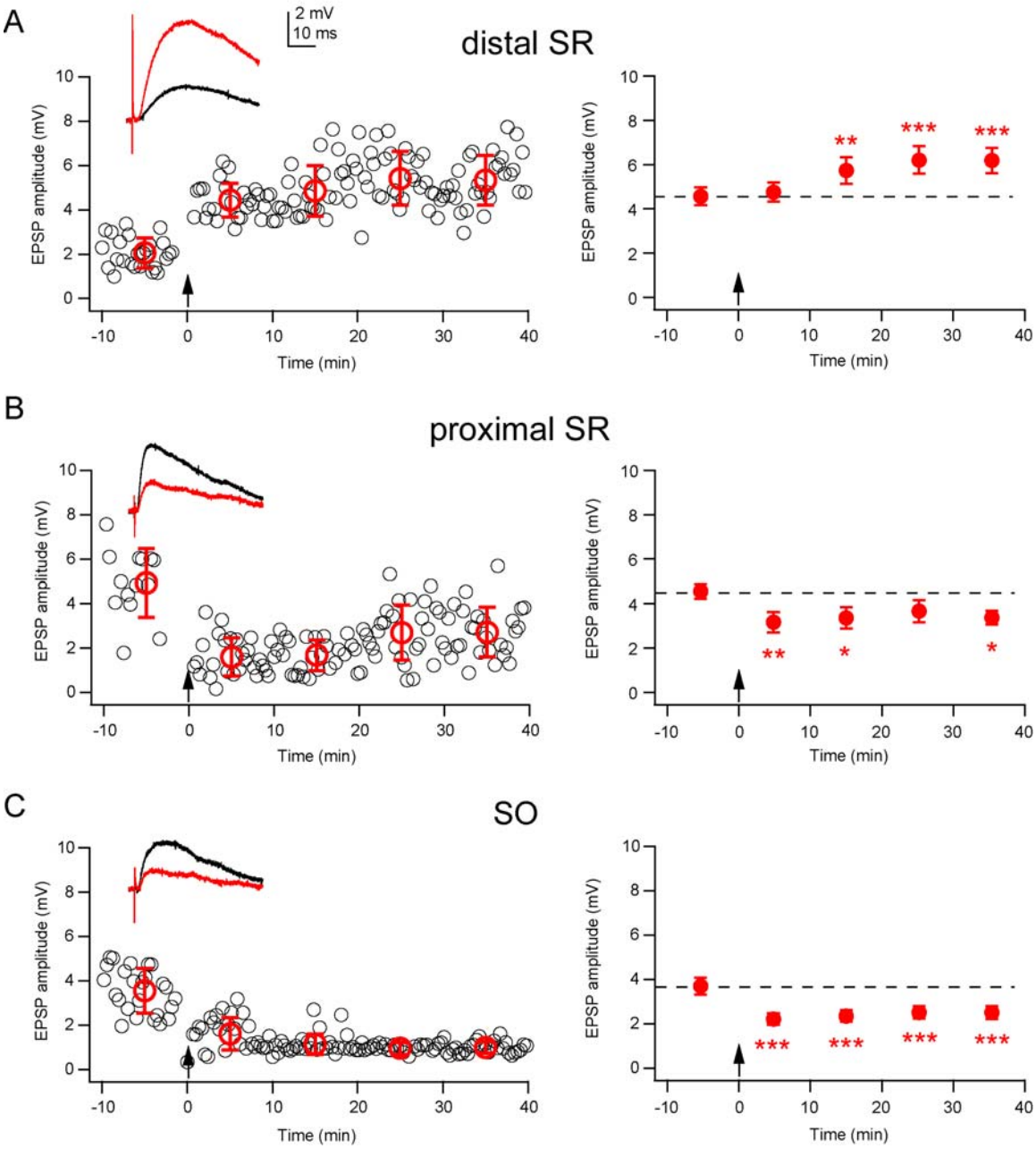
A
2 mV
10 ms
distal SR
EPSP amplitude (mV)
Time (min)
**
***
***
B
proximal SR
EPSP amplitude (mV)
Time (min)
**
*
*
C
SO
EPSP amplitude (mV)
Time (min)
***
***
***
***

Figure 2.3 LTP, but not LTD, at SC synapses in SR requires activation of NMDARs.

Experiments were performed in the presence of N-methyl-D-aspartate (NMDAR) antagonists (50 μM D-AP5 and 20 μM MK-801). For both panels, graphs on the left show data collected from a representative cell for each configuration, and graphs on the right show the average data for the group. Small open circles (black) are the raw data, while large open circles (red) show the average amplitude (± standard deviation) in 10-minute bins. Filled circles (red) show the average (± s.e.m.) for all cells recorded in the given configuration. Arrows indicate the time at which the plasticity-induction stimulus was given (t = 0 min). Dashed lines represent the amplitude during the baseline period. Significance levels, as calculated by a repeated measures ANOVA with Bonferroni post-hoc comparisons, are * = $p < 0.05$. Insets show representative excitatory postsynaptic potentials (EPSPs), recorded before (black) and after (red) induction. The scale bars in A. apply to both insets.

A. Antagonism of NMDARs blocked the induction of long-term potentiation (LTP) at Schaffer collateral (SC) synapses in distal stratum radiatum (SR), as evidenced by the lack of a long-lasting increase in EPSP amplitude ($n = 7$; $p = 0.16$, repeated measures ANOVA). **B.** Antagonism of NMDARs did not affect the induction of synaptic plasticity at SC synapses in proximal SR. As in control conditions, induction resulted in long-term depression (LTD), evidenced by a long-lasting decrease in EPSP amplitude ($n = 5$; $p < 0.05$, repeated measures ANOVA).

Figure 2.3

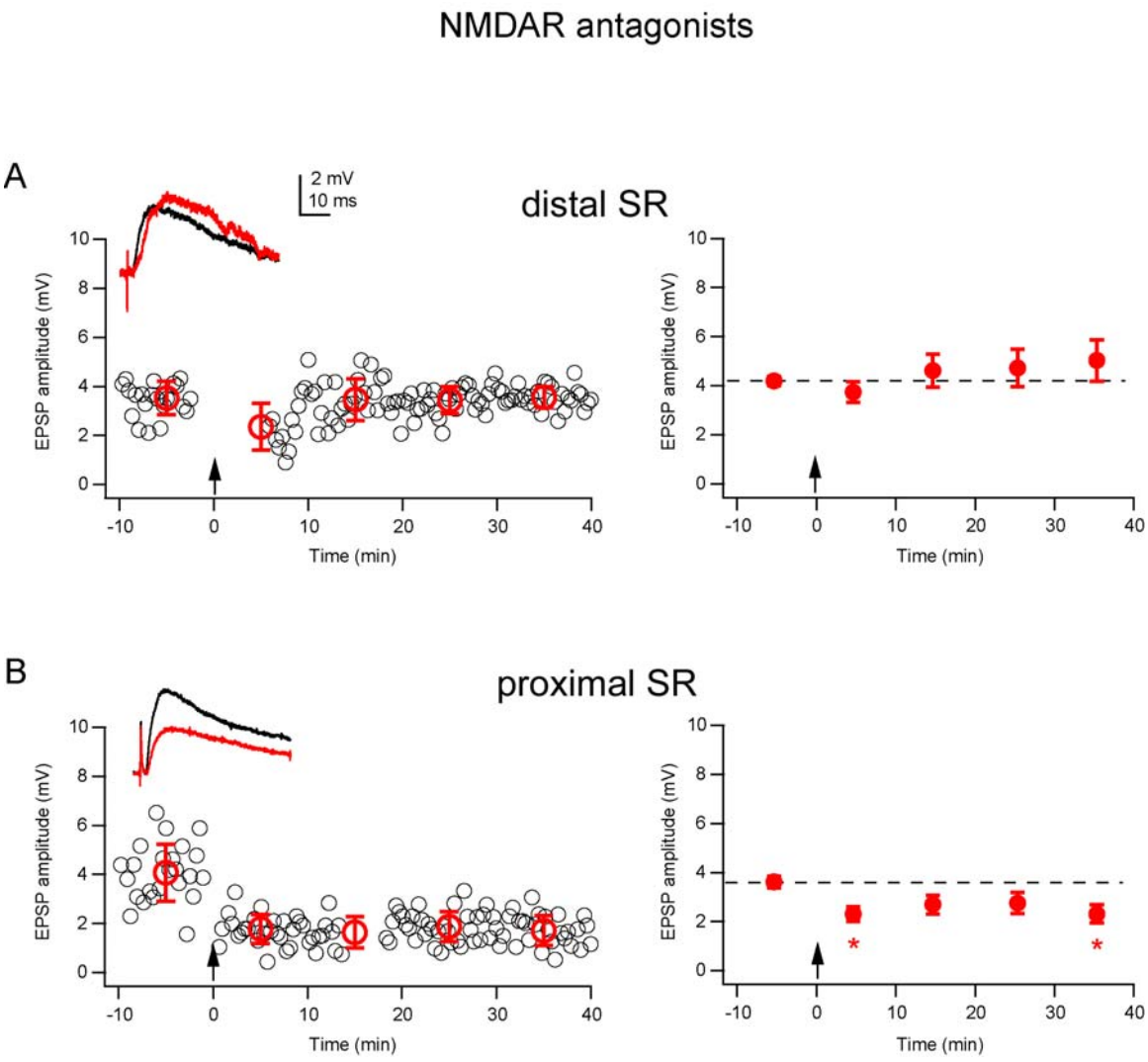
NMDAR antagonists
A
2 mV
10 ms
distal SR
EPSP amplitude (mV)
Time (min)
B
proximal SR
EPSP amplitude (mV)
Time (min)

Figure 2.4 Group I mGluR activation converts LTP into LTD at SC synapses in SR.

Experiments were performed in the presence of antagonists of group I metabotropic glutamate receptors (mGluRs; 25 μM LY367385 and 10 μM MPEP). For all panels, graphs on the left show data collected from a representative cell for each configuration, and graphs on the right show the average data for the group. Small open circles (black) are the raw data, while large open circles (red) show the average amplitude (± standard deviation) in 10-minute bins. Filled circles (red) show the average (± s.e.m.) for all cells recorded in the given configuration. Arrows indicate the time at which the plasticity-induction stimulus was given (t = 0 min). Dashed lines represent the amplitude during the baseline period. Significance levels, as calculated by a repeated measures ANOVA with Bonferroni post-hoc comparisons, are * = $p < 0.05$, ** = $p < 0.01$, and *** = $p < 0.001$. Insets show representative excitatory postsynaptic potentials (EPSPs), recorded before (black) and after (red) induction. The scale bars in A. apply to all insets.

A. Antagonism of group I mGluRs had no affect on the synaptic plasticity induced at Schaffer collateral (SC) synapses in distal stratum radiatum (SR). As in control conditions, induction resulted in long-term potentiation (LTP), evidenced by a long-lasting increase in EPSP amplitude ($n = 6$; $p < 0.01$, repeated measures ANOVA). **B.** Antagonism of group I mGluRs blocked long-term depression (LTD) at SC synapses in proximal SR, evidenced by the lack of a long-lasting decrease in EPSP amplitude that was observed in control conditions. Furthermore, when LTD was prevented, LTP was observed at these synapses ($n = 6$; $p < 0.01$, repeated measures ANOVA). **C.** Antagonism

of group I mGluRs had no effect on the synaptic plasticity induced at SC synapses in stratum oriens (SO). As in control conditions, induction resulted in LTD, evidenced by a long-lasting decrease in EPSP amplitude ($n = 8$; $p < 0.05$, repeated measures ANOVA).

Figure 2.4

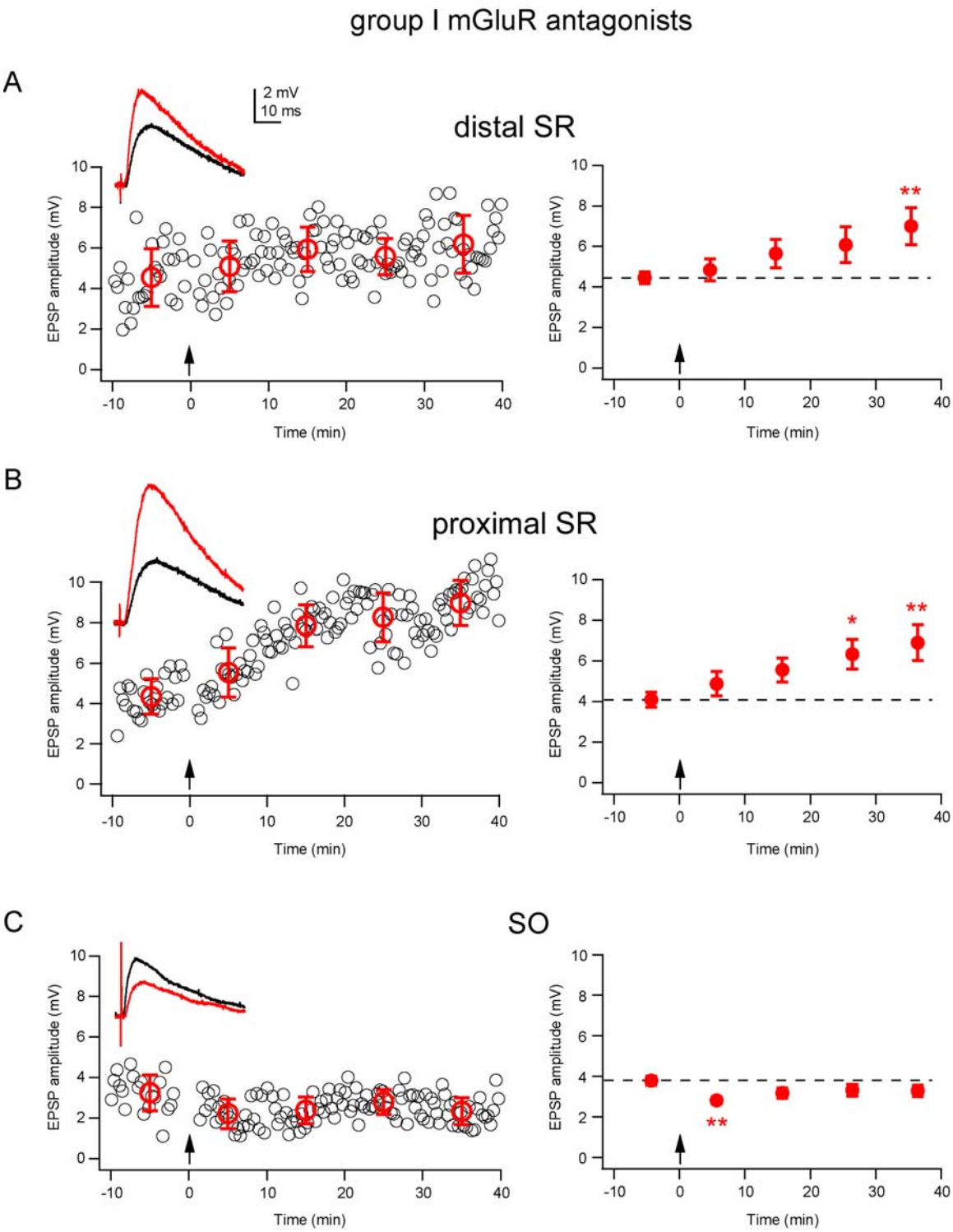
group I mGluR antagonists
A
2 mV
10 ms
distal SR
EPSP amplitude (mV)
Time (min)
**
B
proximal SR
EPSP amplitude (mV)
Time (min)
*
**
C
SO
EPSP amplitude (mV)
Time (min)
**

Figure 2.5 LTD, but not LTP, at SC synapses in SR requires activation of CB1 receptors.

Experiments were performed in the presence of a type 1 cannabinoid (CB1) receptor antagonist (600 nM AM251). For both panels, graphs on the left show data collected from a representative cell for each configuration, and graphs on the right show the average data for the group. Small open circles (black) are the raw data, while large open circles (red) show the average amplitude (± standard deviation) in 10-minute bins. Filled circles (red) show the average (± s.e.m.) for all cells recorded in the given configuration. Arrows indicate the time at which the plasticity-induction stimulus was given (t = 0 min). Dashed lines represent the amplitude during the baseline period. Significance levels, as calculated by a repeated measures ANOVA with Bonferroni post-hoc comparisons, are * = $p < 0.05$, and ** $p < 0.01$. Insets show representative excitatory postsynaptic potentials (EPSPs), recorded before (black) and after (red) induction. The scale bars in A. apply to both insets.

A. Antagonism of CB1 receptors did not affect the induction of synaptic plasticity at Schaffer collateral (SC) synapses in distal stratum radiatum (SR). As in control conditions, induction resulted in long-term potentiation (LTP), evidenced by a long-lasting increase in EPSP amplitude ($n = 5$; $p < 0.01$, repeated measures ANOVA). **B.** Antagonism of CB1 receptors blocked the induction of long-term depression (LTD) at SC synapses in proximal SR, evidenced by the lack of a long-lasting decrease in EPSP amplitude ($n = 6$; $p = 0.35$, repeated measures ANOVA).

Figure 2.5

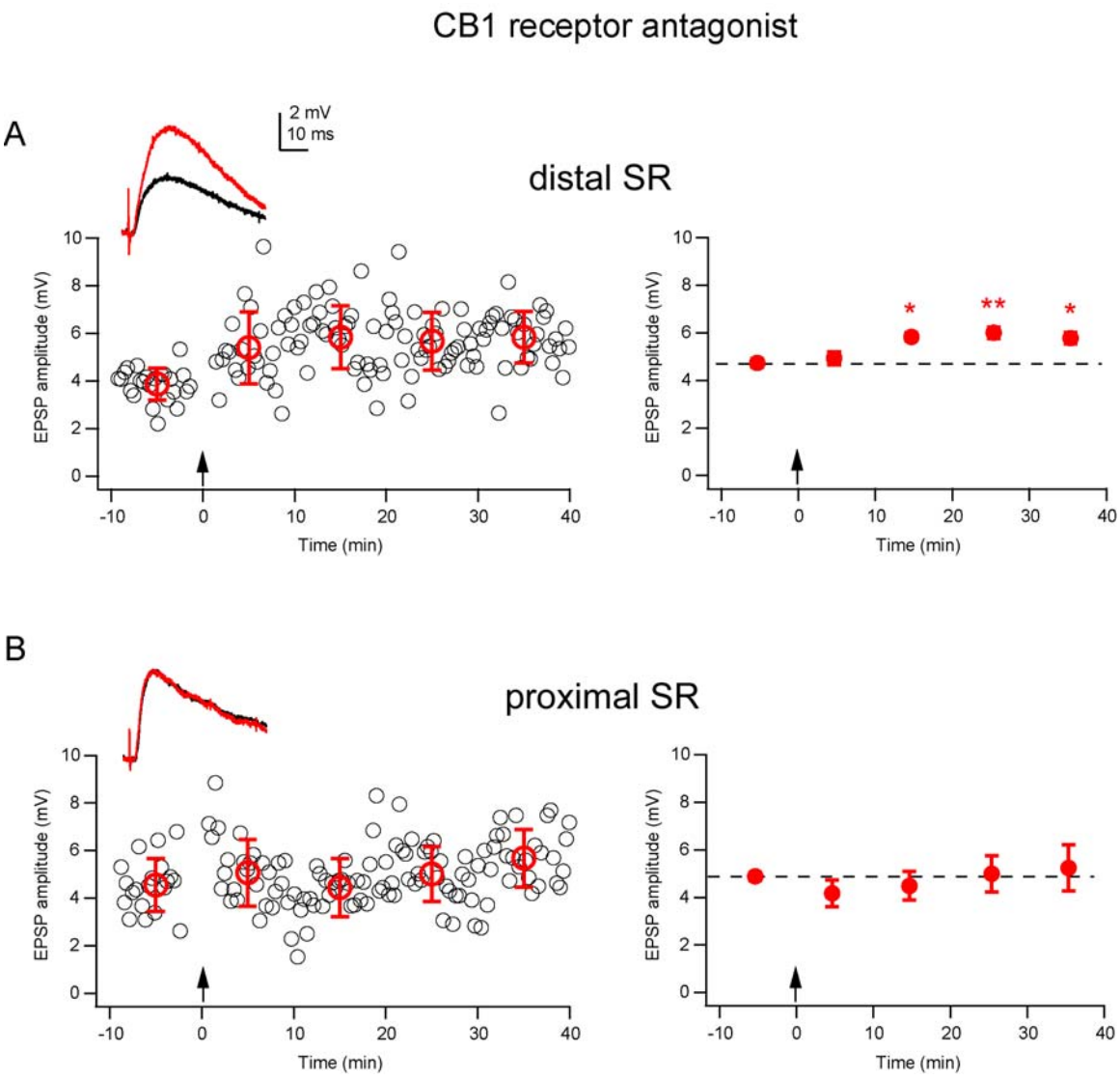
CB1 receptor antagonist
A
2 mV
10 ms
distal SR
EPSP amplitude (mV)
Time (min)
*
**
*
B
proximal SR
EPSP amplitude (mV)
Time (min)

Chapter 3:

Psychostimulant-induced plasticity of intrinsic neuronal excitability in pyramidal neurons of the subiculum

Abstract

Withdrawal from repeated exposure to psychostimulants results in behavioral sensitization as well as long-lasting neuroadaptations, particularly in the mesolimbic reward circuit. These changes may contribute to the transition from drug use to drug abuse. The subiculum provides a strong excitatory input to this reward circuit, and changes in the intrinsic excitability and neuronal output of this region may drive changes in downstream targets, including nucleus accumbens (NAc). Here, we show that long-term (14 days), but not short-term (2 days), withdrawal from five days of amphetamine (AMPH) treatment results in increased locomotor activity in response to a challenge injection of AMPH, compared to saline- (SAL) injected control animals. Conversely, short- but not long-term withdrawal reduces neuronal excitability in subicular pyramidal neurons. This reduced excitability is not observed when AMPH is acutely applied to slices, but can be mimicked by low concentrations of tetrodotoxin (TTX), suggesting that repeated exposure to AMPH results in a transient down-regulation of voltage-gated Na^+ channel function. These findings increase our understanding of the addictive process and may provide novel therapeutic targets for the prevention and treatment of drug abuse.

Introduction

Drugs of abuse have been postulated to assert their addictive effects via powerful activation of the mesolimbic dopamine (DA) system, which is an integral component of the brain reward circuit (Kalivas and Volkow, 2005). Chronic exposure to psychostimulants, such as cocaine and AMPH, produces long-lasting neuroadaptations in this circuit leading to increased dopaminergic neurotransmission, which may underlie the transition from drug use to drug abuse (Robinson and Berridge, 2003). Therefore, determining the nature of these neuroadaptations is an important step in understanding the addictive process and providing therapeutic targets for the treatment and prevention of drug abuse.

The ventral tegmental area (VTA) is the primary source of dopaminergic efferents, which target all other regions of the reward circuit. NAc neurons gate the activity of VTA both directly, through inhibitory projections from medium spiny neurons, and indirectly, via the ventral pallidum, which exerts a tonic inhibitory tone in VTA (Kalivas and Volkow, 2005). NAc neurons, in turn, receive powerful limbic innervation from the subiculum, which constitutes that major output pathway of the hippocampus (Swanson and Cowan, 1977). The subiculum is responsible for controlling NAc output by driving the transition to a depolarized membrane potential, allowing action potentials to be evoked by prefrontal cortical (PFC) input (O'Donnell and Grace, 1995).

Both the NAc and subiculum (particularly ventral regions [vSUB]) are important in mediating reward-related actions and contribute to behavioral responses induced by

psychostimulants. For example, simultaneous *in vivo* recordings demonstrate increased activity in both groups of neurons in response to reward anticipation and reward presentation (Martin and Ono, 2000). In a rat model of cocaine self-administration, selective lesions of the NAc core profoundly attenuated drug-seeking in response to conditioned reinforcers, while lesions of the NAc shell reduced the psychostimulant effects of cocaine (Ito et al., 2004). Likewise, excitotoxic lesions of vSUB decreased cocaine self-administration and attenuated AMPH-induced locomotion (Caine et al., 2001). Furthermore, theta-frequency stimulation of hippocampus resulted in a relapse to drug-seeking in rats that had previously undergone extinction from learned cocaine self-administration (Vorel et al., 2001).

Repeated exposure to psychostimulants has been shown to induce changes in neuronal excitability in NAc neurons. Short-term withdrawal after three days of consecutive cocaine administration resulted in DA D1 receptor-mediated suppression of voltage-gated Na^+ and Ca^{2+} currents (Zhang et al., 1998; Zhang et al., 2002). However, psychostimulant-induced neuroadaptations in the subiculum have not, thus far, been examined. Therefore, the goal of this study was to investigate changes in subthreshold properties and neuronal output of subicular pyramidal neurons, which may profoundly influence the activity of downstream targets, such as NAc, in the brain reward circuit.

Methods

Animals and AMPH administration - All animal procedures were approved by the Northwestern University Animal Care and Use Committee. Male Wistar rats, aged 25-50

days, were used for all experiments. Animals were colony housed on a 12-hour light/dark cycle with free access to food and water. Rats received five daily subcutaneous injections of SAL (1 ml/kg) or AMPH (2.5 mg/kg). At an early withdrawal (EW, 2 days) or late withdrawal (LW, 14 days) time, rats either received an AMPH challenge injection (2.5 mg/kg; for behavioral testing) or were sacrificed with no test injection given (for electrophysiological experiments).

Behavioral testing and analysis - Rats were screened for their baseline locomotor activity in a testing apparatus (34 x 34 inch) for 30 min 1 week before beginning drug treatment. Behavioral sensitization was assessed at EW and LW. On these days, rats were habituated to the test apparatus for 30 min before an AMPH challenge injection (2.5 mg/kg). Stereotyped behaviors were scored by trained observers blind to treatment conditions using procedures previously established (Wolf et al., 1995; Li et al., 1997). Briefly, rats (eight with previous SAL treatment and eight with previous AMPH treatment) were manually scored in sequential 25 s intervals for 2 hours on withdrawal days 2 and 14. Individual rearing bouts and stereotyped continuous rearing and grooming were scored as events if they occurred during the 25 s observation period for each rat. Individual rearing bouts were counted each time both forelimbs were raised off the surface. Grooming bouts were scored if they lasted >10 s. Continuous rearing was counted if both forelimbs were raised off the surface of the test apparatus for the entire 25-s scoring period.

Slice preparation - For EW (36- to 42-day-old rats) and LW (42- to 50-day-old rats), transverse slices hippocampal slices were prepared. Rats were anesthetized with

halothane and intracardially perfused with ice-cold artificial cerebrospinal fluid (ACSF). After approximately 30 s - 1 min, the brain was removed, bisected into hemispheres and mounted at a 60° angle to the horizontal plane using superglue. Slices (300 μm) were cut using a Vibratome (Leica, Nussloch, Germany). These slices were then incubated in a chamber containing warm (34-35°C) ACSF for 20-40 min, after which they were maintained at room temperature. For recording, slices were transferred to a chamber on a fixed stage of a Zeiss Axioscop (Oberkochen, Germany) equipped with differential interference contrast (DIC) optics. Recordings were obtained under visual control using a Dage-MTI (Michigan City, IN) or Hamamatsu (Hamamatsu City, Japan) camera. All experiments were performed during continuous perfusion with ACSF at 32-35°C.

Histological procedures - After recording, the slices were placed in paraformaldehyde (4%) and refrigerated at 4°C for <2 weeks before processing. We stained the biocytin-filled cells using an avidin–horseradish peroxidase reaction with the Vectastain ABC Kit (Vector Labs, Burlingame, CA). Processed slices were mounted on microscope slides using Mowiol. Neuron reconstructions were performed using a Neurolucida system (MicroBrightField, Inc., Williston, VT) and a Leica microscope with a 63x oil immersion objective.

Solutions and drugs - ACSF consisted of (in mM): 125 NaCl, 25 glucose, 25 $NaHCO_3$, 2.5 KCl, 1.25 NaH_2PO_4, 2 $CaCl_2$, and 1 $MgCl_2$, pH 7.2-7.4 (bubbled with 95% O_2 and 5% CO_2). For most experiments, synaptic activity was blocked using a mixture of kynurenic

acid (2.5 mM, to block α-amino-3-hydroxy-5-methyl-4-isoxazolepropionic acid [AMPA] and N-methyl-D-aspartate [NMDA] receptors), SR 95531 (2-4 μM, to block γ-aminobutyric acid $[GABA]_A$ receptors), and atropine (1 μM, to block muscarinic acetylcholinergic receptors [mAChRs]). For experiments involving synaptic stimulation, MK-801 (20 μM, to block NMDA receptors), SR 95531 (2 μM), and CGP 55845(1 μM, to block $GABA_B$ receptors) were included in the bath. The intracellular solution for whole-cell recordings contained (in mM): 115 K-gluconate, 20 KCl, 10 Na_2-phosphocreatine, 10 HEPES, 2 Mg-ATP, and 0.3 Na-GTP, pH 7.3, and 0.1% biocytin (for subsequent morphological identification). All chemicals were purchased from Sigma/RBI (St. Louis, MO).

Electrophysiological recordings - Whole-cell current-clamp recordings were made from the soma of visually identified subicular pyramidal neurons using a BVC-700 amplifier (Dagan, Minneapolis, MN). Patch-clamp electrodes were fabricated from thick-walled borosilicate glass and fire polished to resistances of 3-5 MΩ in the bath. Data were stored on a Power Macintosh G4 (Apple Computers, Cupertino, CA) or Dell Inspiron (Round Rock, TX) computer via an ITC-16 interface (Instrutech, Port Washington, NY). Data acquisition and analysis were performed using custom macros running under Igor Pro (WaveMetrics, Lake Oswego, OR). Voltage was filtered at 5 kHz and digitized at 20 kHz.

In most cases, a somatic current injection designed to mimic synaptically evoked current was used (compare synaptically and current-evoked responses in Figure 3.4). This simulated excitatory postsynaptic current (sEPSC; τ_{rise}=0.2 ms, τ_{decay}= 6 ms) was used to classify subicular neurons as either burst spiking (BS) or regular spiking (RS) because it

is a more physiologically relevant stimulus than a long square pulse. The sEPSC injection was increased in amplitude from 100 to 2000 pA until either a single action potential (RS cells) or a burst of action potentials (BS cells) was elicited. The amount of current necessary to evoke firing was defined as the rheobase for that cell. In RS neurons, we continued to inject larger amplitude sEPSCs (in 100 pA increments) until the cell fired a burst of action potentials. This was considered to be the "burst threshold" for RS cells. In all cases, the sEPSC injection was followed 400 ms later by a 5 ms square step pulse (at half the current amplitude used for the sEPSC injection) to verify accurate bridge balance and capacitance compensation.

For synaptic stimulation, a stimulating electrode was placed in stratum radiatum (SR) in the CA1 region of the hippocampus. The current pulse was adjusted in strength to evoke a 3-5 mV excitatory postsynaptic potential (EPSP) at the soma when the cell was held at -67 mV. This synaptic stimulus was not altered throughout the duration of the recordings to avoid confounds caused by changing stimulus intensity or duration. Current was injected via the amplifier to test neuronal responses across a range of membrane potentials, from -75 to -50 mV or until the cell fired.

Data analysis - Data analysis was performed using IGOR Pro 4.0. To calculate the voltage-dependent variation in the membrane potential, we used the average deviation of 7 sec duration traces with no action potentials present. The average power spectra were calculated for 7 sec traces using a Hamming window. Traces were de-trended using a cubic polynomial fit of the raw data that was subtracted from each trace before

performing the power spectral density analysis to eliminate low-frequency (< 0.1 Hz) DC drift in the recording. With use of either a 600-ms square or sEPSC injection, action potential thresholds were determined by calculating the first derivative (dV/dt) and setting a rate of rise of 30 mV/ms as the criteria for the non-linear inflection point, signifying the beginning of the action potential. The amplitudes of synaptically evoked EPSPs and EPSP-like (sEPSPs) responses to sEPSC injections were calculated as the maximum voltage reached within 25 ms from synaptic stimulation or sEPSC injection. The integrals of EPSPs and sEPSPs were calculated by differentiating the voltage trace and performing trapezoidal integration. The integral calculation began at the time of the maximum amplitude of the voltage deflection and ended when the voltage had decayed back to the prestimulus level. At least six traces were collected and averaged at each holding potential.

Statistics for two groups were performed using paired or unpaired Student's two-tailed t tests on normally distributed data and two-tailed U tests for non-normally distributed data. For multiple groups we used ANOVA with or without repeated measures. *Post hoc* analysis was performed using a Bonferroni corrected *t* test. All analyses were performed on raw data. No more than two cells were used from each rat.

Results

Withdrawal from AMPH produces behavioral sensitization

One effect of repeated exposure to psychostimulants is the development of sensitization, which manifests as an augmented response to drug presentation compared

to that displayed by drug-naïve animals (Segal and Mandell, 1974). This property is thought to contribute to the addictive properties of drugs of abuse, and can be used as an indication of the development of drug addiction (Robinson and Berridge, 2003). We used an established dosing regimen to induce behavioral sensitization of locomotor responses in adult male rats (Wolf et al., 1995). Following five daily subcutaneous injections of SAL or AMPH, rats were tested at 2 (EW) or 14 (LW) days of withdrawal for behavioral responses to a challenge injection of AMPH. The AMPH-treated group displayed increased stereotyped continuous rearing compared to the SAL-treated group at the LW but not EW (stereotypy scores: SAL/EW = 1.3 ± 0.4 (n = 8), AMPH/EW = 2.3 ± 0.6 (n = 8), $p = 0.12$; SAL/LW = 0.6 ± 0.4 (n = 8), AMPH/LW = 3.1 ± 1.1 (n = 8); $p < 0.05$). This result demonstrates that the development and expression of behavioral sensitization occurs not after acute withdrawal from AMPH, but develops over an extended period of time.

Electrophysiology of subicular pyramidal neurons after withdrawal from AMPH

Electrophysiological experiments were performed in slices made from separate groups of rats, subjected to repeated SAL or AMPH treatment, at EW and LW. To avoid possible confounds of AMPH treatment and withdrawal on synaptic drive or response, we determined the electrophysiological characteristics of subicular pyramidal neurons in the presence of antagonists of excitatory (AMPA- and NMDA-mediated), inhibitory ($GABA_A$-mediated), and modulatory (mAChR-mediated) neurotransmission (see Methods). Subicular pyramidal neurons were classified as RS (53%) or BS (47%) on the

basis of the response elicited by just-above threshold, brief somatic current injection (sEPSC). This current injection was designed to mimic the time course of an excitatory postsynaptic current (EPSC) because it represents a more physiologically relevant stimulus than a square current injection. As a result, cells that were classified as weak-burst firing in our previous study (one burst before switching to single action potentials in response to a 1-s long square current injection; Staff et al., 2000) typically emitted single action potentials in response to sEPSCs, and were therefore classified as RS. However, when the amplitude of the sEPSC was increased 30 - 100%, burst firing could also be elicited in these neurons (Figure 3.1).

We found that the numbers of RS and BS neurons in the AMPH and SAL groups at the EW or LW time points were not different, indicating that neither treatment paradigm shifted the proportion of firing patterns in the subiculum. Furthermore, there were no differences in membrane potential or input resistance between any of these groups (Figure 3.2; Table 3.1).

Subthreshold neuronal excitability is reduced at EW, but not LW, from repeated AMPH

Subthreshold activation of voltage-gated Na^+ channels produces membrane-voltage fluctuations, which have the greatest magnitude near threshold (Mattia et al., 1997). We investigated the effects of EW and LW from repeated AMPH by recording these fluctuations, in the presence of antagonists from synaptic transmission, at a range of membrane holding potentials, from -70 to -50 mV, or until action potentials were evoked (Figure 3.3). In both RS and BS, there was a strong, non-linear effect of holding potential

on the peak-to-peak voltage deviation, such that the magnitude of the fluctuations was greatest at the most depolarized membrane voltages. This effect was almost completely blocked by application of TTX (Figure 3.3A), indicating that voltage-dependent activation of Na^+ channels mediates a large component of near-threshold membrane-voltage fluctuations. An analysis of the power spectra revealed a dominant frequency of 3 Hz in the fluctuations, which was not altered with TTX application (although the magnitude of the peak decreased; Figure 3.3B). Because there was no difference between RS and BS in the magnitude of membrane-voltage fluctuations (Figure 3.3C,D), they were combined for subsequent analysis of the effect of AMPH treatment. Short-term withdrawal from AMPH (EW time point) reduced the magnitude of membrane-voltage fluctuations compared to SAL-treated animals (Figure 3.3E), but at the LW time point, there was no difference between AMPH-treated and SAL-treated groups (Figure 3.3F). In all groups, voltage-dependent membrane fluctuations were reduced by application of a TTX (Figure 3.3E,F). Taken together, these results suggest that EW from repeated AMPH reduces, but does not eliminate, voltage-dependent fluctuations of membrane potential in subicular pyramidal neurons, potentially by down-regulating Na^+ channel activity.

In neocortical neurons, synaptic inputs and small somatic current pulses are amplified as a result of subthreshold activation of voltage-gated Na^+ channels (Thomson et al., 1988; Deisz et al., 1991). Synaptic stimulation of SR in CA1, in the presence of NMDA, $GABA_A$, and $GABA_B$ receptor antagonists, produced EPSPs in both RS and BS subicular pyramidal neurons. When these neurons were held at membrane potentials near

threshold, both the amplitude and integral of synaptically evoked EPSPs were profoundly amplified, and these non-linear increases were blocked by application of a low concentration of TTX (Figure 3.4). For comparison, we also examined the effect of membrane holding potential on the response to a sEPSC injection (a sEPSP). Like synaptically-evoked responses, the amplitude and integral of sEPSPs exhibited a strong TTX-sensitive increase at membrane potentials close to threshold. In fact, the magnitudes of these effects were indistinguishable from those observed for EPSPs (Figure 3.4). To examine the consequence of AMPH treatment on amplification of near-threshold inputs, we used sEPSC injections, which avoid the potential confound of AMPH-induced changes in synaptic drive or strength. At the EW time point, AMPH treatment reduced the voltage-dependent amplification of both the amplitude and integral of the sEPSP compared to the SAL-treated group (Figure 3.5A-C). At the LW time point, neither the amplitude nor the integral of the sEPSP was different in the AMPH- and SAL-treated groups (Figure 3.5D). Taken together, these results demonstrate that AMPH induces a transient reduction, but not elimination, of membrane potential-dependent amplification of subthreshold excitatory inputs in subicular pyramidal neurons.

Suprathreshold neuronal excitability is reduced at EW, but not LW, from repeated AMPH

We investigated the effects of withdrawal from repeated AMPH on suprathreshold properties by evoking action potential firing with either a 600-ms square current or a sEPSC injection, and measuring action potential threshold, amplitude, and rise rate. These parameters were not different between RS and BS neurons from rats that

received the same drug treatment paradigm (data not shown), so these cells were pooled to compare the effects of AMPH or SAL treatment at EW or LW time points. Neurons in the AMPH/EW group exhibited reduced neuronal excitability compared to the SAL/EW group. This decreased excitability was characterized by a slower rate of action potential rise (dV/dt), a depolarization of action potential threshold, and a reduction in action potential amplitude (Figure 3.6). Additionally, RS neurons in the AMPH/EW group required a larger amplitude sEPSC injection to fire a burst relative to RS neurons in the SAL/EW group (Table 3.1). However, at the LW time point, none of these parameters were different between the AMPH- and SAL-treated groups (Figure 3.6A-C), indicating that short-term withdrawal from repeated AMPH transiently increases suprathreshold neuronal excitability of subicular pyramidal neurons.

Acute application of AMPH does not induce changes in neuronal excitability

One possible explanation for the reduced neuronal excitability observed in the AMPH-treated group is that the changes are simply due to acute exposure to the drug. To test for this effect, we examined subthreshold and suprathreshold properties in RS and BS subicular pyramidal neurons before and 20 minutes after exposure to AMPH in slices from drug-naïve rats (Figure 3.7). Because responses from RS and BS neurons were not different on any of these measures (data not shown), the data from all cells were combined for subsequent analysis. Subthreshold measures, including the peak-to-peak deviation of membrane voltage fluctuations (Figure 3.7A), and the amplitude and integral of the sEPSP (Figure 3.7C,B), all exhibited a pronounced dependence on voltage. As the

holding potential was progressively depolarized, the magnitude of each of these parameters increased non-linearly. However, acute application of AMPH did not alter the effect of holding potential on any of these parameters (Figure 3.7A-C). Additionally, the effect of acute AMPH application on suprathreshold measures, including rheobase and action potential threshold in response to a sEPSC injection, was investigated. Again, 20 minutes of exposure to AMPH had no affect on either of these parameters (Figure 3.7D). Taken together, these results indicate that reduced neuronal excitability induced by withdrawal from repeated drug treatment is not mediated by acute exposure to AMPH.

Spike timing is disrupted in BS, but not RS, at EW, but not LW, from repeated AMPH

In recordings from lateral geniculate neurons of a cat, the presentation of a visual cue elicits a neuronal response with a shorter latency during burst firing than during tonic (regular) firing, suggesting that bursts are triggered more precisely and immediately by a stimulus than single action potentials (Guido and Sherman, 1998). Therefore, we examined the latency of the spiking response elicited by a sEPSC injection in RS and BS neurons from SAL-treated rats (Figure 3.8). Cells were held at a membrane potential close to threshold (approximately -60 mV) and a sEPSC just large enough to elicit one action potential (RS) or burst (BS) was somatically injected. Analysis showed that, on average, RS displayed a longer latency to action potential generation than BS (Figure 3.8A). Furthermore, the variability in latencies observed for all RS neurons was greater than the variability observed for all BS neurons, indicating that burst spiking is more time-locked to the stimulus than regular spiking. This difference was not a result of

differences in holding potential between these two populations of neurons because there was no correlation between holding potential and latency in either group (Figure 3.8B). Although there was not a difference in the average action potential threshold between RS and BS neurons, there was a significant correlation between threshold and latency in both groups (Figure 3.8B). These results demonstrate, across all cells, a more depolarized action potential threshold increases the latency to for a stimulus to evoke action potential firing, but that this change is not responsible for the longer latency observed in RS neurons compared to BS neurons. Therefore, the intrinsic conductances that contribute to the subthreshold membrane potential preceding action potential generation (such as voltage-gated Na^+ and K^+ channels) must be less efficacious at producing a net depolarization sufficient to reach threshold. Together, this suggests that action potential threshold is independent of holding potential, and that an elevated threshold tends to increase latency to firing in both RS and BS.

We next examined whether withdrawal from repeated AMPH treatment could alter the latencies observed in RS and BS neurons. There was no effect of AMPH treatment at either EW or LW on action potential latency for RS neurons (Figure 3.9A). However, in BS neurons, short-term withdrawal from repeated AMPH (AMPH/EW) increased the average latency for action potential generation (Figure 3.9B). This increased latency was not observed in BS neurons at LW time points (AMPH/LW), when the average latency was indistinguishable from that observed in the SAL-treated group. These results demonstrate that short-term withdrawal from repeated AMPH treatment

selectively increases the average latency to firing in BS neurons, and suggests that this effect may be due to an AMPH-mediated elevation of action potential threshold.

Decreased Na^+ channel availability recapitulates decreased neuronal excitability observed after withdrawal from repeated AMPH

Taken together, our experiments indicate that short-term withdrawal from repeated AMPH treatment results in decreased subthreshold and suprathreshold neuronal excitability, which may be mediated via a reduction in voltage-gated Na^+ channel activity. Therefore, we hypothesized that the effects observed in the AMPH/EW group would be mimicked by application of a low concentration of TTX, which slightly reduces Na^+ channel availability. We continuously monitored sEPSP amplification, action potential threshold, and spike latency once every 10 seconds (0.1 Hz) as TTX was perfused into the bath. This protocol had the advantage of allowing gradual changes in neuronal excitability to be detected as the TTX concentration in the bath steadily increased (reaching 500 nM at steady-state, which completely inhibited all action potential firing). Under these conditions, a minimal decrease in Na^+ channel availability resulted in decreased sEPSP amplification, increased action potential threshold, and increased latency to spike generation (Figure 3.10), as well as decreased near-threshold membrane voltage oscillations (data not shown). These results are in good accordance with data obtained following short-term withdrawal from repeated AMPH, suggesting that this treatment is sufficient to decrease Na^+ channel function, leading to decreased neuronal excitability in subicular pyramidal neurons.

Discussion

Our experiments demonstrate that, in rats, long-term (14 day) withdrawal from repeated exposure to AMPH results in locomotor sensitization, expressed as an increase in stereotyped behaviors (such as grooming and rearing) compared to SAL-treated rats, in response to a challenge injection of AMPH. This enhanced behavioral response is not observed after short-term (2 day) withdrawal, suggesting that sensitization develops over time in the absence of the drug. Conversely, short-term, but not long-term, withdrawal from repeated AMPH induced changes in subthreshold neuronal excitability and suprathreshold neuronal output of subicular pyramidal neurons, which serve as the interface between the memory and reward circuits in the brain. Decreased neuronal excitability was reflected by a reduction in near-threshold membrane voltage fluctuations and reduced amplification of synaptic and somatic subthreshold inputs. Decreased neuronal output was reflected by an elevated action potential threshold, a reduced action potential amplitude, and a slower rate of rise for the action potential. Furthermore, the latency for spike firing in BS neurons, which is usually short and has little variability, was significantly increased, which could lead to disruptions in spike timing of subicular output. These effects could be mimicked by a low concentration of TTX, but not by acute application of AMPH, suggesting withdrawal from repeated AMPH reduces voltage-gated Na^+ channel availability. Taken together, our results demonstrate that withdrawal from repeated AMPH rapidly but transiently decreases neuronal excitability in the subiculum, which may be related to the development of behavioral sensitization, and contribute to the transition from drug use to drug addiction.

Mechanisms of psychostimulant-induced plasticity of intrinsic neuronal excitability

AMPH increases dopaminergic neurotransmission both by reversing the DA transporter (DAT) on dopaminergic terminals (Jones et al., 1998), resulting in stimulus-independent release, and by preventing reuptake of released DA (Heikkila et al., 1975a; Heikkila et al., 1975b). DA has been implicated in mediating or modulating synaptic plasticity in a variety of brain regions, including the prefrontal cortex and hippocampus (Jay and Witter, 1991). The AMPH-induced reduction in neuronal excitability in the subiculum may be caused by enhanced dopaminergic signaling, DA-mediated synaptic changes in afferent input, or both. However, the expression of decreased neuronal excitability is clearly postsynaptic, as it was observed in the presence of antagonists of excitatory and inhibitory neurotransmission, as well as with purely postsynaptic stimulation (sEPSC injections). It appears that decreased neuronal excitability in the subiculum is mediated by a reduction of voltage-gated Na^+ channel activity, because submaximal concentrations of TTX were able to reproduce the effects induced by short-term withdrawal from repeated AMPH treatment.

Similar results, including an elevated action potential threshold and a reduction in action potential amplitude, have been observed in nucleus accumbens (NAc) medium spiny neurons after short-term (1-3 day) withdrawal from repeated cocaine treatment (Zhang et al., 1998). Further, voltage-clamp recordings from these neurons showed decreased whole-cell Na^+ currents (Zhang et al., 1998). Cocaine increases dopaminergic transmission by inhibiting reuptake at dopaminergic terminals (Heikkila et al., 1975a; Ritz et al., 1987). Stimulation of DA D1 receptors activates protein kinase A (PKA),

which can phosphorylate Na^+ channels. Phosphorylation of Na^+ channels results in decreased activity, possibly by increasing the proportion of Na^+ channels in the slow-inactivated state (Carr et al., 2003). Interestingly, the D1/PKA-mediated reduction in Na^+ current has been shown to be voltage-dependent, with a greater degree of inhibition at more depolarized potentials (Cantrell et al., 1999), paralleling the voltage-dependent reduction in neuronal excitability observed after short-term withdrawal from AMPH. Therefore, a possible mechanism underlying the AMPH-mediated decrease in neuronal excitability is an upregulation of PKA signaling by repeated AMPH exposure, leading to increased Na^+ channel phosphorylation, which may drive a larger proportion of Na^+ channels into a slow-inactivated state. This hypothesis could be tested by using specific PKA inhibitors in the internal recording solution, or, more directly, by mutating the amino acids in the Na^+ channel which serve as the targets for PKA-mediated phosphorylation (Murphy et al., 1993).

Effects of AMPH-induced plasticity on information processing in the subiculum

Under physiological conditions, stimulation of glutamatergic subicular efferents increases the excitability of target structures, such as NAc (Finch, 1996). For example, stimulation of subiculum has been shown to drive medium spiny neurons into prolonged (~200-500 ms), depolarized (but subthreshold) “up” states. Cortical projections can only elicit action potential firing from these up states, making subicular afferents critically responsible for gating input to NAc (O'Donnell and Grace, 1995). Therefore, reduced

subicular neuronal excitability may result in diminished ability for NAc neurons to respond to input, leading to disruptions in DA-mediated behaviors.

The precise (ms) timing of coordinated pre- and postsynaptic activity has been shown, in some cases, to determine the direction and magnitude of synaptic plasticity (spike-timing dependent plasticity [STDP]) (Bi and Poo, 1998). After short-term withdrawal from repeated AMPH, we observed a significant decrease in the latency to generate action potentials in BS neurons. This may result in inappropriately timed responses to excitatory drive, which could change the polarity or magnitude of plasticity induced at synapses onto subicular neurons. Furthermore, cooperative or associative plasticity at synapses between the subiculum and its downstream targets, which is potentially important for learning associations, may be strongly reduced in the absence of appropriate synchrony, particularly because burst firing is thought to be important in signaling salient stimuli in the environment (Heien and Wightman, 2006). In addition to the importance of relative timing, the strength of the synaptic input (reflected by the amplitude of the response) also influences the induction of synaptic plasticity. For example, weak synaptic input, with appropriate timing, fails to induce long-term potentiation (LTP), but an additional somatic (postsynaptic) current injection that boosts the EPSP only a few millivolts rescues LTP induction (Sjostrom et al., 2001). Near-threshold membrane voltage fluctuations or voltage-dependent amplification of EPSPs could provide the necessary boosting of synaptic input to permit the induction of LTP. Our finding that withdrawal from repeated AMPH decreases postsynaptic excitability

suggests a novel mechanism by which subicular-dependent associative learning may be impaired.

Behavioral consequences of AMPH-mediated plasticity in subicular neurons

Long-term use of psychostimulants leads to a host of behavioral effects, including sensitized responses to drug presentation, disruptions in associative learning, and impaired dopaminergic neurotransmission (Wise, 1998). In humans, repeated exposure to psychostimulants can induce long-lasting behavioral sensitization associated with addiction and psychosis, such as the development of schizophrenia (Robinson and Berridge, 2003). Our results, in agreement with other reports (Paulson and Robinson, 1991; Wolf et al., 1995), show that long-term withdrawal from repeated AMPH treatment produces behavioral sensitization of locomotor responses. Because AMPH-induced changes in neuronal excitability of subicular neurons were limited to EW time points, this plasticity may contribute to the induction of behavioral sensitization, but is not involved in expression.

Short-term withdrawal from AMPH produces a decline in the ability to learn conditioned associations (Murphy et al., 1993). Selective lesions of vSUB also impair conditioned learning, and disrupt behavioral responses to psychostimulants (Caine et al., 2001). These impairments are reversed by DA antagonists and are exacerbated by AMPH (Caine et al., 2001; Russig et al., 2003). Thus, it appears that precise regulation of dopaminergic tone and activity of the subiculum, particularly vSUB, is critical for proper associative learning.

In a spatial location task, synchronous firing of subicular and NAc neurons predicted anticipation of a reward presentation (Martin and Ono, 2000). Direct stimulation of vSUB increases dopaminergic tone in NAc and increases locomotor activity (Brudzynski and Gibson, 1997). Furthermore enhancement of dopaminergic neurotransmission by administration of AMPH directly into NAc increases the reinforcing effects of subicular self-stimulation (Sweet and Neill, 1999). Together, these data suggest that there is a cooperative relationship between subicular activity and NAc dopaminergic tone that together influence motivated behavior. Decreased subicular neuronal excitability may lead to a reduction in goal-directed actions, perhaps reflected by the lack of energy human patients exhibit during withdrawal symptoms from repeated psychostimulant use.

Figures

Figure 3.1 Examples of RS and BS pyramidal neurons in the subiculum.

Reconstructions of subicular neurons and their spike-firing properties. **A., B.** Regular spiking (RS; *A*) and burst spiking (BS; *B*) neurons with example suprathreshold responses. A_1 (RS neuron) and B_1 (BS neuron) show whole-cell current-clamp recordings in response to a long (600 ms) square current injection of 250 pA. A_2 (RS neuron) and B_2 (BS neuron) show whole-cell current-clamp recordings in response to a simulated excitatory postsynaptic current (sEPSC) injection of 1500 pA (A_2) or 950 pA (B_2). A_3 shows the RS neuron induced to burst by a larger sEPSC injection (2000 pA). The two cells depicted and their recorded traces were randomly chosen from the RS and BS groups. Previous quantitative analyses by our laboratory have shown no morphological differences between the dendritic arborization in RS and BS neurons (Staff et al., 2000).

Figure 3.1

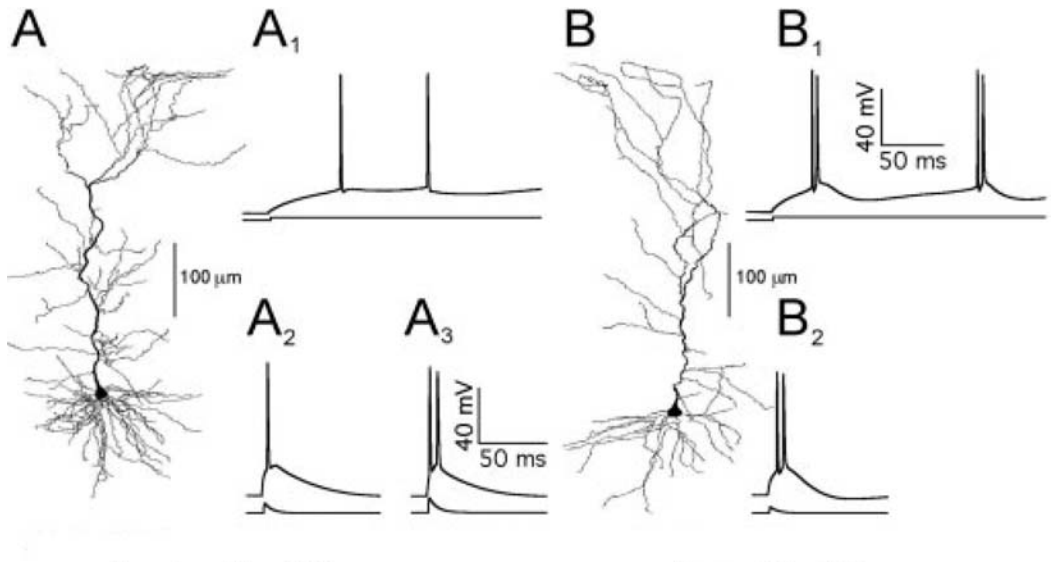

Regular spiking (RS) Burst spiking (BS)

Figure 3.2 The current-voltage relationship is not different between RS and BS neurons.

A. Subthreshold voltage-current (V-I) plot for regular spiking (RS) and burst spiking (BS) neurons in response to series of 600 ms step pulses from -200 to +100 pA . Because there was no difference between groups, the data were pooled and a linear fit was performed on points between the -50 pA to the +50 pA current injections, then extrapolated to the rest of the graph (*solid line*). **B.** Pooled means for the V-I relationship of RS and BS neurons from saline- (SAL) and amphetamine- (AMPH) treated rats at the early (2 - 3 days) withdrawal (EW) time point. Only data from EW are plotted because there were no differences in the V-I curve between EW and late (14 - 15 days) withdrawal (LW)

Figure 3.2

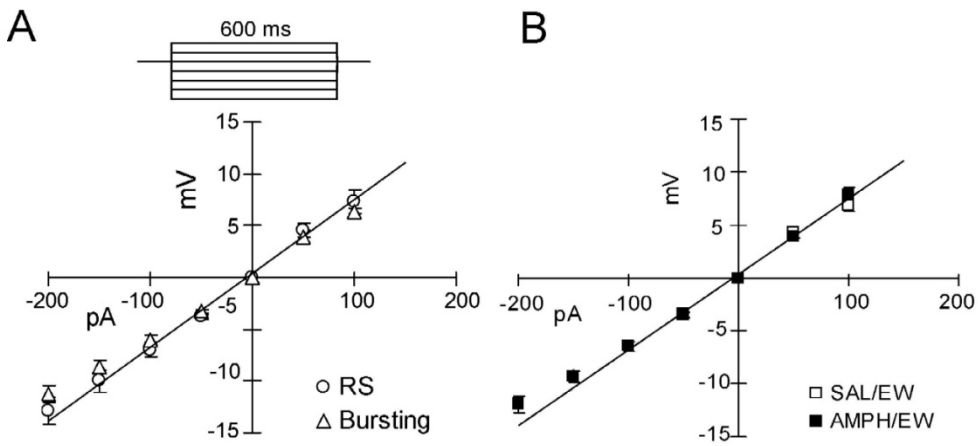
A
600 ms
15
10
5
mV
-200
-100
-5
100
200
pA
-10
-15
○ RS
△ Bursting
B
15
10
5
mV
-200
pA
-100
100
200
-5
-10
-15
□ SAL/EW
■ AMPH/EW

Figure 3.3 Voltage-dependent membrane potential fluctuations are reduced at EW, but not LW, from repeated AMPH.

A. Voltage-dependent increase in near-threshold membrane potential fluctuations, measured before (baseline) and after tetrodotoxin (TTX, 500 nM). The maximum peak-to-peak deviations were 2 - 10 times larger than the average deviation for each trace. **B.** The power spectral density plot of membrane potential fluctuations from pooled regular spiking (RS) and burst spiking (BS) subicular neurons (n = 15) in the saline- (SAL) treated control group at a holding potential of -55 mV, showing a peak at 3Hz . After treatment with TTX, this peak was attenuated, but the dominant frequency did not change. **C., D.** Scatter plot of the average peak-to-peak deviation of the membrane potential fluctuations over a range of holding potentials (-75 to -55 mV) in the SAL/early withdrawal (EW, 2 days) group (*C*) and the amphetamine (AMPH)/EW group (*D*). Small symbols represent data collected from RS and BS, which were not different, and thus were pooled and plotted as large open (SAL) and filled (AMPH) squares. The pooled data showed that both the SAL/EW and AMPH/EW groups exhibit a significant voltage-dependent increase in the magnitude of membrane potential fluctuations (SAL/EW, n = 15, $p < 0.001$; AMPH/EW, n = 19, $p < 0.001$). **E.** Pooled averages (± s.e.m.) of RS and BS neurons for both treatment groups (SAL or AMPH) for the EW time point. Compared to SAL/EW, the AMPH/EW group displayed significantly decreased voltage-dependent amplification of the membrane potential fluctuations in the near-threshold voltage range between -60 and -55 mV (* $p < 0.05$). TTX greatly reduced voltage-dependent amplification the fluctuations and eliminated the differences between SAL and AMPH treatment. **F.** Pooled averages (± s.e.m.) of RS and BS neurons for both treatment groups

(SAL or AMPH) for the late withdrawal (LW, 14 days) time point. No differences were observed between SAL/LW (n = 17) and AMPH/LW (n = 15) groups before or after TTX treatment.

Figure 3.3

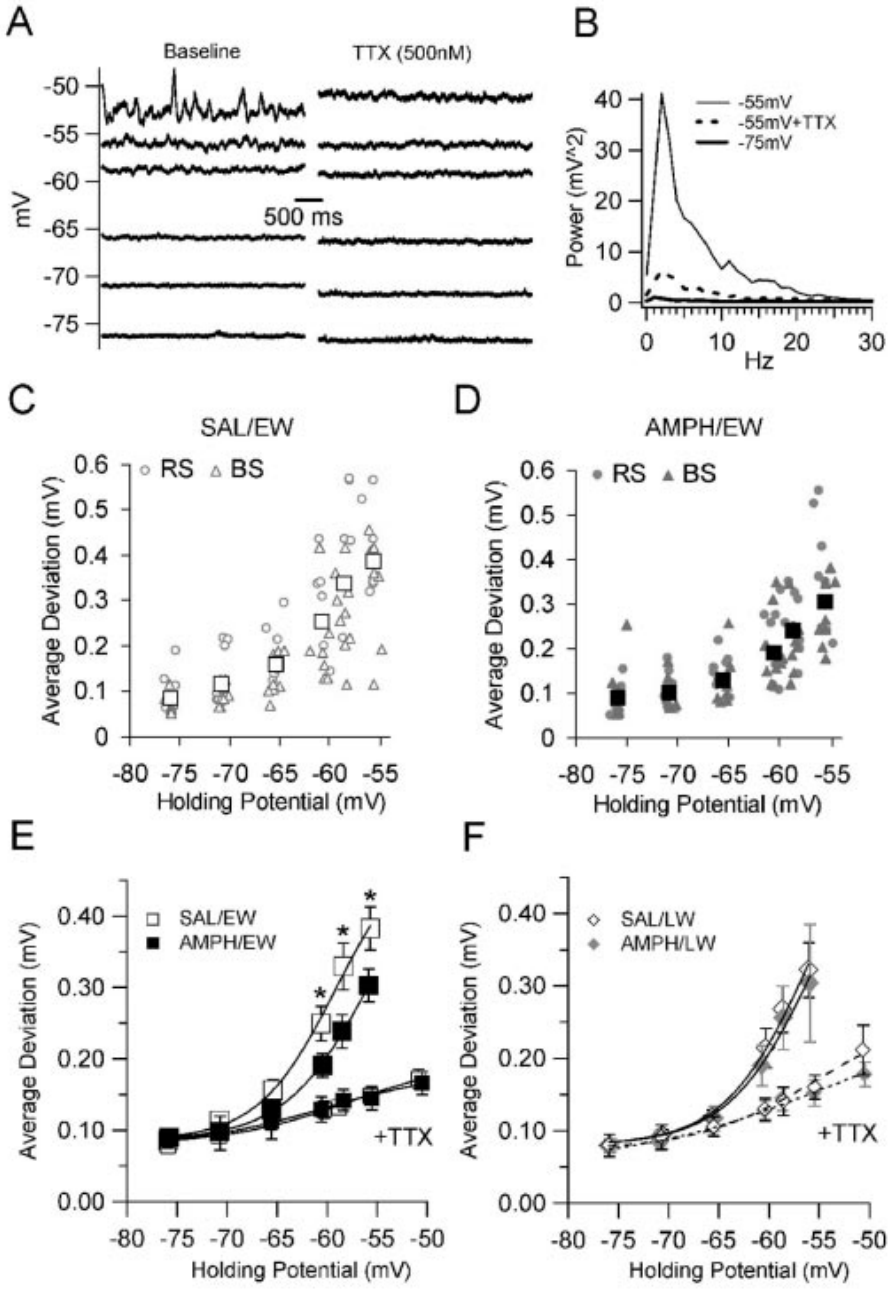
A
Baseline
TTX (500nM)
-50
-55
-60
-65
-70
-75
mV
500 ms
B
-55mV
-55mV+TTX
-75mV
Power (mV^2)
40
30
20
10
0
0
10
20
30
Hz
C
SAL/EW
RS
BS
Average Deviation (mV)
0.6
0.5
0.4
0.3
0.2
0.1
0
-80 -75 -70 -65 -60 -55
Holding Potential (mV)
D
AMPH/EW
RS
BS
Average Deviation (mV)
0.6
0.5
0.4
0.3
0.2
0.1
0
-80 -75 -70 -65 -60 -55
Holding Potential (mV)
E
SAL/EW
AMPH/EW
Average Deviation (mV)
0.40
0.30
0.20
0.10
0.00
*
*
*
+TTX
-80 -75 -70 -65 -60 -55 -50
Holding Potential (mV)
F
SAL/LW
AMPH/LW
Average Deviation (mV)
0.40
0.30
0.20
0.10
0.00
+TTX
-80 -75 -70 -65 -60 -55 -50
Holding Potential (mV)

Figure 3.4 Voltage-dependent amplification of EPSPs and sEPSPs depends on TTX-sensitive Na^+ channels.

A. Scatter plot shows the similarity in voltage-dependent amplification of synaptically evoked excitatory postsynaptic potentials (EPSPs) and somatically evoked simulated EPSPs (sEPSPs; evoked by a simulated excitatory postsynaptic current (sEPSC) injection) over a range of holding potentials, from -75 to approximately -60 mV. EPSPs (*filled squares*) and sEPSPs (*open circles*) were collected in the same sweep, 500 ms apart. The averages for EPSPs (*large filled squares*) and the sEPSPs (*large open circles*) were taken from six consecutive sweeps in both regular spiking (RS) and burst spiking (BS) neurons (n = 4). The inset shows superimposed representative sweeps of EPSPs (*open triangles*) and sEPSPs (*open diamonds*) at both hyperpolarized (-75 mV) and near-threshold holding potentials. **B., C.** Near-threshold EPSP (*B*) and sEPSP (*C*) amplification before (*black traces*) and after (*grey traces*) bath application of a submaximal concentration of tetrodotoxin (TTX; 50 nM). Representative traces are shown from hyperpolarized and near-threshold holding potentials. **D., E.** Average voltage-dependent amplification of the peak (*D*) and integral (*E*) from EPSPs (*squares*) and sEPSPs (*circles*) before (*black*) and after (*grey*) bath application of a submaximal concentration of TTX.

Figure 3.4

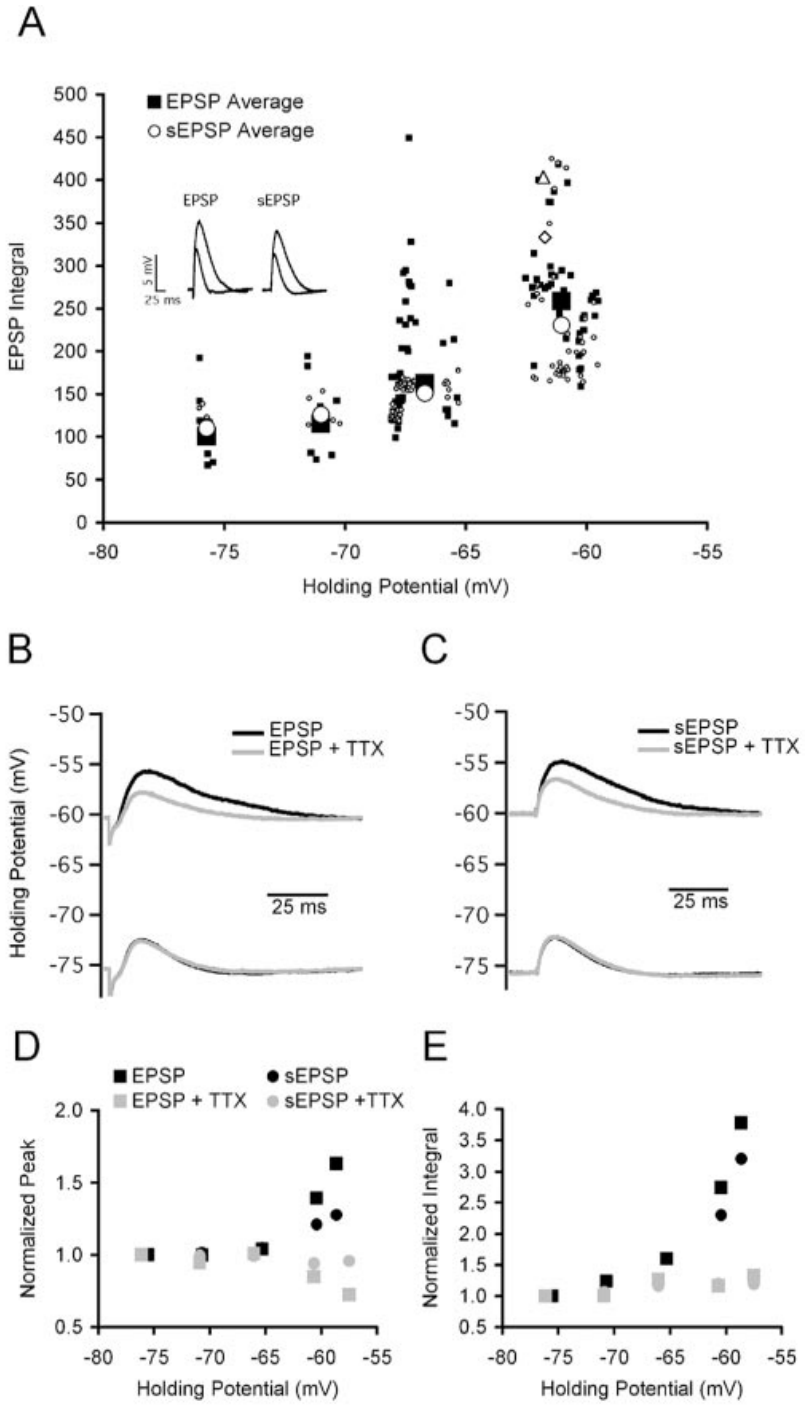
A
EPSP Average
sEPSP Average
EPSP
sEPSP
5 mV
25 ms
EPSP Integral
Holding Potential (mV)
B
EPSP
EPSP + TTX
25 ms
Holding Potential (mV)
C
sEPSP
sEPSP + TTX
25 ms
D
EPSP
sEPSP
EPSP + TTX
sEPSP +TTX
Normalized Peak
Holding Potential (mV)
E
Normalized Integral
Holding Potential (mV)

Figure 3.5 Voltage-dependent amplification of sEPSPs is reduced EW, but not LW, from repeated AMPH.

A., B. Scatter plots of amplification of the amplitude (peak; A) and integral (B) of simulated excitatory postsynaptic potentials (sEPSPs) over a range of holding potentials for the saline/early withdrawal (SAL/EW; *top graphs*) and amphetamine (AMPH)/EW (*bottom graphs*) groups. Small symbols represent data collected from regular spiking (RS) and burst spiking (BS) neurons. Because there were no differences in sEPSP amplification between RS and BS in either group, data were pooled and plotted as large open (SAL) and filled (AMPH) squares on these graphs. Both groups exhibited significant voltage-dependent amplification of sEPSPs ($p < 0.001$). **C.** Compared to SAL/EW, the AMPH/EW group displayed significantly decreased voltage-dependent amplification of both the amplitude (*left graph*) and integral (right graph) of sEPSPs in the near-threshold voltage range between -65 mV and -60 mV (SAL, n=12; AMPH, n=12; * $p < 0.05$, ** $p < 0.01$). **D.** No differences were observed between SAL/late withdrawal (LW) and AMPH/LW groups in amplification of either the amplitude (*left graph*) or the integral (*right graph*) of sEPSPs. All groups consisted of 6 - 12 cells. Error bars are ± s.e.m.

Figure 3.5

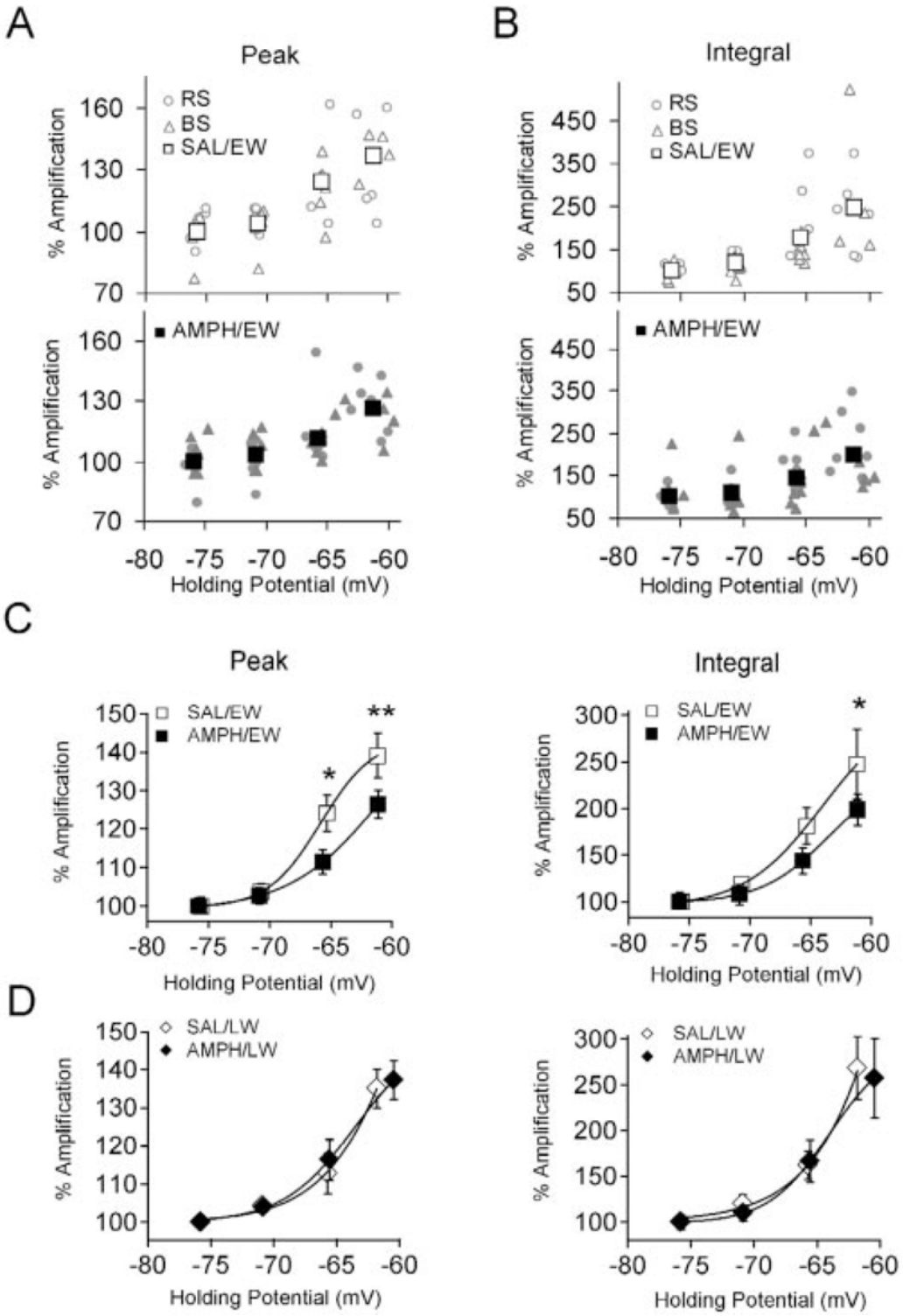
A
Peak
RS
BS
SAL/EW
AMPH/EW
% Amplification
160
130
100
70
-80 -75 -70 -65 -60
Holding Potential (mV)
B
Integral
450
350
250
150
50
C
Peak
Integral
SAL/EW
AMPH/EW
*
**
150
140
120
110
D
SAL/LW
AMPH/LW

Figure 3.6 Action potential properties are reduced at EW, but not LW, from repeated AMPH.

A-C. Compared to the saline /early withdrawal (SAL/EW) group (white), the amphetamine (AMPH)/EW group (black) shows an elevated action potential threshold (A; ** $p < 0.01$), decreased action potential amplitude (B;** $p < 0.01$), and a decreased rate of rise (C;* $p < 0.05$). At late withdrawal (LW), there were no differences on any of these measures between the SAL and AMPH groups. Cells in all treatment groups were held at similar membrane potentials before triggering action potentials (SAL/EW = -67.3 ± 0.3 mV; AMPH/EW = -67.6 ± 0.3 mV; SAL/LW = -67.7 ± 0.2 mV; AMPH/LW = -68.0 ± 0.03 mV). All groups were composed of 16 - 19 cells. Error bars are ± s.e.m. **D.** Responses of representative burst spiking (BS) neurons to just-suprathreshold 600 ms square current injections from the SAL/EW (black) and AMPH/EW (gray) groups. Note that the AMPH/EW trace has an elevated action potential threshold, decreased action potential amplitude, and decreased rate of rise (dV/dt, inset). Rate of rise was calculated as the first derivative of the bursts for each group (dV/dt: SAL/EW = 605 mV/ms; AMPH/EW = 408 mV/ms). There were no differences between the two BS cells in the holding potential before the burst was triggered (SAL/EW = -68.0 mV; AMPH/EW = -67.5 mV).

Figure 3.6

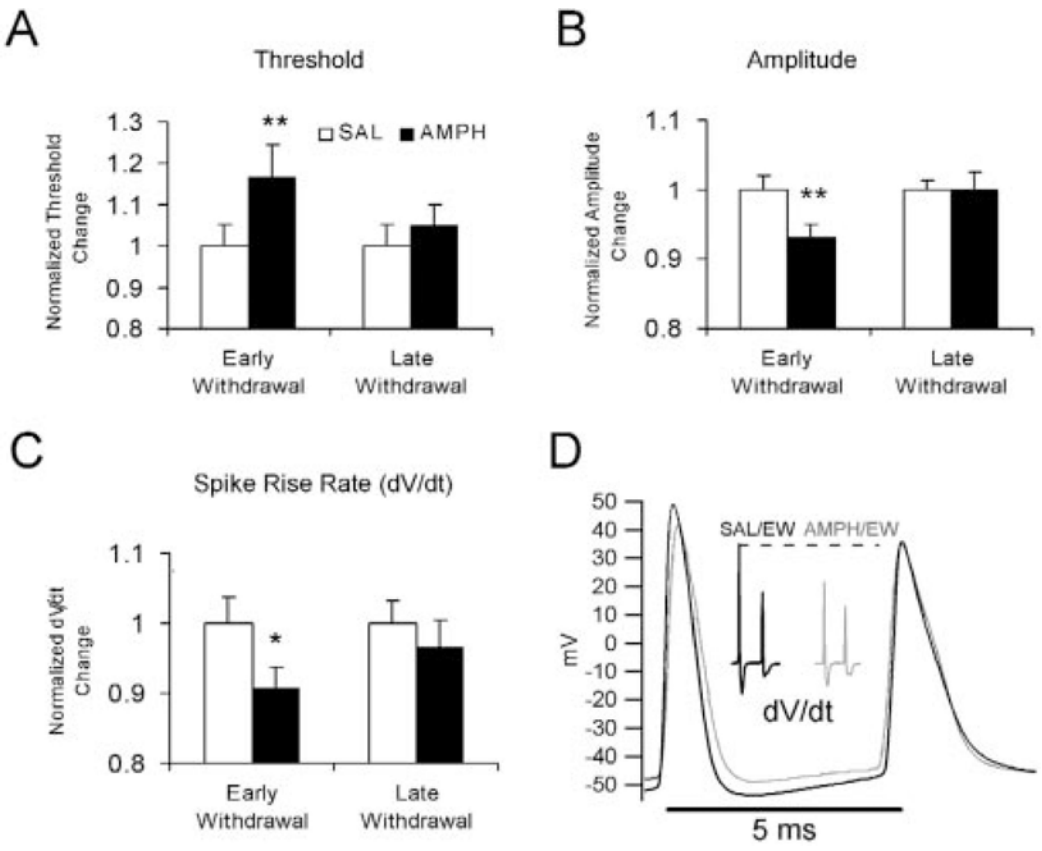
A
Threshold
Normalized Threshold Change
1.3
1.2
1.1
1
0.9
0.8
**
SAL
AMPH
Early Withdrawal
Late Withdrawal
B
Amplitude
Normalized Amplitude Change
1.1
1
0.9
0.8
**
Early Withdrawal
Late Withdrawal
C
Spike Rise Rate (dV/dt)
Normalized dV/dt Change
1.1
1
0.9
0.8
*
Early Withdrawal
Late Withdrawal
D
mV
50
40
30
20
10
0
-10
-20
-30
-40
-50
SAL/EW
AMPH/EW
dV/dt
5 ms

Figure 3.7 Acute application of AMPH does not affect neuronal excitability.

A. Scatter plot depicting voltage-dependent amplification of membrane voltage fluctuations before (baseline, n = 12) and 20 minutes after acute application of amphetamine (AMPH; 25 - 50 μM) over a range of membrane holding potentials, from -75 to -55 mV. Small symbols represent data collected from individual cells and large symbols represent data averaged across cells, before (*open squares*) and after (*filled circles*) AMPH application. Inset shows an example of membrane voltage fluctuations in control conditions (before AMPH application) at holding potentials of -71.3 mV (*bottom trace*) and -55.6 mV (*top trace*). **B., C.** Scatter plots showing voltage-dependent amplification of the amplitude (peak; *B*) and integral (*C*) of simulated excitatory postsynaptic potentials (sEPSP) before (baseline, n = 6) and 20 minutes after acute application of AMPH. Inset shows an example of sEPSP amplification in control conditions (before AMPH application) at holding potential of -76.2 mV (*bottom trace*) and -57.7 mV (*top trace*). **D.** No changes in rheobase or the action potential threshold in response to a simulated excitatory postsynaptic current (sEPSC) injection were observed after 20 minutes of acute AMPH application.

Figure 3.7

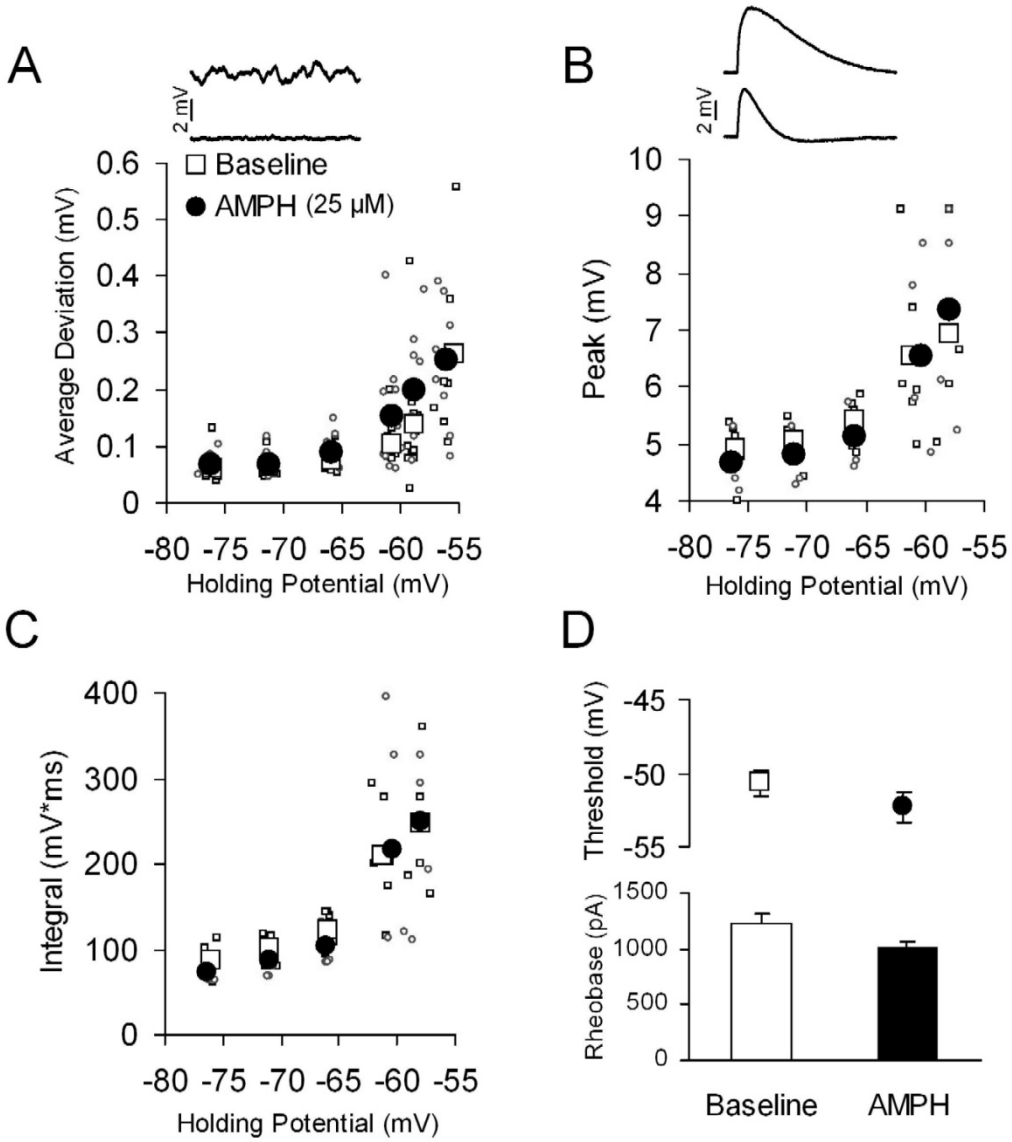
A
2 mV
Baseline
AMPH (25 µM)
Average Deviation (mV)
0.6
0.5
0.4
0.3
0.2
0.1
0
-80 -75 -70 -65 -60 -55
Holding Potential (mV)
B
2 mV
Peak (mV)
10
9
8
7
6
5
4
-80 -75 -70 -65 -60 -55
Holding Potential (mV)
C
Integral (mV*ms)
400
300
200
100
0
-80 -75 -70 -65 -60 -55
Holding Potential (mV)
D
Threshold (mV)
-45
-50
-55
Rheobase (pA)
1500
1000
500
0
Baseline
AMPH

Figure 3.8 Variability in spike timing between RS and BS neurons.

A. Plot of latency to spike firing, elicited by a simulated excitatory postsynaptic current (sEPSC) injection (at time 0 ms), in regular spiking (RS; *top, open circles*; n = 19, combined from saline, early withdrawal [SAL/EW] and saline, late withdrawal [SAL/LW] groups) and burst spiking (BS; *bottom, filled diamonds*; n = 16, combined from SAL/EW and SAL/LW groups) neurons. The median latency, indicated by a solid line for each group, is significantly different between RS and BS neurons (* $p < 0.05$; Mann–Whitney U test). RS and BS neurons were maintained at similar holding potentials (RS = -60.07 ± 0.73 mV; BS = -60.08 ± 0.70 mV), and there were no differences in the amplitudes of the sEPSC injection between groups. Insets show representative RS (*top, indicated in group data by a filled square*) and BS (*bottom, indicated in the group data by an open diamond*) responses. **B.** Scatter plot illustrating the relationship between latency to spike firing and action potential threshold (*top panels*) or latency to spike firing and holding potential (*bottom panels*) in RS (*left panels*) and BS (*right panels*) neurons. The action potential threshold versus latency data were fit by a logarithmic equation (RS: $R^2 = 0.30$, $p < 0.01$; BS: $R^2 = 0.20$, $p < 0.05$). The holding potential versus latency data were fit by a linear equation (RS: $R^2 = 0.005$; BS: $R^2 = 0.004$) The amphetamine (AMPH)/EW group exhibited the same relationship between action potential threshold and latency, as so were plotted on the same graphs (*filled diamonds*; AMPH RS, n=16; AMPH BS, n=10).

Figure 3.8

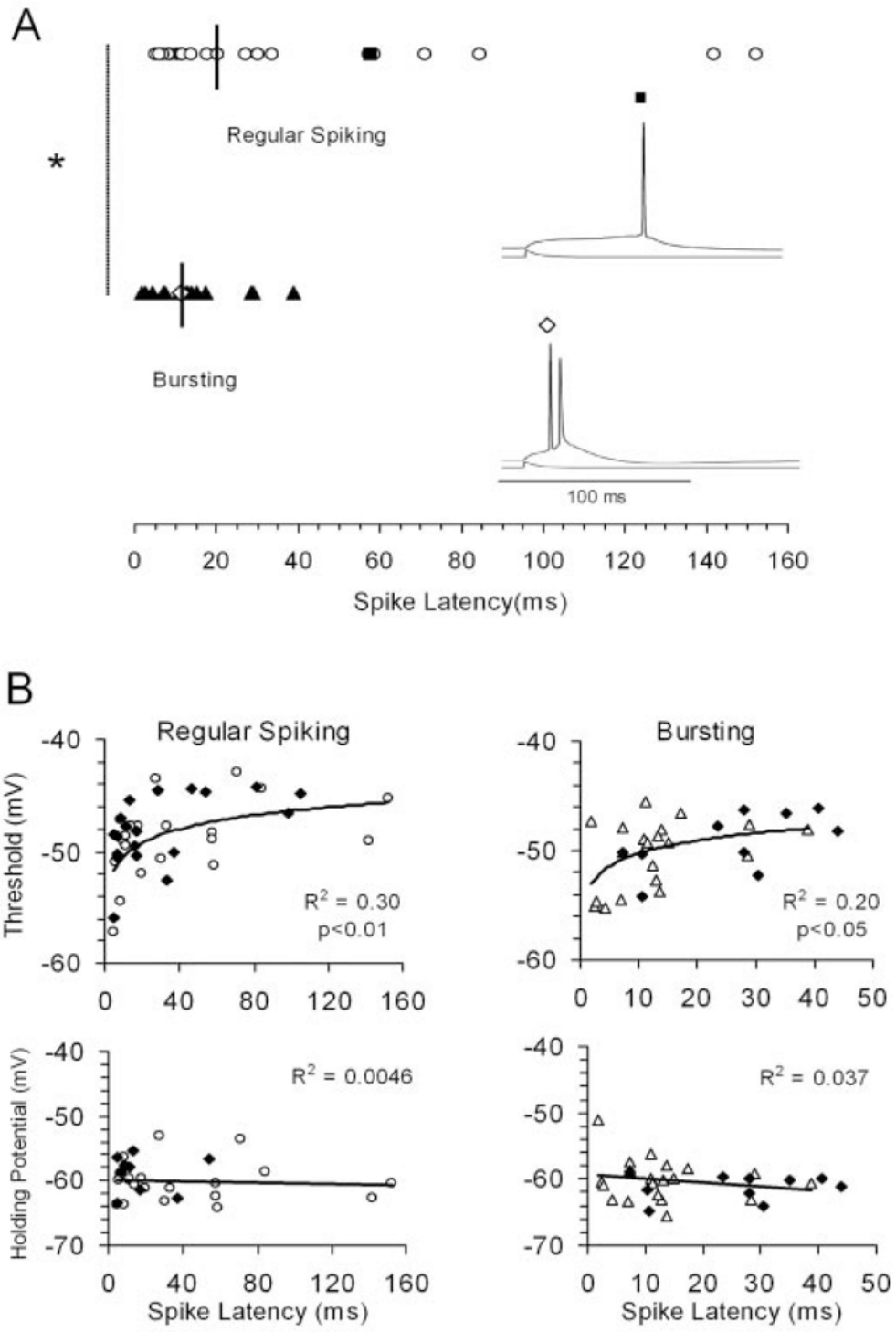
A
Regular Spiking
Bursting
100 ms
0 20 40 60 80 100 120 140 160
Spike Latency(ms)
B
Regular Spiking
Bursting
Threshold (mV)
-40
-50
-60
R2 = 0.30
p<0.01
R2 = 0.20
p<0.05
0 40 80 120 160
0 10 20 30 40 50
Holding Potential (mV)
-70
R2 = 0.0046
R2 = 0.037
Spike Latency (ms)

Figure 3.9 Spike timing of BS, but not RS, neurons is disrupted at EW, but not LW, from repeated AMPH.

A. Plot of latency to spike firing, elicited by a simulated excitatory postsynaptic current (sEPSC) injection (at time 0 ms), in regular spiking (RS) neurons from saline (SAL)/early withdrawal (EW) and amphetamine (AMPH)/EW groups (*top, open circles*; SAL, n = 10; AMPH, n = 8) and SAL/late withdrawal (LW) and AMPH/LW groups (*bottom, filled circles*; SAL, n = 9; AMPH, n = 8). There were no differences in latency to spike firing between any of these groups. **B.** Plot of latency to spike firing, elicited by a sEPSC injection (at time 0 ms), in burst spiking (BS) neurons from SAL/EW and AMPH/EW groups (*top, open triangles*; SAL, n = 8; AMPH, n = 8) and SAL/LW and AMPH/LW groups (*bottom, filled triangles*; SAL, n = 8; AMPH, n = 9). At EW, latency to spike firing was significantly increased in BS neurons in the AMPH-treated compared to the SAL-treated groups (* $p < 0.05$; Mann–Whitney U test). Insets show representative responses from BS neurons in SAL/EW (*top, indicated in the group data by a filled triangle*) and AMPH/EW (*bottom, indicated in the group data by a filled diamond*) groups. All neurons were maintained at similar holding potentials (SAL/EW: RS = -59.5 ± 0.74 mV, BS = -61.3 ± 0.81 mV; AMPH/EW: RS = -58.9 ± 0.96 mV, BS = -61.2 ± 0.62 mV; SAL/LW: RS = -60.6 ± 0.57 mV, BS = -59.2 ± 0.94 mV; AMPH/LW: RS -59.12 ± 0.75 mV, BS = -59.4 ± 1.00 mV), and there were no differences in the amplitudes of the sEPSC injections between groups.

Figure 3.9

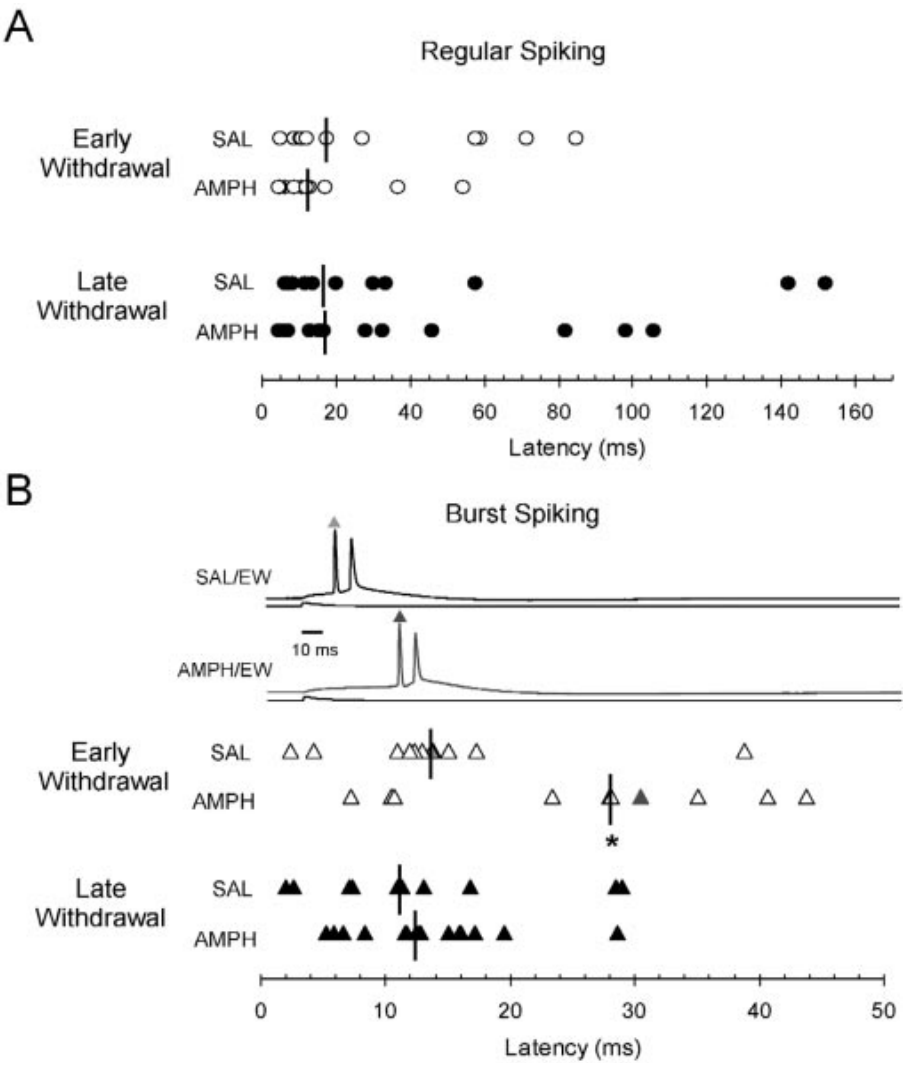
A
Regular Spiking
Early Withdrawal
SAL
AMPH
Late Withdrawal
SAL
AMPH
0
20
40
60
80
100
120
140
160
Latency (ms)
B
Burst Spiking
SAL/EW
10 ms
AMPH/EW
Early Withdrawal
SAL
AMPH
*
Late Withdrawal
SAL
AMPH
0
10
20
30
40
50
Latency (ms)

Figure 3.10 TTX-induced downregulation of voltage-gated Na^+ channels mimics the effects of EW from repeated AMPH.

A. A representative burst response to a simulated excitatory postsynaptic current (sEPSC) injection (400 pA) before (*black trace*) and during (*grey trace*) bath application of tetrodotoxin (TTX; 500 nM). Note that in a submaximal concentration of TTX, action potential threshold is depolarized and latency to spike firing is increased. Action potentials are truncated in the traces. **B.** There is a positive linear correlation ($R^2 = 0.99$) between the depolarization of action potential threshold and increase in latency to spike firing during application of low concentrations of TTX (n = 4). The grey open triangle indicates data for the traces shown in A. The holding potentials were similar before (-60.3 ± 0.38 mV) and after TTX (-60.6 ± 0.45 mV). C. Subthreshold simulated excitatory postsynaptic potentials (sEPSPs) evoked by 200 pA (left) and 300 pA (right) sEPSC injections 400 ms apart, recorded 300 ms before the burst response seen in A. Note that amplification of the sEPSP amplitude and integral (only seen in response to the larger sEPSC) is reduced by TTX. Subthreshold sEPSCs were injected every 300 - 400 ms while TTX washed into the recording chamber. The before- and after-TTX traces shown were 40 s apart. Under our experimental conditions, TTX reached sufficient concentrations in the recording chamber to eliminate action potential firing between 240 and 300 s from beginning of wash-in. Therefore, all TTX data were taken between 30 and 60 s from the beginning of wash-in.

Figure 3.10

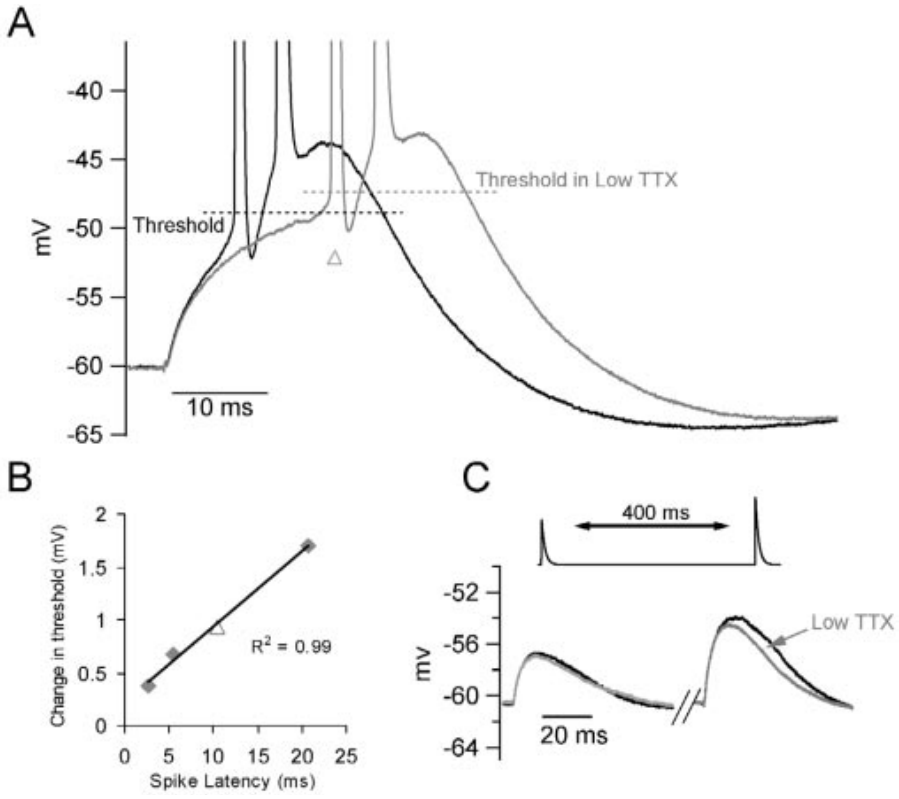
A
-40
-45
-50
-55
-60
-65
mV
Threshold
Threshold in Low TTX
10 ms
B
Change in threshold (mV)
2
1.5
1
0.5
0
0 5 10 15 20 25
Spike Latency (ms)
R² = 0.99
C
400 ms
-52
-56
-60
-64
mv
Low TTX
20 ms

Tables

Table 3.1 Electrophysiological properties of subicular neurons in SAL- or AMPH-treated groups at EW or LW.

Measurements of passive properties, including input resistance (R_N) and resting potential (V_m), and active properties, taken as measurements of evoked action potentials, including half-width, threshold, amplitude, and minimum current needed to trigger an action potential (rheobase), are presented for both regular spiking (RS) and burst spiking (BS) neurons in one of four experimental groups: saline/early withdrawal (SAL/EW), amphetamine/early withdrawal (AMPH/EW), saline/late withdrawal (SAL/LW), or amphetamine/late withdrawal (AMPH/LW). Action potentials were elicited by either a 600 ms square current or simulated excitatory postsynaptic current (sEPSC) injection. In RS cells, the amplitude of the sEPSC injection was increased past rheobase (which elicited a single action potential) until a burst was evoked. The amplitude of the sEPSC needed to evoke burst firing in RS cells was determined to be sEPSC burst rheobase. ANOVA and two-tailed *t* tests were used to compare treatment groups for EW and LW between each neuron classification (RS and BS). All groups were composed of 8 - 19 different cells with no more than 2 cells from a single rat. * $p < 0.05$; ** $p < 0.01$.

Table 3.1

	SAL/EW		AMPH/EW		SAL/LW		AMPH/LW	
	RS	BS	RS	BS	RS	BS	RS	BS
V_m (mV)	-73.4 ± 1.0	-73.1 ± 0.9	-70.5 ± 0.8	-69.3 ± 0.8	-69.9 ± 1.0	-68.9 ± 1.1	-72.1 ± 1.1	-67.8 ± 1.2
R_n (MΩ)	57.5 ± 5.7	65.1 ± 7.6	64.3 ± 5.8	65.0 ± 7.0	54.5 ± 5.0	54.1 ± 7.2	65.4 ± 4.6	56.5 ± 5.6
600 ms rheobase (pA)	135 ± 25	144 ± 19	174 ± 31	198 ± 31	194 ± 27	196 ± 40	135 ± 22	205 ± 24
600 ms threshold (mV)	-48.5 ± 1.1	-50.0 ± 0.8**	-46.9 ± 1.2	-46.6 ± 0.6**	-47.9 ± 1.9	-47.5 ± 1.2	-48.6 ± 1.7	-46.4 ± 0.8
Amplitude (mV)	93.9 ± 2.0	95.5 ± 1.6*	92.6 ± 2.2	89.3 ± 2.8*	95.9 ± 1.6	95.1 ± 1.6	91.3 ± 2.4	95.7 ± 3.6
dV/dt (mV/ms)	479 ± 22	521 ± 29*	451 ± 19	459 ± 25*	557 ± 26	556 ± 26	533 ± 45	511 ± 24
Half-width (ms)	0.72 ± 0.02	0.71 ± 0.02	0.72 ± 0.03	0.69 ± 0.03	0.69 ± 0.03	0.66 ± 0.03	0.66 ± 0.04	0.70 ± 0.03
sEPSC rheobase (pA)	980 ± 150	812 ± 79	1000 ± 109	881 ± 110	846 ± 107	702 ± 115	830 ± 125	974 ± 180
sEPSC burst rheobase (pA)	1113 ± 74**	NA	1570 ± 127*	NA	1280 ± 178	NA	1571 ± 142	NA
sEPSC threshold (mV)	-52.1 ± 1.4	-52.7 ± 0.8*	-50.4 ± 1.0	-49.6 ± 0.9*	-51.9 ± 0.6	-50.4 ± 1.4	-48.6 ± 1.7	-49.3 ± 1.3

Chapter 4:

Bidirectional plasticity of intrinsic burst firing in subicular pyramidal neurons

Abstract

The subiculum, which is the primary efferent pathway of the hippocampus, participates in memory for spatial tasks, relapse to drugs of abuse, and initiation of temporal lobe seizures. An important electrophysiological property of subicular pyramidal neurons is low-threshold burst firing. Here we report that burst firing can be regulated in an activity-dependent manner via synaptic stimulation of afferents from entorhinal cortex and CA1. Unlike synaptic plasticity in subicular pyramidal cells, burst plasticity did not require activation of N-methyl-D-aspartate receptors (NMDARs), synaptic depolarization, or action potential firing. Rather, enhancement of burst firing depended on synergistic activation of group I subtype 1 metabotropic glutamate receptors (mGluRs) and the M_1 subtype of muscarinic acetylcholine receptor (mAChR). When enhancement was blocked, activation of group I subtype 5 mGluRs resulted in suppression of burst firing. These results indicate that output of the subiculum can be strongly and bidirectionally regulated in a state-dependent manner through coordinated activation of glutamatergic inputs within the hippocampus and cholinergic afferents from the septal nucleus.

Introduction

Synaptic plasticity is a leading candidate for the cellular mechanism underlying learning and memory (Maren and Baudry, 1995; Martinez and Derrick, 1996), but a role for non-synaptic plasticity has also been suggested (Daoudal and Debanne, 2003; Zhang and Linden, 2003). Non-synaptic plasticity generally involves the regulation of extra-synaptically localized ligand- or voltage-gated conductances and, compared to synaptic plasticity, represents a more global change in the excitability of a neuron. Unlike synaptic plasticity, the conditions required to induce non-synaptic plasticity are relatively poorly understood. An important issue in this regard is whether the requirements for non-synaptic plasticity parallel those of synaptic plasticity or differ substantially. Resolving this issue will help to determine whether synaptic and non-synaptic plasticity are likely to occur in concert or under separate conditions.

Much of the work on synaptic plasticity has been performed in the hippocampus, an area well known for its role in spatial memory tasks in rodents and declarative memory in humans. A functionally important subregion is the subiculum, which serves as the major output pathway of the hippocampus. Subicular efferents target a variety of cortical and subcortical areas, including prefrontal cortex (Jay and Witter, 1991), nucleus accumbens (Lopes da Silva et al., 1984; Witter et al., 1990), and hypothalamus (Swanson and Cowan, 1977; Kishi et al., 2000). This divergent output makes the subiculum an integral component in networks underlying diverse functions and behaviors, such as regulation of the hypothalamic-pituitary axis and memory for spatial tasks (for review, see O'Mara 2005). Additionally, dysregulation of subicular function has been implicated

in pathological conditions such as epilepsy (Funahashi et al., 1999; Harris and Stewart, 2001b; Cohen et al., 2002) and drug addiction (Caine et al., 2001; Vorel et al., 2001; Cooper et al., 2003; Sun and Rebec, 2003).

The majority of pyramidal neurons in the subiculum respond to brief depolarization just above threshold with a high frequency cluster (> 100 Hz) of 2-3 action potentials (a burst). *In vitro*, burst firing does not require strong correlated synaptic input (Staff et al., 2000; Harris and Stewart, 2001a), but rather depends on activation of voltage-gated Ca^{2+} conductances by a Na^{+}-dependent action potential. The resulting Ca^{2+} tail current, largely mediated by R-type channels, leads to an after-depolarization (ADP) that can drive burst firing. The ADP, as well as burst firing, can be limited by other conductances, including slow Ca^{2+}-activated K^{+} currents (Staff et al., 2000; Jung et al., 2001). Because intrinsic conductances determine this pattern of neuronal output, their modulation can result in robust and distinct changes in burst firing, which therefore provides a good model system for the study of non-synaptic plasticity.

We used whole-cell current-clamp recordings to examine whether synaptic and non-synaptic properties of subicular pyramidal cells can be regulated in an activity-dependent manner. We describe a novel form of bidirectional plasticity, independent of synaptic plasticity that resulted in altered levels of burst firing in these neurons (burst plasticity). The direction of this change depended on the receptor types activated during the induction stimulus. Enhancement of burst firing did not require NMDAR activation, synaptic depolarization, or action potential firing, but rather depended on synergistic activation of group I subtype 1 mGluRs and the M_1 mAChRs. When the enhancement of

burst firing was blocked, a separate process led to suppression of burst firing, mediated by synaptic activation of group I subtype 5 mGluRs (mGluR5). These results support the idea that, separate from synaptic changes, distinct mechanisms can lead to alterations in intrinsic conductances that significantly alter neuronal integration and output.

Methods

Animals – Male Wistar rats, aged 25-45 days, were used for all experiments. Animals were colony housed on a 12-hour light/dark cycle with free access to food and water. All animal procedures were approved by the Northwestern University Animal Care and Use Committee.

Solutions – Artificial cerebrospinal fluid (ACSF) consisted of (in mM): 125 NaCl, 2.5 KCl, 25 $NaHCO_3$, 1.25 NaH_2PO_4, 1 $MgCl_2$, 2 $CaCl_2$, and 25 dextrose (all from Fisher Scientific, Pittsburgh, PA). The pH of the ACSF was 7.2-7.4 and the osmolarity was 305-320 mOsm. ACSF was always oxygenated by constant bubbling with a gas mixture of 95% O_2/5% CO_2. Internal recording solution consisted of: 115 K-gluconate, 20 KCl, 10 sodium phosphocreatine (Na_2-Pcr), 10 HEPES, 2 MgATP, and 0.3 NaGTP with 0.10% biocytin for subsequent determination of morphology (all from Sigma-Aldrich, St. Louis, MO, except KCl and HEPES, which were from Fisher Scientific). 1 M KOH was used to pH the internal solution to 7.3-7.4. The osmolarity was 272-290 mosm.

Unless otherwise indicated, ACSF used to perfuse slices in the recording chamber included 2 μM SR95531, a γ-aminobutyric acid $(GABA)_A$ antagonist (Sigma-Aldrich), and 3 μM CGP52432, a $GABA_B$ antagonist (Tocris-Cookson, Bristol, UK). Where noted, one of the following antagonists or combinations of antagonists (all from Sigma-Aldrich unless otherwise indicated) was also included in the perfusion ACSF and present for the entire duration of recording: 1. N-methyl-D-aspartate (NMDA) receptor antagonists: 50 μM D-2-amino-5-phosphonopentanoate (D-AP5) and 20 μM MK-801; 2. ionotropic glutamate (iGluR) receptor antagonists: 20 μM 6-cyano-7-nitroquinoxaline-2,3-dione (CNQX), 50 μM D-AP5, and 20 μM MK-801; 3. group I metabotropic glutamate (mGluR) receptor antagonists: 25 μM LY367385, an antagonist of mGluR subtype 1, and/or 10 μM 2-methyl-6-(phenylethynyl)-pyridine (MPEP), an antagonist of mGluR subtype 5 (both from Tocris-Cookson); 4. a mAChR antagonist: 10 μM atropine; 5. an antagonist of the M_1 subtype of mAChRs: 50 nM telenzipine (from Tocris-Cookson); 6. a phospholipase C (PLC) inhibitor: 25 μM U-73122 (from Tocris-Cookson). In some experiments, additional drugs were added to the intracellular recording solution: either 10 mM 1,2-bis(2-aminophenoxy)ethane N,N,N,N-tetraacetic acid (BAPTA; from Sigma-Aldrich), a Ca^{2+} chelator, or 2 μM thapsigargin (from Tocris-Cookson), which depletes intracellular Ca^{2+} stores in the endoplasmic reticulum by inhibiting Ca^{2+}-ATPases. To allow time for the intracellular stores to be depleted, cells were exposed to thapsigargin for at least 30 minutes before the induction stimulus was given.

Slice preparation and experimental setup – Rats were anesthetized with halothane, intracardially perfused with ice-cold ACSF for less than 1 min, then decapitated and the brains rapidly removed. A blocking cut was made to each hemisphere at 60^{o} to the horizontal plane before mounting with ventral side up. Transverse hippocampal slices, 300 μm thick, were made with a Vibratome 3000 (Ted Pella, Inc., Redding CA) and transferred to a storage chamber, incubated at 32-35 ^{o}C for 20-30 min. Afterwards, the chamber was maintained at room temperature.

Prior to electrophysiological recordings, slices were transferred to a submerged chamber and maintained at 32-35 ^{o}C by constant perfusion of warmed ACSF, at a rate of approximately 1 mL/s. A Zeiss Axioskop (Oberkochen, Germany) equipped with differential interference contrast (DIC) optics was used in conjunction with a Hamamatsu camera system to visually identify subicular pyramidal cells. The subiculum was distinguished from bordering regions by the diffuse distribution of pyramidal cells, compared to the tightly packed pyramidal cell layer of CA1, and the lack of distinct cortical layers seen in entorhinal cortex. Recording pipettes were fabricated (Flaming/Brown Micropipette Puller, Sutter Instruments, Novato, CA) from thick-walled borosilicate capillary glass (Garner Glass Company, ID = 1.2 ± 0.05 mm, OD = 2.0 ± 0.05 mm) and filled with the K-gluconate-based internal solution to obtain a 3-5 MΩ open-tip resistance in the bath. Using a motorized micromanipulator (Sutter Instruments), the recording pipette was positioned on a subicular pyramidal cell and negative pressure was applied by mouth suction to form a GΩ seal. Brief pulses of negative pressure were

then used to break through the membrane in the patch pipette and achieve whole-cell configuration.

To evoke synaptic responses, an extracellular stimulating pipette, fabricated from borosilicate theta glass (Sutter Instruments) was filled with ACSF and placed (by using a separate motorized micromanipulator, Sutter Instruments) 50-200 μm away from the site of the whole-cell recording on the apical dendritic side either toward CA1 or entorhinal cortex. In both cases, it is likely that CA1 and EC afferents were jointly recruited and contributed to the synaptic response.

Electrophysiological recordings – Whole-cell current-clamp recordings of subicular pyramidal neurons in rat hippocampal slices were made through patch pipettes containing a silver chloride-coated electrode connected to an amplifier (Dagan BVC-700, Minneapolis, MN). Only cells that had a resting potential between -56 mV and -70 mV at break-in were used. Experiments were restricted to burst-firing neurons, which were defined as those that exhibited two or more action potentials with an instantaneous frequency of greater than 100 Hz in response to a just-above threshold, long (600 ms) square pulse.

Neuronal output was monitored once every 20 seconds (0.05 Hz) by using a train of 10 somatic EPSC-like (τ_{rise} = 0.2 ms, τ_{decay} = 6 ms) current injections to evoke action potential firing (Figure 4.1). The frequency (5 Hz, n=38; 7 Hz, n=43; or 10 Hz, n=17) and amplitude (800 pA - 2400 pA) of somatic current injections were set such that, for each train, 2-7 responses were bursts (while the remaining responses were single action

potentials). In all cases, burst firing occurred mostly at the beginning of the train and single action potentials occurred toward the end of the train.

Synaptic strength (EPSP amplitude) and subthreshold voltage response (a reflection of passive membrane properties) were also monitored once every 20 seconds. The synaptic stimulus (0.2 ms square current pulse through the extracellular bipolar electrode; Axon stimulus isolator) was set to elicit EPSPs of 1-6 mV. Subthreshold responses were monitored with EPSC-like somatic current injections (8% of burst-monitoring amplitude). In some neurons, a hyperpolarizing square current injection (5% of burst-monitoring amplitude, 500 ms) was used to monitor and calculate input resistance.

In one set of experiments, a more physiologically realistic stimulus (noisy current injection) was used to evoke action potential firing. To obtain the noisy current, we depolarized the cell to just below action potential threshold by a constant DC current injection and recorded spontaneous membrane potential fluctuations. A scaled version of this trace was then injected back into the cell as a current wave form.

The induction stimulus consisted of theta-burst-patterned synaptic activation (5 stimuli at 100 Hz) paired with somatic current injection (2 ms square current pulse at the burst-monitoring amplitude), repeated at 5 Hz for 3 seconds (Figure 4.1). The TBS induction stimulus was given approximately 30 minutes after whole-cell configuration was achieved (average, all groups: 30 ± 1 min.; range, all groups: 11 - 76 min.). There was no difference in the time of induction relative to break-in across groups ($p=0.57$, one-factor ANOVA).

All neurons were held at membrane potentials between -63 mV and -67 mV for the duration of the recordings (except in voltage-clamp experiments when, during the induction stimulus only, cells were held at -72 mV). Cells that required more than 250 pA of current to maintain these potentials were excluded from the dataset. There were no statistically significant differences in membrane potential between experimental groups over time ($p=0.76$, two-factor ANOVA; Table 4.1). Bridge balance and capacitance compensation were monitored and adjusted throughout the duration of each experiment; recordings in which the series resistance exceeded 45 MΩ were excluded. Cells were generally recorded from for a total of 50-70 minutes, but, in some cases, were held up to 100 minutes.

Data acquisition and statistical analysis – Voltage responses were filtered at 5 kHz, digitized at 50 kHz, and stored via an ITC-16 analog-to-digital converter (Instrutech, Port Washington, NY) on a Dell Dimension PC. All acquisition and analysis procedures were custom programmed in IGOR Pro (Wavemetrics, Lake Oswego, OR). Statistical analyses of group data were performed using paired, two-tailed Student's t-tests, or one- or two-factor repeated measures ANOVA, where appropriate, with Prism software (GraphPad Software, Inc., San Diego, CA). When a significant main effect was detected with ANOVA tests, Bonferroni's post-hoc correction was applied to determine significance between pairwise comparisons. Unless stated otherwise, reported values are mean ± s.e.m. of data collected 30-40 minutes after the induction stimulus was given. Normalized

values are plotted as a percentage of the value during the baseline, and are obtained by dividing the mean at 30-40 minutes by the mean during the 10-minute baseline period.

Results

Theta-burst stimulation induces synaptic and non-synaptic plasticity in the subiculum

Synaptic and non-synaptic responses were assessed using whole-cell current-clamp recordings in burst-firing pyramidal neurons of the subiculum. Theta-burst stimulation (TBS; 5 synaptic pulses at 100 Hz paired with somatic current injections, repeated at 5 Hz), which resembles the activity patterns observed during hippocampus-dependent learning tasks *in vivo* (Larson and Lynch, 1986; Larson et al., 1986; Otto et al., 1991), was used to induce plasticity of neuronal excitability.

Excitatory postsynaptic potentials (EPSPs) were recorded during low-frequency stimulation of afferents from CA1 and entorhinal cortex (EC). After measuring EPSPs for a 10-minute baseline period, 3 seconds of TBS (Figure 4.1B; see Figure 4.2 for example traces recorded during induction for each experimental condition) were delivered to these same afferents. As expected based on previous work (Commins et al., 1998; Commins et al., 1999; Kokaia, 2000; O'Mara et al., 2000; Huang and Kandel, 2005), TBS resulted in long-term potentiation of EPSPs under control conditions, but not when NMDAR antagonists (50 μM D-AP5 and 20 μM MK-801) were present in the bathing medium (Figure 4.3; Table 4.1).

Additionally, neuronal output was monitored by a train of 10 brief, suprathreshold somatic current injections (Figure 4.1A,C). Current injections at the beginning of the

train elicit burst firing while those later in the train elicit single action potentials (Staff et al., 2000; Cooper et al., 2005). During somatic current injection, neuronal output is determined only by activation of intrinsic conductances gated by voltage and/or calcium. Therefore, a change in the number of bursts can be used as a measure of non-synaptic plasticity caused by changes in postsynaptic excitability.

Interestingly, TBS increased the number of bursts elicited by the train of somatic current injections (Figures 4.1 and 4.4A). This enhancement of burst firing (non-synaptic plasticity) developed more gradually than potentiation of EPSPs (synaptic plasticity), and, unlike the synaptic plasticity, was not blocked by NMDAR antagonists (Figure 4.4B; Table 4.1). Furthermore, there was no correlation between the magnitude of the synaptic and non-synaptic plasticity (linear regression, R^2=0.06, p=0.61; data not shown). However, both types of plasticity required TBS (induction), as neither developed over time when the TBS was not delivered (no induction; Figure 4.3 and 4.4A; Table 4.1).

In both the induction and no-induction groups, inhibitory neurotransmission was blocked by the inclusion of $GABA_A$ and $GABA_B$ receptor antagonists (2 μM SR95531 and 3 μM CGP52432, respectively). To test whether enhanced burst firing persists when inhibitory neurotransmission is intact, a more physiologically relevant condition, we delivered TBS in standard solution (no GABA receptor antagonists). A comparable increase in burst firing was observed in these experiments, demonstrating that the induction of enhanced burst firing is not mediated by inhibitory neurotransmission (Figure 4.4C). To isolate the effects of excitatory synaptic innervation, we included $GABA_A$ and $GABA_B$ receptor antagonists in all subsequent experiments.

Enhancement of burst firing requires synaptic activation, but not synaptic depolarization or action potential firing

In a variety of brain regions, including the cortex, cerebellum, and hippocampus, synaptic and non-synaptic plasticity have been shown to require postsynaptic depolarization (Malinow and Miller, 1986; Sastry et al., 1986; Mahon et al., 2003; van Welie et al., 2004). Physiologically, this depolarization can be achieved by action potential firing (Christie et al., 1996; Magee and Johnston, 1997), synaptic activation (Golding et al., 2002; Holthoff et al., 2004), or both. We investigated whether these sources of depolarization were necessary for the induction of enhanced burst firing by separating the induction stimulus (TBS) into its synaptic and action-potential components.

The necessity for synaptic activation in the induction of enhanced burst firing was tested by somatically injecting current at 5 Hz for 3 seconds in the absence of synaptic stimulation. This action potential-only stimulus did not induce increased burst firing (Figure 4.5A; Table 4.1), indicating a requirement beyond simple postsynaptic depolarization mediated by somatic action potential firing.

To test the requirement for action potential firing in the induction of enhanced burst firing, axonal afferents were stimulated in the theta-burst pattern (5 synaptic pulses at 100 Hz paired, repeated at 5 Hz, for 3 s) while the soma was voltage-clamped at -72 mV. Experiments were divided into two groups based on whether action potential firing was eliminated, as evidenced by the lack of visually identifiable escape spikes during the recording (no escape spikes, n=9; escape spikes, n=4). Synaptic stimulation during

somatic voltage clamp resulted in enhancement of burst firing regardless of whether escapes spikes were prevented (Figure 4.5B). This increase was indistinguishable from that observed in the control induction group ($p=0.49$, two-factor repeated measures ANOVA; Table 4.1), demonstrating that somatic action potential firing is not necessary for the induction of burst firing enhancement.

Taken together, the results from these two experiments suggest that synaptic activation of dendrites is required for induction of enhanced burst firing, while action potential firing is neither necessary nor sufficient. However, it is likely that dendritic depolarization was incompletely limited during the voltage-clamp experiments. Therefore, to determine whether dendritic depolarization is required for the induction of burst firing enhancement, experiments were performed in the presence of antagonists of ionotropic glutamate receptors (iGluRs; 20 μM CNQX, 50 μM D-AP5, and 20 μM MK-801 to block AMPA and NMDA receptors, respectively). In these experiments, the somatically recorded voltage during TBS was limited to a maximum of two millivolts (average 1.0 ± 0.4 mV; range 0.4 - 2.0 mV) and no action potentials were triggered. Despite this lack of depolarization, burst firing was enhanced to a degree comparable to that observed in control conditions (Figure 4.5C; Table 4.1).

Synergistic activation of mGluR1 and mAChR is required for enhanced burst firing

A likely explanation for the requirement of synaptic activation, but not AMPA or NMDA-receptor mediated depolarization, is that metabotropic (G-protein coupled) receptors are involved in the induction of burst firing enhancement. We tested this

hypothesis by performing experiments in the presence of antagonists for mGluRs or mAChRs.

Co-application of specific antagonists for group I mGluRs (25 μM LY367385 to block mGluR1 and 10 μM MPEP to block mGluR5) blocked the TBS-induced increase in burst firing observed under control conditions (Figure 4.6A; Table 4.1). When applied separately, the mGluR1 antagonist blocked enhancement of burst firing, and, further, revealed a suppression (Figure 4.6B; Table 4.1). On the other hand, when only the mGluR5 antagonist was used, TBS was still able to induce an enhancement of burst firing (Figure 4.6C; Table 4.1). This suggests that synaptic activation of mGluR1 is required to induce an increase in burst firing, while mGluR5 activation is involved in mediating a decrease.

Application of a general mAChR antagonist (atropine, 10 μM) also blocked an enhancement and revealed a suppression of burst firing (Figure 4.7A). This implies that mAChRs must be activated in addition to mGluRs to induce burst firing enhancement. To explore which mAChR subtype mediates this enhancement, we performed experiments in the presence of an M_1-subtype specific mAChR antagonist (telenzipine, 50 nM). In this condition, induction of enhanced burst firing was prevented (Figure 4.7B). Taken together, these results suggest that activation of the M_1-subtype of mAChRs, in addition to activation of mGluR1, is required for the synaptically-induced enhancement of burst firing.

mGluR1 and M_1 are members of the G-protein-coupled receptor superfamily, and more specifically, both couple to phospholipase C (PLC) activation via the stimulatory

subunit $G_{q\alpha}$. To test the involvement of PLC in an intracellular signaling cascade leading to the induction of burst firing enhancement, a PLC inhibitor (U-73122, 25 μM) was bath-applied to the slice. Under this condition, the increase in burst firing was blocked, and a suppression of burst firing was revealed (Figure 4.8A), suggesting that mGluR1 and/or M_1 act via a PLC-dependent pathway to result in burst firing enhancement. Furthermore, these data argue that PLC activation is not required for burst firing suppression.

PLC catalyzes the breakdown of phosphotidylinositol 4,5-bisphosphate (PIP_2) in the cellular membrane into two reaction products: diacylglycerol (DAG), which remains membrane bound, and inositol-1,4,5-triphosphate (IP_3), which diffuses through the cytosol. IP_3 activates IP_3 receptors on the endoplasmic reticulum, causing release of Ca^{2+} from internal stores. To test the requirement of this Ca^{2+} release in the induction of burst firing enhancement, we depleted internal stores by including a Ca^{2+}-ATPase inhibitor (thapsigargin, 2 μM) in the internal recording solution. When TBS was applied in the presence of the Ca^{2+}-ATPase inhibitor, no increase in burst firing was induced (Figure 4.8B, red circles). As a control, we recorded burst firing in the absence of TBS and observed no time-dependent effects of the Ca^{2+}-ATPase inhibitor on burst firing (Figure 4.8B, black squares). One possibility that may explain these results is that stimulus-evoked release of Ca^{2+} from internal stores is required for the induction of burst firing enhancement.

To determine whether intracellular Ca^{2+} elevation is required for the induction of burst firing enhancement, we included a fast Ca^{2+} chelator (1,2-bis(2-

aminophenoxy)ethane N,N,N,N-tetraacetic acid (BAPTA), 10 mM) in the internal solution. When TBS was applied in the presence of the Ca^{2+} chelator, no enhancement of burst firing was observed (Figure 4.8C, red circles), suggesting that elevation of intracellular Ca^{2+} is required for induction. We also performed control experiments in which burst firing was monitored in the absence of TBS to ensure that there were no time-dependent effects of recording with the Ca^{2+} chelator (Figure 4.8C, black squares). In addition to a lack of burst firing enhancement in the Ca^{2+}-ATPase inhibitor and the Ca^{2+} chelator experiments, no decrease in burst firing was observed suggesting further that induction of burst firing suppression may depend on a rise in intracellular Ca^{2+} concentration, perhaps through release from internal stores.

The results of all experimental manipulations are summarized in Figure 4.9. Groups are color-coded according to one of four conditions: 1. black - no synaptic stimulation during induction, 2. green - synaptic stimulation during induction, resulting in an enhancement of burst firing; 3. red - synaptic stimulation during induction, resulting in a suppression of burst firing; and 4. grey - synaptic stimulation during induction, resulting in no change in burst firing.

A confound in distinguishing the magnitude and direction of burst plasticity, however, is that, in all experimental groups, there was a decrease in action potential threshold (Figure 4.10A) and an increase in the subthreshold voltage response (Figure 4.10B). Either of these changes would be predicted to enhance the neuron's ability to generate bursts of action potentials, exaggerating an enhancement or masking a suppression of burst firing. To quantitatively investigate the relationship between action

potential threshold, subthreshold response, and change in burst firing for each of the four conditions described above, we plotted normalized burst firing against change in action potential threshold (Figure 4.10A_3) and normalized burst firing against normalized subthreshold response (Figure 4.10B_3). The slopes of the best-fit lines were not different from each other, indicating that the strength of the relationship between burst firing and action potential threshold or burst firing and subthreshold response was not different in these conditions (linear regression: $p=0.39$ for action potential threshold; $p=0.21$ for subthreshold response). From these results, one would predict that a given change in action potential threshold or subthreshold voltage response would have an equivalent impact on the burst firing in each condition; in this case, the data for each population would overlap on the graphs of normalized burst firing versus normalized change in action potential threshold and normalized burst firing versus normalized change in subthreshold voltage response. However, the populations do not overlap, which can be quantified by measuring the y-intercept for each best fit line. For both action potential threshold and subthreshold response, there was a difference in elevation of the best-fit lines (linear regression: $p<0.0001$ for action potential threshold; $p<0.0001$ for subthreshold response), which indicates that the magnitude of burst firing enhancement is greater than what can be explained simply by a change in either of these parameters. Therefore, neither a decrease in action potential threshold nor an increase in subthreshold excitability can fully account for the mechanism underlying burst plasticity. Taken together, these results indicate that voltage-gated conductances other than those involved in setting action potential threshold (primarily Na^+ channels) or those active at resting

membrane potentials (such as the "leak" K^+ current), which influence the subthreshold voltage response, must be involved in the induction of burst plasticity.

Theta-burst stimulation increases neuronal excitability in response to a noisy stimulus

To determine the effect of TBS on neuronal excitability in response to a more physiologically relevant stimulus, a noisy current injection (see Methods) was used to evoke action potential firing (Figure 4.11). We plotted a histogram of inter-spike intervals (ISIs) before (black) and after (red) TBS, which revealed two separate populations reflecting different action potential firing patterns. Short ISIs (< 40 ms) were indicative of burst firing, while long ISIs (> 40 ms) reflected single action potentials. One effect of TBS was to increase the overall number of action potentials evoked (for example, a previously subthreshold current injection subsequently reached threshold for an action potential; Figure 4.11B). This increase was reflected in the histogram as an increase in the number of events with long ISIs.

Burst firing responses, which constituted the majority of events, could be further characterized based on the appearance of two distinct peaks in the short-ISI population. The narrower peak contained the shortest ISI values (4-6 ms), which corresponds to the interval between the first and second action potentials in a burst. A broader peak contained a range of longer ISI values (6-40 ms), which represents the interval between additional action potentials in a burst. Following TBS, the number of events with the shortest ISIs did not increase, suggesting that there was no increase in the number of burst events (for example, by conversion of a single action potential into a burst).

However, the number of burst events that included ISIs in the broader peak increased, indicating that, on average, there were more action potentials per burst. This suggests that the nature and timing of inputs to subicular pyramidal neurons (i.e. brief but strong input sufficient to reach action potential threshold versus weaker input arriving during periods of rhythmic oscillations) may be differently affected by TBS; repetitive, strong inputs are likely to generate more burst firing, while weaker inputs are likely to boost the effective release probability of the neuron because more action potentials per burst are generated. Thus, the TBS-induced increase in neuronal excitability was expressed both as a global increase in the probability of reaching threshold for action potential firing, as well as a specific increase in the strength of burst firing.

Discussion

The results of these experiments suggest that theta-burst patterned synaptic stimulation induces a long-term change in the firing of intrinsically bursting pyramidal neurons in the subiculum. This form of plasticity requires synaptic activation of mGluRs and mAChRs, but does not require synaptic activation of AMPA or NMDA-type glutamate receptors, synaptic depolarization, or action potential firing. When mGluR1 or mAChRs are blocked, an activity-dependent suppression of burst firing is observed, which may be mediated by activation of mGluR5. Because bursts are not synaptically driven in these experiments, but are elicited by direct somatic current injection, the observed increases and decreases in burst firing must be caused by alterations in voltage- and/or calcium-activated conductances. Therefore, these experiments demonstrate, for the

first time, activity-dependent bidirectional regulation of intrinsic firing in pyramidal neurons of the subiculum.

Comparison to other forms of non-synaptic plasticity

The burst plasticity we describe here differs markedly from other types of non-synaptic plasticity reported in the literature. Bliss and Lømo's (1973) initial report of activity-dependent changes in synaptic strength also noted an increase in the amplitude of the population spike that was larger than what could be accounted for simply by the increase in EPSP amplitude. There is some evidence to suggest alterations in intrinsic excitability underlie this increased firing probability, referred to as EPSP-to-spike (E-S) potentiation (Chavez-Noriega et al., 1990; Jester et al., 1995; Liao et al., 1995). However, E-S potentiation is mostly blocked by GABA antagonists, and therefore thought to be primarily a result of decreased feedforward inhibition (Gustafsson et al., 1987; Chevaleyre and Castillo, 2003; Cooper et al., 2003). Burst plasticity persists in the presence of antagonists of both $GABA_A$ and $GABA_B$, so changes in network connectivity are unlikely to underlie the observed changes in burst firing. Furthermore, a recent report (Campanac and Debanne, 2007) demonstrates, in the presence of GABAergic antagonists, a change in E-S coupling of CA1 pyramidal cells that occurs together with spike timing-dependent synaptic plasticity, which appear to be mediated by the same induction pathway.

A stronger link between alterations in firing properties and voltage-gated conductances has been demonstrated in cell culture. Chronic isolation from physiological

excitatory inputs resulted in a persistent switch in the firing pattern, from tonic firing to burst firing, during a sustained depolarizing current (Turrigiano et al., 1994). More rapid induction of non-synaptic plasticity was demonstrated in acute cerebellar slices, where high-frequency synaptic stimulation resulted in an increase in the number of action potentials elicited by a depolarizing current step (Aizenman and Linden, 2000). In hippocampal slices, direct depolarization and synaptic stimulation of CA1 pyramidal cells produces local changes in the intrinsic excitability of stimulated dendritic regions within SR (Frick et al., 2004; van Welie et al., 2004). In one study, depolarization combined with cholinergic activation, via the agonist carbachol, induced an increase in the voltage and Ca^{2+} signal produced by distinct dendritic branches (Losonczy et al., 2008). Another previous study showed that an increase in excitability mediated by downregulation of the after-hyperpolarization (AHP) in CA1 pyramidal neurons requires co-activation of glutamatergic and ß-adrenergic receptors (Faas et al., 2002). *In vivo*, training on a hippocampus-dependent trace eye-blink conditioning task results in reduction of the AHP of CA1 neurons in animals that are able to successfully learn the paradigm (i.e. to blink after a tone presentation, but before a puff of air is delivered to the eye) (Moyer et al., 1996). Animals that do not perform this behavior correctly do not display a decreased AHP. However, a reduction in the AHP is not necessary for the expression of the learned behavior because the amplitude of the AHP returns to levels indistinguishable from control, pseudo-conditioned, and non-learners after approximately 7 days, while correct performance on the task (in those animals that learned the paradigm) is exhibited for months, or even years. Together, these results suggest that a

reduction in AHP amplitude is required to learn this hippocampus-dependent task, but is not involved in the storage or retrieval of memory for the paradigm. Intriguingly, this effect is enhanced by upregulation of cholinergic innervation (Disterhoft and Matthew Oh, 2003).

Our experiments complement these previous reports of non-synaptic plasticity by demonstrating a robust change in the firing pattern of subicular pyramidal neurons produced by a protocol resembling firing patterns observed during behavioral tasks that activate the hippocampus, such as exploratory behavior or learning a spatial task. The robust nature of this plasticity suggests that the subiculum can dramatically change its output following activity-dependent modulation of voltage- and/or Ca^{2+}-activated conductances. Furthermore, the requirement for co-activation of glutamatergic and cholinergic receptors suggests the possibility that this form of plasticity could contribute to associative or state-dependent learning mechanisms.

Comparison to synaptic plasticity

A number of features suggest that burst plasticity is distinct from synaptic plasticity in the subiculum. First, the time course of development for burst plasticity is slower than that of synaptic plasticity. This result indicates that the expression of burst plasticity is likely mediated by an intracellular signaling cascade that results in changes in the biochemical state of target proteins (such as ion channels), rather than a fast, diffusion-limited mechanism such as diffusion of ionic receptors (like the AMPAR) into the synapse. Second, synaptic plasticity is blocked by NMDA receptor antagonists, but

burst plasticity is not, demonstrating that synaptic and intrinsic plasticity can be differentially regulated, and suggesting that distinct mechanisms underlie their induction. Third, the requirement for synaptic depolarization and/or action potential firing, which have been well documented for many forms of synaptic plasticity (Kelso et al., 1986; Gustafsson et al., 1987; Golding et al., 2001), is absent for burst plasticity. Rather, the induction of enhanced burst firing requires synergistic activation of at least two metabotropic receptor types (mGluR1 and M_1). The plasticity induction paradigm used in these experiments, when no pharmacological manipulations are present, results in both increased synaptic strength and increased non-synaptic excitability. However, there are likely other induction protocols *in vitro* and behavioral states *in vivo* where activity-dependent synaptic and non-synaptic plasticity may interact in more complex ways to modulate subicular output. For example, hippocampal activity in the absence of medial septal activation could lead to suppression of burst firing. Thus, burst plasticity provides an additional mechanism, complementary to synaptic plasticity, by which subicular pyramidal neurons can modify their properties and influence adaptive behaviors contributing to learning and memory.

Signal transduction mechanisms for induction of burst plasticity

A remarkable feature of burst firing enhancement in the subiculum is the necessity for activation of both mGluR1 and M_1 receptors. Several scenarios could explain this requirement. One possibility is that presynaptic receptors for one transmitter may affect the release of the other. For example, activation of mGluR1 receptors on

cholinergic terminals may be required to permit or promote release of acetylcholine (ACh). Postsynaptically, these receptor subtypes may also interact in complex ways. One example is that different metabotropic receptors have been shown to form heteromers (Enz, 2007). In particular, heteromeric interactions of adenosine or $GABA_B$ receptors with mGluR1 have been reported to regulate transmembrane currents (Ciruela et al., 2001; Tabata et al., 2007). Another possibility is that each receptor subtype is coupled to separate signaling pathways, both of which are required to induce plasticity, or that different subcellular locations of these receptor subtypes recruit signaling pathways in specific neuronal compartments. For example, the actions of mGluR1 and M_1 have been shown to activate extracellular signal-regulated kinase (ERK) in different cellular compartments (Berkeley et al., 2001). Alternatively, activation of postsynaptic mGluR1 and M_1 receptors may converge on a common intracellular signaling pathway to produce a higher level of a critical second messenger. One prediction of such a mechanism is that elevated levels of glutamate or ACh may produce comparable effects on burst firing, even in the absence of synergism. Thus, burst plasticity may require activation of CA1 and/or EC (leading to glutamate release in the subiculum) in addition to activation of the septal nucleus to stimulate release of ACh, or may be induced when either region is more strongly activated. Furthermore, activation of these two receptor types may be sufficient to induce burst plasticity, or they may be necessary but not sufficient. For example, activation of additional receptors could also be required. Although stimulation of afferent fibers in a hippocampal slice may result in release of multiple neurotransmitters, release of different neurotransmitters *in vivo* is likely related to behavioral state.

It is possible that synaptic activation is required to release glutamate, but not ACh, and that basal levels of ACh are sufficient to induce burst plasticity (or, vice versa, that stimulation is required to release ACh, but that basal levels of glutamate are sufficient to induce burst plasticity). This question is difficult to address because, in hippocampal slices, an extracellular stimulating electrode is likely to recruit both glutamatergic and cholinergic release. An antagonist of either receptor blocks the effects of stimulated neurotransmission, but also blocks the effects of basal levels of the neurotransmitter. On the other hand, application of agonists for either receptor type may result in supraphysiological activation and could overcome the requirement for synaptic activation to stimulate release of the other neurotransmitter.

Activation of group I mGluRs and some mAChRs (specifically M_1, M_3, and M_5) releases the $G_{q\alpha}$ subunit, which in turn activates PLC, producing two second messengers: DAG and IP_3. These can directly activate ion channels or cause Ca^{2+} release from intracellular stores. Additionally, they may activate protein kinases such as protein kinase C (PKC) and ERK, which have been shown to play critical roles in synaptic plasticity. Other signal transduction mechanisms may also be involved since activation of mGluR1 and mGluR5, which are both coupled to $G_{q\alpha}$ and PLC, did not have equivalent roles in the induction of burst plasticity. Indeed, it is somewhat surprising that the enhancement of burst firing depends on mGluR1 activation, as immunohistological studies show no or very little staining for mGluR1 in CA1 or the subiculum, while mGluR5 is abundantly expressed (Fotuhi et al., 1994; Shigemoto et al., 1997). Nevertheless, there are a number of electrophysiological studies that report mGluR1-mediated effects in CA1 pyramidal

neurons that are distinct from those observed when mGluR5 is activated alone (Volk et al., 2006; Chaouloff et al., 2007).

In some conditions, when the induction of enhanced burst firing is blocked, a suppression of burst firing is revealed. Because this suppression is not observed in experimental groups that did not receive synaptic stimulation (no-induction and action potentials-only groups), it is likely that suppression of burst firing reflects recruitment of an additional activity-dependent process. Our data suggest that the decreased burst firing depends on synaptically-mediated stimulation of mGluR5, although we can not rule out the possibility that other receptor types also contribute to the induction of burst firing suppression.

Candidate mechanisms for the expression of burst plasticity

An obvious question is which conductances are altered to produce the observed changes in burst firing. Analysis of the bursting responses before and after TBS has yielded few clues as to the nature of the affected conductances, so further work will be required to address this question. Possible candidates that should be considered include voltage-gated Ca^{2+} conductances that drive the ADP following spikes (Su et al., 2001; Metz et al., 2005), voltage-gated Na^{+} conductances that drive spiking and may also affect the ADP (Azouz et al., 1996), and voltage- and/or Ca^{2+}-activated K^{+} channels that may affect spiking, the ADP, and the slow AHP following bursts (Rhoades and Gross, 1994; Staff et al., 2000; Jung et al., 2001; Golomb et al., 2006; Metz et al., 2007). Other types of channels, such as Ca^{2+}-activated non-specific cation channels, including members of

the transient receptor potential (TRP) channel family, are also possible candidates. In addition to simple up- or down-regulation of these channel types, shifts in properties such as slow inactivation of Na^+ channels, which has been shown to affect repetitive burst firing in the subiculum (Cooper et al., 2005), must also be considered.

Functional significance of burst plasticity

Burst firing has been observed in a variety of brain regions and has been posited to play a number of roles. At central nervous system synapses, bursts of two action potentials increase the probability of release per event from 10-50% to over 90% (Stevens and Wang, 1995; Lisman, 1997). Therefore, upregulation of burst firing may represent a relative increase in the strength of a particularly important or salient stimulus, allowing activity to propagate more reliably through the network. Hippocampal sharp-wave bursts are associated with the transition between neocortical down- and up-states (Battaglia et al., 2004), thought to be related to the transition between quiescence and alertness, and can also drive down-to-up state transitions in the nucleus accumbens (Lape and Dani, 2004). In this context, an increase in burst firing in the subiculum may be important in driving transitions between operational states of downstream target regions, particularly because the subiculum is the major output of the hippocampus. In addition, bursts from place cells in the hippocampus provides a more accurate spatial map than all firing considered together (Otto et al., 1991). Likewise, bursts in visual cortex provide more information about the stimulus than do single action potentials (Cattaneo et al.,

1981b, 1981a; Livingstone et al., 1996). Thus, increased burst firing may help to refine cortical maps by strongly, but selectively, activating particular neuronal connections.

Regulation of burst firing may also be important in learning and memory. Increased burst firing in presynaptic neurons increases postsynaptic responsiveness of synaptically connected cells. Increased burst firing in postsynaptic neurons contributes further dendritic and somatic depolarization. Both these changes could result in an increase in correlated activity, which may be a crucial feature contributing to Hebbian synaptic plasticity. Indeed, postsynaptic bursting has been shown to enhance long-lasting synaptic plasticity, such as long-term potentiation (Pike et al., 1999; O'Connor et al., 2005). The requirement for cholinergic activation suggests that increases in burst firing could contribute to learning, as cholinergic activation is well known to enhance learning (Disterhoft et al., 1999; Power et al., 2003). Conversely, activation of the subiculum in the absence of cholinergic modulation could lead to a reversal of burst plasticity and may impede memory formation or retrieval.

Abnormal upregulation of burst firing may contribute to diseases that manifest as hyperexcitability. In acute brain slices from normal rats, seizure-like events were initiated in the subiculum, and maintained even when disconnected from the CA and EC regions (Dreier and Heinemann, 1991; Behr and Heinemann, 1996). In rat models of epilepsy, this type of activity in the subiculum can spread to other structures, including CA1 and the EC (Kemppainen et al., 2002; Benini and Avoli, 2005). Tissue from human patients with temporal lobe epilepsy also demonstrated spontaneous electrical activity initiated in

the subiculum, as well as synaptic and cellular changes associated with increased spontaneous activity (Cohen et al., 2002; Wozny et al., 2005). Therefore, activity-dependent increases in burst firing, such as those demonstrated here, although likely to contribute to normal functioning of the subiculum, may also increase susceptibility to seizure-like activity and influence the propagation of seizure activity to other areas.

Taken together, these results demonstrate a novel form of plasticity, distinct from synaptic plasticity, in burst firing neurons of the subiculum. The ability to increase or decrease burst firing in response to physiologically relevant activity patterns may represent a complementary cellular mechanism for the recognition, coding, and storage of hippocampus-dependent information.

Figures

Figure 4.1 Experimental protocol used to study plasticity of excitability in subicular pyramidal neurons.

Scale bars in A apply to A-C and are 20 mV and 100 ms (A,C) or 150 ms (B). Inset scale bars in A apply to all insets in A and C and are 20 mV and 5 ms. Scale bars in D also apply to E, and are 20 mV and 5 ms.

A. Voltage trace (*top*) from a representative subicular pyramidal neuron illustrating the response to synaptic stimulation (*middle*) followed by somatic current injection (*bottom*). Somatic current injection consisted of a train of 10 EPSC-like pulses. Hash marks indicate a 500 ms waiting period between the end of the synaptic stimulation and the beginning of the train. Note that action potential firing is evoked by somatic current injections alone. Dots above the voltage trace signify burst responses. Insets show a magnified view of responses to the 1^{st}, 6^{th}, and 10^{th} current injections. **B.** Voltage trace (*top*) recorded during TBS (induction stimulus). TBS consisted of 5 synaptic pulses at 100 Hz (*middle*) paired with 1 somatic current injection (*bottom*), repeated at 5 Hz for 3 s. **C.** Voltage trace (*top*) from the same neuron in response to the same stimuli as in A, 30 minutes after TBS. **D.** Magnification of insets from A. **E.** Magnification of insets from C.

Figure 4.1

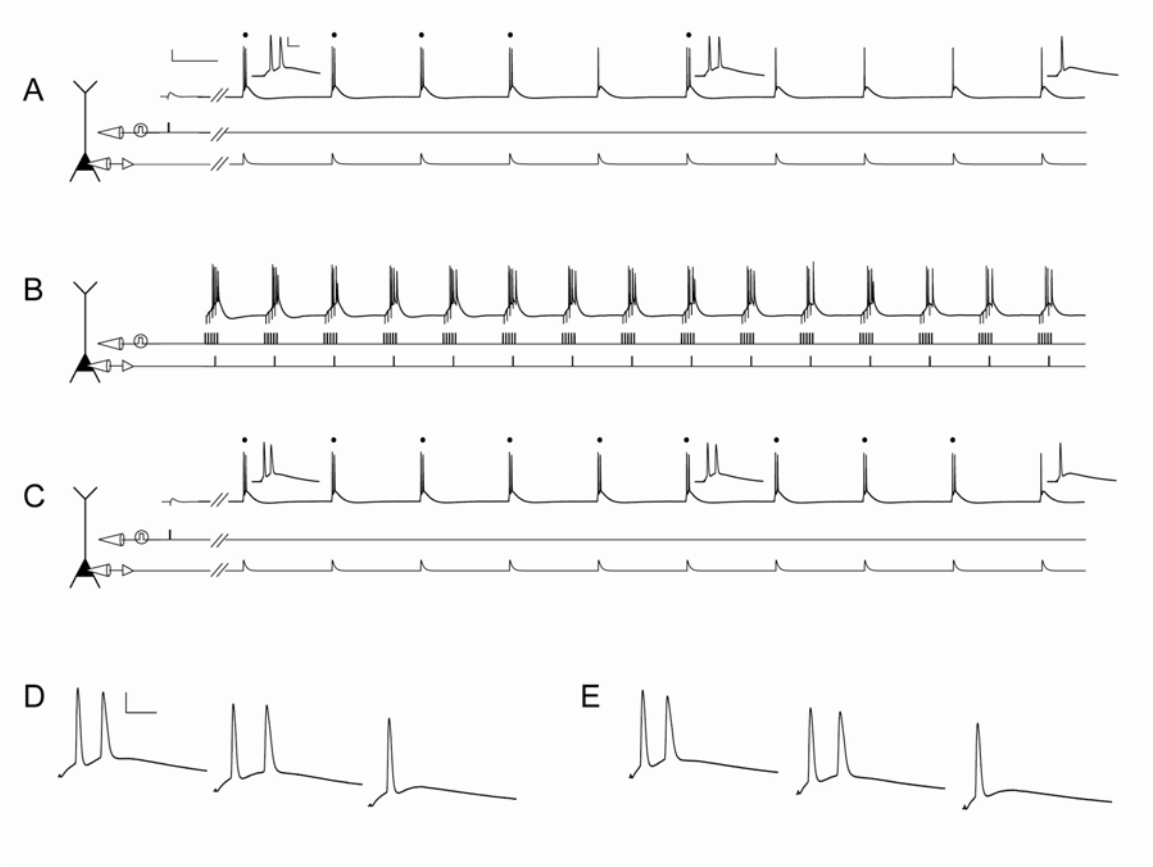

Figure 4.2 Representative traces recorded during TBS under different experimental conditions.

In all panels, the trace recorded (*red*) in response to the induction stimulus (*black*) is shown. All traces were recorded in current-clamp mode, except C. when the soma was voltage-clamped during induction. Note escape spikes are clearly distinguishable, allowing experiments where somatic voltage clamp was ineffective at preventing action potential firing during induction to be easily detected. In E., the induction stimuli *(bottom, black)* and scale bars apply to all conditions shown.

Figure 4.2

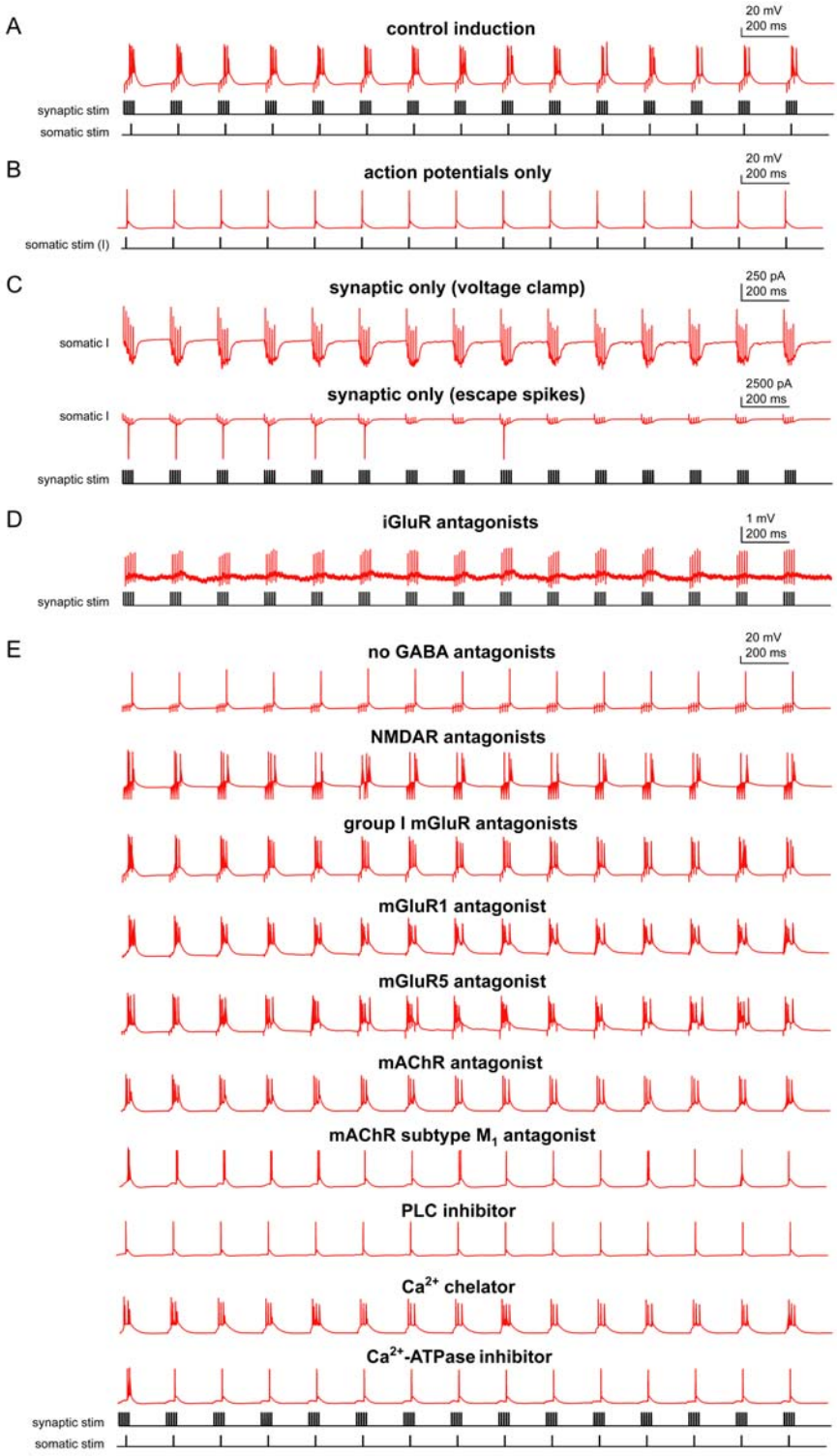
A
control induction
20 mV
200 ms
synaptic stim
somatic stim
B
action potentials only
20 mV
200 ms
somatic stim (I)
C
synaptic only (voltage clamp)
250 pA
200 ms
somatic I
synaptic only (escape spikes)
2500 pA
200 ms
somatic I
synaptic stim
D
iGluR antagonists
1 mV
200 ms
synaptic stim
E
no GABA antagonists
20 mV
200 ms
NMDAR antagonists
group I mGluR antagonists
mGluR1 antagonist
mGluR5 antagonist
mAChR antagonist
mAChR subtype M1 antagonist
PLC inhibitor
Ca2+ chelator
Ca2+-ATPase inhibitor
synaptic stim
somatic stim

Figure 4.3 Synaptic plasticity in subicular pyramidal neurons depends on NMDAR activation.

For both graphs, dotted lines indicate the average EPSP amplitude for the 10-minute baseline period. Arrows indicate when TBS was given. Asterisks indicate a significant effect of time, repeated measures ANOVA: **$p<0.01$.

Left graph: Small open circles (*black*) indicate the EPSP amplitude in response to synaptic stimulation, which was given every 20 seconds. Large open circles (*red*) represent the average EPSP amplitude for each 10-minute period. Error bars are ± standard deviation. Inset shows representative traces before *(left)* and 33 minutes after *(right)* TBS was given. *Right graph:* Group data showing the average EPSP amplitude for each 10-minute period when no TBS was given (*filled black squares*; n=4), when TBS was given in control conditions (*filled red circles*; n=7), or when TBS was given in the presence of N-methyl-D-aspartate receptor (NMDAR) antagonists (*filled blue triangles*; n=4). Error bars are ± s.e.m.

Figure 4.3

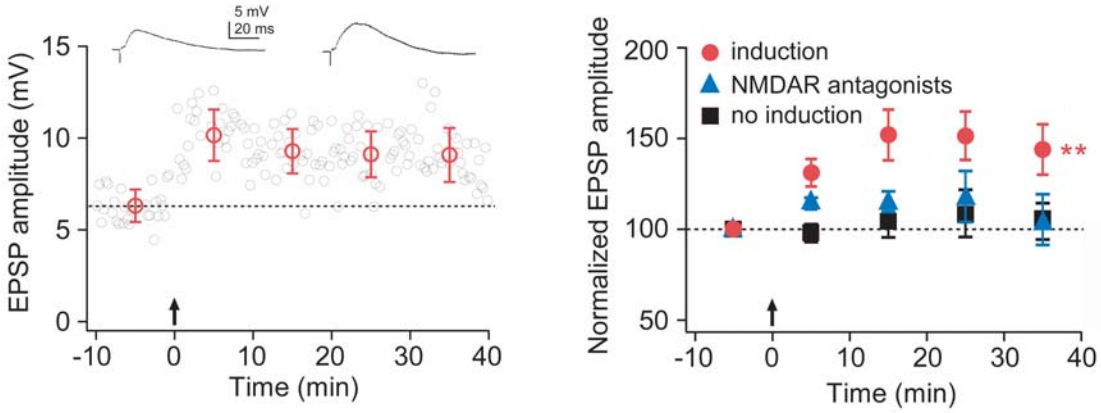
5 mV
20 ms
EPSP amplitude (mV)
15
10
5
0
-10
0
10
20
30
40
Time (min)
Normalized EPSP amplitude
200
150
100
50
induction
NMDAR antagonists
no induction
**
-10
0
10
20
30
40
Time (min)

Figure 4.4 TBS results in an enhancement of burst firing that does not require NMDA or GABA receptor activation.

For all representative-experiment graphs *(left column)*, small open circles (*black*) indicate the number of burst firing responses evoked by a train of 10 EPSC-like somatic current injections. The train was delivered every 20 seconds. Large open circles (*red*) represent the average number of burst firing responses per train for each 10-minute period. Error bars are ± standard deviation. For all group-data graphs *(right column)*, filled symbols represent the average number of burst firing responses per train for each 10-minute period. Error bars are ± s.e.m. For all graphs, dotted lines indicate the average number of burst firing responses per train for the 10-minute baseline period. Arrows indicate when TBS (induction) was given. Asterisks signify a significant effect of time, repeated measures ANOVA: ***$p<0.001$, ****$p<0.0001$.

A. Representative *(left)* and group (*right, red circles;* n=10) data from experiments in which TBS was given in control conditions. Group data (*right, black squares*; n=9) are also shown for experiments in which no TBS was given. **B.** Representative *(left)* and group *(right*; n=8) data from experiments in which TBS was given in the presence of N-methyl-D-aspartate receptor (NMDAR) antagonists (50 μM D-AP5 and 20 μM MK-801) **C.** Representative *(left)* and group (*right*; n=8) data from experiments in which TBS was given in the presence of no γ-aminobutyric acid (GABA) receptor antagonists (standard ACSF only).

Figure 4.4

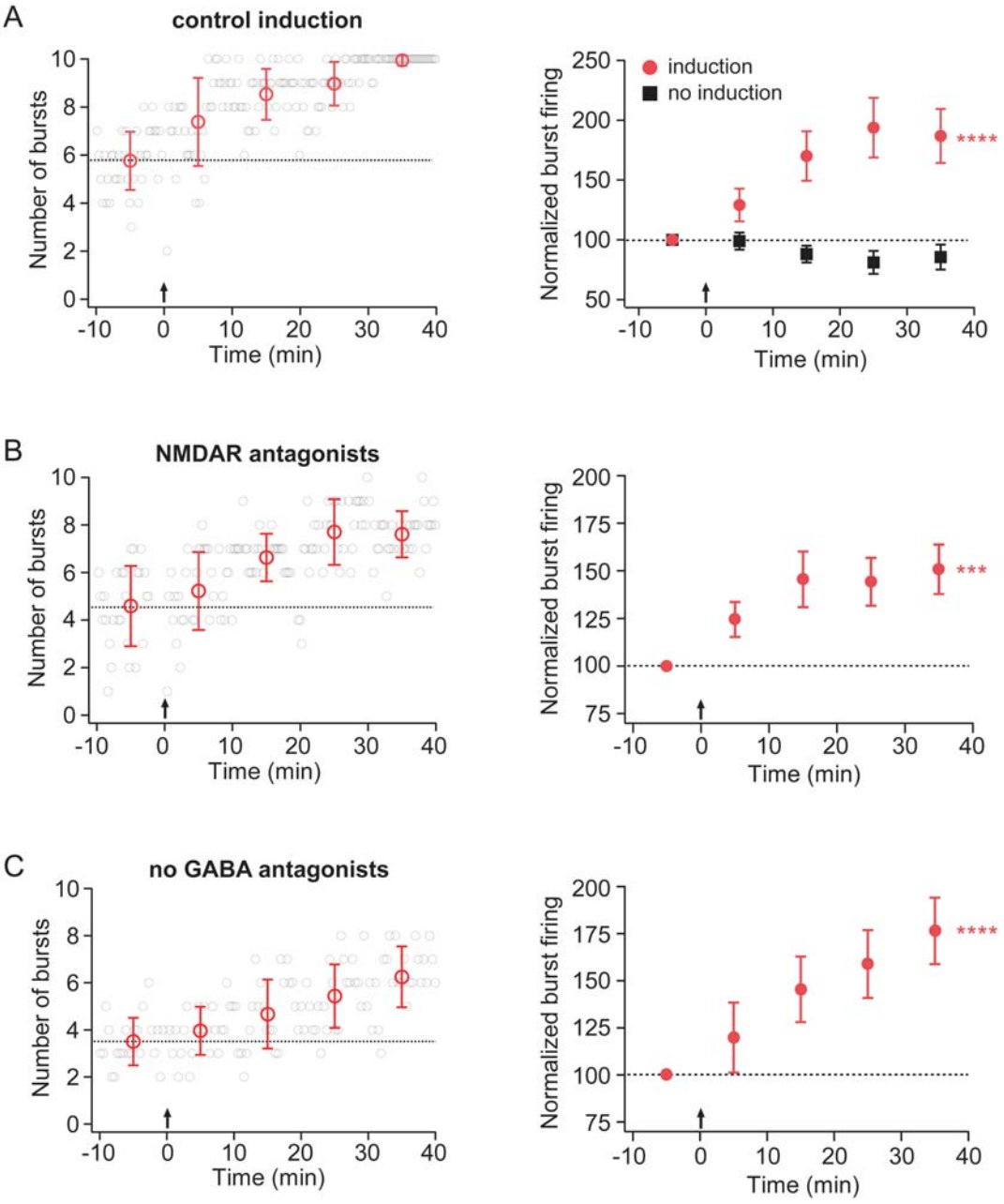
A
control induction
Number of bursts
Time (min)
induction
no induction
Normalized burst firing
****
B
NMDAR antagonists
***
C
no GABA antagonists
****

Figure 4.5 Synaptic stimulation alone is sufficient to induce an enhancement of burst firing.

For all representative-experiment graphs *(left column)*, small open circles (*black*) indicate the number of burst firing responses evoked by a train of 10 EPSC-like somatic current injections. The train was delivered every 20 seconds. Large open circles (*red*) represent the average number of burst firing responses per train for each 10-minute period. Error bars are ± standard deviation. For all group-data graphs *(right column)*, filled symbols represent the average number of burst firing responses per train for each 10-minute period. Error bars are ± s.e.m. For all graphs, dotted lines indicate the average number of burst firing responses per train for the 10-minute baseline period. Arrows indicate when TBS (induction) was given. Asterisks signify a significant effect of time, repeated measures ANOVA: *$p<0.05$, **$p<0.01$, ***$p<0.001$.

A. Representative *(left)* and group (*right*; n=18) data from experiments in which the induction stimulus consisted only of somatic current injections to evoke action potential firing. **B.** Representative *(left)* and group *(right)* data from experiments in which the induction stimulus consisted of synaptic stimulation during somatic voltage clamp (at -72 mV). In the group data, red circles indicate experiments in which somatic voltage clamp was effective at preventing action potential firing (n=9); blue triangles indicate experiments in which escape spikes were observed (n=4). **C.** Representative *(left)* and group (*right*; n=4) data from experiments in which TBS was given in the presence of ionotropic glutamate receptor (iGluR) antagonists (20 μM CNQX, 50 μM D-AP5, and 20 μM MK-801).

Figure 4.5

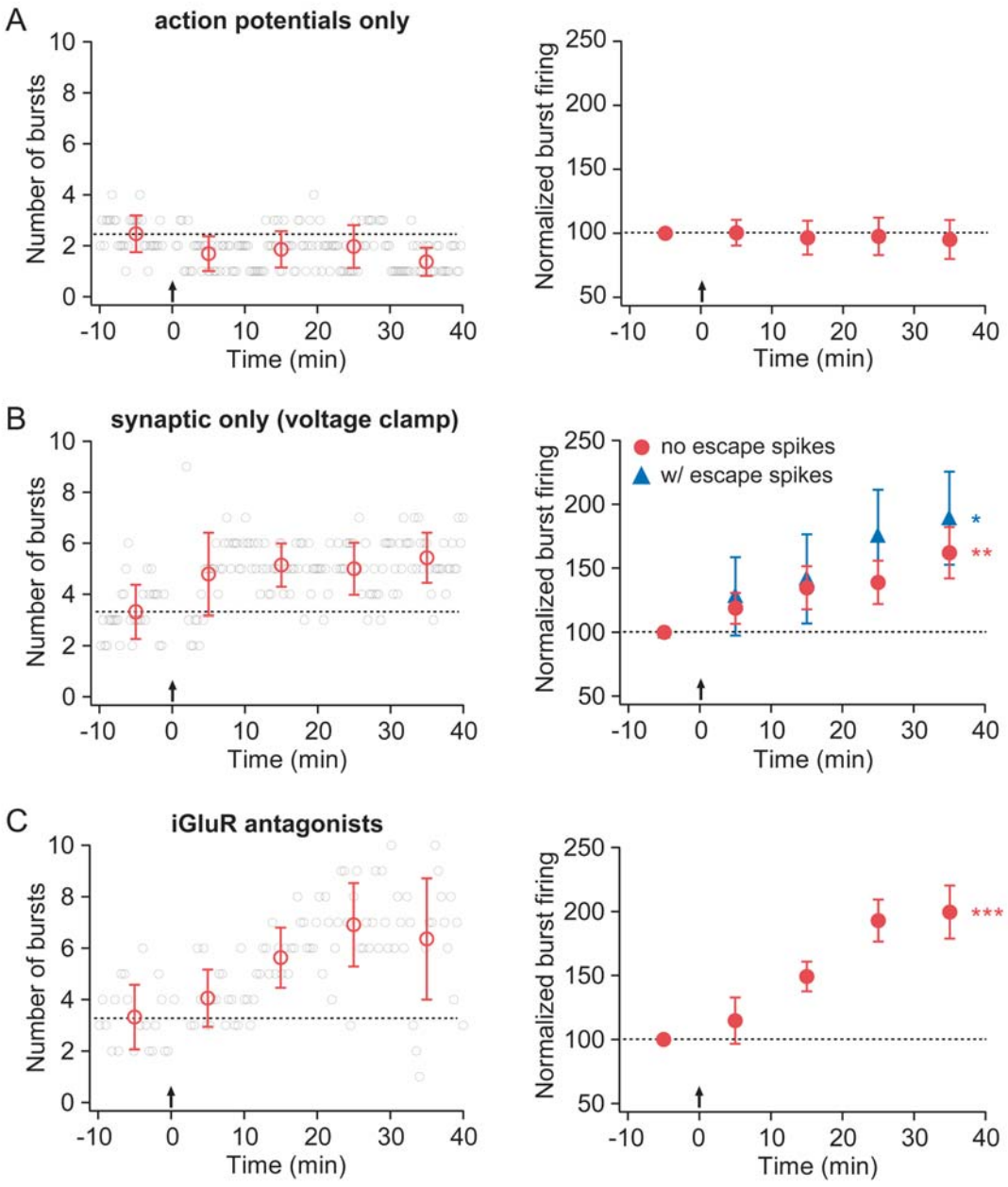
A
action potentials only
Number of bursts
Normalized burst firing
Time (min)
B
synaptic only (voltage clamp)
no escape spikes
w/ escape spikes
*
**
C
iGluR antagonists
***

Figure 4.6 Activation of mGluR1 is required for enhancement of burst firing while activation of mGluR5 promotes suppression of burst firing.

For all representative-experiment graphs *(left column)*, small open circles (*black*) indicate the number of burst firing responses evoked by a train of 10 EPSC-like somatic current injections. The train was delivered every 20 seconds. Large open circles (*red*) represent the average number of burst firing responses per train for each 10-minute period. Error bars are ± standard deviation. For all group-data graphs *(right column)*, filled symbols represent the average number of burst firing responses per train for each 10-minute period. Error bars are ± s.e.m. For all graphs, dotted lines indicate the average number of burst firing responses per train for the 10-minute baseline period. Arrows indicate when TBS (induction) was given. Asterisks signify a significant effect of time, repeated measures ANOVA: **$p<0.01$, ***$p<0.001$.

A. Representative *(left)* and group (*right*; n=8) data from experiments in which TBS was given in the presence of group I mGluR antagonists (25 μM LY367385 and 10 μM MPEP). **B.** Representative *(left)* and group (*right*; n=9) data from experiments in which TBS was given in the presence of the metabotropic glutamate receptor, subtype 1 (mGluR1) antagonist alone (25 μM LY367385). **C.** Representative *(left)* and group (*right*; n=5) data from experiments in which TBS was given in the presence of the metabotropic glutamate receptor, subtype 5 (mGluR5) antagonist alone (10 μM MPEP).

Figure 4.6

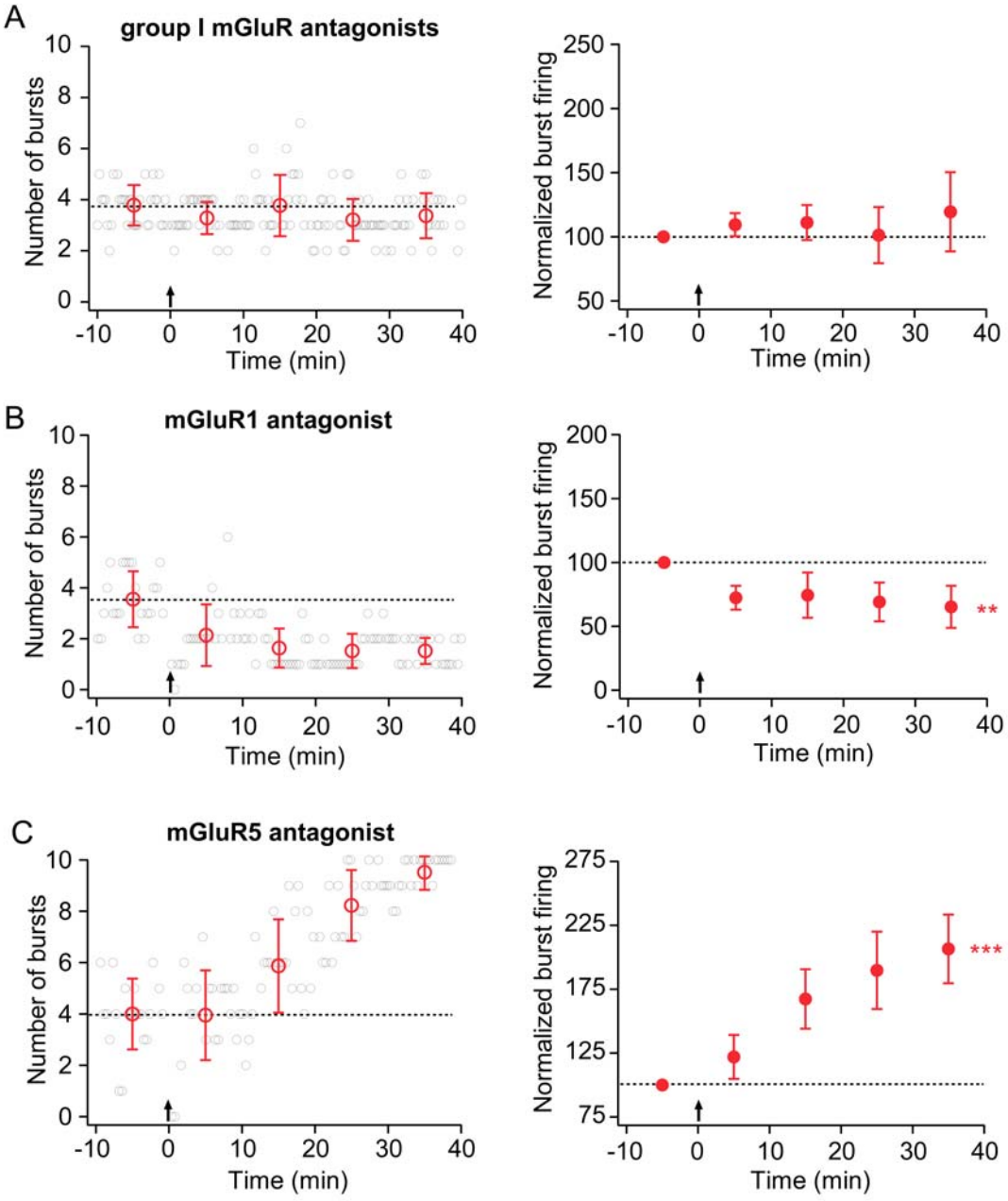
A
group I mGluR antagonists
Number of bursts
Time (min)
Normalized burst firing
Time (min)
B
mGluR1 antagonist
Number of bursts
Time (min)
Normalized burst firing
**
Time (min)
C
mGluR5 antagonist
Number of bursts
Time (min)
Normalized burst firing
***
Time (min)

Figure 4.7 Activation of M_1 mAChRs is required for enhancement of burst firing.

For all representative-experiment graphs *(left column)*, small open circles (*black*) indicate the number of burst firing responses evoked by a train of 10 EPSC-like somatic current injections. The train was delivered every 20 seconds. Large open circles (*red*) represent the average number of burst firing responses per train for each 10-minute period. Error bars are ± standard deviation. For all group-data graphs *(right column)*, filled symbols represent the average number of burst firing responses per train for each 10-minute period. Error bars are ± s.e.m. For all graphs, dotted lines indicate the average number of burst firing responses per train for the 10-minute baseline period. Arrows indicate when TBS (induction) was given. Asterisks signify a significant effect of time, repeated measures ANOVA: ***$p<0.001$.

A. Representative *(left)* and group (*right*; n=6) data from experiments in which TBS was given in the presence of the muscarinic acetylcholine receptor (mAChR) antagonist atropine (10 μM). **B.** Representative *(left)* and group (*right*; n=5) data from experiments in which TBS was given in the presence of the specific M_1 subtype mAChR antagonist, telenzipine (50 nM).

Figure 4.7

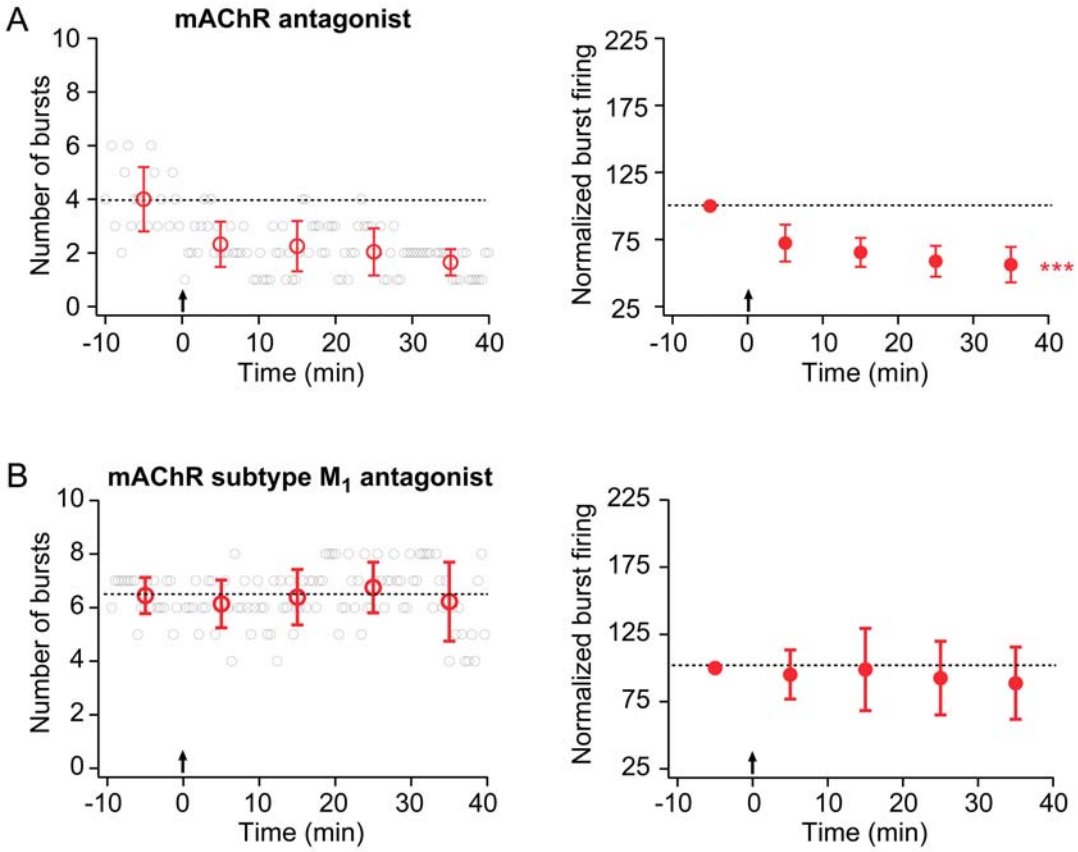
A
mAChR antagonist
Number of bursts
Time (min)
Normalized burst firing
***
B
mAChR subtype M1 antagonist
Number of bursts
Time (min)
Normalized burst firing

Figure 4.8 Enhancement of burst firing requires PLC activation, release of Ca^{2+} from internal stores, and an increase in intracellular Ca^{2+} concentration.

For all representative-experiment graphs *(left column)*, small open circles (*black*) indicate the number of burst firing responses evoked by a train of 10 EPSC-like somatic current injections. The train was delivered every 20 seconds. Large open circles (*red*) represent the average number of burst firing responses per train for each 10-minute period. Error bars are ± standard deviation. For all group-data graphs *(right column)*, filled symbols represent the average number of burst firing responses per train for each 10-minute period. Error bars are ± s.e.m. For all graphs, dotted lines indicate the average number of burst firing responses per train for the 10-minute baseline period. Arrows indicate when TBS (induction) was given. Asterisks signify a significant effect of time, repeated measures ANOVA: **$p<0.01$.

A. Representative *(left)* and group (*right*; n=8) data from experiments in which TBS was given in the presence of a phospholipase C (PLC) inhibitor (U-73122, 25 μM). **B.** Representative *(left)* and group *(right)* data from experiments in which the internal recording solution contained the Ca^{2+}-ATPase inhibitor thapsigargin (2 μM). In the group data, red circles indicate experiments in which TBS was given (n=6). Group data (*right, black squares*; n=6) are also shown for experiments in which no TBS was given. **C.** Representative *(left)* and group *(right)* data from experiments in which the internal recording solution contained the Ca^{2+} chelator (BAPTA, 10 mM). In the group data, red circles indicate experiments in which TBS was given (n=5). Group data (*right, black squares*; n=5) are also shown for experiments in which no TBS was given.

Figure 4.8

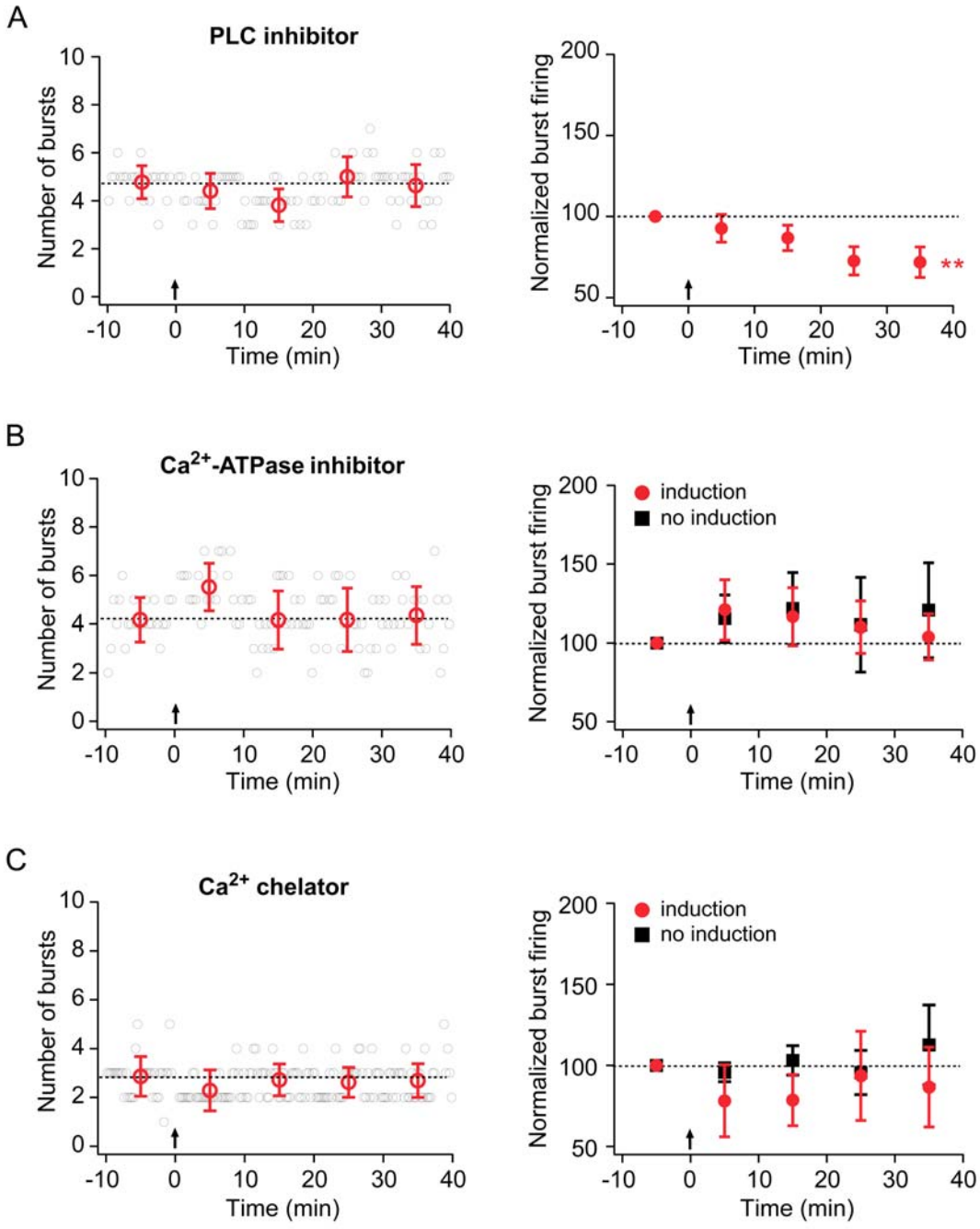
A
PLC inhibitor
Number of bursts
Time (min)
Normalized burst firing
**
B
Ca2+-ATPase inhibitor
induction
no induction
C
Ca2+ chelator

Figure 4.9 Summary of plasticity of burst firing under different experimental conditions.

Normalized burst firing (the average number of burst firing responses per train at 30-40 minutes post-induction as a fraction of the average number of burst firing responses per train in the 10-minute period before TBS was given (or comparable time points in the no-induction group)) is shown for each experimental condition. Bar are color-coded according to one of four conditions: 1. black - no synaptic stimulation during induction, 2. green - synaptic stimulation during induction, resulting in an enhancement of burst firing; 3. red - synaptic stimulation during induction, resulting in a suppression of burst firing; and 4. grey - synaptic stimulation during induction, resulting in no change in burst firing. Numbers at the bottom of the bars indicate n for that group. Error bars are s.e.m. The dotted line indicates no change in the number of burst firing responses compared to the baseline period (100% of baseline). Asterisks indicate a significant effect of time, repeated measures ANOVA: *$p<0.05$, **$p<0.01$, ***$p<0.001$, ****$p<0.0001$.

Figure 4.9

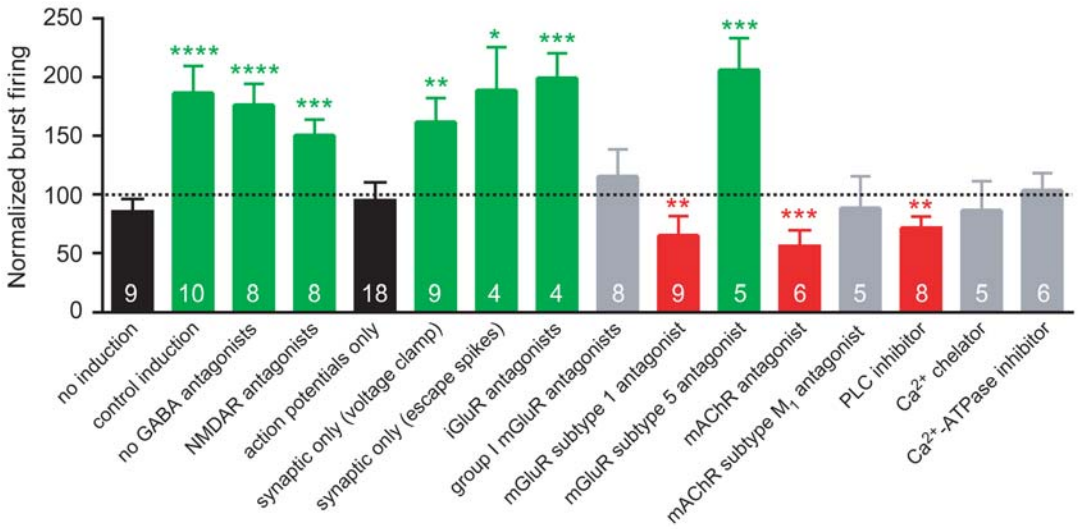
Normalized burst firing
250
200
150
100
50
0
****
****
***
**
*
***
**
***
***
**
9
10
8
8
18
9
4
4
8
9
5
6
5
8
5
6
no induction
control induction
no GABA antagonists
NMDAR antagonists
action potentials only
synaptic only (voltage clamp)
synaptic only (escape spikes)
iGluR antagonists
group I mGluR antagonists
mGluR subtype 1 antagonist
mGluR subtype 5 antagonist
mAChR antagonist
mAChR subtype M1 antagonist
PLC inhibitor
Ca2+ chelator
Ca2+-ATPase inhibitor

Figure 4.10 Decreases in action potential threshold and increases in subthreshold excitability do not underlie the induction of burst firing enhancement.

The change from the 10-minute baseline period to the period 30-40 minutes post-induction (or comparable time points in the no-induction group) is shown for each experimental group. Groups are color-coded by condition as in Fig. 3.7, and data are pooled accordingly in A_2 and B_2. The symbol used to represent each experimental group in A_3 and B_3 are shown above the bars in A_1. In A_1 and B_1, asterisks indicate significance levels as follows: *p<0.05, **p<0.01, ***p<0.001, ****p<0.0001 (one-sample t-test, different from a hypothetical value of 0 mV threshold shift or 0% change in subthreshold voltage response). In A_2 and B_2, asterisks indicate a significant difference compared to the no synaptic stimulation condition (*black*; one-factor ANOVA, ***p<0.001). All error bars are ± s.e.m.

A_1. Average change in action potential threshold for each experimental group. **A_2.** Action potential threshold was more hyperpolarized in groups in which synaptic stimulation led to enhancement of burst firing *(green)* compared to other groups. **A_3.** Plot of change in action potential threshold versus normalized burst firing for each cell in each experimental group. Solid colored lines indicate best fit through pooled data for each condition (linear regression indicates that the slopes are not different (p=0.39), but that the y-intercepts are (p<0.0001)). **B_1.** Average change in subthreshold voltage response (see Experimental Procedures) for each experimental group. **B_2.** The subthreshold voltage response increased more in groups in which synaptic stimulation led to enhancement of burst firing *(green)* compared to other groups. **B_3.** Plot of change in subthreshold voltage

response versus normalized burst firing for each cell in each experimental group. Solid colored lines indicate best fit through pooled data for each condition (linear regression indicates that the slopes are not different ($p=0.21$), but that the y-intercepts are ($p<0.0001$)).

Figure 4.10

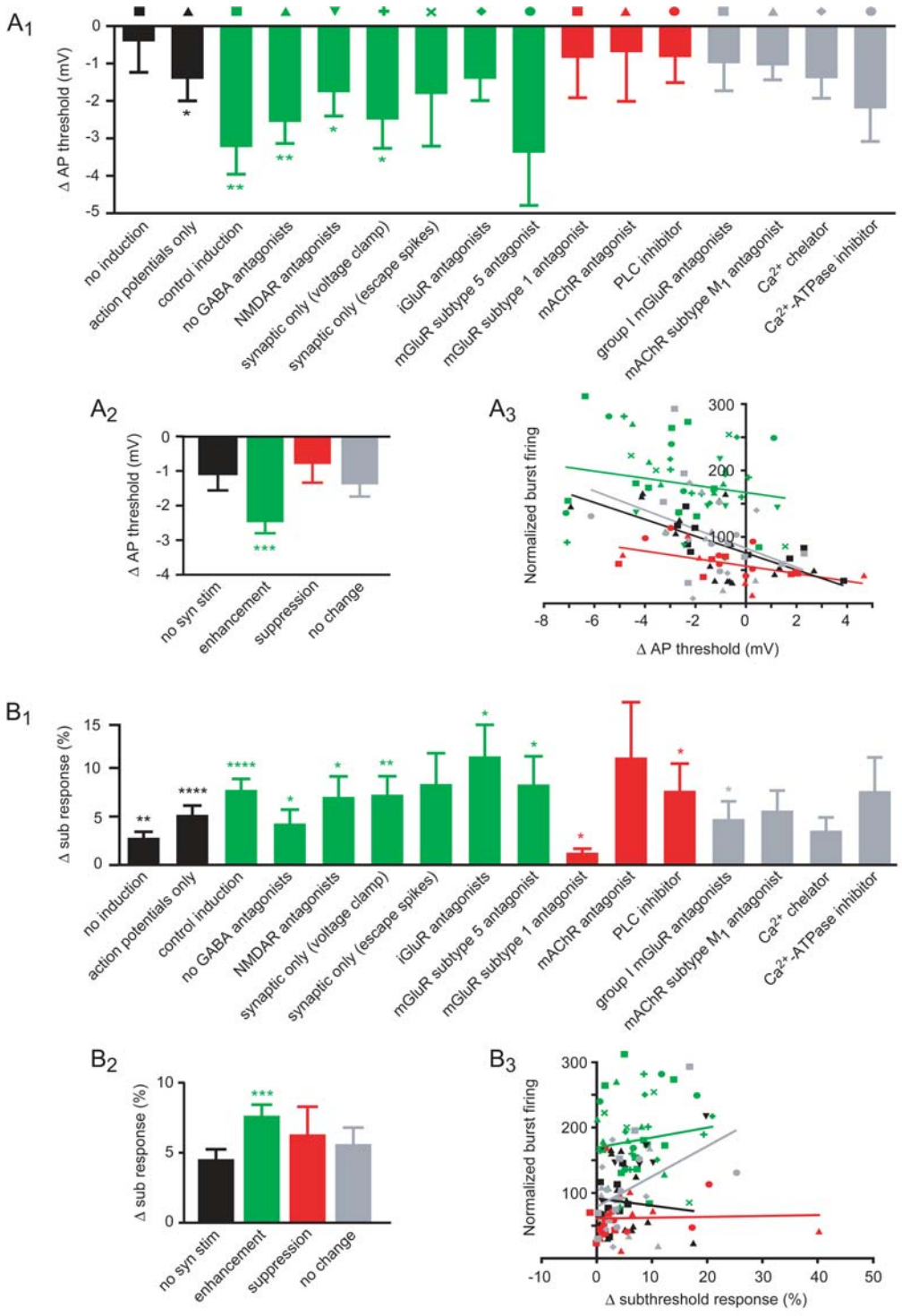
A1
Δ AP threshold (mV)
0
-1
-2
-3
-4
-5
*
**
**
*
*
no induction
action potentials only
control induction
no GABA antagonists
NMDAR antagonists
synaptic only (voltage clamp)
synaptic only (escape spikes)
iGluR antagonists
mGluR subtype 5 antagonist
mGluR subtype 1 antagonist
mAChR antagonist
PLC inhibitor
group I mGluR antagonists
mAChR subtype M1 antagonist
Ca2+ chelator
Ca2+-ATPase inhibitor
A2
Δ AP threshold (mV)
0
-1
-2
-3
-4
***
no syn stim
enhancement
suppression
no change
A3
Normalized burst firing
300
200
100
-8
-6
-4
-2
0
2
4
Δ AP threshold (mV)
B1
Δ sub response (%)
15
10
5
0
**
****
****
*
*
**
*
*
*
*
*
*
*
no induction
action potentials only
control induction
no GABA antagonists
NMDAR antagonists
synaptic only (voltage clamp)
synaptic only (escape spikes)
iGluR antagonists
mGluR subtype 5 antagonist
mGluR subtype 1 antagonist
mAChR antagonist
PLC inhibitor
group I mGluR antagonists
mAChR subtype M1 antagonist
Ca2+ chelator
Ca2+-ATPase inhibitor
B2
Δ sub response (%)
10
5
0
***
no syn stim
enhancement
suppression
no change
B3
Normalized burst firing
300
200
100
-10
0
10
20
30
40
50
Δ subthreshold response (%)

Figure 4.11 TBS results in an increase in excitability of subicular pyramidal neurons.

A. Voltage response to a noisy current injection before *(top, black)* and after *(bottom, red)* TBS. Times indicated are relative to when TBS was given. Scale bars apply to both traces. The boxed area is shown on an expanded scale in C. **B.** Quantification of the increase in number of action potentials, plotted as a percentage of the number of action potentials before TBS induction (n=4; **p<0.01, paired, two-tailed Student's t-test). **C.** Magnified view of boxed area in A. Scale bars apply to both traces. Note that there is an increase in the total number of action potentials and, in most cases, an increase in the number of action potentials per burst event. The traces in the boxed area are shown as insets in D. **D.** An inter-spike interval (ISI) histogram reveals two populations: 1. those with short ISIs (<40 ms), which correspond to burst events, and 2. those with long ISIs (>40 ms), which correspond to regular firing of single action potentials. *Bar graph inset:* A magnified view of the short ISI population shows that burst events can be further characterized based on the appearance of two distinct peaks: the shortest ISIs (4-6 ms) represent the interval between the first and second action potentials in a burst, while slightly longer ISIs (6-40 ms) reflect the time between subsequent (post-second spike) action potentials in a burst. *Trace insets:* Magnified view of action potential firing from the boxed area in C. Scale bars apply to both traces. Numbers above the traces are the ISI, in ms, for each action potential pair.

Figure 4.11

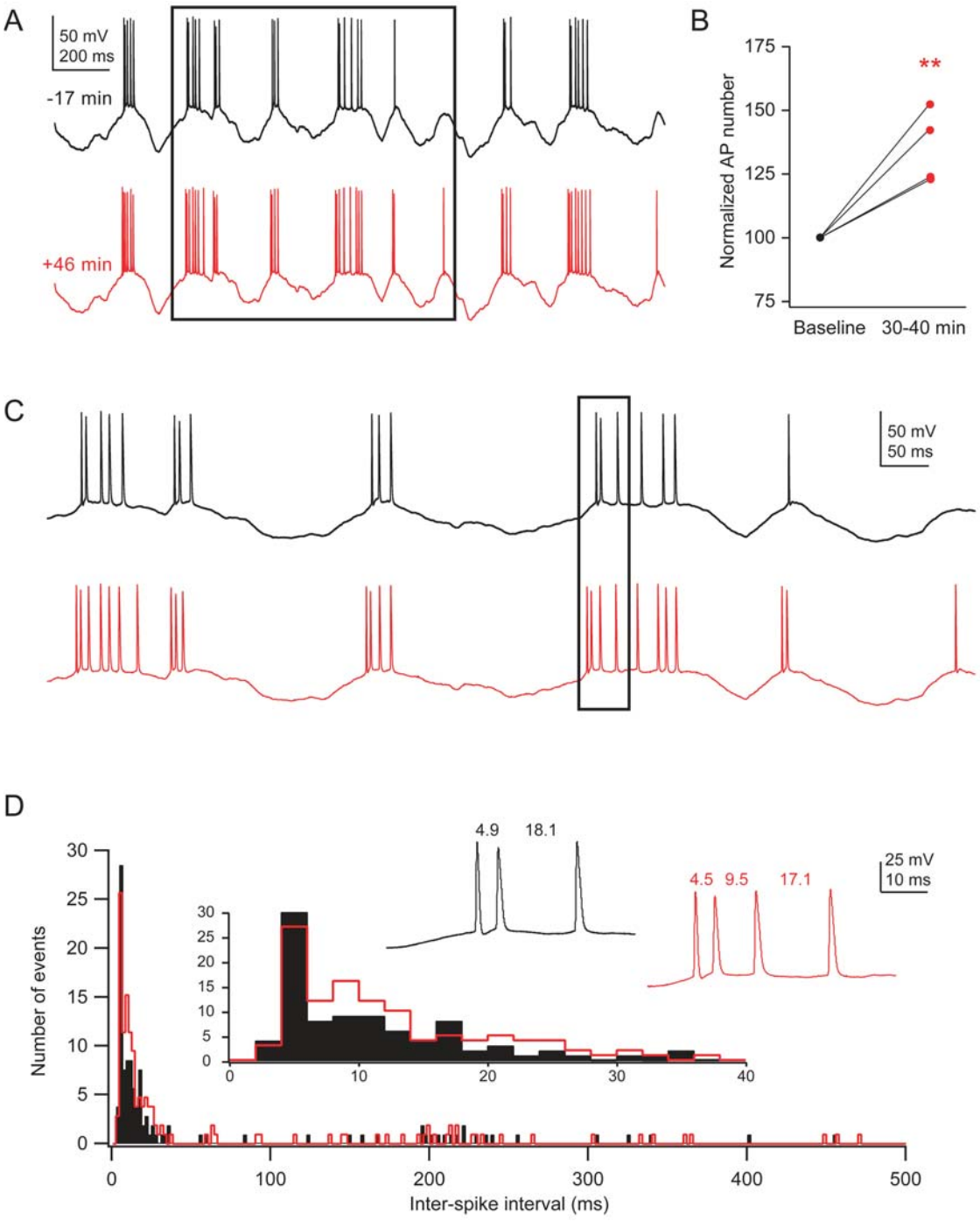
A
50 mV
200 ms
-17 min
+46 min
B
Normalized AP number
175
150
125
100
75
**
Baseline
30-40 min
C
50 mV
50 ms
D
Number of events
Inter-spike interval (ms)
4.9
18.1
4.5
9.5
17.1
25 mV
10 ms

Tables

Table 4.1 Summary of measured parameters under different experimental conditions.

pre = before induction; post = 30-40 min. after induction; AP = action potential. All values are reported as ± s.e.m. Numbers in parentheses are the n for each group. Table entries are left blank if fewer than 3 cells were available for that measure. Asterisks indicate a significant effect of time, repeated measures AVOVA: * = $p<0.05$, ** = $p<0.01$, *** = $p<0.001$, **** = $p<0.0001$.

Table 4.1

	Bursts	EPSP amp	V_m	AP threshold	Subthreshold	Input Resistance	During induction
	Number, pre Number, post	mV, pre mV, post	mV, pre mV, post	mV, pre mV, post	mV, pre mV, post	MΩ, pre MΩ, post	AP number AP range
no induction	3.3 ± 0.4 (9) 2.9 ± 0.7	3.3 ± 0.5 (4) 3.5 ± 0.4	-66 ± 0.3 (9) -66 ± 0.4	-51 ± 1.4 (9) -51 ± 1.6	1.6 ± 0.1 (9) 1.7 ± 0.1	31 ± 2.3 (6) 31 ± 2.4	N/A N/A
control induction	4.5 ± 0.6 (10) 7.8 ± 0.9 ****	5.3 ± 0.5 (7) 7.3 ± 0.6 **	-67 ± 0.2 (10) -67 ± 0.2	-52 ± 0.6 (10) -55 ± 0.8 *	1.4 ± 0.1 (10) 1.5 ± 0.1 ****		22 ± 6 (10) 13 - 73
no GABA antagonists	4.2 ± 0.2 (8) 7.5 ± 0.7	3.3 ± 0.5 (7) 3.3 ± 0.4 *	-65 ± 0.4 (8) -65 ± 0.4	-51 ± 0.4 (7) -54 ± 0.6 *	1.5 ± 0.1 (8) 1.5 ± 0.1 **	30 ± 3.0 (8) 32 ± 3.1 *	16 ± 0.6 (8) 15 - 20
NMDAR antagonists	3.7 ± 0.8 (8) 5.6 ± 1.2 ***	3.0 ± 0.7 (4) 3.0 ± 0.7	-66 ± 0.3 (8) -66 ± 0.2	-53 ± 1.3 (8) -55 ± 0.9	1.4 ± 0.1 (8) 1.5 ± 0.1		35 ± 6 (8) 15 - 60
action potentials only	4.0 ± 0.3 (18) 3.9 ± 0.7	5.4 ± 0.6 (12) 6.3 ± 0.6	-66 ± 0.2 (17) -66 ± 0.4	-52 ± 0.5 (18) -54 ± 0.8	1.6 ± 0.1 (17) 1.6 ± 0.1 *	36 ± 1.5 (17) 39 ± 2.0 **	25 ± 4 (18) 15 - 52
synaptic only (voltage clamp)	3.5 ± 0.3 (9) 5.7 ± 0.9 **	4.5 ± 0.5 (7) 5.6 ± 0.9	-66 ± 0.3 (9) -66 ± 0.5	-52 ± 1.1 (9) -55 ± 1.5	1.5 ± 0.1 (9) 1.6 ± 0.1	34 ± 2.2 (9) 38 ± 2.7 ****	0 (9) 0
synaptic only (w/ escape spikes)	4.4 ± 0.3 (4) 8.2 ± 1.6 *		-66 ± 0.1 (4) -67 ± 0.1	-52 ± 1.6 (4) -53 ± 2.2	1.5 ± 0.1 (4) 1.7 ± 0.1	38 ± 4.8 (4) 42 ± 5.8 **	17 ± 13 (4) 5 - 31
iGluR antagonists	3.5 ± 0.3 (4) 6.9 ± 0.8 ***	0.5 ± 0.1 (4) 0.5 ± 0.1	-65 ± 0.2 (4) -65 ± 0.3	-49 ± 1.5 (4) -51 ± 1.9	1.5 ± 0.1 (4) 1.7 ± 0.1	29 ± 3.9 (4) 34 ± 5.1 **	0 (4) 0
group I mGluR antagonists	4.1 ± 0.5 (8) 4.5 ± 1.1	4.1 ± 1.0 (4) 5.2 ± 2.0	-66 ± 0.2 (8) -66 ± 0.3	-53 ± 0.5 (8) -54 ± 0.8	1.5 ± 0.1 (8) 1.5 ± 0.1 *		34 ± 6 (8) 15 - 58
mGluR subtype 1 antagonist	3.6 ± 0.3 (9) 2.3 ± 0.8 *	4.5 ± 0.6 (7) 8.1 ± 1.8 ***	-65 ± 0.4 (9) -65 ± 0.3	-49 ± 0.6 (9) -50 ± 0.9	1.6 ± 0.1 (9) 1.6 ± 0.1	32 ± 1.4 (9) 33 ± 1.7	47 ± 6 (9) 15 - 63
mGluR subtype 5 antagonist	4.2 ± 0.3 (5) 8.7 ± 0.7 ***	4.0 ± 0.9 (3) 2.3 ± 0.4	-66 ± 0.3 (5) -66 ± 0.2	-50 ± 0.7 (5) -54 ± 1.4 **	1.2 ± 0.1 (5) 1.3 ± 0.1	37 ± 3.5 (5) 39 ± 3.8	46 ± 13 (5) 16 - 86
mAChR antagonist	3.8 ± 0.2 (6) 2.1 ± 0.6 ***	4.4 ± 0.5 (6) 7.3 ± 0.7 ****	-65 ± 0.4 (6) -65 ± 0.9	-51 ± 0.9 (6) -51 ± 1.4	1.4 ± 0.1 (6) 1.6 ± 0.1	42 ± 8.3 (6) 45 ± 9.7	43 ± 5 (6) 24 - 55
mAChR subtype M_1 antagonist	4.9 ± 0.4 (5) 4.3 ± 1.5	4.3 ± 0.4 (5) 6.8 ± 1.3 *	-65 ± 0.4 (5) -65 ± 0.4	-51 ± 1.8 (5) -52 ± 1.6	1.4 ± 0.1 (5) 1.5 ± 0.1	36 ± 4.2 (5) 35 ± 3.0	51 ± 8 (5) 22 - 63
PLC inhibitor	4.4 ± 0.3 (8) 3.2 ± 0.5 *	3.9 ± 0.4 (8) 5.3 ± 1.3 *	-65 ± 0.3 (8) -65 ± 0.3	-53 ± 1.2 (8) -54 ± 1.6	1.4 ± 0.1 (8) 1.9 ± 0.5	36 ± 2.9 (8) 36 ± 3.3	38 ± 7 (8) 15 - 67
Ca^{2+} chelator	4.0 ± 0.4 (5) 3.6 ± 1.2	5.6 ± 0.9 (4) 8.6 ± 2.4 *	-66 ± 0.2 (5) -67 ± 0.3	-50 ± 0.9 (5) -51 ± 0.7	1.7 ± 0.1 (5) 1.8 ± 0.1	35 ± 3.0 (5) 39 ± 9.7 **	54 ± 11 (5) 19 - 78
Ca^{2+}-ATPase inhibitor	4.8 ± 0.3 (6) 5.1 ± 1.0	3.9 ± 0.4 (6) 3.2 ± 0.7	-65 ± 0.4 (6) -66 ± 0.4	-54 ± 0.9 (6) -56 ± 1.5	1.4 ± 0.1 (6) 1.4 ± 0.1	40 ± 6.4 (6) 44 ± 9.9	32 ± 9 (6) 15 - 69

Chapter 5:

Possible mechanisms of induction and expression of burst plasticity in subicular pyramidal neurons

Abstract

Pyramidal neurons in the subiculum exhibit activity-dependent bidirectional plasticity of burst firing, which, unlike synaptic plasticity in these neurons, does not require N-methyl-D-aspartate receptor (NMDAR) activation, synaptically mediated depolarization, or somatic action potential firing. Instead, synaptic activation is required to recruit activation of metabotropic receptors. When a specific subtype of group I metabotropic glutamate receptors (mGluR), mGluR1, is activated coincidently with the M_1 subtype of muscarinic acetylcholine receptors (mAChRs), an enhancement of burst firing is observed. Alternately, when the enhancement of burst firing is prevented (in the presence of an mGluR1 subtype specific antagonist), activation of mGluR5 is required for a suppression of burst firing.

Intracellular signaling cascades that mediate the induction of burst plasticity have begun to be elucidated. For example, both enhancement and suppression of burst firing require an increase in Ca^{2+}, which may be mediated by release from intracellular stores. However, phospholipase C (PLC) activation is only necessary for enhancement of burst firing as a suppression of burst firing is observed even in the presence of a PLC inhibitor. In this chapter, I present a series of unpublished results that further explore the induction

mechanism and speculate about possible expression mechanisms underlying burst plasticity.

Introduction

The subiculum provides the major output pathway of the hippocampus, targeting a variety of cortical and subcortical areas (Amaral and Lavenex, 2007). Therefore, any changes in the neuronal output of the subiculum will affect information processing in networks underlying diverse behaviors, such as spatial navigation and memory formation. Further, dysregulation of subicular function has been implicated in pathological conditions such as epilepsy (Funahashi et al., 1999; Harris and Stewart, 2001b; Cohen et al., 2002) and drug addiction (Caine et al., 2001; Vorel et al., 2001; Cooper et al., 2003; Sun and Rebec, 2003).

The majority of subicular pyramidal neurons are intrinsically burst-firing; brief depolarization just above threshold results in a high frequency cluster (> 100 Hz) of 2-3 action potentials (a burst) (Stewart and Wong, 1993). We have shown that plasticity of burst firing can be induced in response to theta-patterned synaptic stimulation, which was modeled after activity recorded in vivo in awake, behaving rats (Larson and Lynch, 1986; Larson et al., 1986; Otto et al., 1991). Briefly, an enhancement of burst firing was observed in response to synaptic stimulation (but did not require postsynaptic depolarization; Figure 4.5), which recruited synergistic activation of group I subtype 1 (mGluR1) and M_1 muscarinic acetylcholine receptors (mAChRs) (see Figures 4.4 and 4.5). When the enhancement of burst firing was prevented, activation of mGluR5 was required for a suppression of burst firing (Figure 4.6). Furthermore, the enhancement of burst firing depends, at least in part, on activation of phospholipase C (PLC) and Ca^{2+} release from intracellular stores (Figure 4.8). The suppression of burst firing likewise

requires an increase in intracellular Ca^{2+}, and release from intracellular stores may contribute to this signal, but via a PLC-independent pathway.

In this chapter, I will introduce a series of unpublished results that, combined with data collected and presented in Chapter 4, further elucidate the requirements for the induction of burst plasticity. I will present several models that demonstrate the cellular mechanisms underlying the observed requirements for the induction of burst plasticity, and speculate on possible expression mechanisms that may mediate the enhancement or suppression of burst firing.

Methods

Animals – Male Wistar rats, aged 25-45 days, were used for all experiments. Animals were colony housed on a 12-hour light/dark cycle with free access to food and water. All animal procedures were approved by the Northwestern University Animal Care and Use Committee.

Solutions – Artificial cerebrospinal fluid (ACSF) consisted of (in mM): 125 NaCl, 2.5 KCl, 25 $NaHCO_3$, 1.25 NaH_2PO_4, 1 $MgCl_2$, 2 $CaCl_2$, and 25 dextrose (all from Fisher Scientific, Pittsburgh, PA). The pH of the ACSF was 7.2-7.4 and the osmolarity was 305-320 mOsm. ACSF was always oxygenated by constant bubbling with a gas mixture of 95% O_2/5% CO_2. Internal recording solution consisted of: 115 K-gluconate, 20 KCl, 10 sodium phosphocreatine (Na_2-Pcr), 10 HEPES, 2 MgATP, and 0.3 NaGTP with 0.10% biocytin for subsequent determination of morphology (all from Sigma-Aldrich, St. Louis,

MO, except KCl and HEPES, which were from Fisher Scientific). 1 M KOH was used to pH the internal solution to 7.3-7.4. The osmolarity was 272-290 mosm.

Unless otherwise indicated, ACSF used to perfuse slices in the recording chamber included 2 μM SR95531, a γ-aminobutyric acid $(GABA)_A$ antagonist (Sigma-Aldrich), and 3 μM CGP52432, a $GABA_B$ antagonist (Tocris-Cookson, Bristol, UK). In some experiments, an L-type Ca^{2+} channel blocker (nimodipine, 10 μM; Tocris-Cookson, Bristol, UK) was included in the perfusion solution either for the entire duration of the experiment, or beginning just before the induction protocol was delivered.

Slice preparation and experimental setup – Rats were anesthetized with halothane, intracardially perfused with ice-cold ACSF for less than 1 min, then decapitated and the brains rapidly removed. A blocking cut was made to each hemisphere at 60^o to the horizontal plane before mounting with ventral side up. Transverse hippocampal slices, 300 μm thick, were made with a Vibratome 3000 (Ted Pella, Inc., Redding CA) and transferred to a storage chamber, incubated at 32-35 ^oC for 20-30 min. Afterwards, the chamber was maintained at room temperature.

Prior to electrophysiological recordings, slices were transferred to a submerged chamber and maintained at 32-35 ^oC by constant perfusion of warmed ACSF, at a rate of approximately 1 mL/s. A Zeiss Axioskop (Oberkochen, Germany) equipped with differential interference contrast (DIC) optics was used in conjunction with a Hamamatsu camera system to visually identify subicular pyramidal cells. The subiculum was distinguished from bordering regions by the diffuse distribution of pyramidal cells,

compared to the tightly packed pyramidal cell layer of CA1, and the lack of distinct cortical layers seen in entorhinal cortex. Recording pipettes were fabricated (Flaming/Brown Micropipette Puller, Sutter Instruments, Novato, CA) from thick-walled borosilicate capillary glass (Garner Glass Company, ID = 1.2 ± 0.05 mm, OD = 2.0 ± 0.05 mm) and filled with the K-gluconate-based internal solution to obtain a 3-5 MΩ open-tip resistance in the bath. Using a motorized micromanipulator (Sutter Instruments), the recording pipette was positioned on a subicular pyramidal cell and negative pressure was applied by mouth suction to form a GΩ seal. Brief pulses of negative pressure were then used to break through the membrane in the patch pipette and achieve whole-cell configuration.

Electrophysiological recordings – Whole-cell current-clamp recordings of subicular pyramidal neurons in rat hippocampal slices were made through patch pipettes containing a silver chloride-coated electrode connected to an amplifier (Dagan BVC-700, Minneapolis, MN). Only cells that had a resting potential between -56 mV and -70 mV at break-in were used. Experiments were restricted to burst-firing neurons, which were defined as those that exhibited two or more action potentials with an instantaneous frequency of greater than 100 Hz in response to a just-above threshold, long (600 ms) square pulse.

Neuronal output was monitored once every 20 seconds (0.05 Hz) by using a train of 10 somatic excitatory postsynaptic current (EPSC)-like (τ_{rise} = 0.2 ms, τ_{decay} = 6 ms) current injections to evoke action potential firing (Figure 4.1). The frequency and

amplitude of somatic current injections were set such that, for each train, 2-7 responses were bursts (while the remaining responses were single action potentials). In all cases, burst firing occurred mostly at the beginning of the train and single action potentials occurred toward the end of the train.

To induce plasticity, theta-burst-patterned (TBS) synaptic activation (5 stimuli at 100 Hz) was delivered via an extracellular stimulating pipette, and paired with somatic current injection (2 ms square current pulse at the burst-monitoring amplitude), which together were repeated at 5 Hz. The extracellular stimulating pipette, fabricated from borosilicate theta glass (Sutter Instruments) was filled with ACSF and placed (by using a separate motorized micromanipulator, Sutter Instruments) 50-200 μm away from the site of the whole-cell recording on the apical dendritic side either toward CA1 or entorhinal cortex. In both cases, it is likely that CA1 and EC afferents were jointly recruited and activated during the induction protocol.

All neurons were held at membrane potentials between -63 mV and -67 mV for the duration of the recordings (except in voltage-clamp experiments when, during the induction stimulus only, cells were held at -80 mV). Cells that required more than 250 pA of current to maintain these potentials were excluded from the dataset. Bridge balance and capacitance compensation were monitored and adjusted throughout the duration of each experiment; recordings in which the series resistance exceeded 45 MΩ were excluded. Only cells that were recorded from for at least 40 minutes after the induction stimulus was given were included in subsequent analysis.

Data acquisition and statistical analysis – Voltage responses were filtered at 5 kHz, digitized at 50 kHz, and stored via an ITC-16 analog-to-digital converter (Instrutech, Port Washington, NY) on a Dell Dimension PC. All acquisition and analysis procedures were custom programmed in IGOR Pro (Wavemetrics, Lake Oswego, OR). Statistical analyses of group data were performed using repeated measures ANOVA with Prism software (GraphPad Software, Inc., San Diego, CA). When a significant main effect was detected with ANOVA tests, Bonferroni's post-hoc correction was applied to determine significance between pairwise comparisons. Unless stated otherwise, averages in individual experiments are reported as mean ± standard deviation for 10-minute bins. Averages for group data are reported as mean ± standard error of the mean (s.e.m.) for 10-minute bins. Normalized values are plotted as a percentage of the value during the baseline, and are obtained by dividing the mean for each 10-minutes bin by the mean during the 10-minute baseline period.

Results

Enhancement of burst firing requires a threshold level of synaptic activity

Burst firing was assessed using whole-cell current-clamp recordings of subicular pyramidal neurons. Neuronal output was monitored by a train of 10 brief, suprathreshold somatic current injections (refer to Figure 4.1A,C), and quantified as the number of burst responses per train (up to 10 if every current injection elicited a burst). During somatic current injection, neuronal output is determined only by activation of intrinsic conductances gated by voltage and/or calcium. Therefore, a change in the number of

bursts (burst plasticity) can be used as a measure of intrinsic plasticity caused by changes in postsynaptic excitability.

Theta-burst stimulation (TBS; 5 synaptic pulses at 100 Hz paired with somatic current injections, repeated at 5 Hz), which resembles the activity patterns observed during hippocampus-dependent learning tasks *in vivo* (Larson and Lynch, 1986; Larson et al., 1986; Otto et al., 1991), was used to induce plasticity. When this induction protocol was delivered for 3 seconds, TBS resulted in an increase in the number of bursts elicited by the train of somatic current injections (Figure 5.1A; $n=10$; $p<0.0001$). When TBS was given for 2 seconds, the change in burst firing was not statistically significant, but there was a trend towards an increase ($n=6$; $p=0.07$). However, when the induction protocol was given for only 1 second (Figure 5.1C), no change in burst firing was observed ($n=4$; $p=0.73$). Taken together, these results suggest that a threshold level of synaptic activity is required to induce burst plasticity, and in all other experiments, a 3-second induction protocol was used.

L-type Ca^{2+} channel activation is required for the induction, but not the expression, of burst plasticity

In vitro, burst firing does not require strong correlated synaptic input (Staff et al., 2000; Harris and Stewart, 2001a), but rather depends on activation of voltage-gated Ca^{2+} conductances by a Na^{+}-dependent action potential. The resulting Ca^{2+} tail current leads to an after-depolarization (ADP) that can drive burst firing. Modulation of voltage-gated Ca^{2+} channels involved in generating an ADP may therefore be involved in burst

plasticity. However, N- and P/Q-type Ca^{2+} channels are involved in regulating neurotransmission, and, in our experiments, synaptic activation is required for burst plasticity, so their contribution can not be investigated via bath application of antagonists. Further, R- or T-type Ca^{2+} channels are difficult to investigate because no high-affinity, specific antagonists exist for these channels. Therefore, we examined whether L-type Ca^{2+} channels were involved in the induction of burst plasticity by performing experiments in the presence of nimodipine (10 μM), a specific L-type Ca^{2+} channel blocker.

When the L-type Ca^{2+} channel blocker was present in the bath for the entire duration of the experiment, no change in burst firing was observed (Figure 5.2A; n=5; p=0.58). To test whether L-type Ca^{2+} channel activity is required during the induction or expression of burst plasticity, we performed experiments in which the blocker was washed into the bath just after TBS (3 s) was delivered. This treatment did not prevent an increase in burst firing (Figure 5.2B; n=5; $p<0.05$). Taken together, these experiments suggest that L-type Ca^{2+} channels are required for the induction but not the expression of burst plasticity.

In light of other experiments that have demonstrated a lack of necessity for postsynaptic depolarization (see Figure 4.5), it is surprising that L-type Ca^{2+} channels, which are voltage-gated, are required for the induction of burst plasticity. Although L-type Ca^{2+} channels are generally included in the high-voltage activated subfamily, which require significant depolarization from the resting membrane potential to be recruited, some evidence suggests that at least a portion may be active at much more hyperpolarized

potentials near rest (Magee et al., 1996). Fluorescence imaging in CA1 pyramidal neurons demonstrated that the basal Ca^{2+} level is dramatically decreased by voltage-clamping the soma at -80 mV (compared to -50 mV). The magnitude of the decrease was reduced by nimodipine, suggesting that, under normal conditions L-type Ca^{2+} channels contribute to the resting Ca^{2+} concentration in neurons (Magee et al., 1996).

Therefore, if blockade of L-type Ca^{2+} channels prevents the induction of burst plasticity by decreasing the basal Ca^{2+} concentration of the neuron, another manipulation that reduces basal Ca^{2+} should also prevent the induction of burst plasticity. We tested this hypothesis by voltage-clamping the soma at -80 mV for 3 - 5 minutes before TBS was given (the soma remained voltage-clamped throughout the duration of the induction protocol as well). In this condition, no change in burst firing was observed (Figure 5.2C; n=7; p=0.62). Taken together, these results suggest that activation of L-type voltage-gated Ca^{2+} channels contributes to the basal Ca^{2+} concentration in the neuron, and that the induction of burst plasticity is prevented when this level falls below a critical threshold.

Discussion

The results of these experiments serve to further elucidate the complex signaling pathways that underlie the induction of burst plasticity, and provide the first attempts to address the mechanism responsible for the expression of burst plasticity. In summary, combined with data presented in the previous chapter, the induction of burst plasticity requires a threshold level of synaptic activation to recruit signaling through metabotropic glutamate and acetylcholine receptors. An enhancement of burst firing is observed when

both mGluR1 and M_1 mAChRs are synergistically activated, while a suppression of burst firing, requiring activation of mGluR5, is revealed when this enhancement is prevented. The expression of burst plasticity is not due to regulation of L-type voltage-gated Ca^{2+} channels, although they may be involved in regulating the basal Ca^{2+} concentration in the neuron. This resting concentration may have a critical threshold level, which, if not reached, may prevent the subsequent induction of burst plasticity. These data help to develop and refine a model for the mechanisms governing the induction and expression of burst plasticity in subicular pyramidal neurons, which may represent a generalized paradigm for intrinsic plasticity of neuronal output in other brain regions.

The role of L-type voltage-gated Ca^{2+} channels in the induction of burst plasticity

Several lines of evidence demonstrate that the induction of burst plasticity does not require postsynaptic depolarization. No change in burst firing was observed when somatic action potentials alone were used as the induction stimulus (see Figure 4.5), showing that synaptic activation is required for the induction of burst plasticity. When the soma was voltage-clamped at -72 mV to prevent action potential firing during induction, synaptic stimulation alone produced an enhancement of burst firing, illustrating that synaptic activation is sufficient to induce burst plasticity. Furthermore, even when ionotropic glutamate antagonists were included in the bath, which prevented almost all depolarization, synaptic stimulation alone induced an enhancement of burst firing. However, when the soma was voltage-clamped at -80 mV, which also prevented somatic

action potential firing, no change in burst firing was observed. Why would voltage-clamping at different potentials have such drastic effects on the induction of burst plasticity? One possibility is that a voltage-gated channel is active at the more depolarized potential, but inactive at the more hyperpolarized potential. When L-type Ca^{2+} channels (which are voltage-gated) were blocked with nimodipine, no change in burst firing was observed. How can the induction of burst plasticity be independent of postsynaptic depolarization, yet still require activation of a voltage-gated channel? The resolution to these questions may be provided by an intriguing result which demonstrates that the basal Ca^{2+} level in a neuron is higher at more depolarized potentials and lower at more hyperpolarized potentials and that nimodipine reduces the basal Ca^{2+} level near resting membrane potentials (Magee et al., 1996), suggesting that L-type channels contribute to this basal concentration of Ca^{2+}. Taken together, these results suggest that voltage-gated L-type Ca^{2+} channels are not strictly required for the induction of burst plasticity, but instead are necessary to establish the appropriate resting concentration of Ca^{2+}. It would be interesting to perform Ca2+ imaging experiments during burst plasticity experiments in the presence or absence of nimodipine to determine whether the induction of burst firing enhancement is indeed correlated with an increased basal level of Ca^{2+} when L-type Ca^{2+} channels are unblocked. One possibility in this scenario is that if the basal intracellular Ca^{2+} concentration is too low, a synaptically evoked Ca^{2+} signal, provided by group I mGluR and M_1 mAChR-mediated release from intracellular stores, is not sufficient to raise Ca^{2+} to a threshold required to induce burst plasticity. In this case, using EGTA to buffer the intracellular Ca^{2+} concentration (instead of BAPTA as in our

experiments; see Figure 4.8) should not prevent the induction of burst plasticity because EGTA would be too slow to prevent the synaptically evoked Ca^{2+} signal (which is prevented by the faster buffering capacity of BAPTA).

Mechanisms underlying the requirement for synergistic activation of metabotropic receptors for the enhancement of burst firing

This necessity for synaptic activation, but lack of a requirement for postsynaptic depolarization, hinted at the possible involvement of metabotropic receptors. The enhancement of burst firing was prevented when either mGluR1 or M_1 mAChR were blocked (see Figures 4.4 and 4.5), which indicates that synergistic activation of both receptors is required to produce this plasticity. The mechanism of the synergistic interaction between mGluR1 and M_1 mAChR may take several forms, which are diagramed in Figure 5.3. Perhaps the most straightforward possibility is that both receptors converge on a common signaling pathway and that synergistic activation leads to an enhanced level of a critical enzyme or second messenger (such as Ca^{2+}) that must reach a threshold to produce an enhancement of burst firing (Figure 5.3A, left). However, it is also possible that each receptor subtype is coupled to separate signaling pathways, both of which are required to induce this plasticity (Figure 5.3A, right). For example, activation of mGluR1 and M_1 mAChR releases the $G_{q\alpha}$ subunit, which in turn activates PLC, producing two second messengers: diacylglycerol (DAG) and inositol-1,4,5-triphosphate (IP_3). These can directly activate ion channels in the plasma membrane and also cause Ca^{2+} release from intracellular stores. Inhibition of PLC and depletion of

intracellular Ca^{2+} stores both prevent the increase in burst firing (see Figure 4.8), suggesting that at least one of these receptors activates this signaling cascade, which is required for the induction of burst firing enhancement. mGluR1 and M_1 mAChR can also activate protein kinases such as protein kinase C (PKC) and extracellular signal-regulated kinase (ERK), which have been shown to play critical roles in synaptic plasticity. Therefore, one receptor may be required to activate the PLC/IP_3 pathway while the other may mediate required activation of a separate signaling cascade.

A second scenario that may underlie the requirement for synergistic activation of mGluR1 and M_1 mAChR is that one receptor may be located on the presynaptic terminal of the other type of neurotransmitter, regulating its release (Figure 5.3B). For example, activation of mGluR1 receptors on cholinergic terminals may be required to permit or promote release of acetylcholine (ACh), or M_1 mAChR on glutamatergic terminals may affect the release of glutamate in response to synaptic stimulation. In this situation, the requirement for PLC activation could be either presynaptic or postsynaptic, since the inhibitor of this enzyme was bath-applied; however, the requirement for an increase in Ca^{2+} concentration and the involvement of intracellular Ca^{2+} stores must be postsynaptic because the Ca^{2+} chelator and the ATPase inhibitor (which depletes intracellular stores) were both applied via the recording pipette to the postsynaptic neuron alone.

A third mechanism which may be responsible for the synergism between mGluR1 and M_1 mAChR involves more complex interactions between the receptor subunits in the postsynaptic neuron (Figure 5.3C). For example, a metabotropic receptor (or receptor subunit) can modulate the actions of another metabotropic receptor. This effect may

occur independently of G-protein coupled signaling, such as the adenosine A_1 receptor-mediated downregulation of an mGluR1-induced inward current (Tabata et al., 2007). A possible mechanism underlying G-protein independent modulation is via direct interaction between metabotropic receptor subunits. For example, metabotropic receptors can form herteromeric complexes with other metabotropic receptors (Enz, 2007). These heteromers have been shown to result in increased sensitivity of a metabotropic receptor to a neurotransmitter (i.e. mGluR1 and $GABA_BR$ heteromers that increase the sensitivity of mGluR1 to glutamate [Tabata et al., 2004]) and to produce synergistic potentiation of a downstream signal (i.e. mGluR1 and A_1 receptor heteromers that result in an enhanced receptor-evoked Ca^{2+} signal [Ciruela et al., 2001]). Therefore, metabotropic receptors may interact to regulated transmembrane currents or intracellular signaling cascades, which may be involved in the induction of burst plasticity.

Transduction mechanisms involved in suppression of burst firing

Other signal transduction mechanisms may also be involved in the induction of burst plasticity, because antagonism of mGluR1 or mGluR5, which are both coupled to $G_{q\alpha}$ and PLC, did not have equivalent effects on burst firing. When the induction of enhanced burst firing was blocked, a suppression of burst firing was revealed (see Figure 4.6B). Because this suppression was not observed in experimental groups that did not receive synaptic stimulation (no-induction and action potentials-only groups; see Figures 4.4 and 4.5), it is likely that suppression of burst firing reflects recruitment of an additional activity-dependent process. Our data suggest that the decreased burst firing

depends on synaptically mediated stimulation of mGluR5, although we can not rule out the possibility that other receptor types also contribute to the induction of burst firing suppression.

Like the enhancement of burst firing, the suppression of burst firing required an increase in Ca^{2+} and, furthermore, was prevented when intracellular stores of Ca^{2+} were depleted (see Figure 4.8). However, suppression of burst firing persisted when PLC was inhibited, suggesting that a mechanism different from that mediating the enhancement of burst firing (namely, PLC-induced production of IP_3 activating IP_3 receptors on the endoplasmic reticulum) may be responsible for release of Ca^{2+} from intracellular stores. Furthermore, the suppression of burst firing did not require synergistic activation of mGluR and mAChR (see Figure 4.7). One possible cellular mechanism by which plasticity of burst firing is bidirectionally induced is that synergistic activation of subtypes of both receptor (mGluR1 and M_1 mAChR) leads to a larger increase in intracellular Ca^{2+} concentration, which results in an enhancement of burst firing, while activation of mGluR5 in the absence of mAChR signaling results in a smaller Ca^{2+} signal that leads to a suppression of burst firing. Another possibility is that mGluR1 and mGluR5 have different subcellular distributions so that activation of one receptor in a specific neuronal compartment (for example, the apical dendrite) induces an enhancement of burst firing while activation of the other receptor in a different compartment (for example, the soma) produces a suppression of burst firing.

In addition to increasing IP_3 production, PLC activation results in a reduction of PIP_2 in the plasma membrane, which can act as a signaling molecule itself, and also

results in the production of DAG, which activates PKC. These proteins may also be required for the induction of burst plasticity, in addition to the requirement for IP_3-mediated release of Ca^{2+} from intracellular stores. Evidence in support of a possible role for membrane-bound signaling molecules comes from one experiment that demonstrated activation of mGluR1 resulted in a rapid, but transient, suppression of Ca^{2+} conductances (in addition to a slower, sustained suppression), consistent with a membrane-delimited process (Sahara and Westbrook, 1993).

Candidate mechanisms for the expression of burst plasticity

An obvious question is which conductances are altered to produce the observed changes in burst firing. Analysis of the bursting responses before and after TBS has yielded few clues as to the nature of the affected conductances, so further work will be required to address this question. However, based on observations from other work, there are three clear candidate conductances: Na^+, Ca^{2+}, and/or K^+.

Repetitive burst firing in subiculum has been shown to be affected by properties of Na^+ channel inactivation. Increasing the frequency of the somatic current injections decreased the number of burst responses because more Na^+ channels were entering an inactive state, from which recovery was relatively slow (on the order of 1 s for full recovery), while there was no change observed in the magnitude of the Ca^{2+} tail current (Cooper et al., 2005). In our experiments (in agreement with others; see Staff et al., 2000; Cooper et al., 2005), current injections at the beginning of the train elicited burst responses while those later in the train elicited single action potentials. When an

enhancement of burst firing was induced, the switch from burst responses to single action potentials occurred later in the train of current injections. Therefore, the increase in burst firing may be due to a decrease in the proportion of channels entering the slow-inactive state. Likewise, when a suppression of burst firing was observed, the switch from burst responses to single action potentials occurred earlier in the train, consistent with a greater proportion of Na^+ channels entering the slow-inactive state.

Phosphorylation of Na^+ channels at specific residues (Murphy et al., 1993) by PKA (Costa et al., 1982; Costa and Catterall, 1984a) and PKC (Costa and Catterall, 1984b) has been shown to reduce Na^+ channel activity (Li et al., 1992; Li et al., 1993). Specifically phosphorylation resulted in a decrease in the number of available Na^+ channels or a reduction in the peak open probability (Numann et al., 1991). PKC activation, via an mGluR5-dependent increase in PLC-mediated production of DAG, may therefore provide a possible mechanism for the reduction of an inward Na^+ current that reduces the ability of a neuron to generate repeated bursts of action potentials, leading to the observed suppression of burst firing.

On the other hand, the calcium-regulated phosphotase calcineurin is very effective at dephosphorylating Na^+ channels (Murphy et al., 1993; Chen et al., 1995). Basal PKA activity has been shown to tonically decrease Na^+ channel activity, an effect that can be reversed (resulting in larger Na^+ currents) by irreversible inhibition of PKA activity or application of phosphotases (Li et al., 1992). Therefore, an mGluR1- and M_1 mAChR-mediated increase in intracellular Ca^{2+} concentration may activate calcineurin, which dephosphorylates Na^+ channels, resulting in a net increase in an inward current. This

increase in available Na^+ channels or peak open conductance may underlie the enhancement of burst firing.

Intrinsic burst firing in subicular pyramidal neurons is mediated by a Ca^{2+} tail current, which is activated by a Na^+-dependent action potential. Blocking or reducing this tail current reduces burst firing (Staff et al., 2000; Jung et al., 2001). Therefore, an increase in a Ca^{2+} conductance that contributes to the tail current may be the mechanism responsible for the increase in burst firing, and, conversely, a decrease in this type of conductance may underlie the suppression of burst firing.

Activation of group I mGluRs have been shown to suppress Ca^{2+} conductances, particularly N- and L-type, via a G-protein coupled signaling pathway (Sahara and Westbrook, 1993). This observation may provide a mechanism for the suppression of burst firing: mGluR5 activation may lead to a decrease in one, or both, of these Ca^{2+} conductances, reducing the amplitude of the ADP following a Na^+-dependent action potential such that the depolarization is not sufficient to reach threshold for a subsequent action potential. One experiment that would test this hypothesis is to perform recordings in the presence of the mGluR1 antagonist (to prevent the enhancement and reveal the suppression of burst firing) and the L-type Ca^{2+} channel blocker (N-type Ca^{2+} channels could not be blocked because they mediate glutamatergic neurotransmission, and synaptic activation is required for the induction of burst firing suppression). If a reduction in an L-type conductance is required for the expression of a decrease in burst firing, this manipulation should prevent burst firing suppression.

Furthermore, the requirement for both mGluR1 and M_1 mAChR activation in the enhancement of burst firing may be due to the need to overcome an mGluR5-mediated suppression. In this scenario, mGluR1 and M_1 mAChR activation may provide a potentiation of the effects of downstream molecules, such as extensive phosphorylation of ion channels, such as voltage-gated Na^+ channels, through elevated PKC or calcium/calmodulin-dependent kinase (CaMKII) activity, leading to a lasting increase in inward (depolarizing) current.

Action potential firing and the ADP can be limited by voltage and/or Ca^{2+}-activated K^+ currents, which also increase the slow AHP following bursts (Rhoades and Gross, 1994; Staff et al., 2000; Jung et al., 2001; Golomb et al., 2006; Metz et al., 2007). Modulation of these channels may result in an increased K^+ current, either by directly altering K^+ channel properties or by increasing sensitivity to Ca^{2+}, which would likely result in a suppression of burst firing. On the other hand, if these currents were downregulated, it would be easier to reach threshold for action potential firing and more burst responses would be generated.

Group I mGluR activation has been shown to inhibit a Ca^{2+}-sensitive K^+ current (I_{AHP}) via an IP_3-dependent pathway that does not depend on PKA or PKC activity (Abdul-Ghani et al., 1996). This observation parallels the pharmacological results from our experiments, suggesting that the enhancement of burst firing may be due to a mGluR1- and/or M_1 mAChR-mediated increase in IP_3 signaling, which reduces an outward (inhibitory) K^+ current.

Although these conductances are some of the most likely candidates for the cellular mechanism underlying the expression of burst plasticity, there are several other conductances that should also be considered. For example, mGluR agonists have been shown to induce non-specific inward cationic currents, independent of Ca^{2+} mobilization (Guatteo et al., 1999; Rae and Irving, 2004), and to modulate Ca^{2+}-activated non-specific cation channels (Crepel et al., 1994), including members of the transient receptor potential (TRP) channel family (Gee et al., 2003). High frequency synaptic activation may increase constitutive activity of these conductances, or could increase sensitivity to neurotransmitters, such as glutamate, so that basal levels present in the synaptic cleft could persistently activate an inward current, resulting in an enhancement of burst firing. Likewise, a decrease in constitutive activity, or a decrease in sensitivity to neurotransmitter may lead to a suppression of burst firing.

Future directions

In addition to experiments designed to address the question of the mechanism of expression for burst plasticity, it will be interesting to compare the magnitude of plasticity (either enhancement or suppression) observed in different conditions. In these experiments, a train of only 10 somatic current injections was used to assess burst firing, but, after induction, many neurons were able to generate bursts in response to each input in the train. Therefore, the magnitude of the enhancement of burst firing may be confounded by a ceiling effect, which makes direct comparison of the amount of burst plasticity observed in different experimental conditions difficult to interpret. However,

this comparison may serve to dissect the signaling pathways involved in burst plasticity and may ultimately elucidate the mechanisms by which an enhancement or suppression of burst firing is both induced and expressed.

Figures

Figure 5.1 Plasticity of burst firing is activity-dependent.

For all representative-experiment graphs *(left column)*, small open circles (*black*) indicate the number of burst firing responses evoked by a train of 10 EPSC-like somatic current injections. The train was delivered every 20 seconds. Large open circles (*red*) represent the average number of burst firing responses per train for each 10-minute period. Error bars are ± standard deviation. For all group-data graphs *(right column)*, filled symbols represent the average number of burst firing responses per train for each 10-minute period. Error bars are ± s.e.m. For all graphs, dotted lines indicate the average number of burst firing responses per train for the 10-minute baseline period. Arrows indicate when TBS (induction) was given. Asterisks signify a significant effect of time, repeated measures ANOVA: ****$p<0.0001$.

A. Representative (*left*) and group (*right, red circles*; n=10; $p<0.0001$) data from experiments in which TBS was given for 3 s. Note that panel A shows the same data as Figure 4.4A, and is repeated here for ease of comparison between protocols.

B. Representative (*left*) and group (*right, red circles*; n=6; $p=0.07$) data from experiments in which TBS was given for 2 s. **C.** Representative (*left*) and group (*right, red circles*; n=4; $p=0.73$) data from experiments in which TBS was given for 1 s.

Figure 5.1

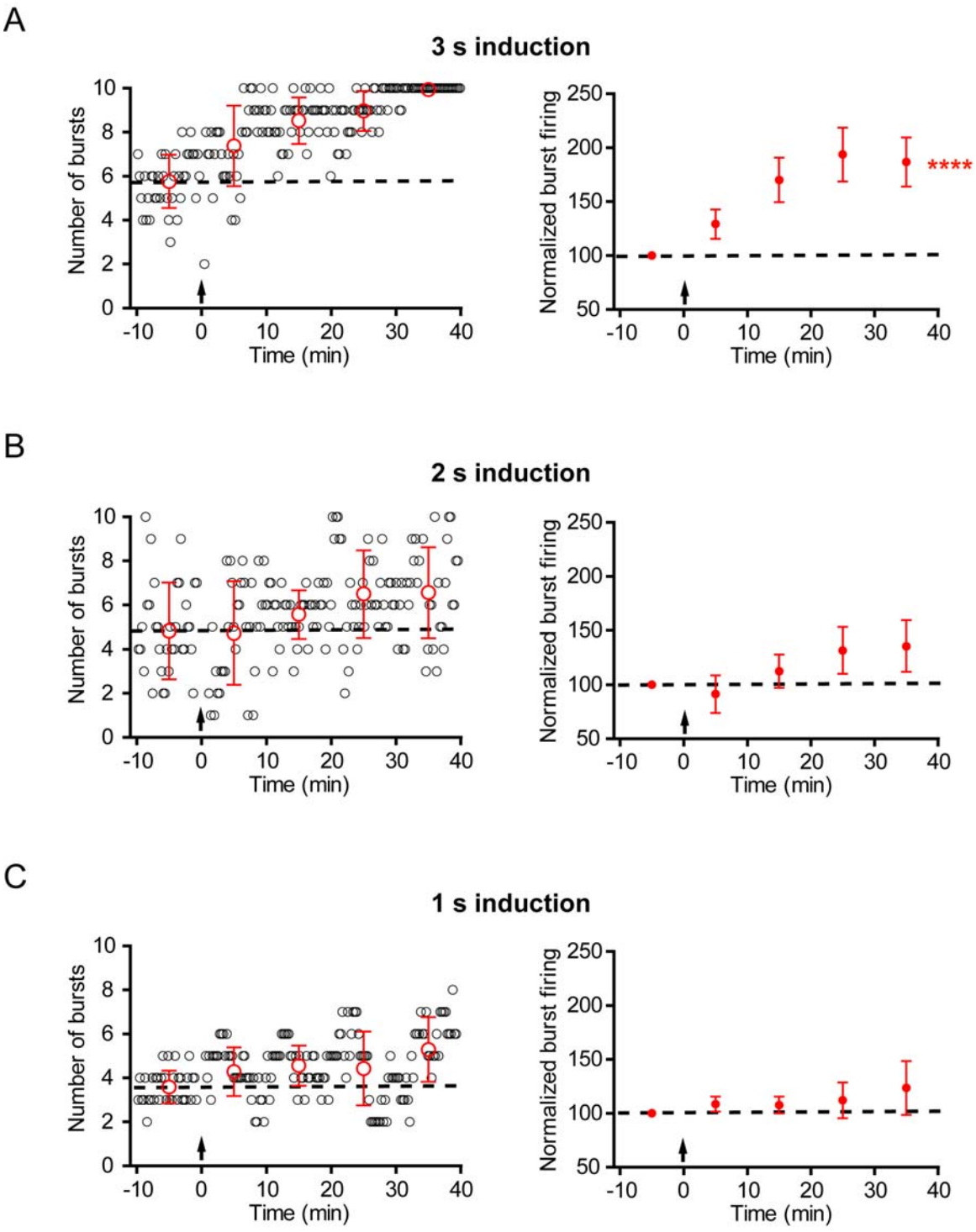
A
3 s induction
Number of bursts
Time (min)
Normalized burst firing
****
B
2 s induction
C
1 s induction

Figure 5.2 L-type Ca^{2+} channel block and somatic voltage clamp at -80 mV prevents the induction, but not expression, of burst plasticity.

For all representative-experiment graphs *(left column)*, small open circles (*black*) indicate the number of burst firing responses evoked by a train of 10 EPSC-like somatic current injections. The train was delivered every 20 seconds. Large open circles (*red*) represent the average number of burst firing responses per train for each 10-minute period. Error bars are ± standard deviation. For all group-data graphs *(right column)*, filled symbols represent the average number of burst firing responses per train for each 10-minute period. Error bars are ± s.e.m. For all graphs, dotted lines indicate the average number of burst firing responses per train for the 10-minute baseline period. Arrows indicate when TBS (induction) was given. Asterisks signify a significant effect of time, repeated measures ANOVA: *$p<0.05$.

A. Representative (*left)* and group (*right*; n=5; p=0.58) data from experiments in which an L-type Ca^{2+} channel blocker (10 μM nimodipine) was present for the duration of the recording (the yellow bar indicates when nimodipine was present). **B.** Representative (*left*) and group (*right*; n=5; $p<0.05$) data from experiments in which an L-type Ca^{2+} channel blocker (10 μM nimodipine) was washed in after the induction stimulus was given (the yellow bar indicates when nimodipine was present). **C.** Representative (*left*) and group (*right*; n=7; p=0.62) data from experiments in which the induction stimulus consisted of synaptic stimulation during somatic voltage clamp (at -80 mV).

Figure 5.2

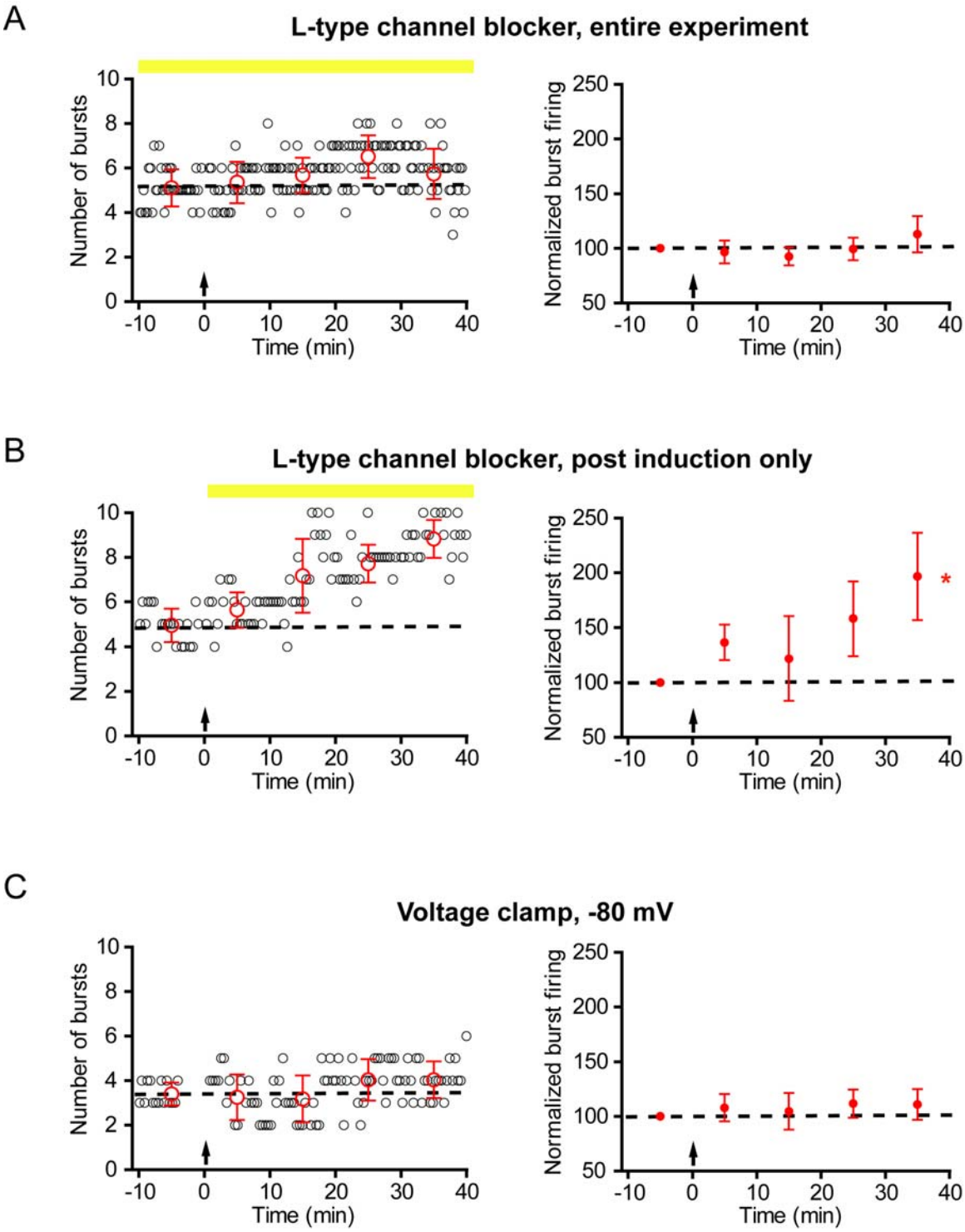
A
L-type channel blocker, entire experiment
Number of bursts
Time (min)
Normalized burst firing
Time (min)
B
L-type channel blocker, post induction only
Number of bursts
Time (min)
Normalized burst firing
Time (min)
*
C
Voltage clamp, -80 mV
Number of bursts
Time (min)
Normalized burst firing
Time (min)

Figure 5.3 Possible mechanisms of synergism between metabotropic receptors, which is required for the enhancement of burst firing.

Panels show several potential ways in which metabotropic receptors may interact, leading to the observed synergism required for the enhancement of burst firing.

A. In this model, synaptic activation leads to signaling via both mGluR1 and M_1 mAChR. These signals may converge at some point along the pathway or may recruit two independent pathways which are both required for the enhancement of burst firing. **B.** In this model, synaptic activation results in stimulation of one receptor (which could be either mGluR1 or M_1 mAChRs; note: the two possibilities are diagramed on either side of the dashed line in the center) located on the presynaptic terminal of the other neurotransmitter, which modulates its release. The other receptor is activated by this neurotransmitter and results in downstream signaling that leads to the enhancement of burst firing. **C.** Activation of mGluR1 and M_1 mAChR heteromers may regulate a transmembrane current or modulate an intracellular signaling cascade, leading to the induction of burst plasticity.

Figure 5.3

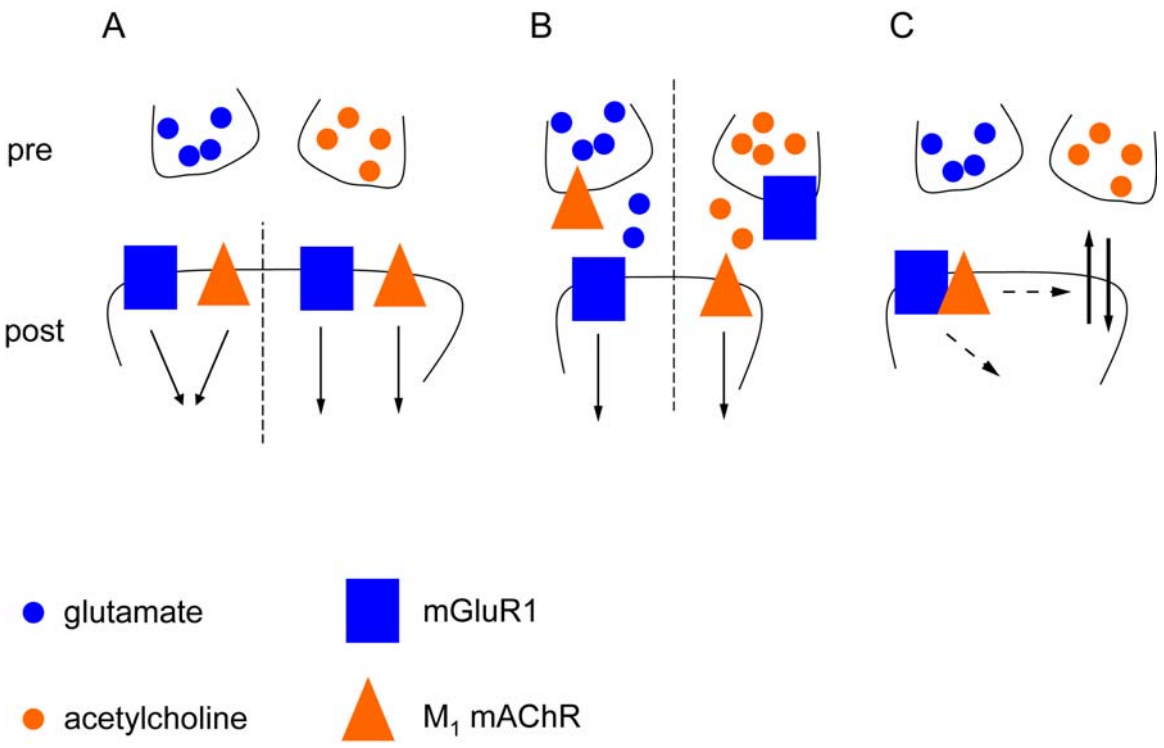

Figure 5.4 Possible models for the induction and expression of burst plasticity.

The enhancement of burst firing requires activation of both mGluR1 and M_1 mAChR, which may lead to enhanced activation of PLC. PLC catalyzes the hydrolysis of membrane phospholipids, and results in the production of IP_3, which causes the release of Ca^{2+} from intracellular stores via activation of IP_3 receptors. This Ca^{2+} signal results in the modulation of one (or more) voltage-gated conductances in the neuron (or may result in heteromerization of mGluR1 and M_1 mAChR which can regulate a separate transmembrane current) to result in an increase in the number of burst responses to a stereotyped input (a train of somatic current injections), as illustrated in the inset traces.

The suppression of burst firing is mediated by the activation of mGluR5 and also requires an increase in intracellular Ca^{2+}. This signal, perhaps because it is smaller than the signal in response to synergistic activation of mGluR1 and M_1 mAChR, differentially modulates voltage-gated conductances in the neuron, resulting in a decrease in the number of burst responses to the stereotyped input, as illustrated in the inset traces.

Figure 5.4

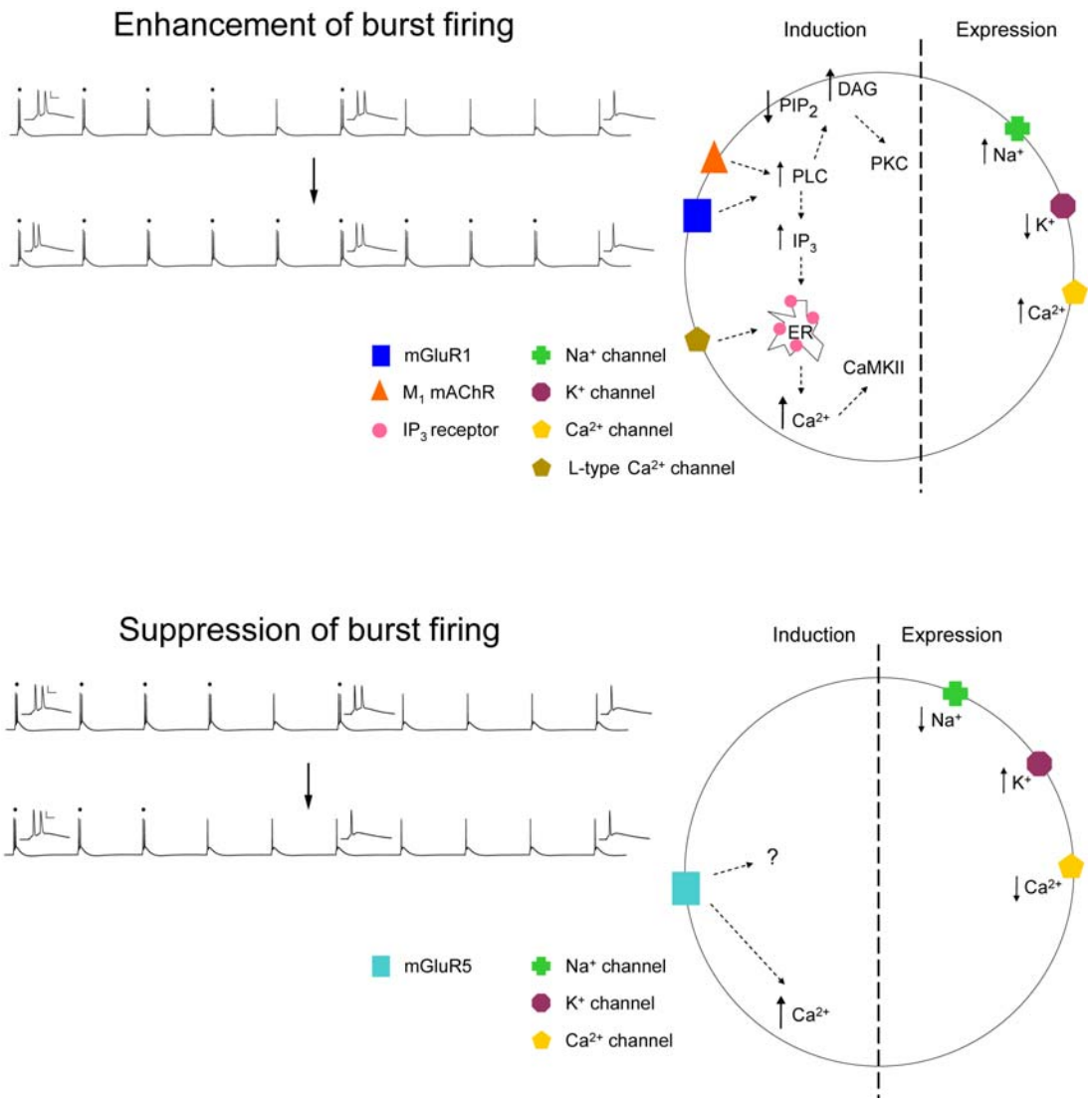
Enhancement of burst firing
Induction
Expression
PIP2
DAG
PKC
PLC
IP3
ER
CaMKII
Ca2+
Na+
K+
Ca2+
mGluR1
M1 mAChR
IP3 receptor
Na+ channel
K+ channel
Ca2+ channel
L-type Ca2+ channel
Suppression of burst firing
Induction
Expression
?
Ca2+
Na+
K+
Ca2+
mGluR5
Na+ channel
K+ channel
Ca2+ channel

Chapter 6:

Conclusions

The hippocampus is integrally involved in spatial and declarative memory, while dysfunction of hippocampal processing contributes to diverse diseases, such as epilepsy, Alzheimer's disease (AD), and addiction to drugs of abuse. The subiculum serves as the major output pathway of the hippocampus, targeting a variety of cortical and subcortical regions. Thus, plasticity of neuronal function in the subiculum, or areas targeting the subiculum, such as CA1, are likely to profoundly effect the way in which hippocampally-dependent information is processed and distributed in both physiological and pathological conditions. The experiments presented in this thesis explored the induction of plasticity of both synaptic and intrinsic properties in hippocampal pyramidal neurons. An understanding of the ways in which hippocampal processing may be affected by activity and environmental stimuli provides insights into general principles of neuronal processing in the brain, as well as providing potential targets for therapeutic interventions aimed at ameliorating the effects of diseases involving the hippocampus.

Synaptic plasticity in CA1 pyramidal neurons

Neurons receive thousands of synaptic contacts from both excitatory and inhibitory afferents. Input from different regions carry specific types of information, and may be clustered together or dispersed across the dendritic tree. The location of these inputs, the properties of the postsynaptic region where contact is made, and the

characteristics of the presynaptic terminals all influence the way in which information is integrated and processed to elicit action potential output. To investigate the location-specific capacity for synaptic plasticity of synapses at different dendritic locations, we used CA1 pyramidal neurons as a model system (Chapter 2). Schaffer collateral (SC) efferents from CA3 carry hippocampally processed information, and synapse on the apical and radial oblique dendrites in stratum radiatum (SR) and on basal dendrites in stratum oriens (SO) (Megias et al., 2001). By placing an extracellular stimulating electrode in specific regions, we could selectively activate SC synapses in distal stratum radiatum (furthest from the soma), proximal SR, or SO.

Interestingly, SC synapses in distal SR exhibited a robust increase in the amplitude of evoked excitatory postsynaptic potentials (EPSPs; long-term potentiation [LTP]) after repeated synaptic activation, but SC synapses, both in proximal SR and SO, exhibited a long-lasting decrease in EPSP amplitude (long-term depression [LTD]). This suggests that input arriving at specific dendritic locations can be separately modulated, perhaps as a means of normalizing the somatic response to synaptic activation in different regions of the dendritic tree.

Furthermore, the direction of plasticity was influenced by the receptors that were activated on the postsynaptic neuron. LTP at SC synapses in distal SR depended on NMDAR activation, but was insensitive to signaling via group I metabotropic glutamate receptors (mGluRs). Conversely, LTD at SC synapses in proximal SR did not require activation of NMDARs, but was dependent on activation of group I mGluRs. In fact, when subtype-specific group I mGluR antagonists were present during the experiment,

not only was LTD prevented, but LTP was induced. However, LTD at SC synapses in SO was not converted to LTP by group I mGluR antagonists, which suggests that target-specific heterogeneity can exist at synapses that are formed at similar distances from the soma. This disparity suggests that there is a specific subcellular distribution of postsynaptic receptors or their effectors such that different dendritic compartments have unique molecular machinery. Furthermore, distinct dendritic regions may be compartmentalized, with intracellular signaling or effects restricted to a specific area.

Synaptic plasticity is regarded as one of the most promising candidates for the cellular mechanism underlying learning and memory. These results demonstrate that the strength of connections can be influenced in complex ways, depending not only on the source of input, but the unique characteristics of the postsynaptic target. This may provide a cellular mechanism by which neurons can selectively attune to relevant information and alter the relative contribution of different afferents, depending on behavioral modulation (such as attention).

Intrinsic plasticity in subicular pyramidal neurons

Axons from CA1 neurons form a dense, topographically-organized projection to the subiculum (Amaral and Witter, 1989), which in turn targets a variety of cortical and subcortical regions (Swanson and Cowan, 1977). As the final output of the hippocampus, neuronal processing in the subiculum exerts a strong influence over the contribution of hippocampally processed information to diverse functions and behaviors. To investigate alterations in intrinsic properties of subicular pyramidal neurons, we examined two

plasticity-inducing paradigms: repeated treatment with a psychostimulant drug of abuse and electrical stimulation patterned after activity observed in CA1 during exploratory behavior (Chapters 3 and 4).

Nearly all potentially addictive drugs profoundly affect dopaminergic signaling in a collection of brain regions that together comprise the reward circuit (Kalivas and Volkow, 2005). Acute exposure to amphetamine, a psychostimulant, directly increases extracellular dopamine levels by reversing the dopamine transporter (DAT), which prevents the reuptake of dopamine, and causes additional dopamine to be released, independently of the stimulus (Heikkila et al., 1975b). Repeated exposure induces neuroadaptations in the reward circuit, which transiently or persistently modulate neurological and behavioral responses to further presentations of the drug. Transient neuroadaptations are likely required for the induction of long-lasting alterations, while persistent neuroadaptations may reflect the neural substrate underlying the manifestation of addiction (Dong et al., 2005).

After short-term (2-3 days) withdrawal from repeated amphetamine treatment, we identified a transient decrease in neuronal excitability in the subiculum, likely mediated by a reduction in Na^+ channel function (Chapter 3). In both regular firing and burst firing subicular pyramidal neurons, sensitivity to near-threshold input was decreased (via an attenuation of voltage-dependent amplification) and the ability to generate action potentials was impaired (via an increase in action potential threshold). In addition, the precise timing of burst firing (but not regular firing), relative to the input, was disrupted. Normally, a burst is reliably generated within a narrow time window shortly after a

stimulus. In contrast, single action potentials have longer latencies relative to an input, and are elicited with more variable timing. In fact, it has been suggested that bursts encode relevant information and that single action potentials represent noise in the system (Lisman, 1997). However, after short-term withdrawal, the latency and variability of burst firing resembled that observed in regular firing neurons, suggesting that the association between input and related output may be weakened, lessening the fidelity of information transfer. Furthermore, desynchronization of spike timing with respect to presynaptic input may lead to inappropriate induction of synaptic plasticity in a spike-timing dependent paradigm. Taken together, short-term withdrawal from repeated amphetamine markedly perturbs hippocampal processing and reduces excitatory drive to downstream targets, which may profoundly affect subsequent plasticity in those regions.

The nucleus accumbens (NAc), which receives a strong glutamatergic projection from the ventral subiculum, would be particularly affected. Subicular efferents directly excite medium spiny neurons in NAc, and further, gate additional glutamatergic input, particularly from prefrontal cortex (PFC), by driving the transition between a quiescent "down" state, from which medium spiny neurons do not fire action potentials, to an active "up" state, where cortical input can drive NAc output (O'Donnell and Grace, 1995). PFC is responsible for decision-making and formulating strategies to obtain desired goals, while NAc projects to ventral pallidum, thus providing an interface between the limbic and motor systems, enabling subsequent expression of behavior (Kalivas and Volkow, 2005). Taken together, a disruption in the PFC-NAc connection would severely impair goal-directed performance, and may contribute to symptoms of

short-term withdrawal observed in humans, including lack of energy (anergia) and flattened affect, particularly towards appetitive stimuli (anhedonia).

One theory concerning the molecular mechanisms underlying addiction is that drugs of abuse activate cellular processes involved in learning and memory in an unregulated and maladaptive manner (Wolf et al., 2004). In this context, decreased activity of medium spiny neurons may affect long-lasting changes in synaptic connections projecting to and emanating from NAc. For example, if input from the subiculum or PFC does not result in NAc output, Hebbian plasticity would lead to a decrease in the strength of the connection between the two regions. Subsequent responses to adaptive stimuli, such as food presentation, which normally produce a modest increase in dopamine, would be markedly attenuated. On the other hand, further presentations of the maladaptive stimulus, such as the drug of abuse, may still be able to evoke a response because of the supra-physiological increase in dopamine elicited. Thus, neurological and behavioral output induced by the maladaptive stimulus would be relatively strengthened compared to other stimuli. This process may contribute to behavioral sensitization observed in addiction, as well as decreased motivation to obtain non-drug rewards.

To more directly examine changes in intrinsic neuronal excitability in the subiculum, which may contribute to adaptive learning or may be hijacked by maladaptive stimuli such as drugs of abuse, we used whole-cell current-clamp recordings in hippocampal slices (Chapter 4). Activity recorded *in vivo* in CA1 during spatial exploration demonstrates a prominent oscillatory rhythm at in the theta frequency range (4-12 Hz) (Buzsaki, 2002; Hasselmo, 2005). Interestingly, stimulation of hippocampal

efferents at theta frequency can induce a relapse to cocaine-seeking in rats that have previously undergone extinction (Vorel et al., 2001). In our experiments, theta-patterned electrical stimulation resulted in a long-lasting increase in burst firing of intrinsically bursting subicular pyramidal neurons.

Burst firing likely has special consequences for signal processing and information transfer within neuronal networks. In some regions during specific tasks, bursts provide a more precise representation of a stimulus than single action potentials, or all firing considered together. For example, using burst responses to diagram place cells in the hippocampus, which fire when an animal is in a particular location in space (O'Keefe, 1976), results in refined spatial tuning and a consistent corticotopic representation of the external environment (Otto et al., 1991). Therefore, an increase in burst firing may represent an increase in the relay of detailed information about the environment and may contribute to the refinement of neural representations of places and events.

Additionally, compared to tonic (regular) firing of single action potentials, burst firing provides a robust signal that is more reliably propagated to postsynaptic targets, because a burst dramatically increases the overall release probability at a synapse (Lisman, 1997). In this context, enhanced burst firing in the subiculum may represent an increase in the relative contribution of hippocampally-dependent information to downstream processes and behaviors and provide a strong signal for the development of learned associations. For example, rats reliably learn to run to a specific place in an environment in response to a tone, which predicts presentation of a reward. Interestingly, after the reward is delivered, an increase in burst firing is observed (Martin and Ono,

2000), which may serve to consolidate the memory of where the reward was obtained. In animals and humans, a strong association is formed between drug experience and the environment in which it occurs. In fact, robust behavioral sensitization may be elicited in the context in which the drug was given, but fails to be expressed in a novel context (Anagnostaras and Robinson, 1996). These location-dependent cues may be a strong trigger that elicits relapse to drug-seeking, even after extended periods of abstinence from a drug.

In addition to characterizing the enhancement of neuronal excitability in response to physiologically relevant activity patterns, we also examined the cellular mechanisms involved in mediating the intrinsic plasticity (Chapter 4). Intriguingly, we found that the induction of burst plasticity, unlike synaptic plasticity, did not depend on activation of ionotropic receptors, but instead required synergistic activation of two metabotropic receptors: group I metabotropic glutamate receptors (mGluRs) and muscarinic acetylcholine receptors (mAChRs). This is the first demonstration that synaptic and intrinsic plasticity can be differentially induced, thereby providing complementary, rather than redundant, mechanisms by which experience-dependent information may be stored. Furthermore, our results raise the possibility that different behavioral states, which have unique neuromodulatory characteristics, may preferentially utilize independent mechanisms to encode information.

Although the role of intrinsic plasticity in learning and memory has received much less attention compared to synaptic plasticity, a number of studies have now demonstrated that plasticity of intrinsic properties occurs in a variety of regions (Zhang

and Linden, 2003). It is likely that these global alterations in neuronal excitability provide a complementary mechanism to synaptic plasticity by which neurons can modify their output in response to specific experiences. However, inappropriate changes in neuronal properties may underlie the induction, maintenance, and expression of maladaptive behaviors, such as addiction to drugs of abuse. By continuing to refine our knowledge of the detailed interactions between synaptic and intrinsic alterations in neural networks, we may elucidate the molecular mechanisms involved in physiological processes, such as learning and memory, as well as identify novel targets for the prevention and treatment of devastating diseases.

References

Abdul-Ghani MA, Valiante TA, Carlen PL, Pennefather PS (1996) Metabotropic glutamate receptors coupled to IP3 production mediate inhibition of IAHP in rat dentate granule neurons. J Neurophysiol 76:2691-2700.

Abe T, Sugihara H, Nawa H, Shigemoto R, Mizuno N, Nakanishi S (1992) Molecular characterization of a novel metabotropic glutamate receptor mGluR5 coupled to inositol phosphate/Ca2+ signal transduction. J Biol Chem 267:13361-13368.

Ackerman JM, White FJ (1990) A10 somatodendritic dopamine autoreceptor sensitivity following withdrawal from repeated cocaine treatment. Neurosci Lett 117:181-187.

Aizenman CD, Linden DJ (2000) Rapid, synaptically driven increases in the intrinsic excitability of cerebellar deep nuclear neurons. Nat Neurosci 3:109-111.

Akers RF, Lovinger DM, Colley PA, Linden DJ, Routtenberg A (1986) Translocation of protein kinase C activity may mediate hippocampal long-term potentiation. Science 231:587-589.

Alger BE, Nicoll RA (1980) Epileptiform burst afterhyperolarization: calcium-dependent potassium potential in hippocampal CA1 pyramidal cells. Science 210:1122-1124.

Amaral D, Lavenex P (2007) Hippocampal Neuroanatomy. In: The Hippocampus Book (Andersen P, Morris R, Amaral D, Bliss T, O'Keefe J, eds). New York: Oxford University Press.

Amaral DG (1978) A Golgi study of cell types in the hilar region of the hippocampus in the rat. J Comp Neurol 182:851-914.

Amaral DG, Dent JA (1981) Development of the mossy fibers of the dentate gyrus: I. A light and electron microscopic study of the mossy fibers and their expansions. J Comp Neurol 195:51-86.

Amaral DG, Witter MP (1989) The three-dimensional organization of the hippocampal formation: a review of anatomical data. Neuroscience 31:571-591.

Amaral DG, Dolorfo C, Alvarez-Royo P (1991) Organization of CA1 projections to the subiculum: a PHA-L analysis in the rat. Hippocampus 1:415-435.

Anagnostaras SG, Robinson TE (1996) Sensitization to the psychomotor stimulant effects of amphetamine: modulation by associative learning. Behav Neurosci 110:1397-1414.

Andersen P, Sundberg SH, Sveen O, Wigstrom H (1977) Specific long-lasting potentiation of synaptic transmission in hippocampal slices. Nature 266:736-737.

Andersen P, Morris R, Amaral D, Bliss T, O'Keefe J (2007) Historical Perspective: Proposed Functions, Biological Characteristics, and Neurobiological Models of the Hippocampus. In: The Hippocampus Book (Andersen P, Morris R, Amaral D, Bliss T, O'Keefe J, eds). New York: Oxford University Press.

Andrasfalvy BK, Magee JC (2001) Distance-dependent increase in AMPA receptor number in the dendrites of adult hippocampal CA1 pyramidal neurons. J Neurosci 21:9151-9159.

Anwyl R (1999) Metabotropic glutamate receptors: electrophysiological properties and role in plasticity. Brain Res Brain Res Rev 29:83-120.

Armano S, Rossi P, Taglietti V, D'Angelo E (2000) Long-term potentiation of intrinsic excitability at the mossy fiber-granule cell synapse of rat cerebellum. J Neurosci 20:5208-5216.

Azouz R, Jensen MS, Yaari Y (1996) Ionic basis of spike after-depolarization and burst generation in adult rat hippocampal CA1 pyramidal cells. J Physiol 492 (Pt 1):211-223.

Bain A (1855) The senses and the intellect: J.W. Parker, London.

Banke TG, Bowie D, Lee H, Huganir RL, Schousboe A, Traynelis SF (2000) Control of GluR1 AMPA receptor function by cAMP-dependent protein kinase. J Neurosci 20:89-102.

Baskys A, Malenka RC (1991a) Agonists at metabotropic glutamate receptors presynaptically inhibit EPSCs in neonatal rat hippocampus. J Physiol 444:687-701.

Baskys A, Malenka RC (1991b) Trans-ACPD depresses synaptic transmission in the hippocampus. Eur J Pharmacol 193:131-132.

Battaglia FP, Sutherland GR, McNaughton BL (2004) Hippocampal sharp wave bursts coincide with neocortical "up-state" transitions. Learn Mem 11:697-704.

Beau FE, Alger BE (1998) Transient suppression of GABAA-receptor-mediated IPSPs after epileptiform burst discharges in CA1 pyramidal cells. J Neurophysiol 79:659-669.

Behr J, Heinemann U (1996) Low Mg2+ induced epileptiform activity in the subiculum before and after disconnection from rat hippocampal and entorhinal cortex slices. Neurosci Lett 205:25-28.

Bekkers JM, Stevens CF (1990) Presynaptic mechanism for long-term potentiation in the hippocampus. Nature 346:724-729.

Benini R, Avoli M (2005) Rat subicular networks gate hippocampal output activity in an in vitro model of limbic seizures. J Physiol 566:885-900.

Bernard C, Wheal HV (1996) A role for synaptic and network plasticity in controlling epileptiform activity in CA1 in the kainic acid-lesioned rat hippocampus in vitro. J Physiol 495 (Pt 1):127-142.

Bernard C, Anderson A, Becker A, Poolos NP, Beck H, Johnston D (2004) Acquired dendritic channelopathy in temporal lobe epilepsy. Science 305:532-535.

Bi GQ, Poo MM (1998) Synaptic modifications in cultured hippocampal neurons: dependence on spike timing, synaptic strength, and postsynaptic cell type. J Neurosci 18:10464-10472.

Blackstad TW, Brink K, Hem J, Jeune B (1970) Distribution of hippocampal mossy fibers in the rat. An experimental study with silver impregnation methods. J Comp Neurol 138:433-449.

Bliss TV, Lømo T (1973) Long-lasting potentiation of synaptic transmission in the dentate area of the anaesthetized rabbit following stimulation of the perforant path. J Physiol 232:331-356.

Bliss TV, Collingridge GL (1993) A synaptic model of memory: long-term potentiation in the hippocampus. Nature 361:31-39.

Blumcke I, Becker AJ, Klein C, Scheiwe C, Lie AA, Beck H, Waha A, Friedl MG, Kuhn R, Emson P, Elger C, Wiestler OD (2000) Temporal lobe epilepsy associated up-regulation of metabotropic glutamate receptors: correlated changes in mGluR1 mRNA and protein expression in experimental animals and human patients. J Neuropathol Exp Neurol 59:1-10.

Bortolotto ZA, Collingridge GL (1993) Characterisation of LTP induced by the activation of glutamate metabotropic receptors in area CA1 of the hippocampus. Neuropharmacology 32:1-9.

Bortolotto ZA, Collingridge GL (1995) On the mechanism of long-term potentiation induced by (1S,3R)-1-aminocyclopentane-1,3-dicarboxylic acid (ACPD) in rat hippocampal slices. Neuropharmacology 34:1003-1014.

Bortolotto ZA, Bashir ZI, Davies CH, Collingridge GL (1994) A molecular switch activated by metabotropic glutamate receptors regulates induction of long-term potentiation. Nature 368:740-743.

Browman KE, Badiani A, Robinson TE (1996) Fimbria-fornix lesions do not block sensitization to the psychomotor activating effects of amphetamine. Pharmacol Biochem Behav 53:899-902.

Brudzynski SM, Gibson CJ (1997) Release of dopamine in the nucleus accumbens caused by stimulation of the subiculum in freely moving rats. Brain Res Bull 42:303-308.

Burns LH, Robbins TW, Everitt BJ (1993) Differential effects of excitotoxic lesions of the basolateral amygdala, ventral subiculum and medial prefrontal cortex on responding with conditioned reinforcement and locomotor activity potentiated by intra-accumbens infusions of D-amphetamine. Behav Brain Res 55:167-183.

Buzsaki G (2002) Theta oscillations in the hippocampus. Neuron 33:325-340.

Caine SB, Humby T, Robbins TW, Everitt BJ (2001) Behavioral effects of psychomotor stimulants in rats with dorsal or ventral subiculum lesions: locomotion, cocaine self-administration, and prepulse inhibition of startle. Behav Neurosci 115:880-894.

Callaway JC, Ross WN (1995) Frequency-dependent propagation of sodium action potentials in dendrites of hippocampal CA1 pyramidal neurons. J Neurophysiol 74:1395-1403.

Campanac E, Debanne D (2008) Spike timing-dependent plasticity: a learning rule for dendritic integration in rat CA1 pyramidal neurons. J Physiol 586:779-793.

Cantrell AR, Scheuer T, Catterall WA (1999) Voltage-dependent neuromodulation of Na+ channels by D1-like dopamine receptors in rat hippocampal neurons. J Neurosci 19:5301-5310.

Carr DB, Day M, Cantrell AR, Held J, Scheuer T, Catterall WA, Surmeier DJ (2003) Transmitter modulation of slow, activity-dependent alterations in sodium channel availability endows neurons with a novel form of cellular plasticity. Neuron 39:793-806.

Castillo PE, Weisskopf MG, Nicoll RA (1994) The role of Ca2+ channels in hippocampal mossy fiber synaptic transmission and long-term potentiation. Neuron 12:261-269.

Castillo PE, Janz R, Sudhof TC, Tzounopoulos T, Malenka RC, Nicoll RA (1997) Rab3A is essential for mossy fibre long-term potentiation in the hippocampus. Nature 388:590-593.

Cattaneo A, Maffei L, Morrone C (1981a) Patterns in the discharge of simple and complex visual cortical cells. Proc R Soc Lond B Biol Sci 212:279-297.

Cattaneo A, Maffei L, Morrone C (1981b) Two firing patterns in the discharge of complex cells encoding different attributes of the visual stimulus. Exp Brain Res 43:115-118.

Chavez-Noriega LE, Halliwell JV, Bliss TV (1990) A decrease in firing threshold observed after induction of the EPSP-spike (E-S) component of long-term potentiation in rat hippocampal slices. Exp Brain Res 79:633-641.

Chavis P, Shinozaki H, Bockaert J, Fagni L (1994) The metabotropic glutamate receptor types 2/3 inhibit L-type calcium channels via a pertussis toxin-sensitive G-protein in cultured cerebellar granule cells. J Neurosci 14:7067-7076.

Chavis P, Fagni L, Bockaert J, Lansman JB (1995) Modulation of calcium channels by metabotropic glutamate receptors in cerebellar granule cells. Neuropharmacology 34:929-937.

Chavis P, Fagni L, Lansman JB, Bockaert J (1996) Functional coupling between ryanodine receptors and L-type calcium channels in neurons. Nature 382:719-722.

Chen TC, Law B, Kondratyuk T, Rossie S (1995) Identification of soluble protein phosphatases that dephosphorylate voltage-sensitive sodium channels in rat brain. J Biol Chem 270:7750-7756.

Chevaleyre V, Castillo PE (2003) Heterosynaptic LTD of hippocampal GABAergic synapses: a novel role of endocannabinoids in regulating excitability. Neuron 38:461-472.

Chevaleyre V, Takahashi KA, Castillo PE (2006) Endocannabinoid-mediated synaptic plasticity in the CNS. Annu Rev Neurosci 29:37-76.

Choi S, Lovinger DM (1996) Metabotropic glutamate receptor modulation of voltage-gated Ca2+ channels involves multiple receptor subtypes in cortical neurons. J Neurosci 16:36-45.

Christie BR, Magee JC, Johnston D (1996) The role of dendritic action potentials and Ca2+ influx in the induction of homosynaptic long-term depression in hippocampal CA1 pyramidal neurons. Learn Mem 3:160-169.

Ciruela F, Escriche M, Burgueno J, Angulo E, Casado V, Soloviev MM, Canela EI, Mallol J, Chan WY, Lluis C, McIlhinney RA, Franco R (2001) Metabotropic glutamate 1alpha and adenosine A1 receptors assemble into functionally interacting complexes. J Biol Chem 276:18345-18351.

Cohen AS, Abraham WC (1996) Facilitation of long-term potentiation by prior activation of metabotropic glutamate receptors. J Neurophysiol 76:953-962.

Cohen I, Navarro V, Clemenceau S, Baulac M, Miles R (2002) On the origin of interictal activity in human temporal lobe epilepsy in vitro. Science 298:1418-1421.

Collingridge GL, Kehl SJ, McLennan H (1983) Excitatory amino acids in synaptic transmission in the Schaffer collateral-commissural pathway of the rat hippocampus. J Physiol 334:33-46.

Commins S, Gigg J, Anderson M, O'Mara SM (1998) The projection from hippocampal area CA1 to the subiculum sustains long-term potentiation. Neuroreport 9:847-850.

Commins S, Anderson M, Gigg J, O'Mara SM (1999) The effects of single and multiple episodes of theta patterned or high frequency stimulation on synaptic transmission from hippocampal area CA1 to the subiculum in rats. Neurosci Lett 270:99-102.

Conn PJ, Pin JP (1997) Pharmacology and functions of metabotropic glutamate receptors. Annu Rev Pharmacol Toxicol 37:205-237.

Contractor A, Rogers C, Maron C, Henkemeyer M, Swanson GT, Heinemann SF (2002) Trans-synaptic Eph receptor-ephrin signaling in hippocampal mossy fiber LTP. Science 296:1864-1869.

Cooper DC (2002) The significance of action potential bursting in the brain reward circuit. Neurochem Int 41:333-340.

Cooper DC, Chung S, Spruston N (2005) Output-Mode Transitions Are Controlled by Prolonged Inactivation of Sodium Channels in Pyramidal Neurons of Subiculum. PLoS Biol 3:e175.

Cooper DC, Moore SJ, Staff NP, Spruston N (2003) Psychostimulant-induced plasticity of intrinsic neuronal excitability in ventral subiculum. J Neurosci 23:9937-9946.

Costa MR, Catterall WA (1984a) Cyclic AMP-dependent phosphorylation of the alpha subunit of the sodium channel in synaptic nerve ending particles. J Biol Chem 259:8210-8218.

Costa MR, Catterall WA (1984b) Phosphorylation of the alpha subunit of the sodium channel by protein kinase C. Cell Mol Neurobiol 4:291-297.

Costa MR, Casnellie JE, Catterall WA (1982) Selective phosphorylation of the alpha subunit of the sodium channel by cAMP-dependent protein kinase. J Biol Chem 257:7918-7921.

Crepel F, Jaillard D (1991) Pairing of pre- and postsynaptic activities in cerebellar Purkinje cells induces long-term changes in synaptic efficacy in vitro. J Physiol 432:123-141.

Crepel V, Aniksztejn L, Ben-Ari Y, Hammond C (1994) Glutamate metabotropic receptors increase a Ca(2+)-activated nonspecific cationic current in CA1 hippocampal neurons. J Neurophysiol 72:1561-1569.

D'Angelo E, Rossi P, Armano S, Taglietti V (1999) Evidence for NMDA and mGlu receptor-dependent long-term potentiation of mossy fiber-granule cell transmission in rat cerebellum. J Neurophysiol 81:277-287.

Daoudal G, Debanne D (2003) Long-term plasticity of intrinsic excitability: learning rules and mechanisms. Learn Mem 10:456-465.

David HN, Abraini JH (2001) Differential modulation of the D1-like- and D2-like dopamine receptor-induced locomotor responses by group II metabotropic glutamate receptors in the rat nucleus accumbens. Neuropharmacology 41:454-463.

Deisz RA, Fortin G, Zieglgansberger W (1991) Voltage dependence of excitatory postsynaptic potentials of rat neocortical neurons. J Neurophysiol 65:371-382.

Denslow MJ, Eid T, Du F, Schwarcz R, Lothman EW, Steward O (2001) Disruption of inhibition in area CA1 of the hippocampus in a rat model of temporal lobe epilepsy. J Neurophysiol 86:2231-2245.

Derkach V, Barria A, Soderling TR (1999) Ca2+/calmodulin-kinase II enhances channel conductance of alpha-amino-3-hydroxy-5-methyl-4-isoxazolepropionate type glutamate receptors. Proc Natl Acad Sci U S A 96:3269-3274.

Desai NS, Rutherford LC, Turrigiano GG (1999) Plasticity in the intrinsic excitability of cortical pyramidal neurons. Nat Neurosci 2:515-520.

Di Ciano P, Everitt BJ (2002) Reinstatement and spontaneous recovery of cocaine-seeking following extinction and different durations of withdrawal. Behav Pharmacol 13:397-405.

Disterhoft JF, Matthew Oh M (2003) Modulation of cholinergic transmission enhances excitability of hippocampal pyramidal neurons and ameliorates learning impairments in aging animals. Neurobiol Learn Mem 80:223-233.

Disterhoft JF, Wu WW, Ohno M (2004) Biophysical alterations of hippocampal pyramidal neurons in learning, ageing and Alzheimer's disease. Ageing Res Rev 3:383-406.

Disterhoft JF, Moyer JR, Jr., Thompson LT, Kowalska M (1993) Functional aspects of calcium-channel modulation. Clin Neuropharmacol 16 Suppl 1:S12-24.

Disterhoft JF, Kronforst-Collins M, Oh MM, Power JM, Preston AR, Weiss C (1999) Cholinergic facilitation of trace eyeblink conditioning in aging rabbits. Life Sci 64:541-548.

Dong Y, Nasif FJ, Tsui JJ, Ju WY, Cooper DC, Hu XT, Malenka RC, White FJ (2005) Cocaine-induced plasticity of intrinsic membrane properties in prefrontal cortex pyramidal neurons: adaptations in potassium currents. J Neurosci 25:936-940.

Dreier JP, Heinemann U (1991) Regional and time dependent variations of low Mg2+ induced epileptiform activity in rat temporal cortex slices. Exp Brain Res 87:581-596.

Edwards DA, Kim J, Alger BE (2006) Multiple mechanisms of endocannabinoid response initiation in hippocampus. J Neurophysiol 95:67-75.

Enz R (2007) The trick of the tail: protein-protein interactions of metabotropic glutamate receptors. Bioessays 29:60-73.

Faas GC, Adwanikar H, Gereau RWt, Saggau P (2002) Modulation of presynaptic calcium transients by metabotropic glutamate receptor activation: a differential role in acute depression of synaptic transmission and long-term depression. J Neurosci 22:6885-6890.

Finch DM (1996) Neurophysiology of converging synaptic inputs from the rat prefrontal cortex, amygdala, midline thalamus, and hippocampal formation onto single neurons of the caudate/putamen and nucleus accumbens. Hippocampus 6:495-512.

Fitzgerald LW, Ortiz J, Hamedani AG, Nestler EJ (1996) Drugs of abuse and stress increase the expression of GluR1 and NMDAR1 glutamate receptor subunits in the rat ventral tegmental area: common adaptations among cross-sensitizing agents. J Neurosci 16:274-282.

Fray PJ, Sahakian BJ, Robbins TW, Koob GF, Iversen SD (1980) An observational method for quantifying the behavioural effects of dopamine agonists: contrasting effects of d-amphetamine and apomorphine. Psychopharmacology (Berl) 69:253-259.

Frick A, Magee J, Johnston D (2004) LTP is accompanied by an enhanced local excitability of pyramidal neuron dendrites. Nat Neurosci 7:126-135.

Funahashi M, Harris E, Stewart M (1999) Re-entrant activity in a presubiculum-subiculum circuit generates epileptiform activity in vitro. Brain Res 849:139-146.

Gee CE, Benquet P, Gerber U (2003) Group I metabotropic glutamate receptors activate a calcium-sensitive transient receptor potential-like conductance in rat hippocampus. J Physiol 546:655-664.

Gold LH, Swerdlow NR, Koob GF (1988) The role of mesolimbic dopamine in conditioned locomotion produced by amphetamine. Behav Neurosci 102:544-552.

Golding NL, Kath WL, Spruston N (2001) Dichotomy of action-potential backpropagation in CA1 pyramidal neuron dendrites. J Neurophysiol 86:2998-3010.

Golding NL, Staff NP, Spruston N (2002) Dendritic spikes as a mechanism for cooperative long-term potentiation. Nature 418:326-331.

Golding NL, Mickus TJ, Katz Y, Kath WL, Spruston N (2005) Factors mediating powerful voltage attenuation along CA1 pyramidal neuron dendrites. J Physiol 568:69-82.

Golomb D, Yue C, Yaari Y (2006) Contribution of persistent Na+ current and M-type K+ current to somatic bursting in CA1 pyramidal cells: combined experimental and modeling Study. J Neurophysiol 96:1912-1926.

Greene JR, Totterdell S (1997) Morphology and distribution of electrophysiologically defined classes of pyramidal and nonpyramidal neurons in rat ventral subiculum in vitro. J Comp Neurol 380:395-408.

Guatteo E, Mercuri NB, Bernardi G, Knopfel T (1999) Group I metabotropic glutamate receptors mediate an inward current in rat substantia nigra dopamine neurons that is independent from calcium mobilization. J Neurophysiol 82:1974-1981.

Guido W, Sherman SM (1998) Response latencies of cells in the cat's lateral geniculate nucleus are less variable during burst than tonic firing. Vis Neurosci 15:231-237.

Gustafsson B, Wigstrom H, Abraham WC, Huang YY (1987) Long-term potentiation in the hippocampus using depolarizing current pulses as the conditioning stimulus to single volley synaptic potentials. J Neurosci 7:774-780.

Harris E, Stewart M (2001a) Propagation of synchronous epileptiform events from subiculum backward into area CA1 of rat brain slices. Brain Res 895:41-49.

Harris E, Stewart M (2001b) Intrinsic connectivity of the rat subiculum: II. Properties of synchronous spontaneous activity and a demonstration of multiple generator regions. J Comp Neurol 435:506-518.

Harris E, Witter MP, Weinstein G, Stewart M (2001) Intrinsic connectivity of the rat subiculum: I. Dendritic morphology and patterns of axonal arborization by pyramidal neurons. J Comp Neurol 435:490-505.

Hasselmo ME (2005) What is the function of hippocampal theta rhythm?--Linking behavioral data to phasic properties of field potential and unit recording data. Hippocampus 15:936-949.

Hasselmo ME, Schnell E (1994) Laminar selectivity of the cholinergic suppression of synaptic transmission in rat hippocampal region CA1: computational modeling and brain slice physiology. J Neurosci 14:3898-3914.

Hebb DO (1949) The organization of behavior; a neuropsychological theory. New York,: Wiley.

Hebert LE, Scherr PA, Bienias JL, Bennett DA, Evans DA (2003) Alzheimer disease in the US population: prevalence estimates using the 2000 census. Arch Neurol 60:1119-1122.

Heien ML, Wightman RM (2006) Phasic dopamine signaling during behavior, reward, and disease states. CNS Neurol Disord Drug Targets 5:99-108.

Heikkila RE, Orlansky H, Cohen G (1975a) Studies on the distinction between uptake inhibition and release of (3H)dopamine in rat brain tissue slices. Biochem Pharmacol 24:847-852.

Heikkila RE, Orlansky H, Mytilineou C, Cohen G (1975b) Amphetamine: evaluation of d- and l-isomers as releasing agents and uptake inhibitors for 3H-dopamine and 3H-norepinephrine in slices of rat neostriatum and cerebral cortex. J Pharmacol Exp Ther 194:47-56.

Henry DJ, White FJ (1995) The persistence of behavioral sensitization to cocaine parallels enhanced inhibition of nucleus accumbens neurons. J Neurosci 15:6287-6299.

Henry DJ, Greene MA, White FJ (1989) Electrophysiological effects of cocaine in the mesoaccumbens dopamine system: repeated administration. J Pharmacol Exp Ther 251:833-839.

Higashi H, Inanaga K, Nishi S, Uchimura N (1989) Enhancement of dopamine actions on rat nucleus accumbens neurones in vitro after methamphetamine pre-treatment. J Physiol 408:587-603.

Holthoff K, Kovalchuk Y, Yuste R, Konnerth A (2004) Single-shock LTD by local dendritic spikes in pyramidal neurons of mouse visual cortex. J Physiol 560:27-36.

Huang YY, Kandel ER (2005) Theta frequency stimulation up-regulates the synaptic strength of the pathway from CA1 to subiculum region of hippocampus. Proc Natl Acad Sci U S A 102:232-237.

Huerta PT, Lisman JE (1995) Bidirectional synaptic plasticity induced by a single burst during cholinergic theta oscillation in CA1 in vitro. Neuron 15:1053-1063.

Isaac JT, Nicoll RA, Malenka RC (1995) Evidence for silent synapses: implications for the expression of LTP. Neuron 15:427-434.

Isaac JT, Hjelmstad GO, Nicoll RA, Malenka RC (1996) Long-term potentiation at single fiber inputs to hippocampal CA1 pyramidal cells. Proc Natl Acad Sci U S A 93:8710-8715.

Ishihara K, Sasa M, Momiyama T, Ujihara H, Nakamura J, Serikawa T, Yamada J, Takaori S (1993) Abnormal excitability of hippocampal CA3 pyramidal neurons of spontaneously epileptic rats (SER), a double mutant. Exp Neurol 119:287-290.

Ishizuka N (2001) Laminar organization of the pyramidal cell layer of the subiculum in the rat. J Comp Neurol 435:89-110.

Ito R, Robbins TW, Everitt BJ (2004) Differential control over cocaine-seeking behavior by nucleus accumbens core and shell. Nat Neurosci 7:389-397.

Jack CR, Jr., Petersen RC, Xu YC, Waring SC, O'Brien PC, Tangalos EG, Smith GE, Ivnik RJ, Kokmen E (1997) Medial temporal atrophy on MRI in normal aging and very mild Alzheimer's disease. Neurology 49:786-794.

Jaffe D, Johnston D (1990) Induction of long-term potentiation at hippocampal mossy-fiber synapses follows a Hebbian rule. J Neurophysiol 64:948-960.

Jarrard LE (1993) On the role of the hippocampus in learning and memory in the rat. Behav Neural Biol 60:9-26.

Jay TM, Witter MP (1991) Distribution of hippocampal CA1 and subicular efferents in the prefrontal cortex of the rat studied by means of anterograde transport of Phaseolus vulgaris-leucoagglutinin. J Comp Neurol 313:574-586.

Jensen MS, Yaari Y (1997) Role of intrinsic burst firing, potassium accumulation, and electrical coupling in the elevated potassium model of hippocampal epilepsy. J Neurophysiol 77:1224-1233.

Jester JM, Campbell LW, Sejnowski TJ (1995) Associative EPSP--spike potentiation induced by pairing orthodromic and antidromic stimulation in rat hippocampal slices. J Physiol 484 (Pt 3):689-705.

Jones SR, Gainetdinov RR, Wightman RM, Caron MG (1998) Mechanisms of amphetamine action revealed in mice lacking the dopamine transporter. J Neurosci 18:1979-1986.

Jung HY, Staff NP, Spruston N (2001) Action potential bursting in subicular pyramidal neurons is driven by a calcium tail current. J Neurosci 21:3312-3321.

Kalivas PW, Volkow ND (2005) The neural basis of addiction: a pathology of motivation and choice. Am J Psychiatry 162:1403-1413.

Kandel E, Schwartz J, Jessell T (2000) Principles of Neural Science, 4th Edition. New York: Oxford University Press.

Kelso SR, Ganong AH, Brown TH (1986) Hebbian synapses in hippocampus. Proc Natl Acad Sci U S A 83:5326-5330.

Kemppainen S, Jolkkonen E, Pitkanen A (2002) Projections from the posterior cortical nucleus of the amygdala to the hippocampal formation and parahippocampal region in rat. Hippocampus 12:735-755.

Kishi T, Tsumori T, Ono K, Yokota S, Ishino H, Yasui Y (2000) Topographical organization of projections from the subiculum to the hypothalamus in the rat. J Comp Neurol 419:205-222.

Kokaia M (2000) Long-term potentiation of single subicular neurons in mice. Hippocampus 10:684-692.

Kullmann DM, Nicoll RA (1992) Long-term potentiation is associated with increases in quantal content and quantal amplitude. Nature 357:240-244.

Lape R, Dani JA (2004) Complex response to afferent excitatory bursts by nucleus accumbens medium spiny projection neurons. J Neurophysiol 92:1276-1284.

Laroche S, Jay TM, Thierry AM (1990) Long-term potentiation in the prefrontal cortex following stimulation of the hippocampal CA1/subicular region. Neurosci Lett 114:184-190.

Larson J, Lynch G (1986) Induction of synaptic potentiation in hippocampus by patterned stimulation involves two events. Science 232:985-988.

Larson J, Wong D, Lynch G (1986) Patterned stimulation at the theta frequency is optimal for the induction of hippocampal long-term potentiation. Brain Res 368:347-350.

Lee YS, Chay TR, Ree T (1983) On the mechanism of spiking and bursting in excitable cells. Biophys Chem 18:25-34.

Levy WB, Steward O (1979) Synapses as associative memory elements in the hippocampal formation. Brain Res 175:233-245.

Li M, West JW, Lai Y, Scheuer T, Catterall WA (1992) Functional modulation of brain sodium channels by cAMP-dependent phosphorylation. Neuron 8:1151-1159.

Li M, West JW, Numann R, Murphy BJ, Scheuer T, Catterall WA (1993) Convergent regulation of sodium channels by protein kinase C and cAMP-dependent protein kinase. Science 261:1439-1442.

Li Y, Vartanian AJ, White FJ, Xue CJ, Wolf ME (1997) Effects of the AMPA receptor antagonist NBQX on the development and expression of behavioral sensitization to cocaine and amphetamine. Psychopharmacology (Berl) 134:266-276.

Liao D, Hessler NA, Malinow R (1995) Activation of postsynaptically silent synapses during pairing-induced LTP in CA1 region of hippocampal slice. Nature 375:400-404.

Lisman J, Schulman H, Cline H (2002) The molecular basis of CaMKII function in synaptic and behavioural memory. Nat Rev Neurosci 3:175-190.

Lisman JE (1997) Bursts as a unit of neural information: making unreliable synapses reliable. Trends Neurosci 20:38-43.

Livingstone MS, Freeman DC, Hubel DH (1996) Visual responses in V1 of freely viewing monkeys. Cold Spring Harb Symp Quant Biol 61:27-37.

Lopes da Silva FH, Arnolds DE, Neijt HC (1984) A functional link between the limbic cortex and ventral striatum: physiology of the subiculum accumbens pathway. Exp Brain Res 55:205-214.

Lorente de Nó R (1933) Studies on the structure of the cerebral cortex. I. The area entorhinalis. Journal für Psychologie und Neurologie 45:381-438.

Lorente de Nó R (1934) Studies on the structure of the cerebral cortex. II. Continuation of the study of ammonic system. Journal für Psychologie und Neurologie 46:113-177.

Losonczy A, Makara JK, Magee JC (2008) Compartmentalized dendritic plasticity and input feature storage in neurons. Nature 452:436-441.

Lu W, Man H, Ju W, Trimble WS, MacDonald JF, Wang YT (2001) Activation of synaptic NMDA receptors induces membrane insertion of new AMPA receptors and LTP in cultured hippocampal neurons. Neuron 29:243-254.

Lynch G, Larson J, Kelso S, Barrionuevo G, Schottler F (1983) Intracellular injections of EGTA block induction of hippocampal long-term potentiation. Nature 305:719-721.

Lynch GS, Dunwiddie T, Gribkoff V (1977) Heterosynaptic depression: a postsynaptic correlate of long-term potentiation. Nature 266:737-739.

Maccaferri G, Lacaille JC (2003) Interneuron Diversity series: Hippocampal interneuron classifications--making things as simple as possible, not simpler. Trends Neurosci 26:564-571.

MacDermott AB, Mayer ML, Westbrook GL, Smith SJ, Barker JL (1986) NMDA-receptor activation increases cytoplasmic calcium concentration in cultured spinal cord neurones. Nature 321:519-522.

Magee JC, Johnston D (1997) A synaptically controlled, associative signal for Hebbian plasticity in hippocampal neurons. Science 275:209-213.

Magee JC, Cook EP (2000) Somatic EPSP amplitude is independent of synapse location in hippocampal pyramidal neurons. Nat Neurosci 3:895-903.

Magee JC, Avery RB, Christie BR, Johnston D (1996) Dihydropyridine-sensitive, voltage-gated Ca2+ channels contribute to the resting intracellular Ca2+ concentration of hippocampal CA1 pyramidal neurons. J Neurophysiol 76:3460-3470.

Mahon S, Casassus G, Mulle C, Charpier S (2003) Spike-dependent intrinsic plasticity increases firing probability in rat striatal neurons in vivo. J Physiol 550:947-959.

Malenka RC, Nicoll RA (1997) Silent synapses speak up. Neuron 19:473-476.

Malenka RC, Nicoll RA (1999) Long-term potentiation--a decade of progress? Science 285:1870-1874.

Malinow R, Miller JP (1986) Postsynaptic hyperpolarization during conditioning reversibly blocks induction of long-term potentiation. Nature 320:529-530.

Malinow R, Tsien RW (1990) Presynaptic enhancement shown by whole-cell recordings of long-term potentiation in hippocampal slices. Nature 346:177-180.

Malinow R, Schulman H, Tsien RW (1989) Inhibition of postsynaptic PKC or CaMKII blocks induction but not expression of LTP. Science 245:862-866.

Manahan-Vaughan D, Reymann KG (1997) Group 1 metabotropic glutamate receptors contribute to slow-onset potentiation in the rat CA1 region in vivo. Neuropharmacology 36:1533-1538.

Maren S, Baudry M (1995) Properties and mechanisms of long-term synaptic plasticity in the mammalian brain: relationships to learning and memory. Neurobiol Learn Mem 63:1-18.

Martin JL, Sloviter RS (2001) Focal inhibitory interneuron loss and principal cell hyperexcitability in the rat hippocampus after microinjection of a neurotoxic conjugate of saporin and a peptidase-resistant analog of Substance P. J Comp Neurol 436:127-152.

Martin PD, Ono T (2000) Effects of reward anticipation, reward presentation, and spatial parameters on the firing of single neurons recorded in the subiculum and nucleus accumbens of freely moving rats. Behav Brain Res 116:23-38.

Martinez JL, Jr., Derrick BE (1996) Long-term potentiation and learning. Annu Rev Psychol 47:173-203.

Masu M, Tanabe Y, Tsuchida K, Shigemoto R, Nakanishi S (1991) Sequence and expression of a metabotropic glutamate receptor. Nature 349:760-765.

Mattia D, Kawasaki H, Avoli M (1997) Repetitive firing and oscillatory activity of pyramidal-like bursting neurons in the rat subiculum. Exp Brain Res 114:507-517.

Mayer ML, Westbrook GL, Guthrie PB (1984) Voltage-dependent block by Mg2+ of NMDA responses in spinal cord neurones. Nature 309:261-263.

McNaughton BL, Douglas RM, Goddard GV (1978) Synaptic enhancement in fascia dentata: cooperativity among coactive afferents. Brain Res 157:277-293.

Megias M, Emri Z, Freund TF, Gulyas AI (2001) Total number and distribution of inhibitory and excitatory synapses on hippocampal CA1 pyramidal cells. Neuroscience 102:527-540.

Mellor J, Nicoll RA (2001) Hippocampal mossy fiber LTP is independent of postsynaptic calcium. Nat Neurosci 4:125-126.

Metz AE, Spruston N, Martina M (2007) Dendritic D-type potassium currents inhibit the spike afterdepolarization in rat hippocampal CA1 pyramidal neurons. J Physiol.

Metz AE, Jarsky T, Martina M, Spruston N (2005) R-type calcium channels contribute to afterdepolarization and bursting in hippocampal CA1 pyramidal neurons. J Neurosci 25:5763-5773.

Moyer JR, Jr., Thompson LT, Disterhoft JF (1996) Trace eyeblink conditioning increases CA1 excitability in a transient and learning-specific manner. J Neurosci 16:5536-5546.

Muller W, Misgeld U (1991) Picrotoxin- and 4-aminopyridine-induced activity in hilar neurons in the guinea pig hippocampal slice. J Neurophysiol 65:141-147.

Murphy BJ, Rossie S, De Jongh KS, Catterall WA (1993) Identification of the sites of selective phosphorylation and dephosphorylation of the rat brain Na+ channel alpha subunit by cAMP-dependent protein kinase and phosphoprotein phosphatases. J Biol Chem 268:27355-27362.

Mutel V, Ellis GJ, Adam G, Chaboz S, Nilly A, Messer J, Bleuel Z, Metzler V, Malherbe P, Schlaeger EJ, Roughley BS, Faull RL, Richards JG (2000) Characterization of [(3)H]Quisqualate binding to recombinant rat metabotropic glutamate 1a and 5a receptors and to rat and human brain sections. J Neurochem 75:2590-2601.

Németh B, Ledent C, Freund TF, Hájos N (2008) CB1 receptor-dependent and -independent inhibition of excitatory postsynaptic currents in the hippocampus by WIN 55,212-2. Neuropharmacology 54:51-57.

Nicholson DA, Trana R, Katz Y, Kath WL, Spruston N, Geinisman Y (2006) Distance-dependent differences in synapse number and AMPA receptor expression in hippocampal CA1 pyramidal neurons. Neuron 50:431-442.

Nishi A, Liu F, Matsuyama S, Hamada M, Higashi H, Nairn AC, Greengard P (2003) Metabotropic mGlu5 receptors regulate adenosine A2A receptor signaling. Proc Natl Acad Sci U S A 100:1322-1327.

Nowak L, Bregestovski P, Ascher P, Herbet A, Prochiantz A (1984) Magnesium gates glutamate-activated channels in mouse central neurones. Nature 307:462-465.

Numann R, Catterall WA, Scheuer T (1991) Functional modulation of brain sodium channels by protein kinase C phosphorylation. Science 254:115-118.

O'Connor DH, Wittenberg GM, Wang SS (2005) Graded bidirectional synaptic plasticity is composed of switch-like unitary events. Proc Natl Acad Sci U S A 102:9679-9684.

O'Donnell P, Grace AA (1995) Synaptic interactions among excitatory afferents to nucleus accumbens neurons: hippocampal gating of prefrontal cortical input. J Neurosci 15:3622-3639.

O'Keefe J (1976) Place units in the hippocampus of the freely moving rat. Exp Neurol 51:78-109.

O'Mara SM, Commins S, Anderson M (2000) Synaptic plasticity in the hippocampal area CA1-subiculum projection: implications for theories of memory. Hippocampus 10:447-456.

O'Mara SM, Commins S, Anderson M, Gigg J (2001) The subiculum: a review of form, physiology and function. Prog Neurobiol 64:129-155.

Office of National Drug Control Policy (2004) The Economic Costs of Drug Abuse in the United States, 1992-2002.

Ohno M, Sametsky EA, Silva AJ, Disterhoft JF (2006) Differential effects of alphaCaMKII mutation on hippocampal learning and changes in intrinsic neuronal excitability. Eur J Neurosci 23:2235-2240.

Okamoto N, Hori S, Akazawa C, Hayashi Y, Shigemoto R, Mizuno N, Nakanishi S (1994) Molecular characterization of a new metabotropic glutamate receptor mGluR7 coupled to inhibitory cyclic AMP signal transduction. J Biol Chem 269:1231-1236.

Otto T, Eichenbaum H, Wiener SI, Wible CG (1991) Learning-related patterns of CA1 spike trains parallel stimulation parameters optimal for inducing hippocampal long-term potentiation. Hippocampus 1:181-192.

Paulson PE, Robinson TE (1991) Sensitization to systemic amphetamine produces an enhanced locomotor response to a subsequent intra-accumbens amphetamine challenge in rats. Psychopharmacology (Berl) 104:140-141.

Paulson PE, Camp DM, Robinson TE (1991) Time course of transient behavioral depression and persistent behavioral sensitization in relation to regional brain monoamine concentrations during amphetamine withdrawal in rats. Psychopharmacology (Berl) 103:480-492.

Pickard L, Noel J, Duckworth JK, Fitzjohn SM, Henley JM, Collingridge GL, Molnar E (2001) Transient synaptic activation of NMDA receptors leads to the insertion of native AMPA receptors at hippocampal neuronal plasma membranes. Neuropharmacology 41:700-713.

Pierce RC, Kalivas PW (1997) Repeated cocaine modifies the mechanism by which amphetamine releases dopamine. J Neurosci 17:3254-3261.

Pierce RC, Bell K, Duffy P, Kalivas PW (1996) Repeated cocaine augments excitatory amino acid transmission in the nucleus accumbens only in rats having developed behavioral sensitization. J Neurosci 16:1550-1560.

Pike FG, Meredith RM, Olding AW, Paulsen O (1999) Rapid report: postsynaptic bursting is essential for 'Hebbian' induction of associative long-term potentiation at excitatory synapses in rat hippocampus. J Physiol 518 (Pt 2):571-576.

Power AE, Vazdarjanova A, McGaugh JL (2003) Muscarinic cholinergic influences in memory consolidation. Neurobiol Learn Mem 80:178-193.

Power JM, Wu WW, Sametsky E, Oh MM, Disterhoft JF (2002) Age-related enhancement of the slow outward calcium-activated potassium current in hippocampal CA1 pyramidal neurons in vitro. J Neurosci 22:7234-7243.

Queiroz CM, Mello LE (2007) Synaptic plasticity of the CA3 commissural projection in epileptic rats: an in vivo electrophysiological study. Eur J Neurosci 25:3071-3079.

Rae MG, Irving AJ (2004) Both mGluR1 and mGluR5 mediate Ca2+ release and inward currents in hippocampal CA1 pyramidal neurons. Neuropharmacology 46:1057-1069.

Ramón j Cajal S (1893) Estructura del asta de Ammon y fascia dentata. Ann Soc Esp Hist Nat 22.

Reid CA, Dixon DB, Takahashi M, Bliss TV, Fine A (2004) Optical quantal analysis indicates that long-term potentiation at single hippocampal mossy fiber synapses is expressed through increased release probability, recruitment of new release sites, and activation of silent synapses. J Neurosci 24:3618-3626.

Reid MS, Berger SP (1996) Evidence for sensitization of cocaine-induced nucleus accumbens glutamate release. Neuroreport 7:1325-1329.

Remy S, Spruston N (2007) Dendritic spikes induce single-burst long-term potentiation. Proc Natl Acad Sci U S A 104:17192-17197.

Rhoades BK, Gross GW (1994) Potassium and calcium channel dependence of bursting in cultured neuronal networks. Brain Res 643:310-318.

Ritz MC, Lamb RJ, Goldberg SR, Kuhar MJ (1987) Cocaine receptors on dopamine transporters are related to self-administration of cocaine. Science 237:1219-1223.

Robinson TE, Berridge KC (2003) Addiction. Annu Rev Psychol 54:25-53.

Rossi P, D'Angelo E, Taglietti V (1996) Differential long-lasting potentiation of the NMDA and non-NMDA synaptic currents induced by metabotropic and NMDA receptor coactivation in cerebellar granule cells. Eur J Neurosci 8:1182-1189.

Rothe T, Bigl V, Grantyn R (1994) Potentiating and depressant effects of metabotropic glutamate receptor agonists on high-voltage-activated calcium currents in cultured retinal ganglion neurons from postnatal mice. Pflugers Arch 426:161-170.

Russig H, Durrer A, Yee BK, Murphy CA, Feldon J (2003) The acquisition, retention and reversal of spatial learning in the morris water maze task following withdrawal from an escalating dosage schedule of amphetamine in wistar rats. Neuroscience 119:167-179.

Sahara Y, Westbrook GL (1993) Modulation of calcium currents by a metabotropic glutamate receptor involves fast and slow kinetic components in cultured hippocampal neurons. J Neurosci 13:3041-3050.

Sander JW, Shorvon SD (1996) Epidemiology of the epilepsies. J Neurol Neurosurg Psychiatry 61:433-443.

Sastry BR, Goh JW, Auyeung A (1986) Associative induction of posttetanic and long-term potentiation in CA1 neurons of rat hippocampus. Science 232:988-990.

Sayer RJ, Schwindt PC, Crill WE (1992) Metabotropic glutamate receptor-mediated suppression of L-type calcium current in acutely isolated neocortical neurons. J Neurophysiol 68:833-842.

Scharfman HE (1994) Synchronization of area CA3 hippocampal pyramidal cells and non-granule cells of the dentate gyrus in bicuculline-treated rat hippocampal slices. Neuroscience 59:245-257.

Scoville WB, Milner B (1957) Loss of recent memory after bilateral hippocampal lesions. J Neurol Neurosurg Psychiatry 20:11-21.

Segal DS, Mandell AJ (1974) Long-term administration of d-amphetamine: progressive augmentation of motor activity and stereotypy. Pharmacol Biochem Behav 2:249-255.

Segal DS, Weinberger SB, Cahill J, McCunney SJ (1980) Multiple daily amphetamine administration: behavioral and neurochemical alterations. Science 207:905-907.

Shen Y, Specht SM, De Saint Ghislain I, Li R (1994) The hippocampus: a biological model for studying learning and memory. Prog Neurobiol 44:485-496.

Shigemoto R, Kinoshita A, Wada E, Nomura S, Ohishi H, Takada M, Flor PJ, Neki A, Abe T, Nakanishi S, Mizuno N (1997) Differential presynaptic localization of metabotropic glutamate receptor subtypes in the rat hippocampus. J Neurosci 17:7503-7522.

Sjostrom PJ, Turrigiano GG, Nelson SB (2001) Rate, timing, and cooperativity jointly determine cortical synaptic plasticity. Neuron 32:1149-1164.

Staff NP, Jung HY, Thiagarajan T, Yao M, Spruston N (2000) Resting and active properties of pyramidal neurons in subiculum and CA1 of rat hippocampus. J Neurophysiol 84:2398-2408.

Stafstrom CE (2005) The role of the subiculum in epilepsy and epileptogenesis. Epilepsy Curr 5:121-129.

Stevens CF, Wang Y (1994) Changes in reliability of synaptic function as a mechanism for plasticity. Nature 371:704-707.

Stevens CF, Wang Y (1995) Facilitation and depression at single central synapses. Neuron 14:795-802.

Steward O (1976) Topographic organization of the projections from the entorhinal area to the hippocampal formation of the rat. J Comp Neurol 167:285-314.

Steward O, Scoville SA (1976) Cells of origin of entorhinal cortical afferents to the hippocampus and fascia dentata of the rat. J Comp Neurol 169:347-370.

Stewart M (1997) Antidromic and orthodromic responses by subicular neurons in rat brain slices. Brain Res 769:71-85.

Stewart M, Wong RK (1993) Intrinsic properties and evoked responses of guinea pig subicular neurons in vitro. J Neurophysiol 70:232-245.

Su H, Alroy G, Kirson ED, Yaari Y (2001) Extracellular calcium modulates persistent sodium current-dependent burst-firing in hippocampal pyramidal neurons. J Neurosci 21:4173-4182.

Su H, Sochivko D, Becker A, Chen J, Jiang Y, Yaari Y, Beck H (2002) Upregulation of a T-type Ca2+ channel causes a long-lasting modification of neuronal firing mode after status epilepticus. J Neurosci 22:3645-3655.

Sugiyama H, Ito I, Hirono C (1987) A new type of glutamate receptor linked to inositol phospholipid metabolism. Nature 325:531-533.

Sun W, Rebec GV (2003) Lidocaine inactivation of ventral subiculum attenuates cocaine-seeking behavior in rats. J Neurosci 23:10258-10264.

Surmeier DJ, Foehring R (2004) A mechanism for homeostatic plasticity. Nat Neurosci 7:691-692.

Swanson LW, Cowan WM (1977) An autoradiographic study of the organization of the efferent connections of the hippocampal formation in the rat. J Comp Neurol 172:49-84.

Swartz KJ (1993) Modulation of Ca2+ channels by protein kinase C in rat central and peripheral neurons: disruption of G protein-mediated inhibition. Neuron 11:305-320.

Swartz KJ, Bean BP (1992) Inhibition of calcium channels in rat CA3 pyramidal neurons by a metabotropic glutamate receptor. J Neurosci 12:4358-4371.

Swartz KJ, Merritt A, Bean BP, Lovinger DM (1993) Protein kinase C modulates glutamate receptor inhibition of Ca2+ channels and synaptic transmission. Nature 361:165-168.

Sweet KL, Neill DB (1999) Amphetamine injections into the nucleus accumbens enhance the reward of stimulation of the subiculum. Ann N Y Acad Sci 877:828-830.

Tabata T, Araishi K, Hashimoto K, Hashimotodani Y, van der Putten H, Bettler B, Kano M (2004) Ca2+ activity at GABAB receptors constitutively promotes metabotropic glutamate signaling in the absence of GABA. Proc Natl Acad Sci U S A 101:16952-16957.

Tabata T, Kawakami D, Hashimoto K, Kassai H, Yoshida T, Hashimotodani Y, Fredholm BB, Sekino Y, Aiba A, Kano M (2007) G protein-independent neuromodulatory action of adenosine on metabotropic glutamate signalling in mouse cerebellar Purkinje cells. J Physiol 581:693-708.

Taepavarapruk P, Floresco SB, Phillips AG (2000) Hyperlocomotion and increased dopamine efflux in the rat nucleus accumbens evoked by electrical stimulation of the ventral subiculum: role of ionotropic glutamate and dopamine D1 receptors. Psychopharmacology (Berl) 151:242-251.

Tamamaki N, Abe K, Nojyo Y (1987) Columnar organization in the subiculum formed by axon branches originating from single CA1 pyramidal neurons in the rat hippocampus. Brain Res 412:156-160.

Tanabe Y, Masu M, Ishii T, Shigemoto R, Nakanishi S (1992) A family of metabotropic glutamate receptors. Neuron 8:169-179.

Tanabe Y, Nomura A, Masu M, Shigemoto R, Mizuno N, Nakanishi S (1993) Signal transduction, pharmacological properties, and expression patterns of two rat metabotropic glutamate receptors, mGluR3 and mGluR4. J Neurosci 13:1372-1378.

Taube JS (1993) Electrophysiological properties of neurons in the rat subiculum in vitro. Exp Brain Res 96:304-318.

Thomas MJ, Beurrier C, Bonci A, Malenka RC (2001) Long-term depression in the nucleus accumbens: a neural correlate of behavioral sensitization to cocaine. Nat Neurosci 4:1217-1223.

Thomson AM, Girdlestone D, West DC (1988) Voltage-dependent currents prolong single-axon postsynaptic potentials in layer III pyramidal neurons in rat neocortical slices. J Neurophysiol 60:1896-1907.

Troyer MD, Blanton MG, Kriegstein AR (1992) Abnormal action-potential bursts and synchronized, GABA-mediated inhibitory potentials in an in vitro model of focal epilepsy. Epilepsia 33:199-212.

Turrigiano G, Abbott LF, Marder E (1994) Activity-dependent changes in the intrinsic properties of cultured neurons. Science 264:974-977.

Turrigiano G, LeMasson G, Marder E (1995) Selective regulation of current densities underlies spontaneous changes in the activity of cultured neurons. J Neurosci 15:3640-3652.

Urban NN, Barrionuevo G (1996) Induction of hebbian and non-hebbian mossy fiber long-term potentiation by distinct patterns of high-frequency stimulation. J Neurosci 16:4293-4299.

van Welie I, van Hooft JA, Wadman WJ (2004) Homeostatic scaling of neuronal excitability by synaptic modulation of somatic hyperpolarization-activated Ih channels. Proc Natl Acad Sci U S A 101:5123-5128.

Vanderschuren LJ, Everitt BJ (2004) Drug seeking becomes compulsive after prolonged cocaine self-administration. Science 305:1017-1019.

Verwer RW, Meijer RJ, Van Uum HF, Witter MP (1997) Collateral projections from the rat hippocampal formation to the lateral and medial prefrontal cortex. Hippocampus 7:397-402.

Vorel SR, Liu X, Hayes RJ, Spector JA, Gardner EL (2001) Relapse to cocaine-seeking after hippocampal theta burst stimulation. Science 292:1175-1178.

Walker M, Chan D, Thom M (2007) Hippocampus and Human Disease. In: The Hippocampus Book (Andersen P, Morris R, Amaral D, Bliss T, O'Keefe J, eds). New York: Oxford University Press.

Williams S, Johnston D (1989) Long-term potentiation of hippocampal mossy fiber synapses is blocked by postsynaptic injection of calcium chelators. Neuron 3:583-588.

Wise RA (1998) Drug-activation of brain reward pathways. Drug Alcohol Depend 51:13-22.

Witter MP (1993) Organization of the entorhinal-hippocampal system: a review of current anatomical data. Hippocampus 3 Spec No:33-44.

Witter MP, Groenewegen HJ (1990) The subiculum: cytoarchitectonically a simple structure, but hodologically complex. Prog Brain Res 83:47-58.

Witter MP, Amaral DG (1991) Entorhinal cortex of the monkey: V. Projections to the dentate gyrus, hippocampus, and subicular complex. J Comp Neurol 307:437-459.

Witter MP, Ostendorf RH, Groenewegen HJ (1990) Heterogeneity in the Dorsal Subiculum of the Rat. Distinct Neuronal Zones Project to Different Cortical and Subcortical Targets. Eur J Neurosci 2:718-725.

Wolf ME, Sun X, Mangiavacchi S, Chao SZ (2004) Psychomotor stimulants and neuronal plasticity. Neuropharmacology 47 Suppl 1:61-79.

Wolf ME, Dahlin SL, Hu XT, Xue CJ, White K (1995) Effects of lesions of prefrontal cortex, amygdala, or fornix on behavioral sensitization to amphetamine: comparison with N-methyl-D-aspartate antagonists. Neuroscience 69:417-439.

Wozny C, Knopp A, Lehmann TN, Heinemann U, Behr J (2005) The subiculum: a potential site of ictogenesis in human temporal lobe epilepsy. Epilepsia 46 Suppl 5:17-21.

Wu K, Leung LS (2003) Increased dendritic excitability in hippocampal ca1 in vivo in the kainic acid model of temporal lobe epilepsy: a study using current source density analysis. Neuroscience 116:599-616.

Wyvell CL, Berridge KC (2000) Intra-accumbens amphetamine increases the conditioned incentive salience of sucrose reward: enhancement of reward "wanting" without enhanced "liking" or response reinforcement. J Neurosci 20:8122-8130.

Yeckel MF, Kapur A, Johnston D (1999) Multiple forms of LTP in hippocampal CA3 neurons use a common postsynaptic mechanism. Nat Neurosci 2:625-633.

Zalutsky RA, Nicoll RA (1990) Comparison of two forms of long-term potentiation in single hippocampal neurons. Science 248:1619-1624.

Zhang W, Linden DJ (2003) The other side of the engram: experience-driven changes in neuronal intrinsic excitability. Nat Rev Neurosci 4:885-900.

Zhang XF, Hu XT, White FJ (1998) Whole-cell plasticity in cocaine withdrawal: reduced sodium currents in nucleus accumbens neurons. J Neurosci 18:488-498.

Zhang XF, Cooper DC, White FJ (2002) Repeated cocaine treatment decreases whole-cell calcium current in rat nucleus accumbens neurons. J Pharmacol Exp Ther 301:1119-1125.

Zhang XF, Hu XT, White FJ, Wolf ME (1997) Increased responsiveness of ventral tegmental area dopamine neurons to glutamate after repeated administration of cocaine or amphetamine is transient and selectively involves AMPA receptors. J Pharmacol Exp Ther 281:699-706.